UNIVERSITY OF CATANIA

INTERNATIONAL PhD IN CHEMICAL SCIENCES - XXIV CYCLE

CURRICULUM: ORGANIC CHEMISTRY

Bhusainahalli Vedamurthy Maheswarappa

NATURAL POLYPHENOLS AS LEAD COMPOUNDS IN THE SYNTHESIS OF ANTITUMOR AGENTS AND OTHER USEFUL PRODUCTS

Tutor: Prof. CORRADO TRINGALI

ACADEMIC YEARS 2009-2011

ABBREVIATIONS

BOP	Benzotriazole-1-yl-oxy-tris-(dimethylamino)-phosphonium hexafluorophosphate
BuLi	*n*-Butyl lithium
^{13}C NMR	Carbon Nuclear Magnetic Resonance
CD	Circular Dichroism
COSY	COrrelation SpectroscopY
DNA	Deoxyribonucleic acid
DCM	Dichloromethane
DCC	*N,N*-Dicyclohexylcarbodiimide
DMAP	Dimethylaminopyridine
DIC	*N,N*-Diisopropylcarbodiimide
DMF	*N*,*N*-dimethylformamide
DPPH	2,2-diphenyl-1-picrylhydrazyl
EWG	Electron Withdrawing Group
EtOH	Ethanol
EtOAc	Ethyl acetate
HSQC	Heteronuclear Single Quantum Coherence
HMBC	Heteronuclear Multiple-Bond Correlation
HPLC	High Performance Liquid Chromatography
HRP	Horseradish Peroxidase
HOBt	*N*-hydroxybenzotriazole
LPO	Laccase from *Pleurotus ostreatus*
LTV	Laccase from *Trametes versicolor*
MeOH	Methanol
MW	Microwave
NOESY	Nuclear Overhauser Enhancement Spectroscopy
RT	Room Temperature
^{1}H NMR	Proton Nuclear Magnetic Resonance
THF	Tetrahydrofuran
TLC	Thin Layer Chromatography
TMP	Trimethylpyridine
UV	Ultraviolet

ACKNOWLEDGEMENTS

This work was carried out at the Department of Chemistry, Faculty of Mathematical, Physical and Natural Sciences, University of Catania, (Italy) and Institut de Chimie Moléculaire de l'Université de Bourgogne (ICMUB), Dijon, France (during a short period visit).

I want to express my immense depth acknowledgement to:

Supervisor of this thesis Prof. Corrado Tringali, who accepted me as doctorate student for his project and was the main source of the great ideas, techniques and backbone of this thesis. I experienced with him great warmth of care, and we experienced together all the ups and downs of routine work, the shared happiness of success and the depression of failure when (sometimes) everything went wrong in laboratory. He managed to teach me how to write scientific reports and reproduce them in scientific journals. It is a real pleasure to work and communicate with such a polite, honest, helping natured and open-minded person.

Co-supervisor - Dr. Carmela Spatafora, who guided me organic chemistry in laboratory activities. She took lot of care towards me and she has helped me greatly during all three years, special appreciation for the proofreading (her patience is valuable) and language translation from Italian to English for all administrative work and has always been extremely supportive and nice to me. It was her great help in science and beyond science life that I got the chance to initiate and complete this thesis. It is great pleasure to work with such an optimistic genteel lady. I felt great love and affection from both guide and co-guide in my three years research work.

I would like to acknowledge Prof. Dominique Fasseur-Vervandier and Dr. Malik Chalal for their love and affection in my short period of stay in ICMUB, Dijon.

I would like to express my immense depth acknowledgement to Prof. Vincenzo Amico to providing laboratory space to complete my research work. I want to say thanks to Prof. Sebastiano Sciuto, Prof.ssa Rosa Chillemi, and all Professors from Chemistry Department, who gave positive critics and suggestions in my yearly viva to improve quality of this thesis. I would like to thank Prof. Antonio Rescifina for theoretical calculations.

Also I want to thanks, an external examiner Prof. Philippe Cotelle from University of Lille, who gave me suggestions in my annual presentations.

I want to express my acknowledgement to Prof. B.S. Sherigara, Prof.Tapas Kumar Kundu, Prof. S. Sampath, Prof. J. Keshavayya, Prof. K.S. Rangappa, Dr. Lokesh, Dr. K.M. Lingu, Dr. A. Hari Kishore, who gave me dimension and shape in research.

I would like to thank present and former colleagues of "Bioactive natural product group", for their assistance and providing an excellent working atmosphere: Dr. Carmelo Daquino, Nino Marino, Ionella Ranno, Lella Susinna, Maria Rita Nobile, Rita Tosto, Carmelo Girmenia, Danilo Aleo and all others.

I want to thanks all 24th cycle International Ph.D program students: Valentina La Paglia Fragola, Martina Pannuzzo, Zelica Minniti, Valentina Greco, Pietro Gemmellaro and Salvatore Battiato and Noufal kandoth for enjoyable outings in Catania.

I want to express my gratitude towards JNCASR. IISc Professors and friends who made my stay in campus fruitful, and M.Sc friends, Bhasker H. G, Pradeep P.C, Harsha V, Ravindra, Siddesh, Maruthi rao, Manthesh, Niranjan, etc for their constant encouragement and cooperation.

I would like to thank my maternal uncles, who feed me immediately after my birth to till my life. Umapathy B.C, Shivalingappa B.C, Shadaksharappa B.C, Onkarappa B.C, Shivappa B.C, Parameshwarappa B.C, Shekrappa B.C, and Basappa B.C. and also I want to acknowledge my all aunts' who took care towards me from childhood to till know. I want to express my gratitude towards, my sisters, my sibling brothers and sisters who gave me company to make my childhood joy able.

I would like to thank my father Maheshwarappa B.M, who was dreaming of my bright future in his life time and I want to dedicate this thesis for his 4th year death anniversary. Last but not least my mother Sakamma B.C, without she, I am an imagination. I had unforgettable love from her, she is praying god each and every movement for my success. How can I express thanks to her? No, it is not possible. Simply I want to say love you Amma....

1. INTRODUCTION

Polyphenols or, more properly, the plant metabolites originated by the shikimic acid pathway show a noticeable structural variety, ranging from simple phenolic acids, for instance gallic acid or caffeic acid, to oligomers (tannins) and polymers (lignins or melanins). This large group of chemical substances, mainly found in higher plants, include more than 8.000 compounds, many of whom display important biological properties. In recent years, an increasing attention towards many dietary polyphenols has been also due to their recognised antioxidative and cancer chemopreventive properties.[1] Indeed, a considerable number of studies is concentrated on a limited number of low molecular weight dietary polyphenols, such as the stilbenoid resveratrol (**1**) found in grape and red wine, the green tea catechins, and in particular epigallocatechin-3-gallate (EGCG, **2**), the hop chalcone xanthohumol (**3**), the soya isoflavone genistein (**4**), the yellow pigment curcumin (**5**) found in turmeric (curry), ellagic acid (**6**), a component of pomegranate, the widespread caffeic acid (**7**) and its natural derivatives chlorogenic acid and (**8**) and CAPE (**9**), this latter found in honeybee propolis. In particular, resveratrol (**1**) is considered one of the most important polyphenols with cancer chemopreventive activity and displays an impressive variety of biological activities.[2]

Some dimeric polyphenols, biosynthetically related to phenolic acids or stilbenoids, collectively named 'lignans' are of high biomedical importance. A well-known example is podophyllotoxin (**10**), a natural aryldihydrolignan with cytotoxic properties, which was submitted to chemical modifications to obtain the anticancer drug etoposide (**11**). Many other dimeric lignans have been reported in the literature, some of them with unusual structures or displaying promising biological properties like antibacterial, anticancer, antiestrogenic,

antiviral, fungistatic, estrogenic, antioxidant, and insecticidal activities.[3] Other lignans are reported as anti-mitotic, anti-angiogenic and anti-radical agents.[4]

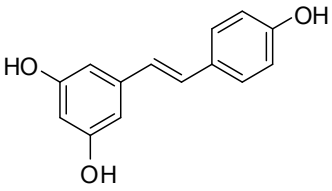

1

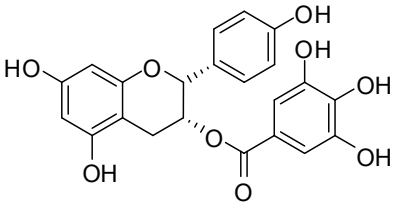

2

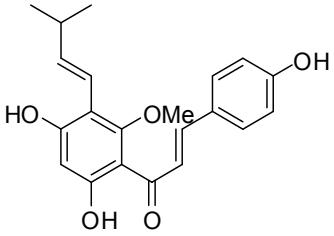

3

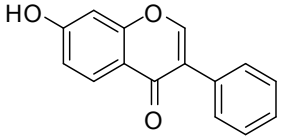

4

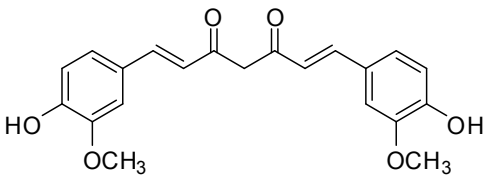

5

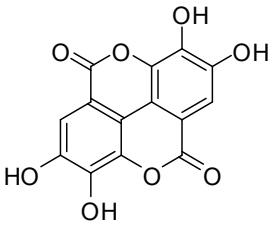

6

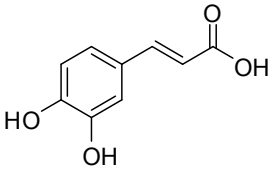

7

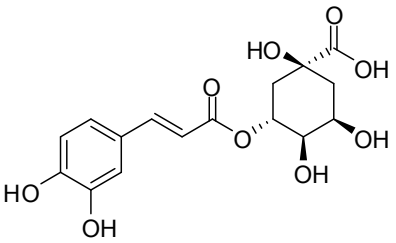

8

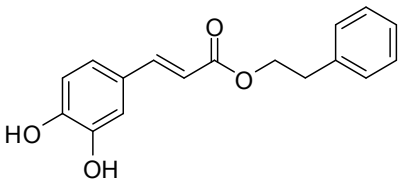

9

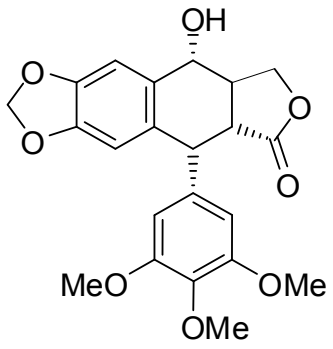

10

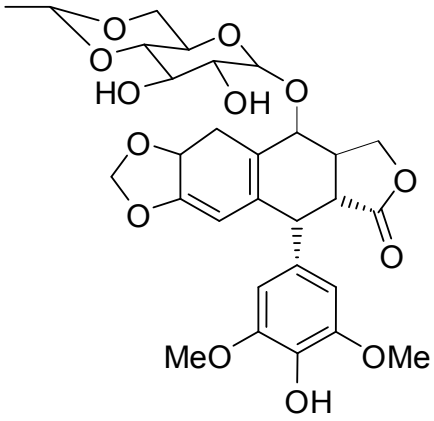

11

From a biosynthetic point of view, lignans are dimers generated by *β-β'* (8-8') oxidative coupling of two cinnamic acid residues. Many lignans and neolignans include a heterocycle in their structure. This is normally generated through intramolecular cyclization of a reactive intermediate formed in the oxidative coupling step, as exemplified by the biosynthesis of the lignan (+)-pinoresinol (**14**) (Scheme1).

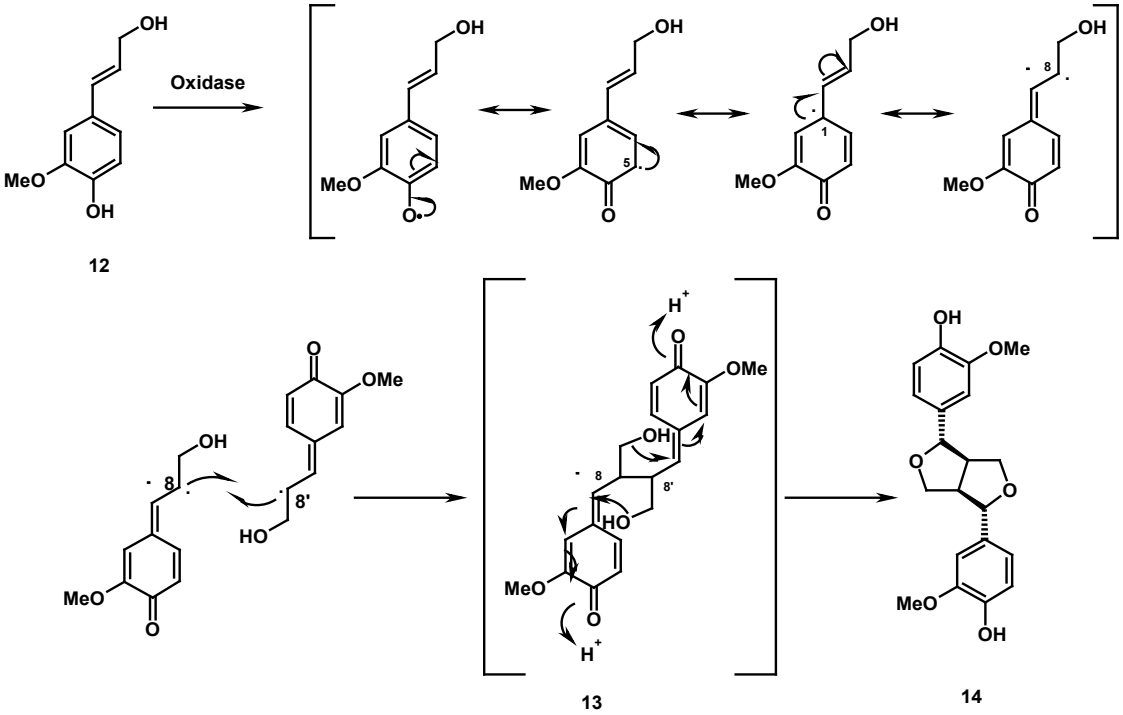

Scheme 1

This biosynthetic pathway has been widely studied and it is known that pinoresinol originates from the monolignol coniferyl alcohol (**12**): in the first step an oxidase enzyme gives rise to the coniferyl alcohol radical, reported here as mesomeric forms. Subsequently, a coupling reaction affords a reactive quinone-methide intermediate (**13**) which by cyclization gives the final product **14**.[2]

According to the IUPAC recommendations 2000,[5,6] 'neolignans' are distinguished in referring to dimers with a carbon linkage between two C_6C_3 units different from 8-8', as for example (+)-dehydrodiconiferyl alcohol (**16**), whose biosynthesis, outlined in Scheme 2, proceeds via the quinone-methide intermediate **15** formed through an 8-5' coupling of coniferyl radicals.[7]

The term 'oxyneolignans,' should be reserved to dimers linked by an ether oxygen atom where there are no direct carbon–carbon bonds between the C_6C_3 units. An important point on lignan and lignin biosynthesis is that the regio- and stereospecificity of bimolecular phenoxy radical coupling is not controlled by peroxidases, laccases or other oxidases, as demonstrated by the formation of racemic mixtures as product of *in vitro* oxidative coupling experiments[8].

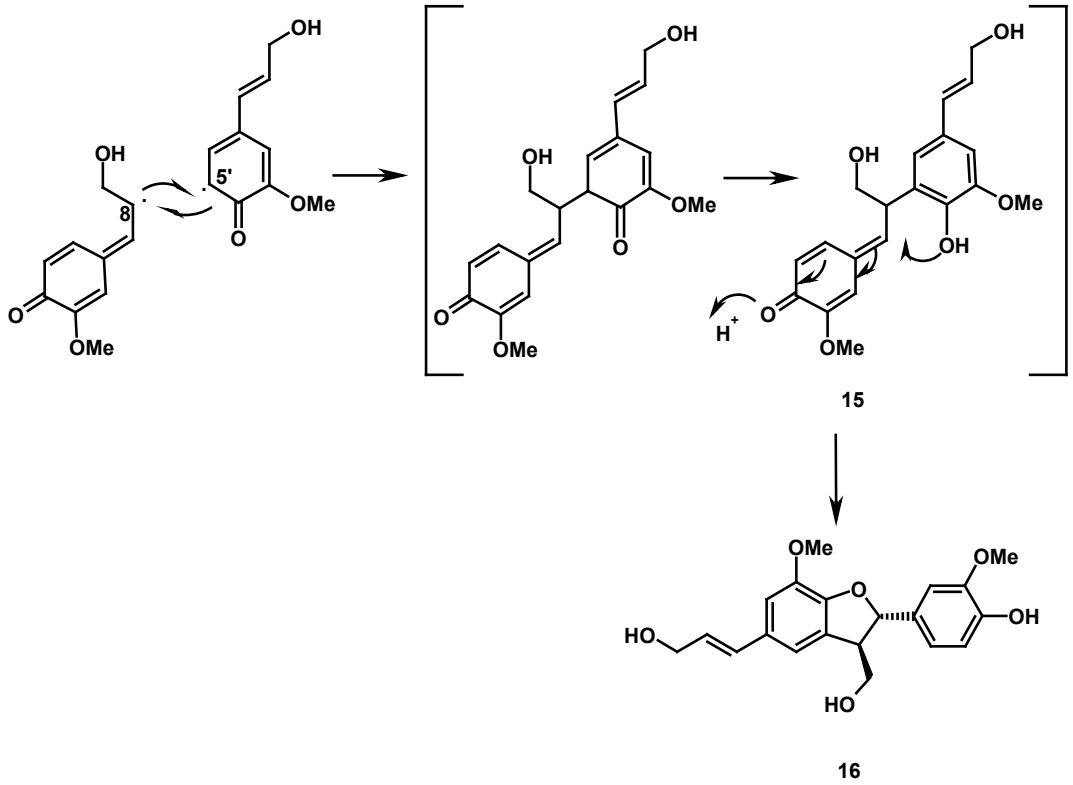

Scheme 2

As shown by Graph 1, the number of references (articles) retrieved through Scifinder Scholar using the term 'lignans' is in constant growth since 1997 to 2010 and a similar trend is observed if the search is restricted to the patents. These data confirm the biomedical importance of this family of natural products: in fact, the most interesting bioactive lignas are an attractive target for chemical synthesis and pharmacological optimization.

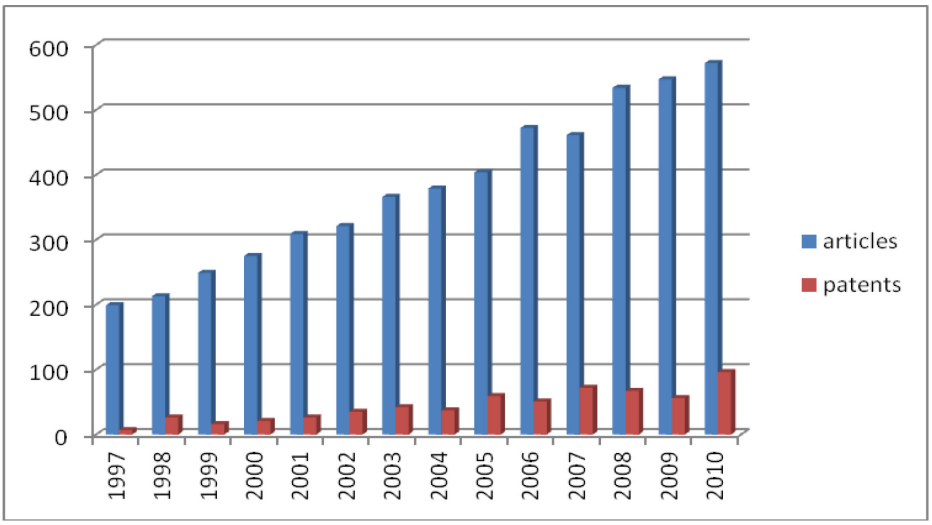

Graph 1

Among the various synthetic methodologies employed in the synthesis of lignans, biomimetic coupling reactions are frequently carried out on natural precursors, and may afford 'unnatural' products through a radical phenolic oxidative coupling mechanism mimicking the 'natural' biosynthetic process. Thus, it is possible in principle to obtain compounds unprecedented in literature although maintaining a basic 'natural' skeleton and possibly offering a bioactivity profile similar to, or better than, that of a natural analogue. Due to the lack of stereocontrol both in metal- or enzyme mediated phenolic radical coupling, racemic mixtures are frequently obtained.[10] Nevertheless, a number of interesting products has been obtained in such a way, and in some cases the bioactive racemate has been resolved to obtain the most active enantiomer. In this regard, one interesting example is the reported dimerization of methyl caffeate (**17**) with Ag_2O[4] which afforded a neolignan racemate related to the natural dimer 3',4-di-*O*-methylcedrusin (**18**). This latter was isolated as one of the active principles of 'dragon's blood', the blood-red latex produced by some *Croton* spp. growing in South America and employed in traditional medicine for its wound-healing and anti-cancer properties. The racemate was then resolved to give the (2*R*,3*R)*-enantiomer (**19**) showing promising antitumor properties against breast cancer cell lines and resulting most potent than its (2*S*,3*S)*-enantiomer not only as antiproliferative but also as antiangiogenic agent.[9] In addition, the related neolignan racemate (±)-**20** (only the 2*R*,3R-enantiomer is reported) resulted highly active against chloroquine-resistant *Plasmodium falciparum* and *Leishmania donovani*.

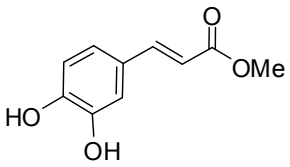

17

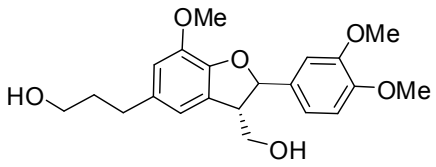

18

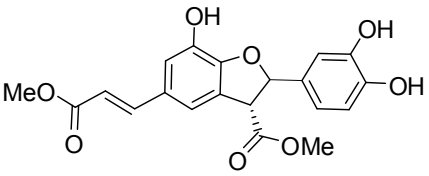

19

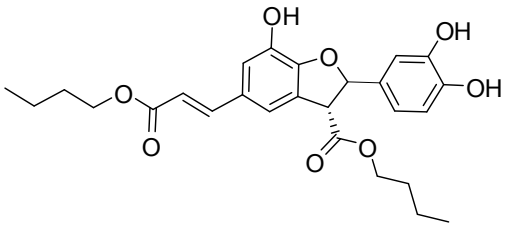

20

Ralph *et al*[10] employed ethyl ferulate **21** as substrate and Ag_2O (in dry acetone) as the oxidative agent; an intermediate quinone-methide **22** is formed by 8-5' coupling of the electron-delocalized phenoxy radical and this gives rise to the cyclization product, the racemic *trans* 2,3-dihydrobenzofuran neolignan **23** (only one enantiomer is reported), obtained in ca 30% yield, according to Scheme 3.

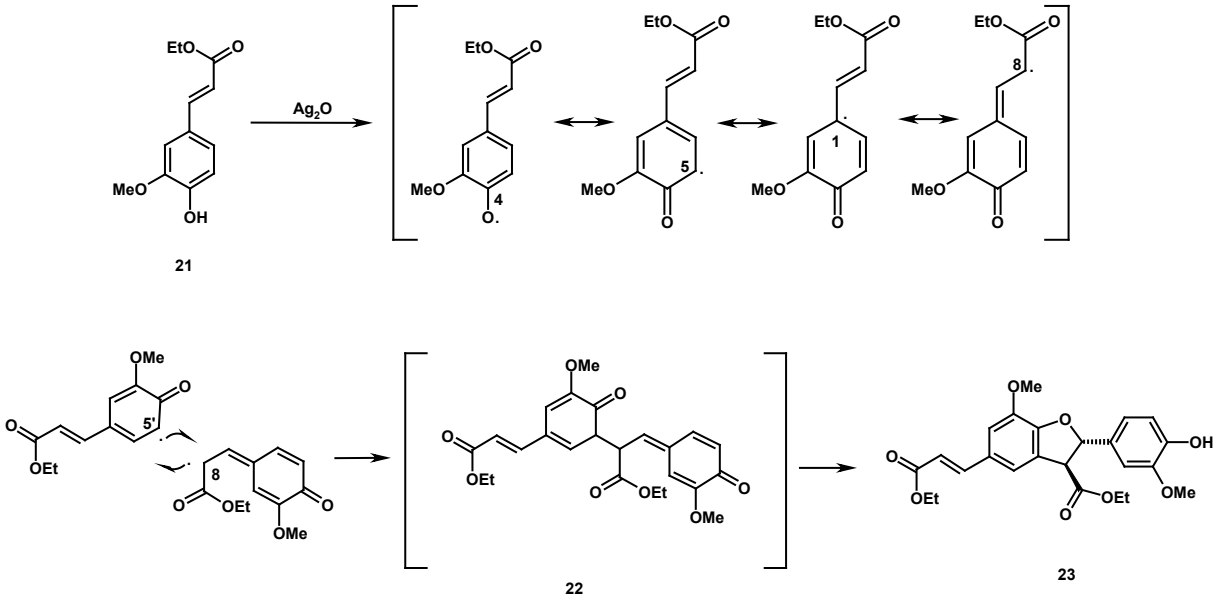

Scheme 3

In the last decade, metal-mediated biomimetic syntheses based on phenolic oxidative coupling have been frequently paralleled by coupling methods mediated by enzymes, mainly peroxidases or laccases.

Laccases (Figure 1**)** are oxidoreductases belonging to the multinuclear copper-containing oxidases; these enzymes are widely distributed in fungi and in some bacteria and higher plants and are able to catalyse the monoelectronic oxidation of substrates at the expense of molecular oxygen.[11] The active site of these enzymes consists of a metallic cluster containing four copper atoms, all of them being involved in the redox process via a radical cyclic mechanism[12] (Figure 2a). The oxidation of a specific phenolic derivative depends on the redox potential difference between the target compound and the so called 'T1'-copper. The overall outcome of the catalytic cycle is the reduction of one molecule of oxygen to two molecules of water and the concomitant oxidation of four substrate molecules to produce four radicals[13] (Figure 2b). These reactive intermediates can then produce dimers, oligomers and polymers.

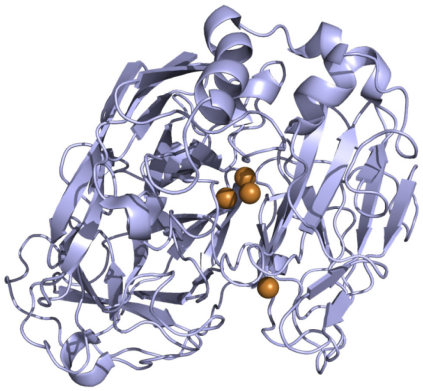

Figure 1: Model structure of *Trametes versicolor* Laccase

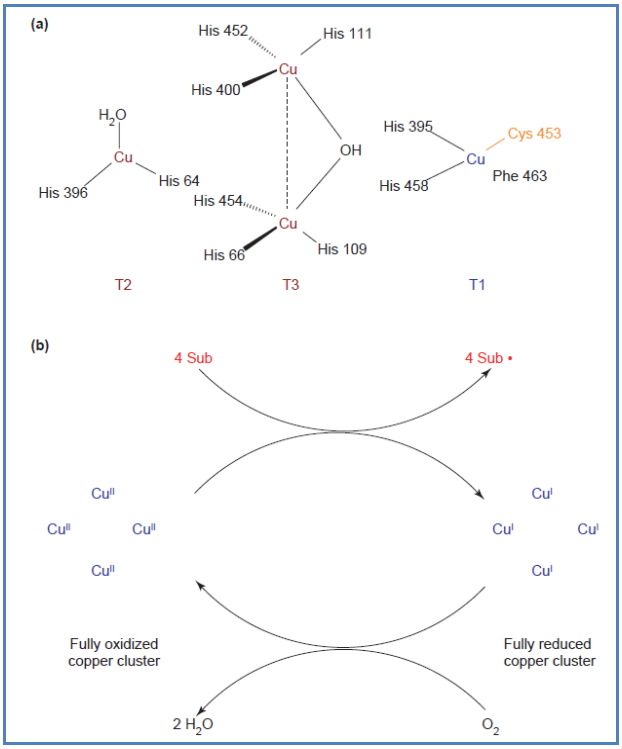

Figure 2: Laccases: active-site structure and catalytic cycle. (**a**) Model of the catalytic cluster of the laccase from *Trametes versicolor* made of four copper atoms. Type I (T1) copper confers the typical blue colour to the protein and is the site where substrate oxidation takes place. Type 2 (T2) and Type 3 (T3) copper form a trinuclear cluster, where reduction of molecular oxygen and release of water takes place.[14] (**b**) Schematic representation of a laccase catalytic cycle producing two molecules of water from the reduction of one molecule of molecular oxygen and the concomitant oxidation (at the T1 copper site) of four substrate molecules to the corresponding radicals.[22] Sub: substrate molecule; Sub: oxidized substrate radicals.

Laccases show exceptional substrate versatility and therefore are potentially suitable biocatalysts for the mild oxidation of organic compounds. Interest in these essentially 'eco-friendly' enzymes, working with air and producing water as the only by-product, has grown significantly in recent years. So far, the main limitation to their use has been their scarce availability. However, mainly to satisfy the demand for new 'green' processes by the textile and pulp and paper industries, some of these enzymes have recently been cloned and overexpressed and are becoming commercially available.[15] Following the

increased interest in these essentially 'green' catalysts, significant number of reports has been published in the past decade, focusing on the biochemical properties of these proteins and/or on their applications in technological and bioremediation processes in addition to their use in chemical reactions.

Peroxidases act on phenols by H_2O_2-dependent one-electron oxidation. Horseradish Peroxidase (HRP) (Figure 3) in the presence of H_2O_2 is one of the most frequently used enzymes for phenolic oxidative coupling (Figure 4).

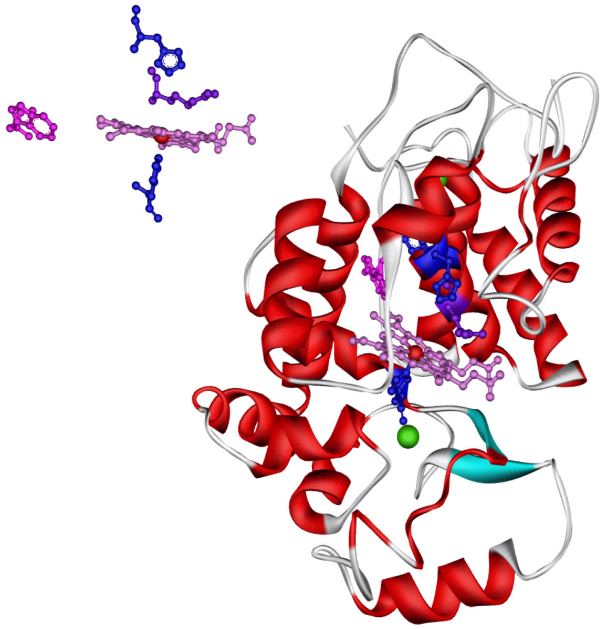

Figure 3: Model structure of Horseradish Peroxidase

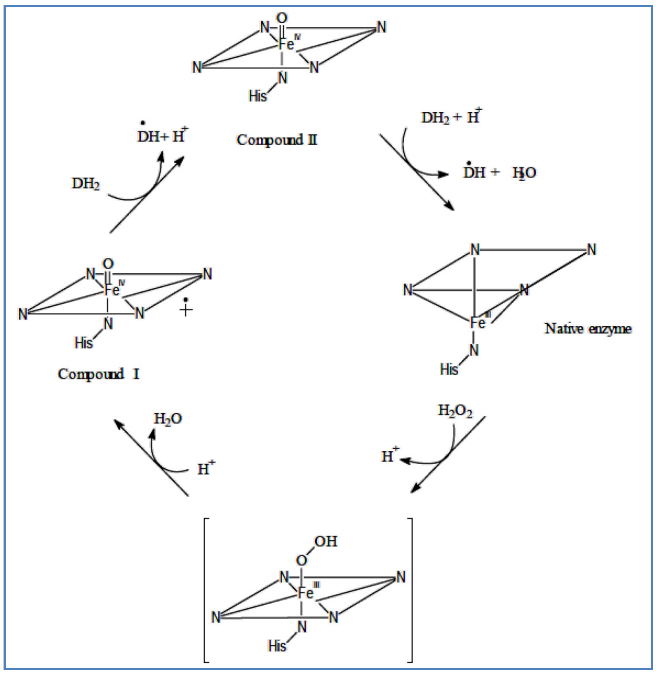

Figure 4: Mechanism of Horseradish Peroxidase (HRP)

Various HRP-mediated dimerizations of phenolic precursors have been carried out; for instance, the 4-allylphenol **25** was used by Liu *et al.*[16] as a putative biogenetic precursor of the oligomeric neolignans isolated from *Illicium* spp., linked through the aromatic rings and exemplified by magnolol (**25**), a dimeric *o,o*-coupled product displaying neuroprotective activity and other promising biological properties.[17] The biomimetic synthesis of **25** was carried out by HRP-catalysed dimerization of **24** with 40% yield, significantly higher than that obtained by the conventional chemical methods.

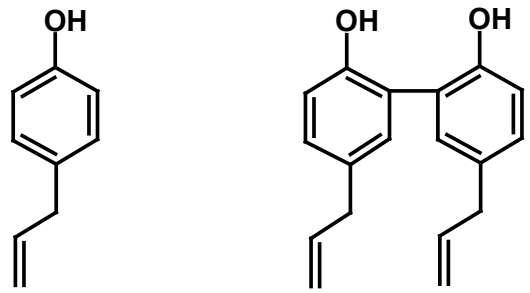

24 **25**

Nitrogenated lignanes are quite rare in nature; two antifeedant lignanamides isolated from *Xylopia aethiopica*[18] were obtained by chemical and enzymatic synthesis. This latter was carried out treating the phenolic amide **26** with HRP/H_2O_2 and afforded the same products of the chemical synthesis in better yields, namely (±)-**27** (18%) and (-)-**28** (10%).

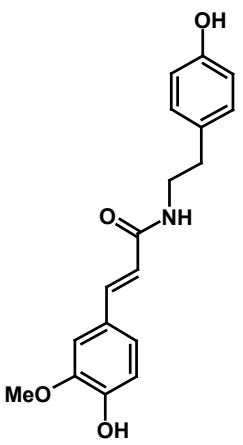

26

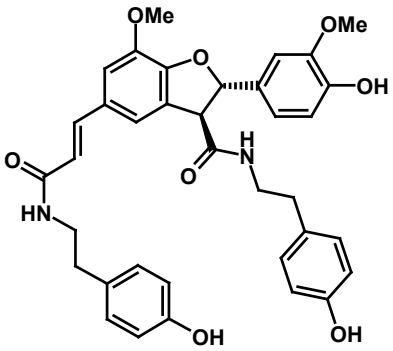

27

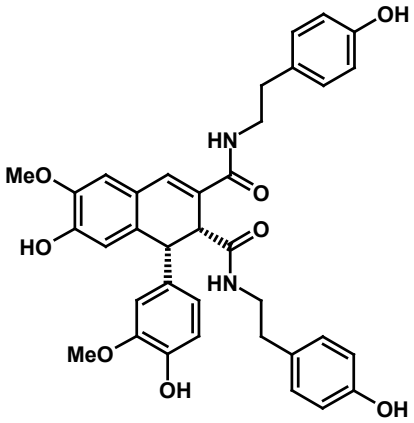

28

1.1 **Stilbenolignans**

Dimeric products have been also obtained by oxidative coupling of polyphenols different from phenylpropanoids. In particular, many chemists have studied the oxidative coupling of resveratrol (or resveratrol analogues) under a variety of conditions because resveratrol oligomers have unusual structures and a wide range of biological activities,[19,20,21] but low natural abundance; ε-viniferin (**29**) firstly isolated in 1977,[22] is a typical example of stilbenoid dimers. Viniferins exhibit a variety of biological activities, among them anti-HIV, antimicrobial, anti-inflammatory and anticarcinogenic.[19, 23] Their biosynthetic origin is reasonably due to oxidative coupling of a stilbenoid precursor, so we include these dimers within the class of stilbenolignans, although this term has been mainly used for mixed dimers with a stilbenoid portion.

In synthetic radical coupling of resveratrol (**1**), the main product most frequently obtained was the 5–8-coupling product, that is, resveratrol *trans*-dehydrodimer (**30**) or δ-viniferin, regardless of whether enzymes (peroxidase[24] or laccase[25]) or inorganic oxidants were used.

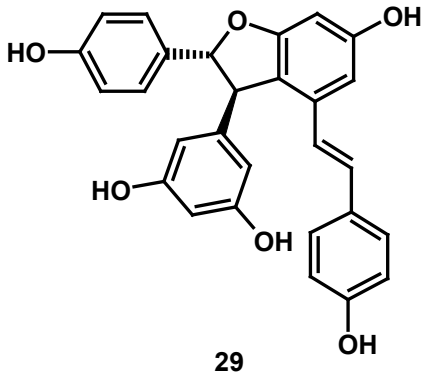

29

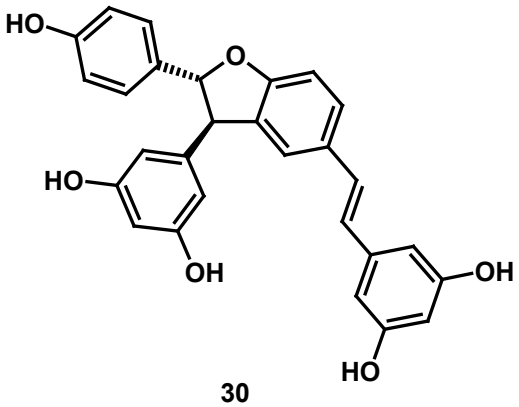

30

By treating **1** with 2,2-diphenyl-1-picrylhydrazyl free radical (DPPH) a major product was isolated in 18% yield and identified as **30**.[26] On the other hand, the treatment of **1** with $FeCl_3$ failed to give **30**, affording the isomeric dimer ε-viniferin (**29**) as the sole product.[27] Riva *et al*[28] reported that the laccase enzyme-mediated dimerization of resveratrol afforded **30**. In a more recent work the same authors reported the laccase enzyme-mediated dimerization of a series of resveratrol analogues.[29] An exemplificative product of this synthesis is again the stilbenoid dimer **30** (type A structure, Scheme 4) but two other kinds of structure, type B and C, are reported.[28]

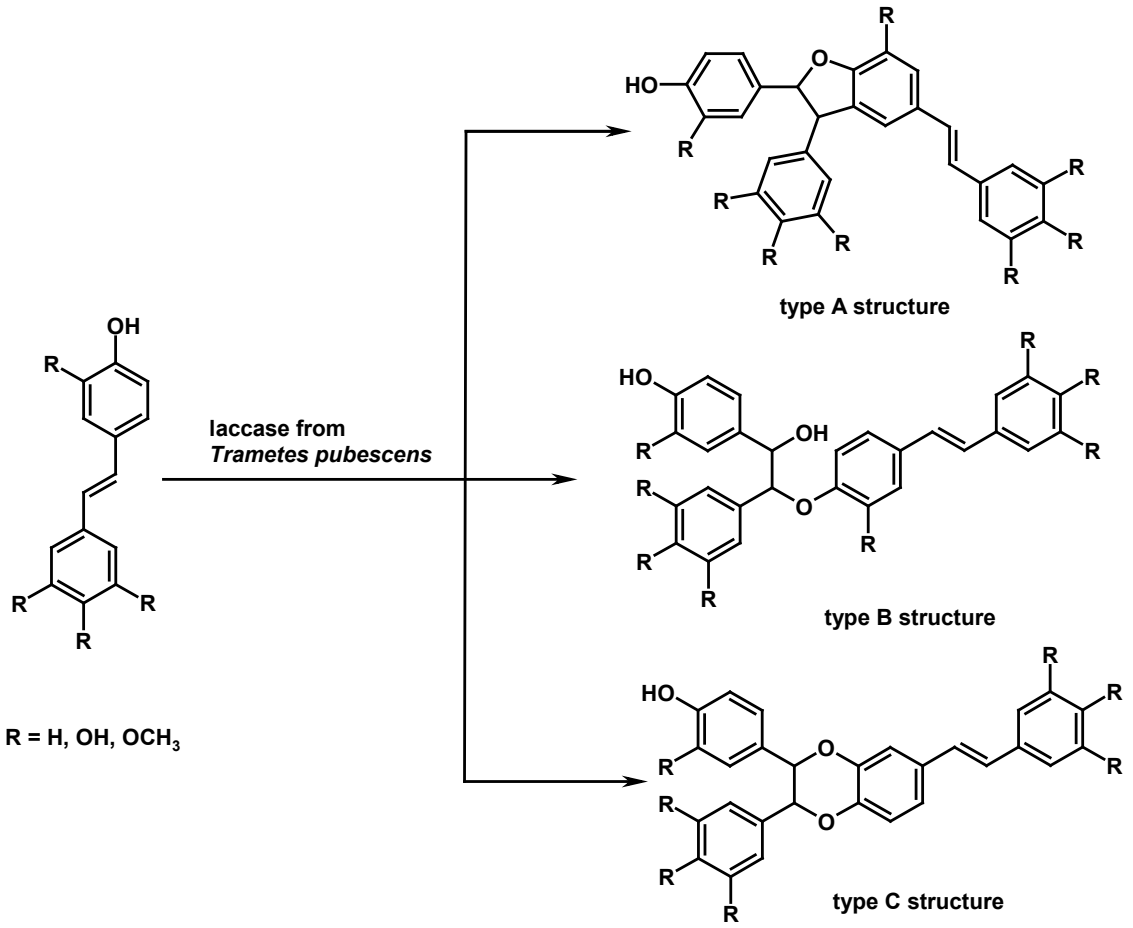

Scheme 4

A recent paper by Snyder *et al*.[30] describes elegant and versatile routes to a few dimeric species by adding and/or constructing additional rings onto brominated stilbenes. Some key steps include intramolecular Friedel–Crafts alkylation. Sako described the non-enzymatic synthesis of **30** involving the treatment of **1** with AgOAc and other metallic oxidants.[31] Similarly, Takaya and co-workers described the treatment of **1** with several oxidizing reagents and found that $Tl(NO_3)_3$ and $K_3[Fe(CN)_6]$ were the best oxidants to transform **1** into **29**, whereas $FeCl_3$ in acetone and MnO_2 in dichloromethane were the best catalysts to produce the dimer **30**.[32] Fang *et al*[33] investigated the radical scavenging activity and detailed mechanism of resveratrol **1** and its analogues (ArOHs) by the reaction kinetics with galvinoxyl (GO•) and 2,2-diphenyl-1-

picrylhydrazyl (DPPH•) radicals in ethanol and ethyl acetate at 25 °C, using UV-Vis spectroscopy: they found that the reaction rates increase with increasing the electron-rich environment in the molecules, and the compound bearing *o*-dihydroxyl groups (3,4-dihydroxy-*trans*-stilbene) is the most reactive one among the examined resveratrol analogues. Lin's group described the oxidative coupling of isorhapontigenin (**31**) by means of formic acid and one electron oxidants (Ag_2O, $FeCl_3 \cdot 6H_2O$).[34] These researchers managed to obtain dimeric species of various natural skeletons, mainly of the δ-viniferin or ε-viniferin type. Hou and co-workers dimerized a cleverly designed resveratrol derivative with help of the horseradish peroxidase.[35] The bulky substituents did not allow the enzyme to convert the substrate into a δ-viniferin analogue and subsequently quadrangularin A (**32**) was obtained.

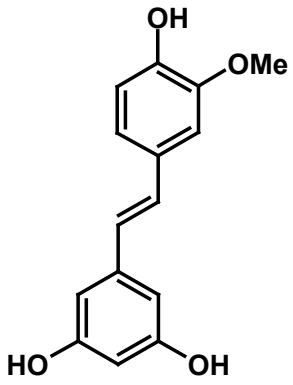

31

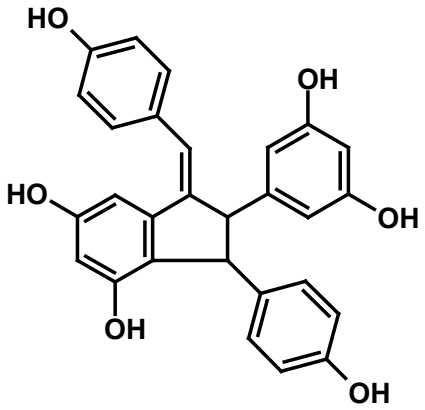

32

S. Velu *et al*[36] achieved biomimetic synthesis of unnatural derivatives by subjecting three resveratrol analogues to oligomerization by means of one-electron oxidants. Upon varying the metal oxidant, the solvent, and the oxygenated substitution pattern of the starting material, these researchers

managed to obtain a series of unusual oligomeric stilbenes, among them compounds **33** and **34**.

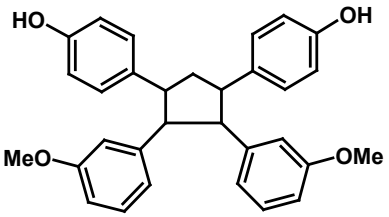

33

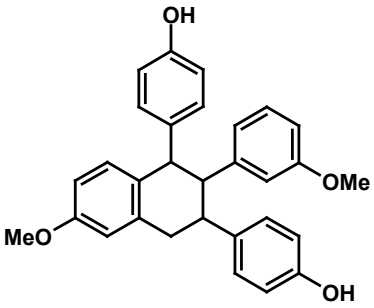

34

The dimeric compound with an 1,4-benzodioxane ring, (-)-aiphanol (**37**) is an unprecedented natural dimer where the dioxane bridge connects a phenylpropane unit with a stilbene unit. This mixed stilbenolignan was recently obtained through bioassay-guided isolation from the seeds of *Aiphanes aculeata*[37] and resulted a potent inhibitor of both COX-1 (IC_{50} = 1.9 μM) and COX-2 (IC_{50} = 9.9 μM). A synthesis of **37** as a racemic mixture has been carried out by Banwell *et al.*[38] through a cross-coupling between stilbenoid and phenylpropanoid substrates. In this synthesis (Scheme 5), the natural stilbenoid piceatannol (**35**), prepared by condensation of a suitable ylide and an aromatic aldehyde (followed by deprotection of the primary product) undergoes an Ag_2CO_3-promoted oxidative coupling with sinapyl alcohol **36** affording (±)-aiphanol (only the levorotatory 2*R*,3*R*-enantiomer is reported here) and a mixture of related dimers (**33** - **40**). All these compounds inhibited both COX-1 and COX-2 (IC_{50} in the range 0.17–9.5 μM). Interestingly, (±)-aiphanol proved to be a potent anti-angiogenic agent, completely inhibiting blood vessels growth at 100 μg/mL. Also compounds **39** and **38** were comparable angiogenesis inhibitors, whereas **40** resulted less active. Compounds **38** - **40** proved more active than PI-88, an anti-angiogenic polysulphated oligosaccharide now in clinical development as anti-cancer agent.[39] In the frame of this work,

piceatannol (**35**) was tested as anti-angiogenic inhibitor and resulted almost active as (±)-aiphanol.

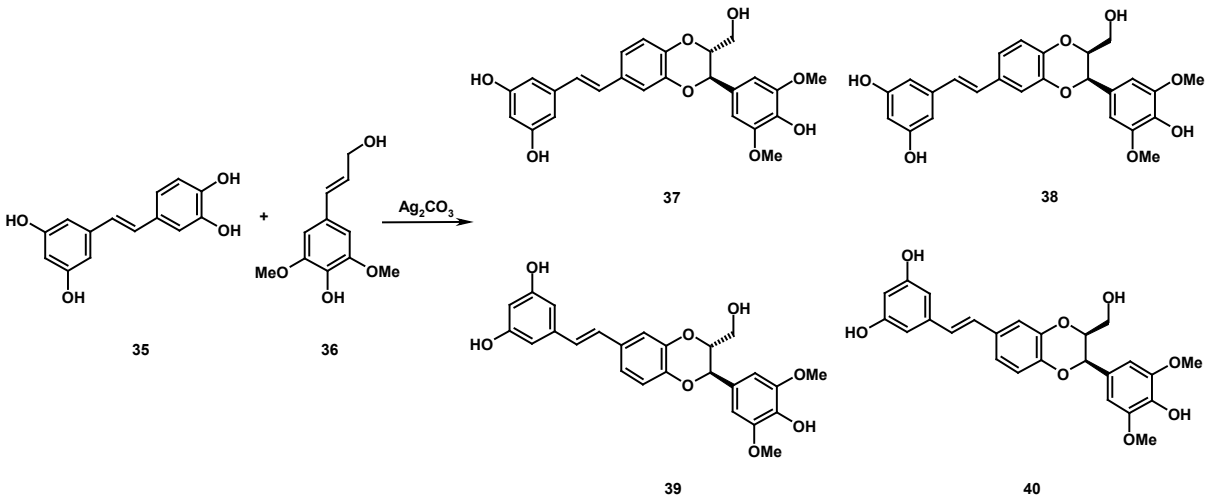

Scheme 5

1.2 Benzo[*k,l*]xanthene lignans

Benzo[*kl*]xanthene lignans are very rare polyphenolic chemical compounds both among natural products and synthetic analogues. Recently reported representatives are yunnaneic acid H (**41**), rufescidride (**42**) and mongolicumin A (**43**) isolated respectively from *Salvia yunnanensis*,[40] *Cordia rufescens*,[41] and *Taraxacum mongolicum*.[42] Interestingly, the aryldihydronaphtalene lignan rabdosiin (**44**) was also isolated from *S*. y*unnanensis*, It is also worth noting that, due to their rarity in nature and the low yield of previous synthetic reactions to obtain analogues,[43] and these compounds are almost unexplored with regard to their biological properties and possible pharmacological applications. Even for the previously known rufescidride (**42**), the only available reference about its biological properties is, to the best of our knowledge, a patent referring to its antimicrobial activity.[44]

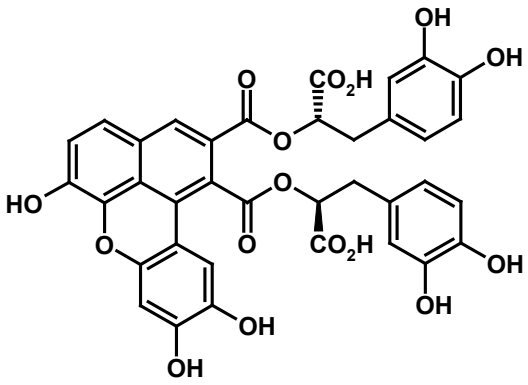

41

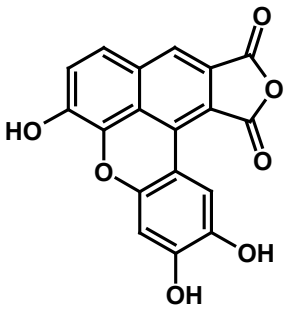

42

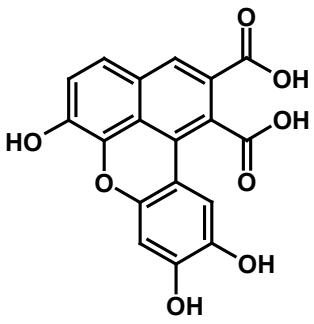

43

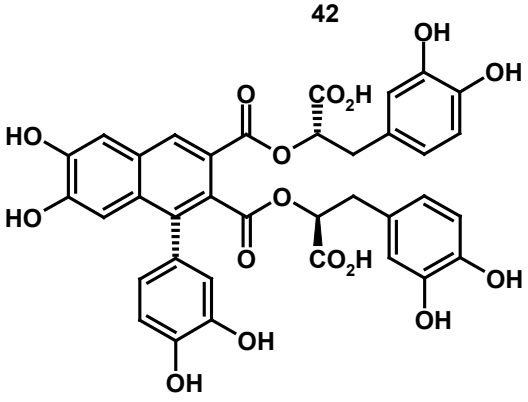

44

Among the few synthetic reactions affording benzoxanthene lignans there is a study of Maeda *et al*; they prepared **45** from the natural coumarin esculetin; the reaction of **45** with Ag_2O in benzene-acetone (Scheme 6), followed by acetylation of the reaction mixture, afforded the aryldihydronaphtalene (**46**) (28% yield) accompanied by the unusual benzo[*kl*]xanthene (**47**) (10%) as major products. Without acetylation, **46** was obtained in 22% yield. Minor amounts of the benzo[*kl*]xanthene (**48**) and the 1,4-benzodioxane (**49**) were also obtained. The formation of dihydrobenzofuran neolignans (8-5' coupling) is blocked by the presence of the methoxy group at C-2 position. A hypothetical mechanism for the formation of the benzoxanthenes, through biradical intermediates, was also proposed. Compounds **46**, **47** and **49** resulted much more effective inhibitors of lipid peroxidation in rat liver microsomes than α-tocopherol. Differently from benzoxanthene lignans, many natural analogs of

the aryldihydronaphtalene lignan **46** are known, among them magnoshinin,[45] thomasic acid,[46] thomasidioic acid[47] and rabdosiin.[48]

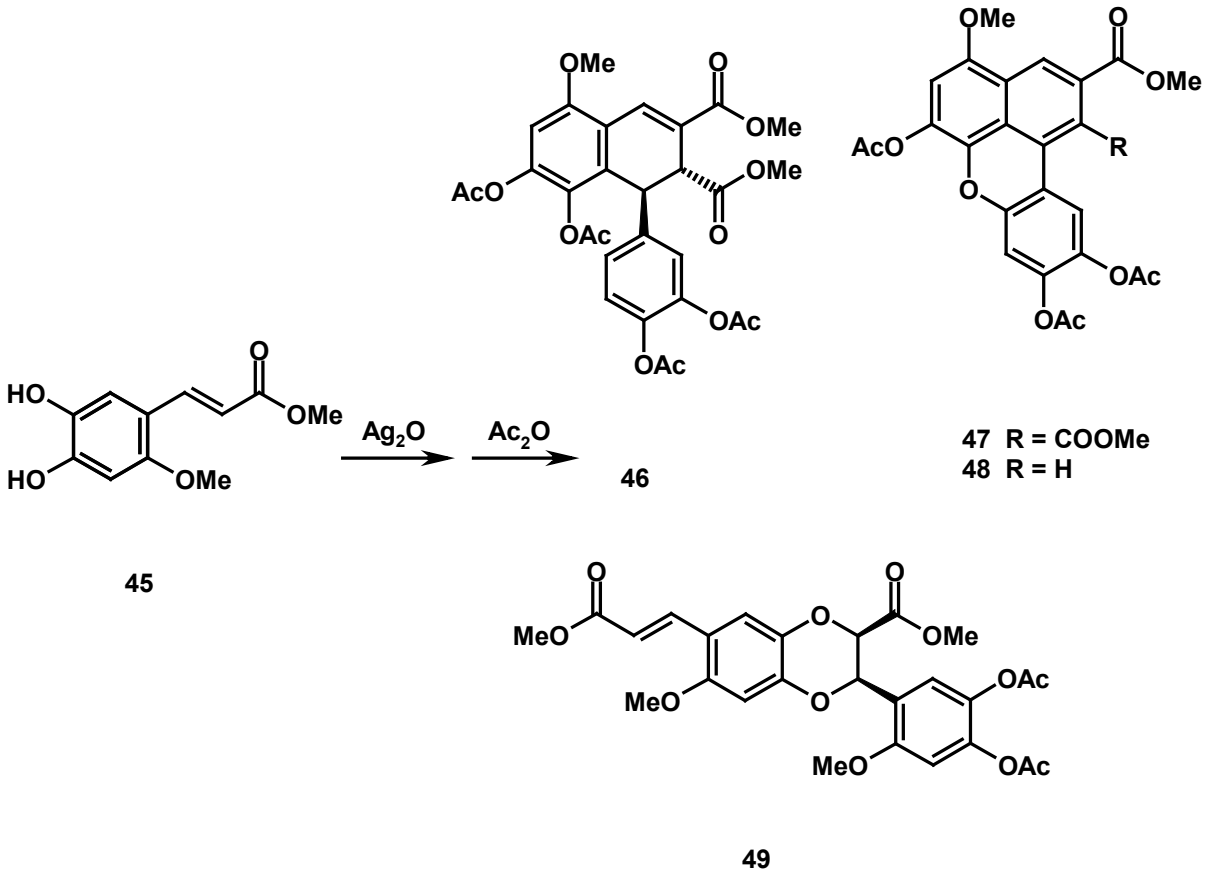

Scheme 6

Recently, C. Tringali *et al*,[49] employed MnO_2 as oxidative agent in a biomimetic coupling reaction of caffeic acid phenethyl ester (CAPE, **9**). This natural product is a component of propolis and it is reported as anti-inflammatory, antioxidant and antitumoral agent.[50]

According to Scheme 7, the manganese-mediated reaction afforded with good yield the benzo[*kl*]xanthene lignan (**50**) as major product, accompanied by minor amounts of the aryldihydronaphtalene lignan (**51**). Interestingly, when Ag_2O was employed as oxidative agent, the neolignan **52** was obtained as major product.[51]

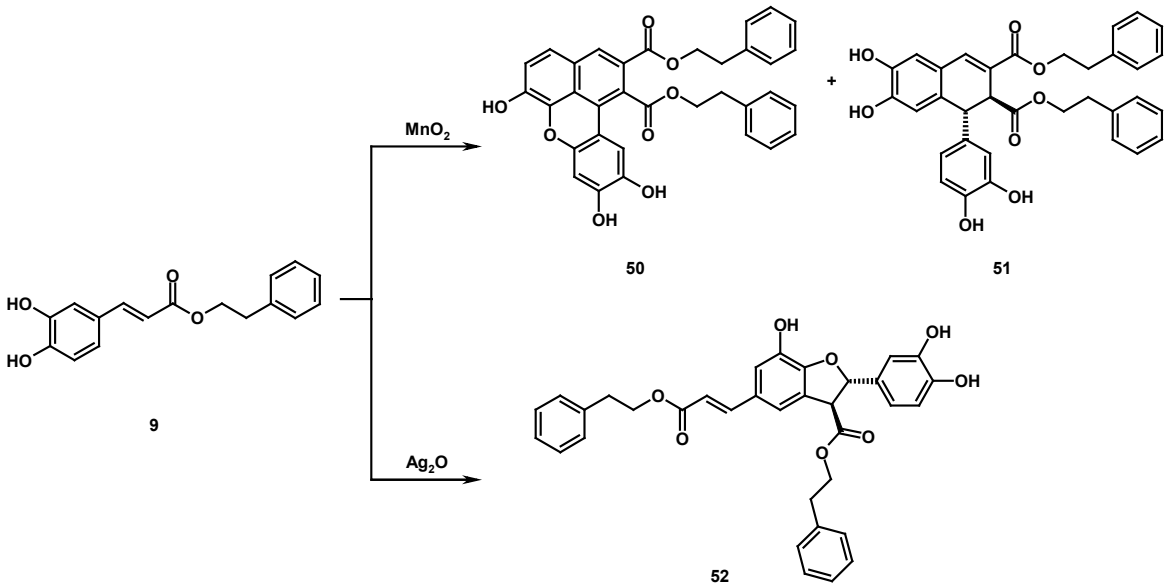

Scheme 7

Very recently, G. Bifulco *et al*[52] investigated interaction of six synthetic benzo[*kl*]xanthene lignans (**50**, **53**, **54**, **55**, **56**, **57**) and the natural metabolite rufescidride **42** with DNA through a combined STD-NMR and molecular docking approach, paralleled by *in vitro* biological assays on their antiproliferative activity towards two different cancer cell lines: SW 480 (Figure 5) and HepG2.

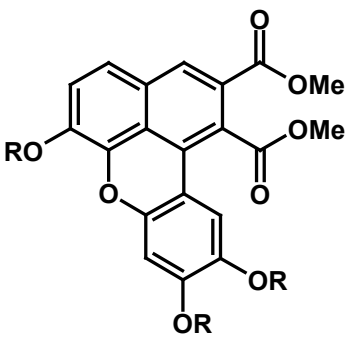

53. H
54. CH_3
55. $COCH_3$

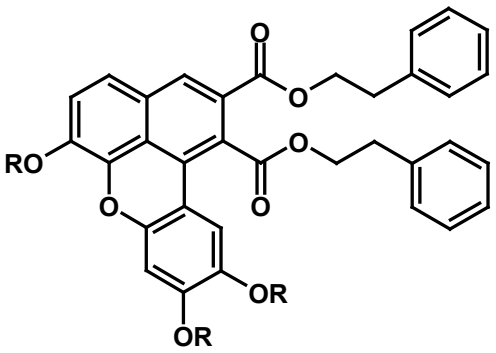

50. H
56. CH_3
57. $COCH_3$

The most active compound was the benzo[*kl*]xanthene lignan **50**, potently active both on colon (IC_{50} = 2.57 mM) and hepatic cancer cells (IC_{50} = 4.76 mM). Also the three-acetylated derivative **53** strongly inhibits the cellular

proliferation after a 48 h treatment, selectively on colon cells (IC_{50} = 3.21 mM), and to a lesser extent, on hepatic cells (IC_{50} = 26.66 mM). It is worth noting that compounds **50** and **57**, bearing the phenylethyl pendants at positions 1 and 2, are significantly more active than compounds **53** and **55**, which have methyl ester groups in the same positions.

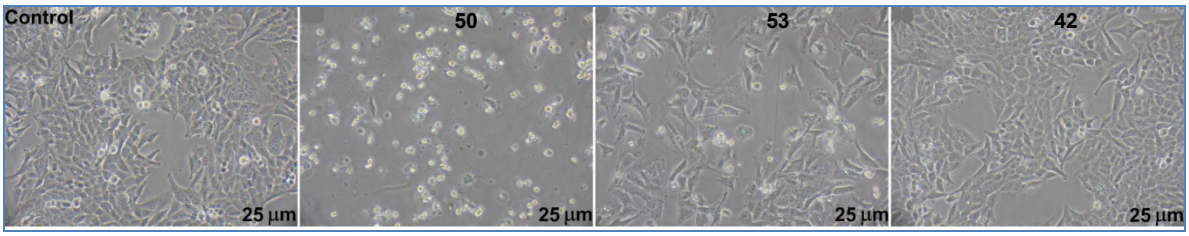

Figure 5: Phase contrast microscopy observation of SW480 colon cancer cells treated or not for 48 h with **50**, **53** and **42**.

The study of intercalation between base pairs was performed taking into account two binding cavities (Figure 6), in order to evaluate if this type of interaction to the DNA, and the consequent hydrogen bond formations, were base-dependent.

Within both models A and B, the common polycyclic aromatic moiety intercalates between base pairs forming *π-π* interactions with the macromolecular counterparts and the two phenylethyl groups are accommodated along the minor groove establishing van derWaals contacts(see Ref. 54 for more details) (Figure 7). Finally, Bifulco *et al* data suggest that the benzo[*kl*]xanthene lignans are suitable lead compounds for the design of DNA selective ligands with potential antitumour properties.

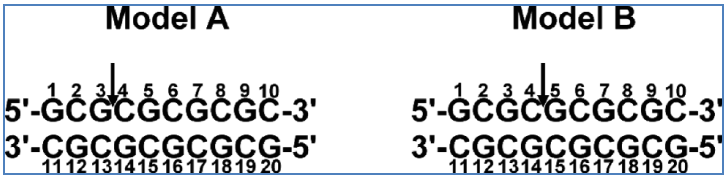

Figure 6: Schematic representation of DNA models (A and B) used in docking calculations

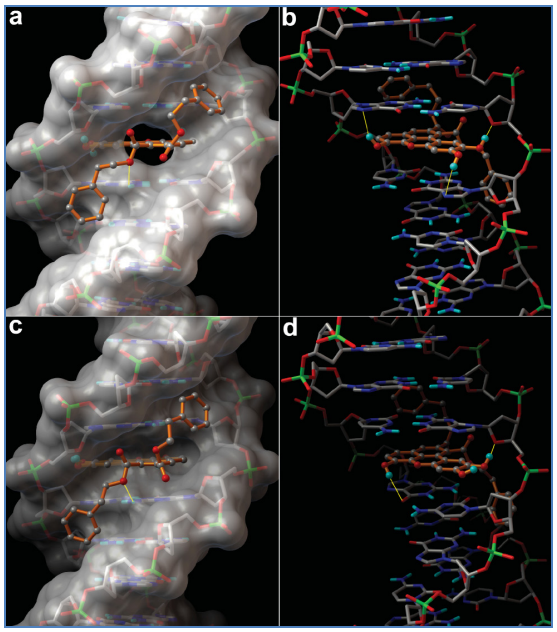

Figure 7: 3D interactions of **50**-model A (a and b) and **50**-model B (c and d) complexes

1.3 Hydantoins

As will be detailed in the following, the above reported analysis of the literature was the basis to a research work carried out during three years with the aim to obtain new bioactive stilbenolignans and benzoxanthene lignans. A step of this work was the synthesis of caffeoyl amides, and in this occasion we observed the formation of caffeoyl *N*-acylurea an unexpected product in specific reaction conditions. We tried to exploit this unexpected product as starting material for the preparation of previously unreported dimers through an enzyme-mediated oxidative coupling; promising results were obtained with Laccase from *Trametes versicolor* (LTV) enzyme. This reaction afforded again an unexpected product, which was submitted to spectral analysis and established as a hydantoin-related compound. Thus, we report here a summary of literature data on hydantoins.

Hydantoin (**57**) which is also known as glycolilurea, was discovered in 1861 by Baeyer, who isolated it as one of the reduction products of allantoin (**58**) a

product of purine metabolic degradation, during the course of his now classic study of uric acid.[53] The new substance was named “hydantoin”, since it had been obtained through the reduction, or hydrogenation, of allantoin. The hydantoin moiety is found in several natural products, including some unusual compounds of marine origin, such as midpacamide (**59**),[54] isolated from a marine sponge of the genus *Agelas*, or the hydantoin-related compounds **60** - **62**, [55, 56,57] obtained from the red sea sponge *Hemimycale arabica*. Among these, **60** showed potent in vitro anti-growth and anti-invasive properties against PC-3M prostate cancer cells in MTT and spheroid disaggregation assays.[58] Hydantoin **60** also showed anti-invasive activity in orthotopic xenograft of PC-3M cells in nude mice model. Some 1-phenethyl and 5-(*E*)-benzylidene hydantoins, as **63**, inhibited EGFR autophosphorylation and polyGAT phosphorylation and were found to inhibit the growth and proliferation of human A-431 cells.[59,60] Therefore, these hydantoins were considered good scaffolds for future design of tyrosine kinase inhibitors.

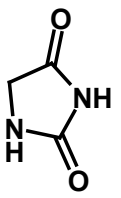

57

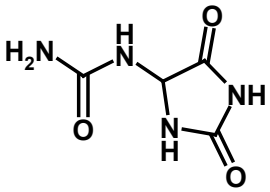

58

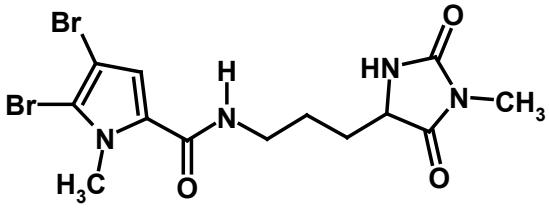

59

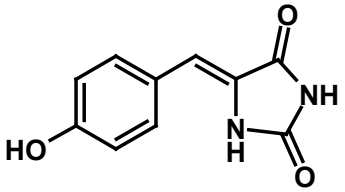

60

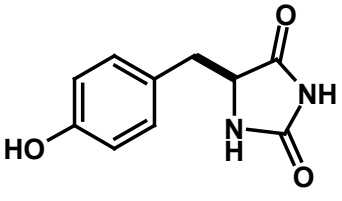

61

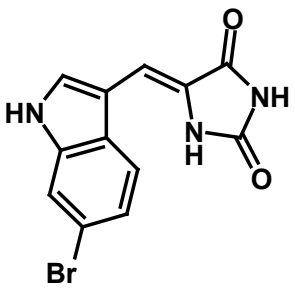

62

Hydanthoin-related compounds are also known as useful drugs, such as phenytoin **64**, employed for the treatment of epilectic seizures.[61] Phenylmethylenehydantoins substituted with alkyl groups, for instance **65**, were found to exhibit good anticonvulsant activity[62]

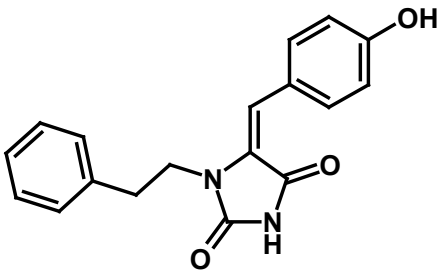

63

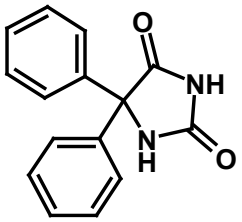

64

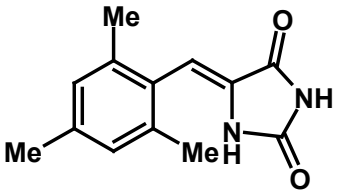

65

Hydantoins have been investigated for other promising pharmacological activities. In fact, hydantoin derivatives have been identified as antimuscarinics,[63] antiulcers, and antiarrythmics,[64] antivirals, antidiabetics,[65] serotonin and fibrinogen receptor antagonists,[66] inhibitors of the glycine binding site of the NMDA receptor[67] and antagonists of leukocyte cell adhesion acting as allosteric inhibitors of the protein–protein interaction.[68] Peptide hydantoin analogs were patented for their ability to inhibit thrombocyte aggregation, metastasis, and osteoclast binding to bone surfaces.[69]

Moreover, substituted hydantoins are important building blocks for the synthesis of unnatural amino acids both in racemic form by alkaline degradation[70] and in an enantioselective way by enzymatic resolution.[71] In fact, hydantoins can serve as useful intermediates in the synthesis of optically pure amino acids employing hydantoinases and other related biocatalysts.[72]

For this reason, there is high interest in developing new strategies for a straightforward synthesis of selectively substituted hydantoins both in solution

and in the solid phase. A classical synthesis of hydantoins is that of Bucherer–Bergs from ketones or cyanohydrins, treated with ammonium carbonate and potassium cyanide respectively to give hydantoins.[73]

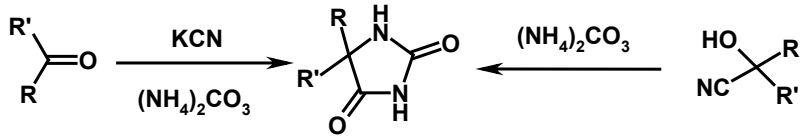

Scheme 8

S. Paul *et al*[74] synthesized 1,5-disubstituted hydantoins/thiohydantoins **68** in good yield by a microwave-promoted solvent-free condensation of arylaldehydes **66** and phenylurea/thiourea **67** using polyphosphoric ester (PPE) as a reaction mediator.

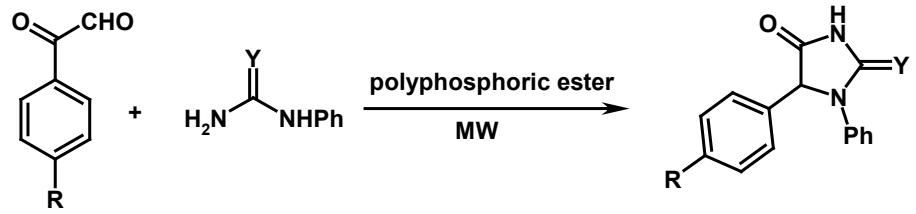

66 **67** **68**

Y: O, S

Scheme 9

A novel intermolecular α-amination process of esters using CuCl as catalyst and di-*tert*-butyldiaziridinone as nitrogen source forms hydantoins effectively under mild reaction conditions. Yian Shi *et al*[75] found that ester **69** can be aminated at the R position using di-*tert*-butyldiaziridinone (**70**)[76] as a nitrogen source and CuCl as a catalyst, leading to a direct formation of hydantoin (**71**).

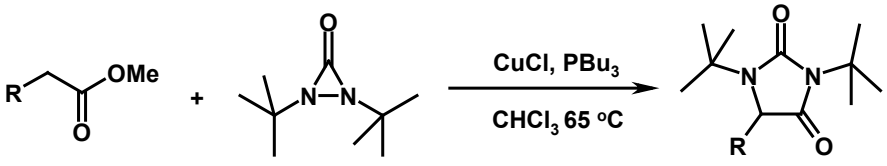

69 **70** **71**

R = Ar, vinyl

Scheme 10

Enantiomerically pure hydantoins **73** are prepared from optically pure α-amino amides **72** utilizing triphosgene. A mechanism for the racemization observed with 1,1'-carbonyldiimidazole (CDI) for this type of reaction is proposed.[77]

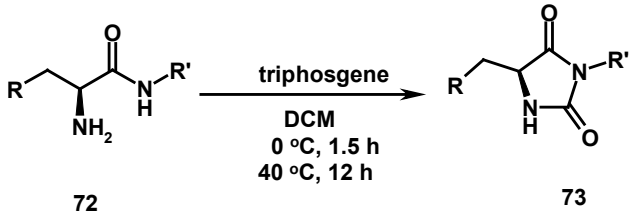

72 **73**

Scheme 11

Carbodiimides[78] such as dicyclohexylcarbodiimide (DCC) and diisopropylcarbodiimide (DIC) are very popular reagents often used to activate carboxylic acid groups to nucleophilic substitution.[79] The mechanism and kinetics of reaction of carbodiimides with carboxylic acids have been extensively investigated.[80] A. Volonterio *et al*[81] recently demonstrated that carbodiimides **75** when treated with suitable carboxylic acids **74**, namely, activated α,β-unsaturated acids, in the absence of a nucleophile are useful reagents for the straightforward synthesis of 1,3,5-trisubstituted hydantoins **76** through a regiospecific domino process consisting of a condensation step between the two reactants, leading to the formation of *O*-acyl isourea intermediates that undergo nucleophilic aza-Michael reaction or halogen displacement, respectively, followed by a final N-O acyl migration step.

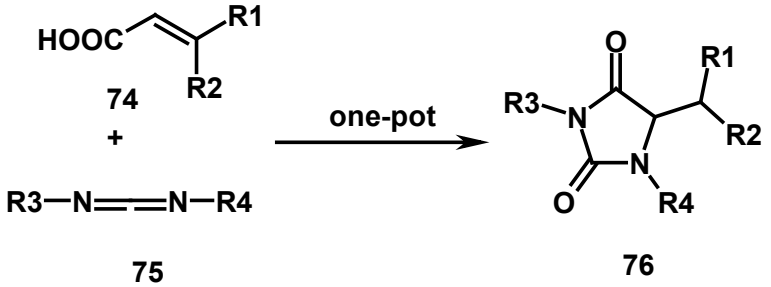

75 **76**

R_1 = EWG, R_2 = H, COOEt, CF_3
R_3 = alkyl or aryl, R_4 = alkyl or aryl

Scheme 12

Recently, the same group[82] developed a general, straightforward method for the preparation of 1,5-disubstituted hydantoins in good to excellent yields through a two-step strategy relying on a highly regioselective domino reaction between *N*-*tert*-butyl- or *N*-trityl-substituted carbodiimides and activated α,β-unsaturated carboxylic acids or α-haloarylacetic acids followed by selective deprotection of the tertiary alkyl substituent at the 3-position of the ring.

In another work A. Volonterio *et al*[83] carried out reaction of carbodiimide **75** with α-Br(Cl)-aryl acetic acids **76** produces *N,N'*-substituted 5-arylhydantoins **77** under very mild conditions and high yields. When the carbodiimides are generated *in situ* by Staudinger reaction, the process becomes a one-pot, three-component sequential synthesis of libraries of differently substituted 5-arylhydantoins.

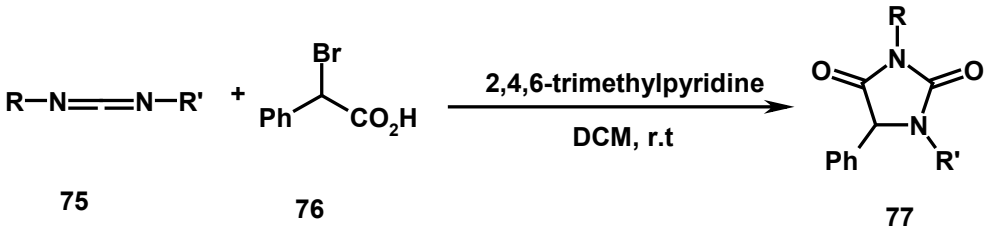

75 **76** **77**

Scheme 13

1.4 Main Objectives

The above reported data show that some polyphenol dimers, such as lignans, neolignans and stilbenoid compounds, because of their biological properties as well as their structural variety, are an attractive target for chemical synthesis or modification. Thus, these polyphenols may be considered 'lead compounds' to obtain products with useful properties, in particular as possible antitumor agents. The observation that lignans, neolignans and related compounds can be obtained by a biomimetic oxidative coupling starting from a phenolic precursor prompted us to carry out a research project aimed to obtain new bioactive products by using biomimetic synthetic methodologies.

In particular, the main objectives pursued during this three year research work have been oriented to the synthesis of new dimers of simple derivatives of natural polyphenols such as resveratrol or caffeic acid and their analogues. To this purpose, we employed both chemical and enzymatic methods, as detailed in the Discussion.

1.4.1 Biomimetic synthesis of stilbenolignans

The biological activity of natural stilbenolignans prompted us to carry out a to biomimetic synthesis of resveratrol synthetic analogues, to obtain new 'unnatural' derivatives; dimerization was obtained by means of one-electron oxidants and employing horseradish peroxidase and Laccase from *Trametes versicolor*. Radical dimerization, both metal- or enzyme-mediated, normally affords racemic mixtures, but enantiopure neolignans could be obtained by resolution of the racemic mixture through chiral HPLC.

1.4.2 Biomimetic synthesis of benzo[*k,l*]xanthene lignanamides

Nitrogenated lignans (Lignanamides) are quite rare respect to oxygenated lignans and their biological activity has not been extensively evaluated. As reported above from C.Tringali *et al*, benzo[*k,l*]xanthene related compounds can be obtained by oxidative coupling of phenolic precursors, employing metal-mediated processes. The above biological results inspired the synthesis of new nitrogenated DNA ligands designed for establishing additional minor groove contacts, improving the affinity for the biological target and contributing to sequence selectivity of the DNA-interacting compounds. Thus, part of this doctorate project has been devoted to carry out some coupling reactions finalized to optimize the biomimetic synthesis of new benzo[k,l]xanthene lignanamides, starting from natural polyphenols and in particular from caffeic acid derivatives. To this purpose, we planned to employ the metal-mediated

oxidative coupling reaction of caffeoyl amides employing $Mn(OAc)_3$ as oxidative agent.

1.4.3. Enzymatic synthesis of hydantoin-related compounds

As mentioned above hydantoin-related compounds are interesting small molecules exhibiting promising biological activities. Thus we tried to exploit some unexpected results of this research work to synthesize hydantoins by a simple biocatalyzed method starting from caffeic *N*-acylureas.

1.4.4. Structural characterization, biological evaluation and SAR studies

The final goal of the above reported project was to obtain a library of bioactive compounds to be addressed to biological evaluation with the aim to establish structure-activity relationships for a future optimization of the most promising products. This work was completed only for a group of stilbenolignans and is in progress for the other families of compounds. Of course, this required a careful spectroscopic characterization of all the intermediates and final products obtained, in order to establish unambiguously their structures.

Biological evaluation has been carried out (or is in progress) in cooperation with other laboratories: antiproliferative and pro-apoptotic activity will be examined primarily, in parallel with DNA-interacting properties for benzoxanthene lignans. Other biological evaluations such as antiangiogenic, antioxidative activity (radical scavenging, DNA-protective, etc.), inhibition of tubulin polimerization and others, will be carried out as a prosecution of this work.

2. RESULTS AND DISCUSSION

The research activity carried out in these three years has been addressed to the main objectives of my doctorate project, as outlined in the Introduction. This was focused on the biomimetic synthesis of new lignans and stilbenolignans in both enzymatic- and metal-mediated ways. Some of these dimeric polyphenols may be considered as 'lead compounds' to obtain optimized products, in particular as possible antitumor agents. More generally, our goal was to obtain useful products employing natural polyphenols as starting material. As detailed below, the main part of my doctorate research activity has been devoted to the synthesis of stilbenolignans, dimeric compounds related to viniferins, natural dimers of the stilbenoid polyphenol resveratrol (Section 2.1). The compounds obtained were evaluated for antiproliferative activity toward tumor cells and the results are reported here. A second project was focused on synthetic approaches to benzo[k,l]xanthene lignanamides, obtained as oxidative coupling products of caffeic acid amides (Section 2.2). Benzo[*k,l*]xanthene lignans are rare natural products with antiproliferative and DNA-interacting properties, and the lignanamides have never been previously synthesized and submitted to biological evaluation. During the preparation of these dimeric products, some unexpected reactions occurred in the presence of Laccase enzyme, leading to hydantoin-related products (Section 2.3); because of the biological properties of hydantoins, also this synthetic methodology, of possible interest in 'green chemistry', is discussed.

2.1 Biomimetic synthesis of stilbenolignans

The synthesis of stilbenolignans dimers and their evaluation as antiproliferative agents has been carried out in collaboration with Prof. Dominique Fasseur-

Vervandier, at the Institut de Chimie Moléculaire de l'Université de Bourgogne, Dijon (France). I have worked for a period in this laboratory, in particular for the synthesis of two new stilbenoid monomers, discussed in detail in the following (see below structures **83** and **86**). Further six stilbenoid monomers were gained from French laboratory. All eight monomers were subjected to metal- and/or enzyme–mediated oxidative coupling in our laboratory, which afforded eight dimers as racemic mixtures. All the synthesized dimers were subjected in France to antiproliferative activity bioassays against colon cancer cells SW480, and apart from (±)-**104** and (±)-**105**, all the other racemic mixtures resulted significantly active; therefore these mixtures were subjected to separation of the pure enantiomers. Among these dimers three stilbenolignans, namely, (±)-**99**, (±)-**100** and (±)-**105** are new compounds, which have been carefully characterized through mass spectrometry, mono and bidimensional NMR spectroscopy to assign all proton and carbon signals. The remaining dimers have been previously reported in literature, although their biological activity has not been investigated before this work. Unfortunately, one of the monomers synthesized in France (namely **98**) was not available for a new synthesis of the active dimer (±)-**106**; so this mixture could not be separated into enantiomers and also not characterized thoroughly. Thus, five racemic mixtures were separated into five couples of pure enantiomers through preparative chiral HPLC and their Circular Dichroism (CD) spectra were run to establish their absolute configuration.

A detailed discussion of all this work is reported below In Sections from 2.1.1 to 2.1.4

2.1.1 Synthesis of monomers

2.1.1.1 *Synthesis of monomer **83***

During my stay in France, I have synthesized the stilbenoid monomer **83** (4-(4-vinylstyryl)phenol) through Wittig reaction; in this reaction the protected aldehyde **80** reacts with a triphenylphosphonium ylide **82** to give the alkene **83** and triphenylphosphine oxide. Thus, the first steps were the preparation of both the protected aldehyde and the Wittig reagent.

Step1: Preparation of hydroxy protected benzaldehyde **80**

The commercially available *p*-hydroxy benzaldehyde (**78**) was employed as starting material and chlorotrimethylsilane (CTMS, **79**) as protecting agent (Scheme14). The reaction mixture was refluxed in pyridine for 10 hours under argon. After removal of the solvent under reduced pressure, the protected benzaldehyde **80** was obtained. ^{1}H NMR spectrum is reported in Figure 9 and data are reported in experimental part.

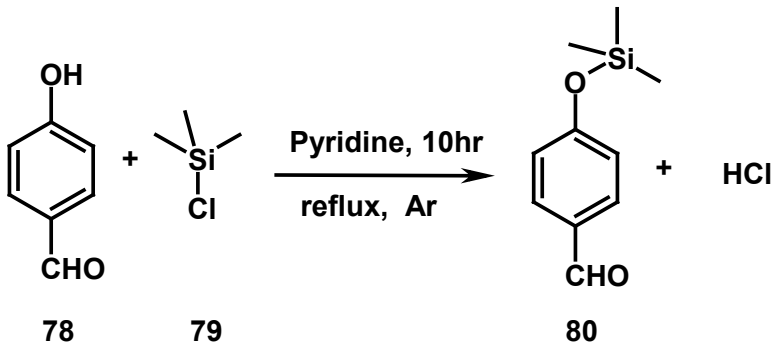

Scheme 14

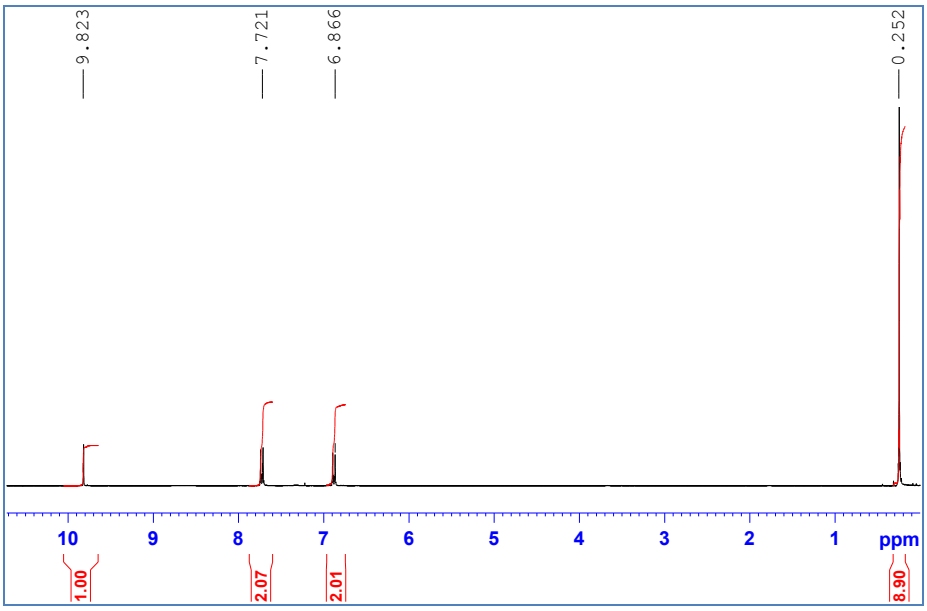

Figure 9: ^{1}H NMR spectrum of **80**

Step2: Preparation of triphenyl phosphonium salt **82**

1-Iodomethyl-4-vinylbenzene (**81**) and triphenylphosphine were refluxed in dry toluene solvent for 4 hours (Scheme 15). After observing the formation of the insoluble triphenylphosphonium ylide **82**, the product was filtered off from the reaction mixture and dried under reduced pressure. ^{1}H and ^{31}P NMR spectra are reported in Figure 10 and 11 respectively and data are reported in experimental part.

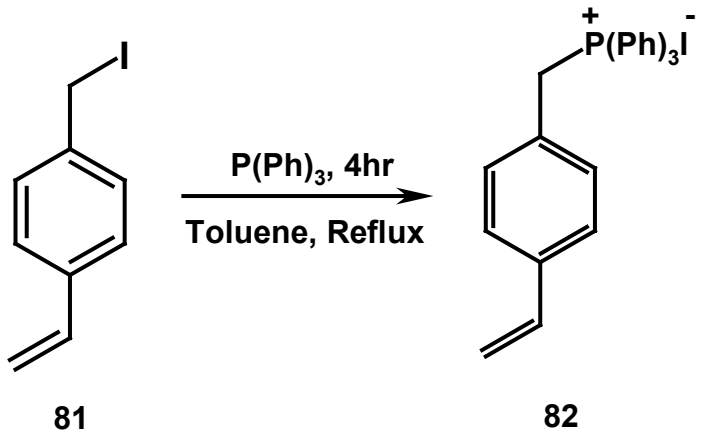

Scheme 15

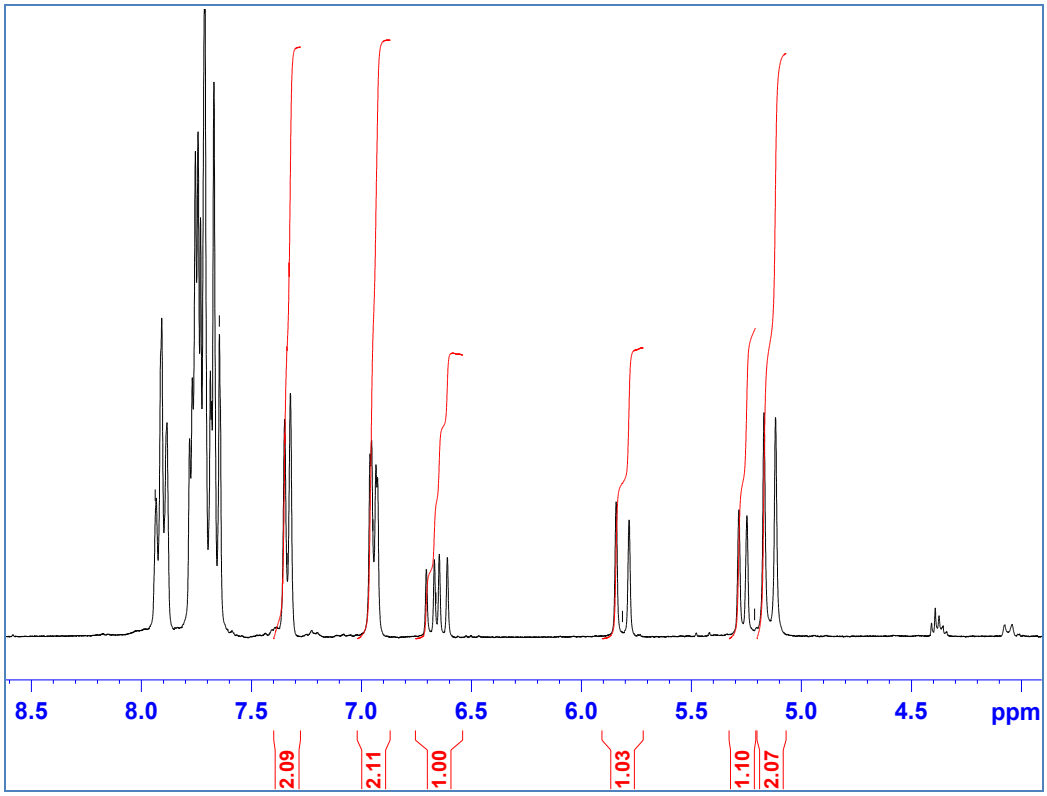

Figure 10: ^{1}H NMR spectrum of **82**

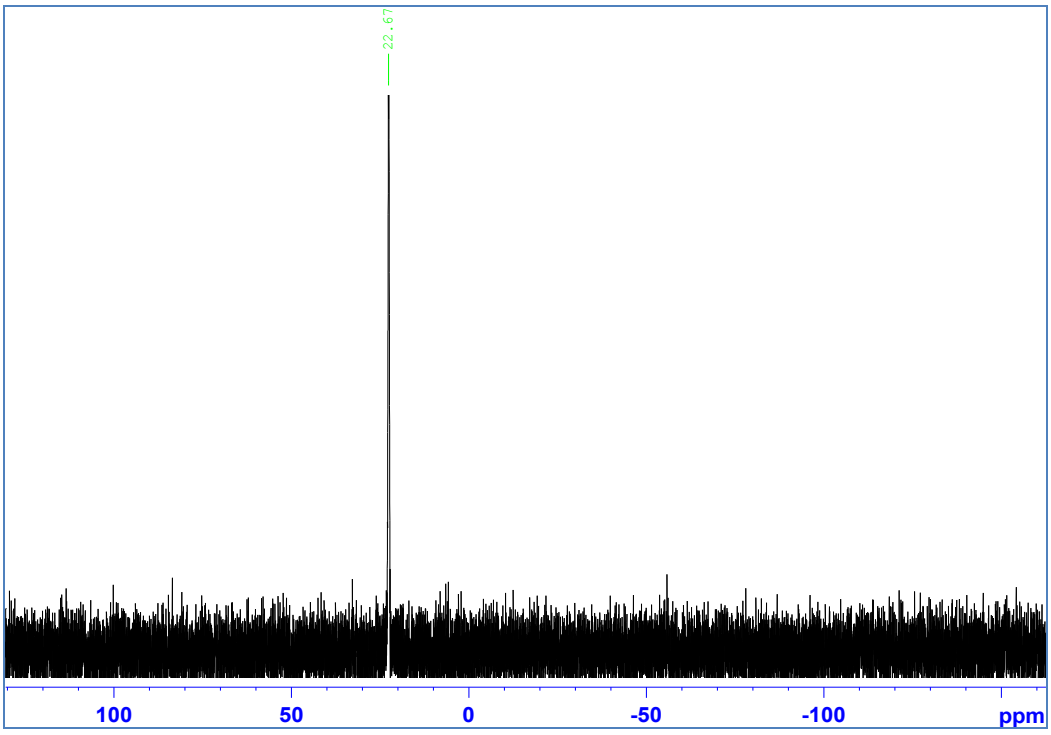

Figure 11: ^{31}P NMR spectrum of **82**

Step3: Preparation of compound **83**

The reaction between **80** and **82** was carried out in dry THF at – 80 ^{o}C by adding the butyl lithium basic reagent in ether solution (Scheme 16). The

reaction is sensitive to atmospheric oxygen, thus it was carried out under argon atmosphere. It furnished a mixture of the *E* and *Z*-isomers of the compound **83** (4-hydroxy-4'-ethenylstilbene). The *trans*-isomer was separated from the *cis*-isomer through preparative silica-gel column chromatography. ^{1}H NMR spectrum is reported in Figure 12 and data are reported in experimental part.

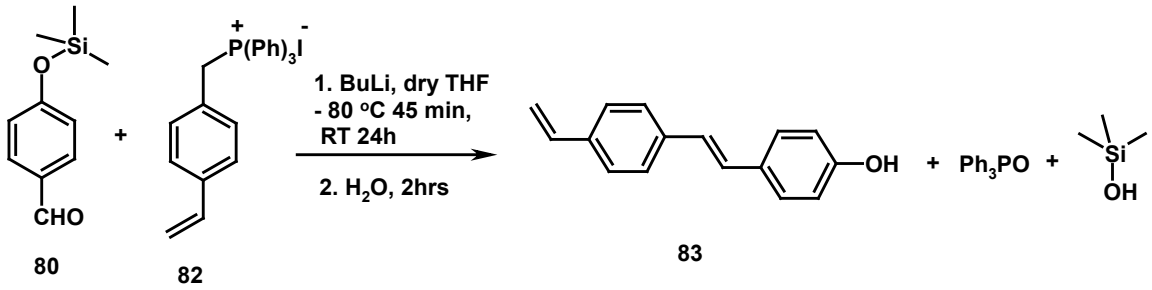

Scheme 16

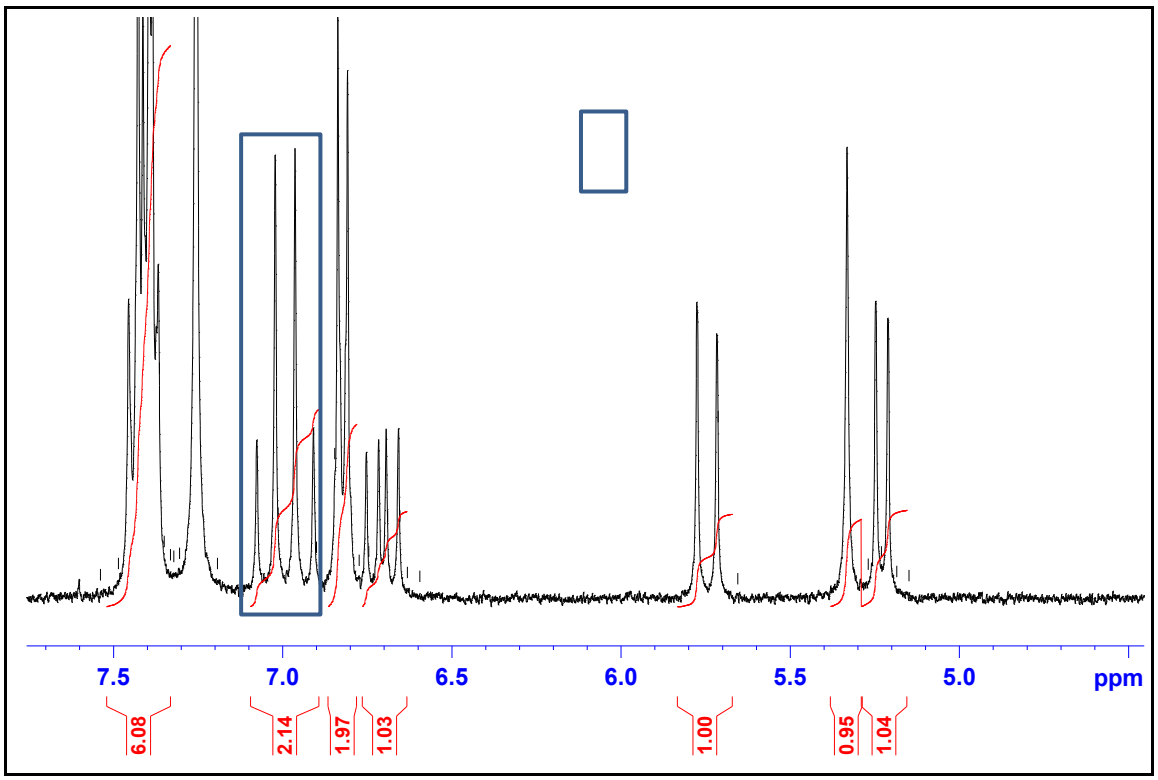

Figure 12: ^{1}H NMR spectrum of **83**

*2.1.1.2 Synthesis of monomer **86***

During my stay in France, I have synthesized the stilbenoid monomer **86** (4-hydroxy-4'-bromostilbene) through Wittig reaction; in this reaction the protected aldehyde **80** reacts with a triphenylphosphonium ylide **85** to give the alkene **86**

and triphenylphosphine oxide. Thus, the first steps were the preparation of both the protected aldehyde and the Wittig reagent.

Step1: Preparation of compound **85**

1-bromo-4-(bromomethyl)benzene (**84**) and triphenylphosphine were refluxed in dry toluene solvent for 4 hours (Scheme 17). After observing the formation of the insoluble triphenylphosphonium ylide **85**, the product was filtered off from the reaction mixture and dried under reduced pressure. ^{1}H and ^{31}P NMR spectra are reported in Figure 13 and 14 respectively and data are reported in experimental part.

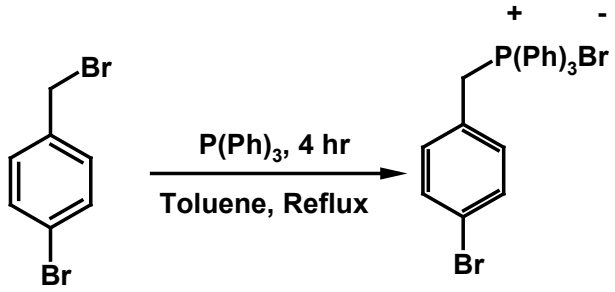

84 **85**

Scheme 17

Step2: Preparation of compound **86**

The reaction between **80** and **85** was carried out in dry THF at – 80 ^{o}C by adding the butyl lithium basic reagent in ether solution (Scheme 18). The reaction is sensitive to atmospheric oxygen, thus it was carried out under argon atmosphere. It furnished a mixture of the *E* and *Z*-isomers of the compound **86** (4-[2-(4-bromophenyl)ethenyl]phenol). The *trans*-isomer was separated from the *cis*-isomer through preparative silica-gel column chromatography. The characterization of the stilbene **86** was made by ^{1}H and ^{13}C NMR spectra (Figure 15 and 16) and data are reported in experimental part.

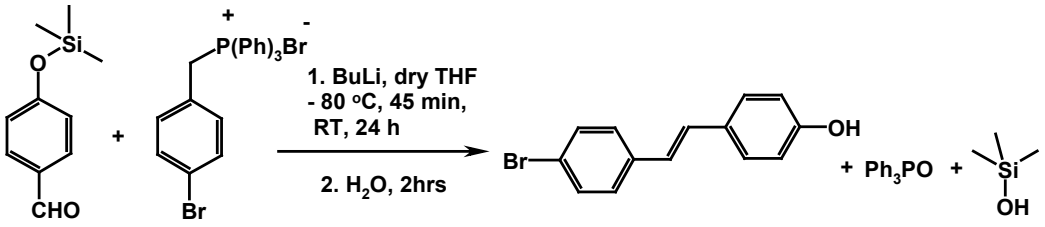

80 85 86

Scheme 18

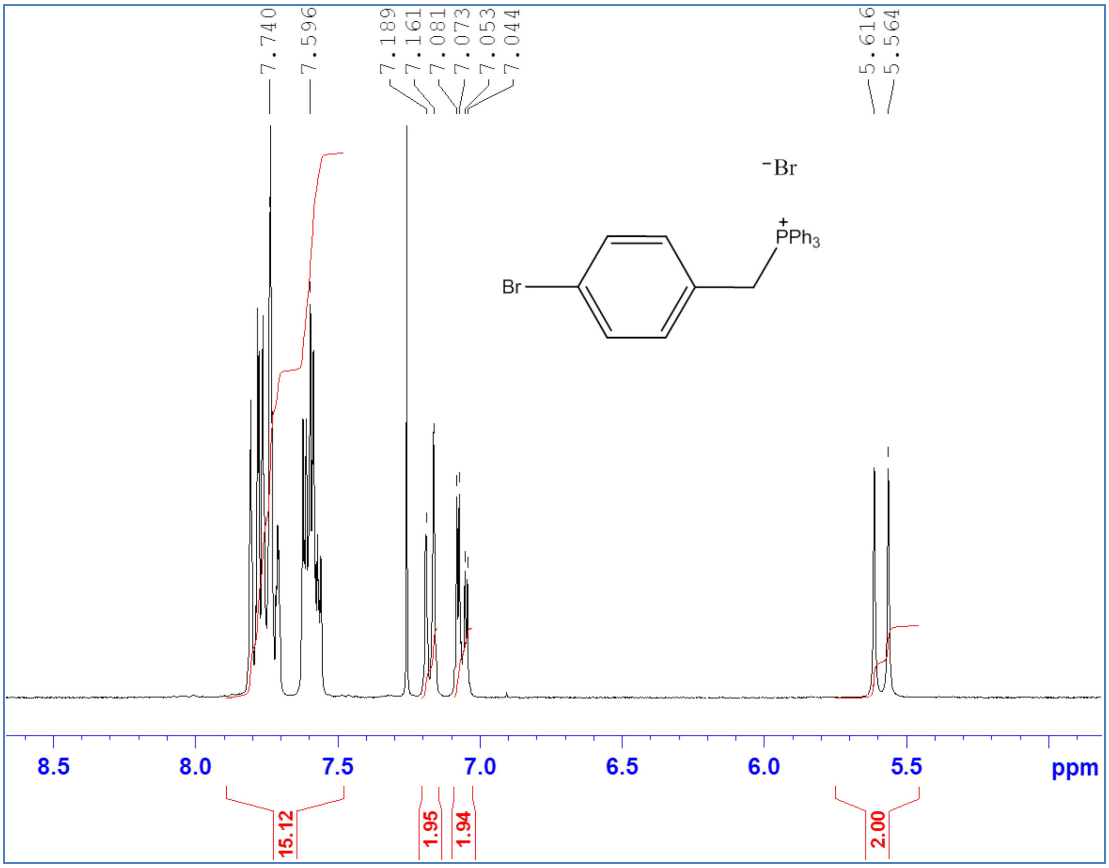

Figure 13: ^{1}H NMR spectrum of **85**

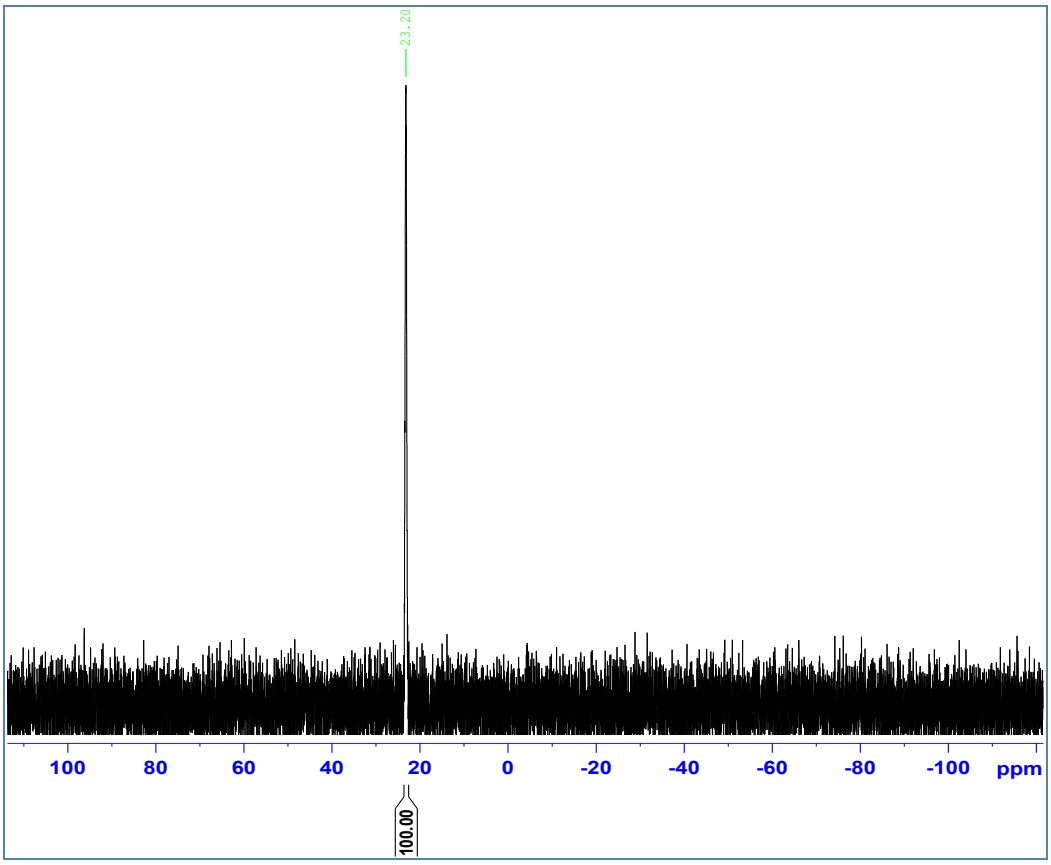

Figure 14: ^{31}P NMR spectrum of **85**

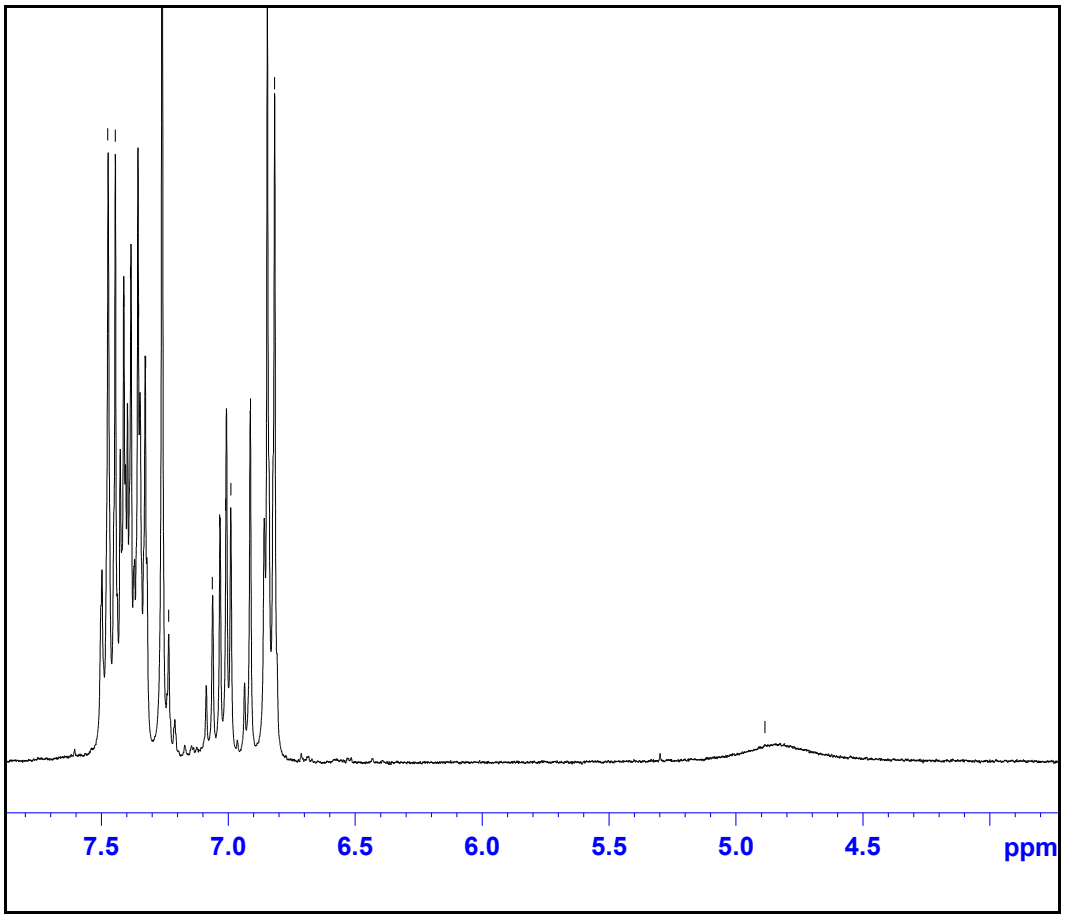

Figure 15: ^{1}H NMR spectrum of compound **86**

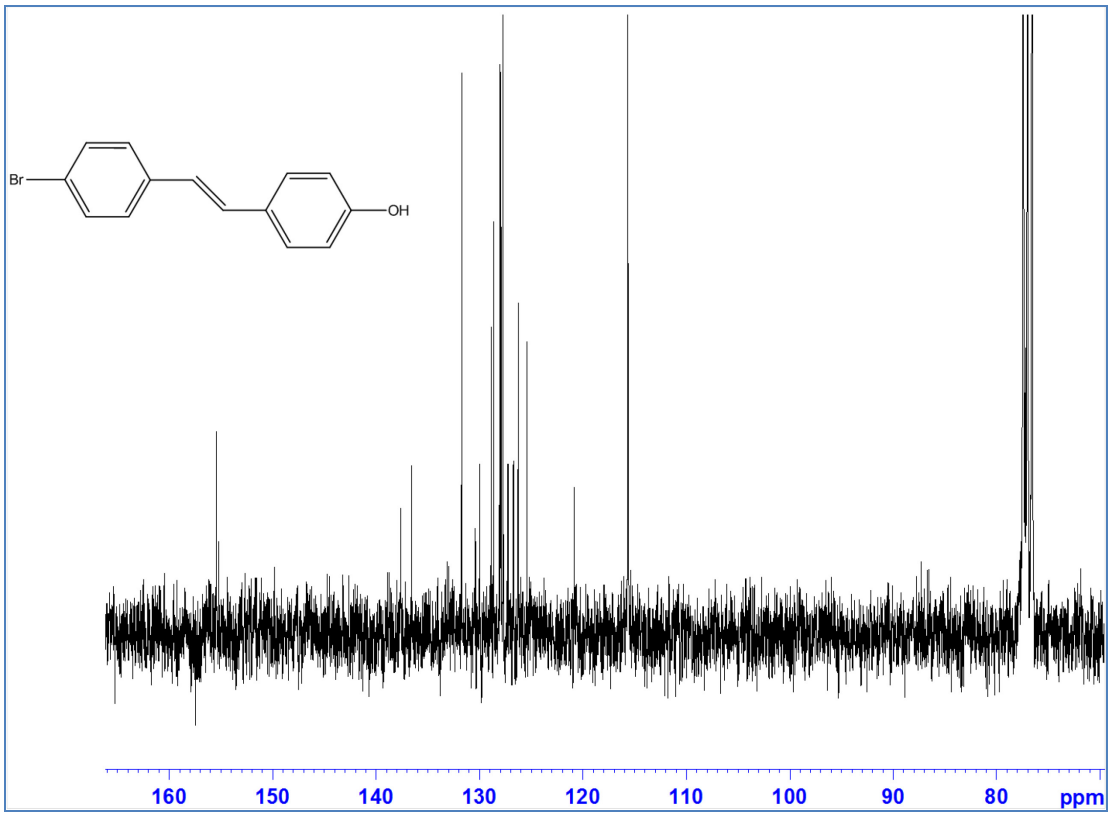

Figure 16: ^{13}CNMR spectrum of compound **86**

*2.1.1.3 Synthesis of monomers **90-92***

These monomers were gained from French laboratory by collaboration with Prof. Dominique Fasseur-Vervandier, at the Institut de Chimie Moléculaire de l'Université de Bourgogne, Dijon (France)

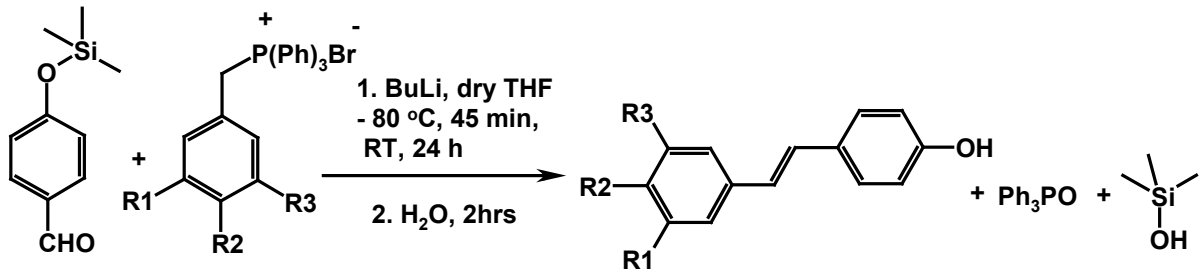

80 **87 - 89** **90 - 92**

87. $R_1 = R_2 = R_3 = H$
88. $R_1 = R_3 = H, R_2 = OMe$
89. $R_1 = R_3 = OMe, R_2 = H$

90. $R_1 = R_2 = R_3 = H$
91. $R_1 = R_3 = H, R_2 = OMe$
92. $R_1 = R_3 = OMe, R_2 = H$

Scheme 19

*2.1.1.4 Synthesis of monomers **95-96***

These monomers were gained from French laboratory by collaboration with Prof. Dominique Fasseur-Vervandier, at the Institut de Chimie Moléculaire de l'Université de Bourgogne, Dijon (France). The synthesis of these monomers is reported in the Scheme 20

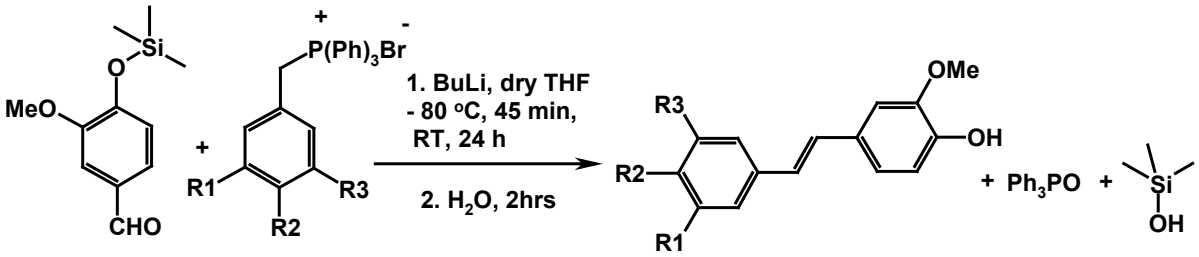

93 **88, 94** **95-96**

88. $R_1 = R_3 = H$, $R_2 = OMe$
94. $R_1 = R_2 = R_3 = OMe$

95. $R_1 = R_3 = H$, $R_2 = OMe$
96. $R_1 = R_2 = R_3 = OMe$

Scheme 20

*2.1.1.5 Synthesis of monomer **98***

This monomer was gained from French laboratory by collaboration with Prof. Dominique Fasseur-Vervandier, at the Institut de Chimie Moléculaire de l'Université de Bourgogne, Dijon (France). The synthesis of this monomers is reported in the Scheme 21

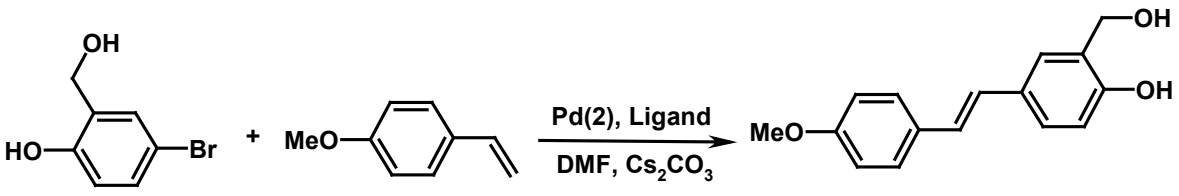

97a **97b** **98**

Scheme 21

2.1.2 Synthesis of Dimers

2.1.2.1 *Biomimetic synthesis of stilbenolignan (±)-**99***

In order to obtain previously unreported stilbenolignans, new stilbenoid monomers were synthesized in cooperation with the laboratory of Prof. Dominique Vervandier-Fasseur. One of these substrates is compound **83** (*E*)-4-(4-vinylstyryl)phenol which was used as substrate, in the presence of Laccase from *Trametes versicolor* (LTV), acetate buffer (pH = 4.7) and EtOAc as co-solvent (Scheme 22).

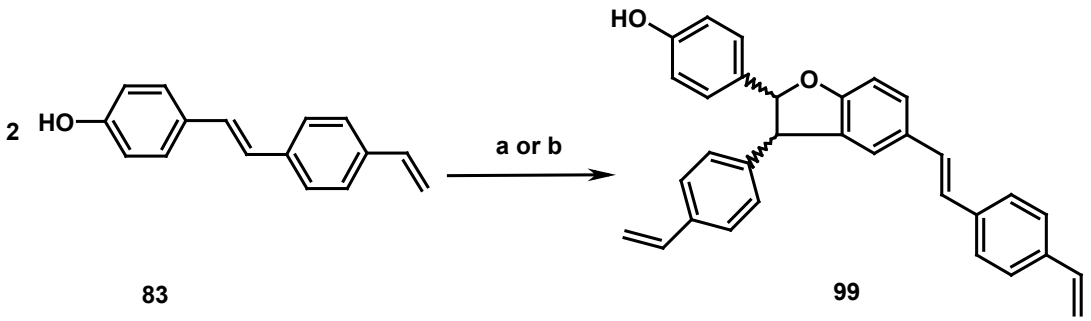

83 **99**

a) LTV, acetate buffer pH 4.7, EtOAc, 24hr.
b) Mn(III)Ac, CH_2Cl_2, 24 hrs.

Sc

Scheme 22

The dimerization afforded the product (±)-**99** as racemic mixture in 24% yield. This reaction was carried out also with $Mn(OAc)_3$ in dichloromethane but this method gives very poor yield (ca 10%). After purification on DIOL silica gel column with petroleum ether: ethyl acetate 9.5:0.5 as the eluent. A spectroscopic characterization of the product was carried out. The structure of this product has not been previously reported, so we employed both mono and two-dimensional NMR methods (COSY and HSQC) to assign all the signals and to establish the structure apart from previously reported data. The ^{1}H and ^{13}C NMR spectra are reported in Figure 17 and 18, respectively, and Table 1; assignments were aided by the careful analysis of COSY, HSQC, and HMBC spectra, reported in Figure 19 ,20 and 21, respectively. The mass spectrum

shows ESI-MS peak at *m*/*z* 465.1 $[M + Na]^+$ confirming the formation of a dimer with molecular formula $C_{32}H_{26}O_2$ and spectrum is reported in Figure 22.

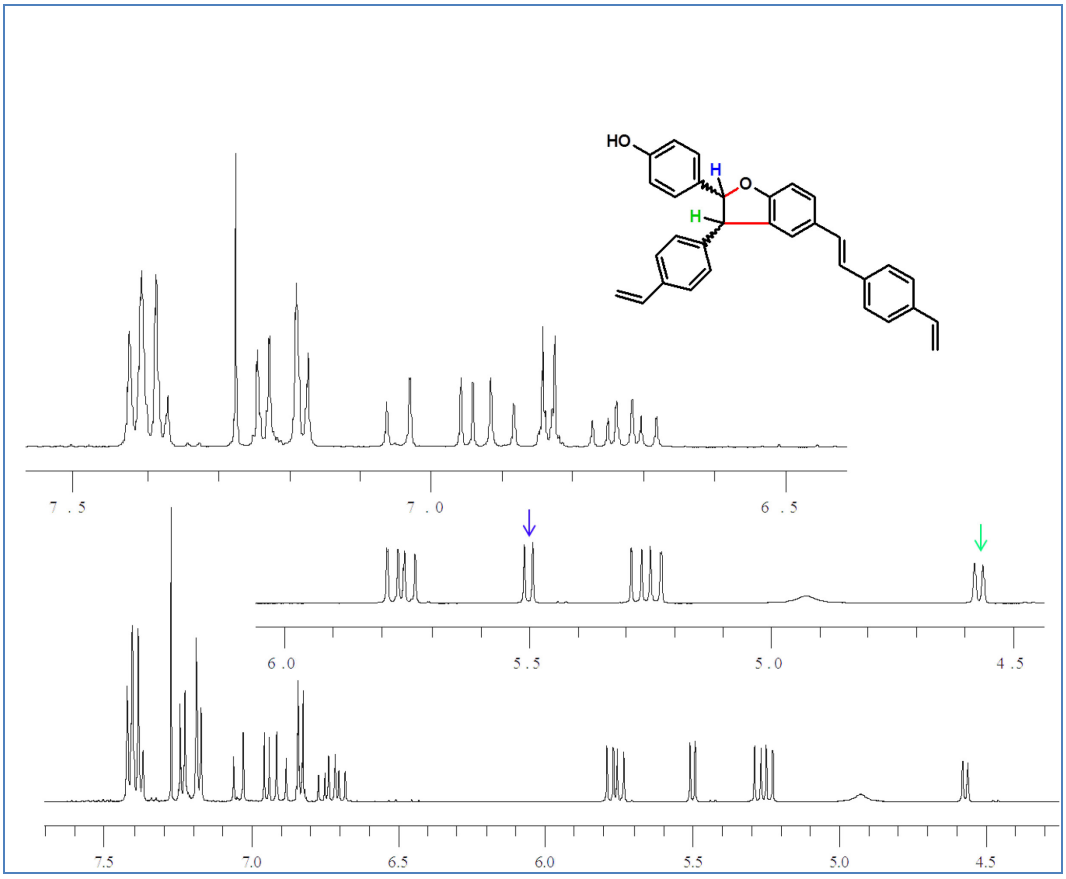

Figure 17: ^{1}H NMR spectrum of (±)-**99**

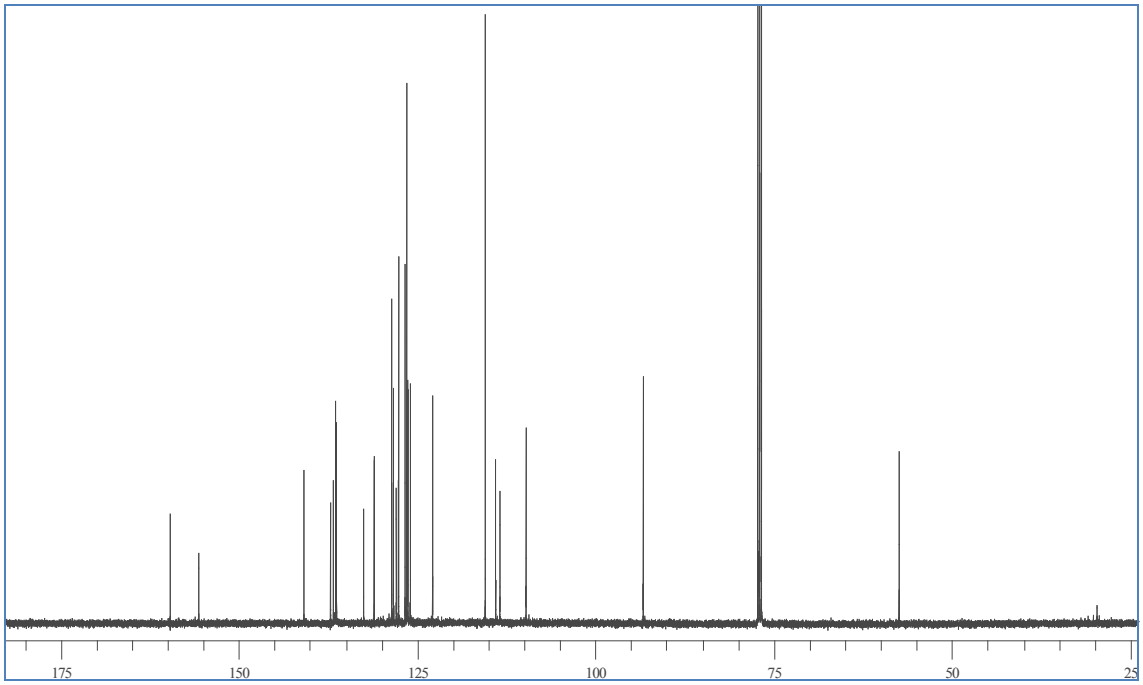

Figure 18:.^{13}C NMR spectrum of (±)-**99**

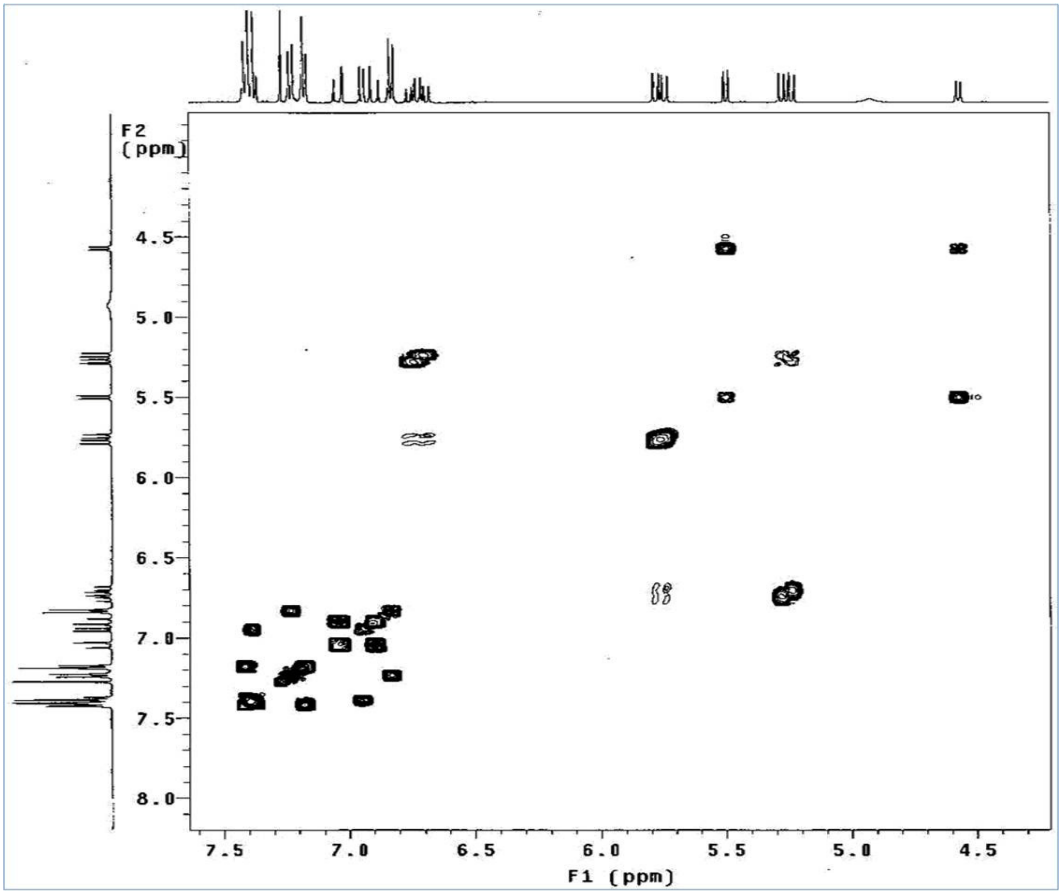

Figure 19: COSY spectrum of (±)-**99**

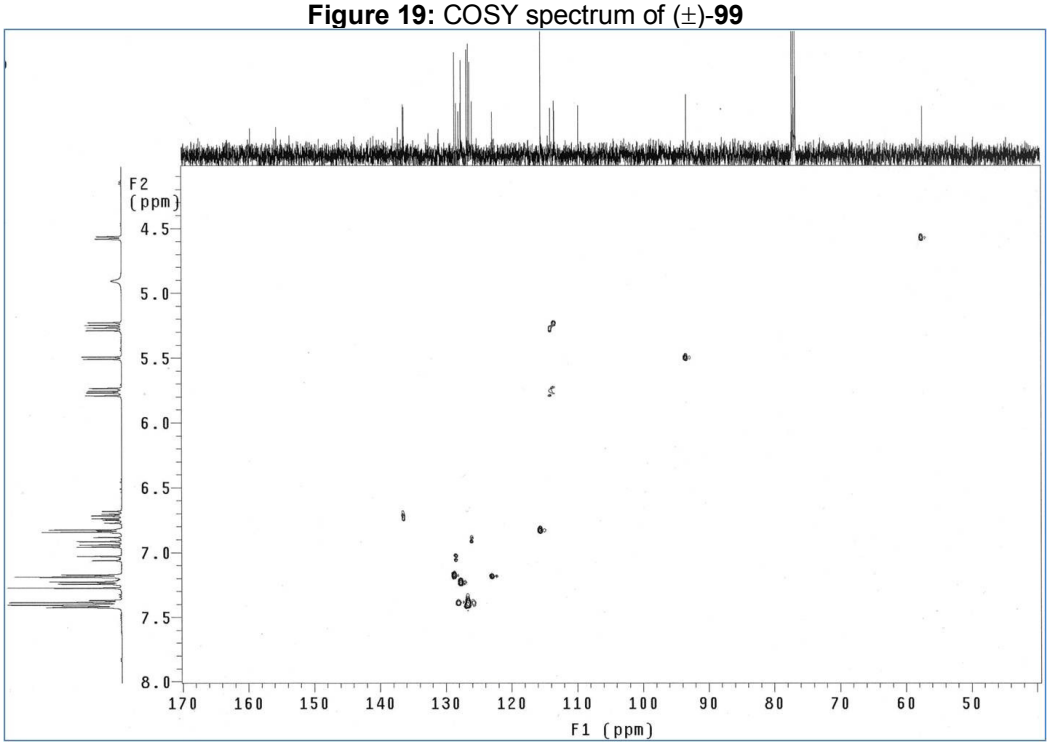

Figure 20: HSQC spectrum of (±)-**99**

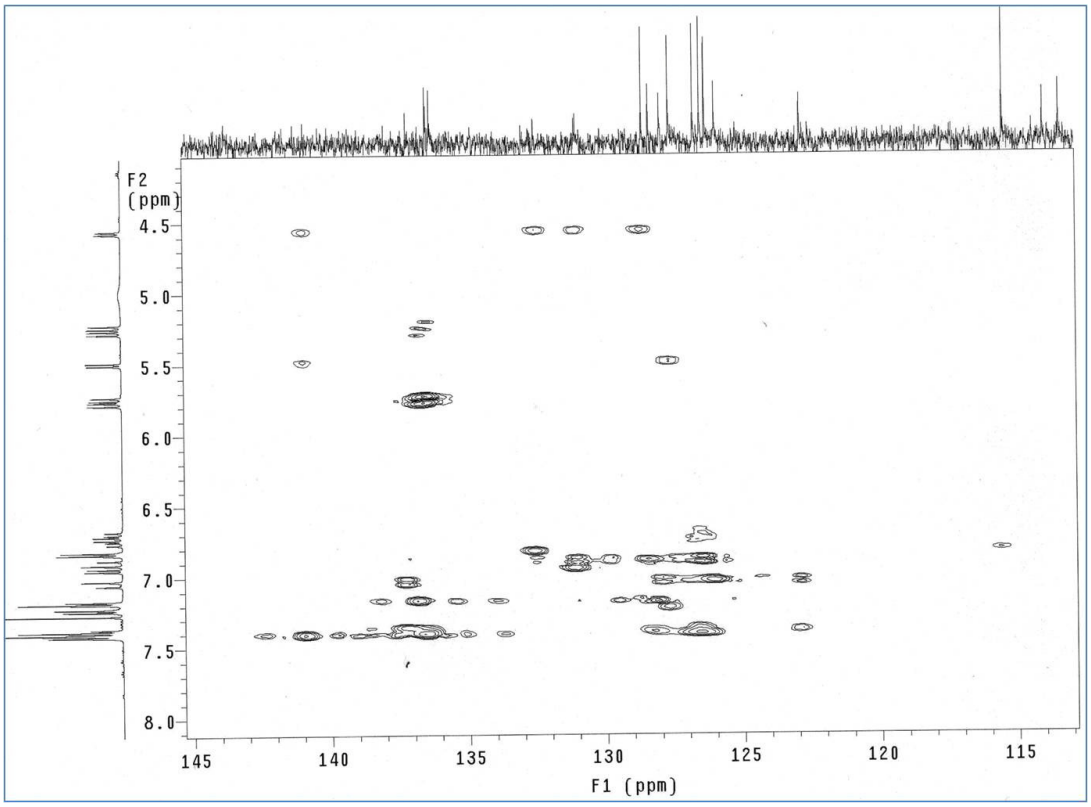

Figure 21: HMBC spectrum of (±)-**99**

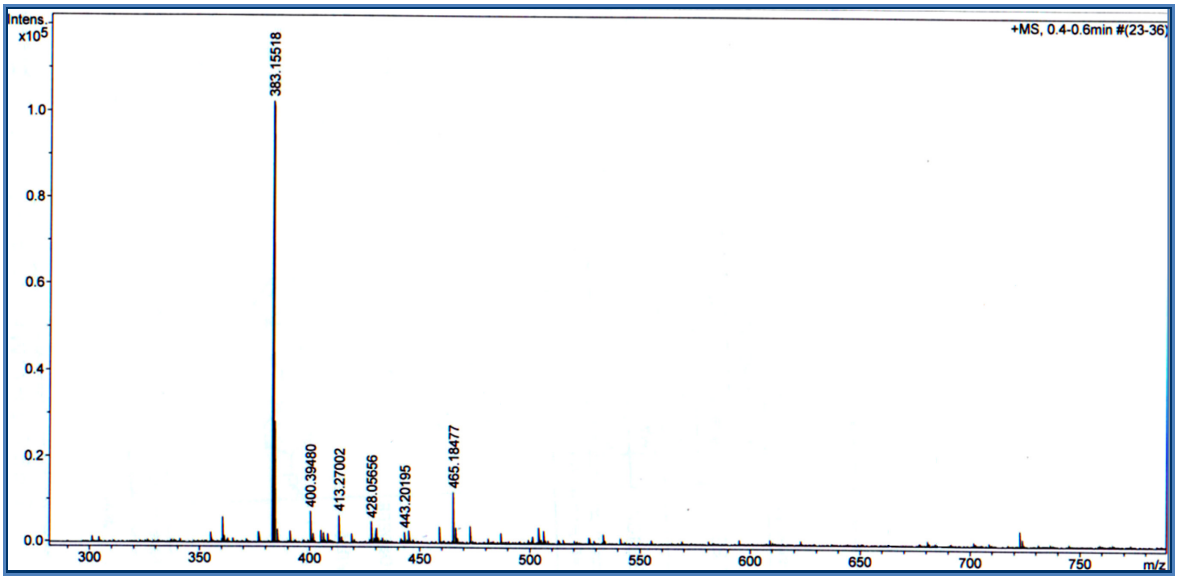

Figure 22: Mass spectrum of (±)-**99**

Table1: ^{1}H and ^{13}C NMR data of (±)-**99**

H	δ_H (mult, J Hz) in $CDCl_3$	C	δ_C in $CDCl_3$
		C-1	132.5
H-2,6	7.22 (d,8.5, 2H)	C-2,6	127.9
H-3,5	6.82 (d,8.5, 2H)	C-3,5	115.5
		C-4	155.6
H-7	5.49 (d,8.75, 1H)	C-7	93.2
H-8	4.56 (d,8.75, 1H)	C-8	57.4
		C-9	140.9
H-10,14	7.17 (d,8.5, 2H)	C-10,14	128.6
H-11,13	7.26 (m,2H)	C-11,13	126.3
		C-12	137.0
H-15a	6.74 (dd,17.5, 10.5, 1H.)	C-15	136.5
H-16b	5.24 (d,10.5, 1H)	C-16	113.9
H-16c	5.75 (d, 17.5, 1H)		
		C-1'	128.4
H-2'	7.35 (bs,1H)	C-2'	125.9
H-3’	6.94 (d,8.5, 1H)	C-3'	109.7
		C-4'	159.6
		C-5'	128.6
H-6'	7.19 (bs,1H)	C-6'	122.8
H-7'	7.02 (d,16.25, 1H)	C-7'	131.0
H-8'	6.88 (d,16.25, 1H)	C-8'	126.7
		C-9'	136.0
H-10',14'	7.36 (d,7.5, 2H)	C-10',14'	127.6
H-11',13'	7.41 (d, 8.5, 2H)	C-11',13'	126.4
		C-12'	137.2
H-15’a	6.70 (dd,17.5, 10.5, 1H)	C-15’	136.4
H-16’b	5.28 (d,10.5, 1H)	C-16’	113.4
H-16’c	5.78 (d, 17.5, 1H)		
OH	4.9 (bs, 1H)		

The ^{13}C NMR spectrum showed 25 signals: the majority of the signals were in the sp^2 region (from 159.6 to 109.7 ppm), but two methine signals in the sp^3 region (57.4 and 93.2 ppm) were also observed, suggesting the formation of a dihydrobenzofuran ring. In the sp^2 region there are 9 quaternary carbon

signals, 12 CH signals, and 2 CH_2 signals. The ^{1}H NMR spectrum of (±)-**99** in the region from 7.42 and 6.82 ppm shows clear similarities with the spectra of the above discussed dihydrobenzofuran neolignans. In particular, a COSY correlation was observed between the two doublet signals at δ = 7.37 and 6.94 ppm assigned to a four-proton AA'BB' system, and between the two doublets at δ = 7.41 and 7.18 ppm, integrating for eight protons (two AA'BB' systems).

These signals indicates that there are three *para* substituted aromatic rings (see below); the ^{13}C chemical shift analysis and HSQC spectrum indicated that one of these rings bear a phenol group whereas the other two, bearing an ethenyl group, give isochronous signals (Figure 23).

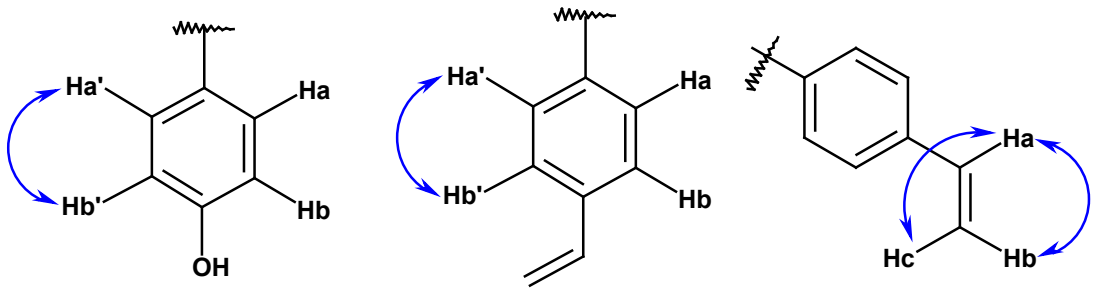

Figure 23

The signals of the two ethenyl groups are partly overlapped and also in this case the COSY/HSQC analysis proved useful, showing the spin-spin couplings in these two ABC systems, as reported below: both '**a**' signals, closer to the aromatic ring, resonate at lower fields (6.74 and 6.70 ppm), whereas the other proton signals (**b** and **c**) are appear at higher fields (5.24, 5.28, 5.76 and 5.78 ppm).

Two further doublets at δ = 7.04 and 6.90 ppm (1H each) show a cross-peaks correlation in the COSY spectrum, and may be assigned to AB system with a large coupling constant (16.3 Hz), clearly due to two *trans* olefinic protons (Figure 24)

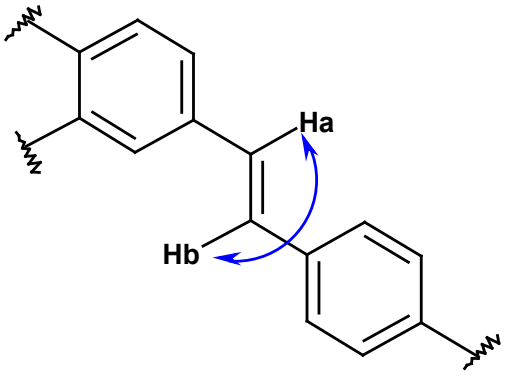

Figure 24

An aromatic ABC spin system (δ = 7.23, 6.82 and 7.37 ppm) was also evidenced by the COSY experiment; in fact, the signal at 7.37 ppm is partially overlapped with a signal of one AA'BB' system but clear COSY correlations were observed for the three protons. The chemical shift analysis and HSQC data, of course aided by the basic knowledge of the oxidative coupling mechanism, strongly indicated that this further trisubstituted aromatic ring was joined to the dihydrobenzofuran ring, whose signals, as cited above, appear as two coupled doublets at (4.56 and 5.49 ppm), Figure 25

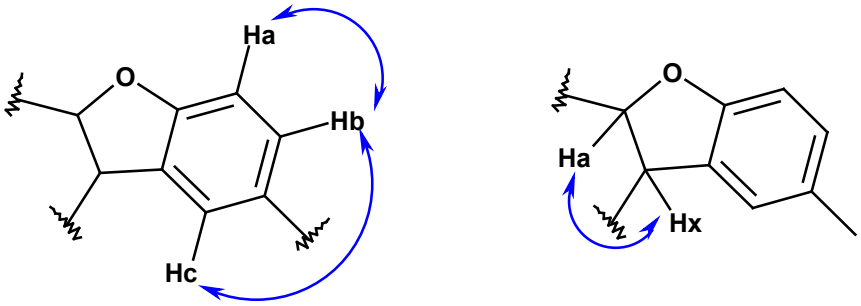

Figure 25

Finally, a broad singlet at δ = 4.86 ppm is present, obviously due to a phenolic OH, because no HSQC correlation is observed for this proton signal.

Although the above discussed partial structure may be reasonably assembled in structure (±)-**99** on the basis of the coupling mechanism, some COSY *long range* correlations, e.g. between the signals 6.82 and 7.04, 4.57 and 7.17,

allowed us to connect the sub-structures and establish the structure of the dimer Figure 26.

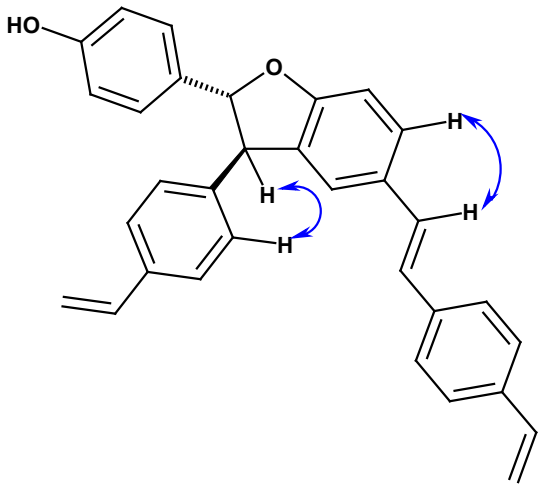

Figure 26

*2.1.2.2 Biomimetic synthesis of stilbenolignan (±)-**100***

4-[(*E*)-2-(4-bromophenyl)ethenyl]phenol (**86**) was used as substrate, in the presence of Laccase from *Trametes versicolor* (LTV), acetate buffer (pH = 4.7) and EtOAc as co-solvent and this reaction was taken 5 days (Scheme 22). The same reaction was carried out in metal-mediated method by using $Mn(OAc)_3$ and dichloromethane As solvent: this reaction was fast (1 day) compared to the enzyme reaction. This suggests that stilbenoids containing bromine gives poor results with LTV enzymes.

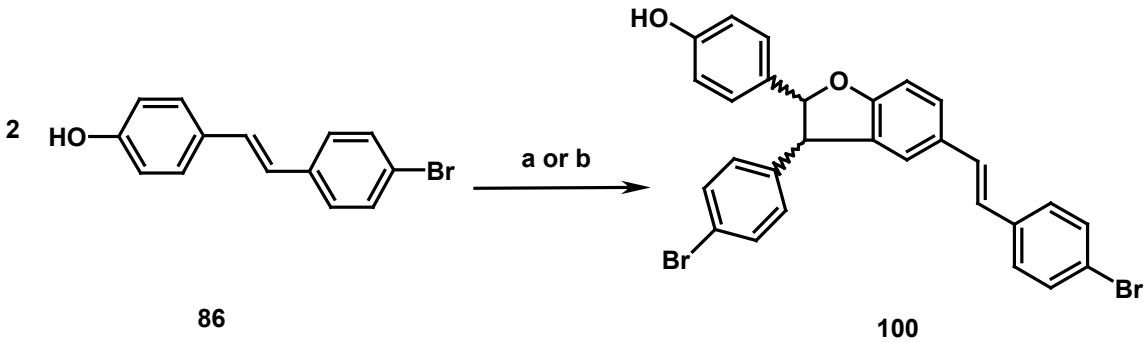

a) LTV, acetate buffer pH 4.7, EtOAc, 5 days.
b) Mn(III)Ac, CH_2Cl_2, 24 hrs.

Scheme 22

Purification of the crude mixture resulted very difficult because the substrate and the dimer have very similar chromatographic properties. Therefore first purification was carried out with silica gel column using petroleum ether: ethyl acetate 9:1 as the eluent. Subsequent purifications were carried out by using preparative thin layer chromatographic method by using 30% EtOAc, petroleum ether solvent mixture.

The complete spectroscopic characterization of the product (±)-**100** was carried out on the pure dimer. The structure of this product has not been previously reported, so we employed both mono and two-dimensional NMR methods (COSY, HSQC and HMBC) to assign all the signals and to establish the structure apart from previously reported data. Mass spectrum shows a ESI-MS peak at *m*/*z* 546.9 $[M-H]^-$ confirming the formation of a dimer with molecular formula $C_{28}H_{20}Br_2O_2$ and spectrum is reported in Figure 27; the ^1H and ^{13}C NMR, COSY, HSQC and HMBC spectra are reported in Figure 28, 29, 30, 31 and 32 respectively, and Table 2

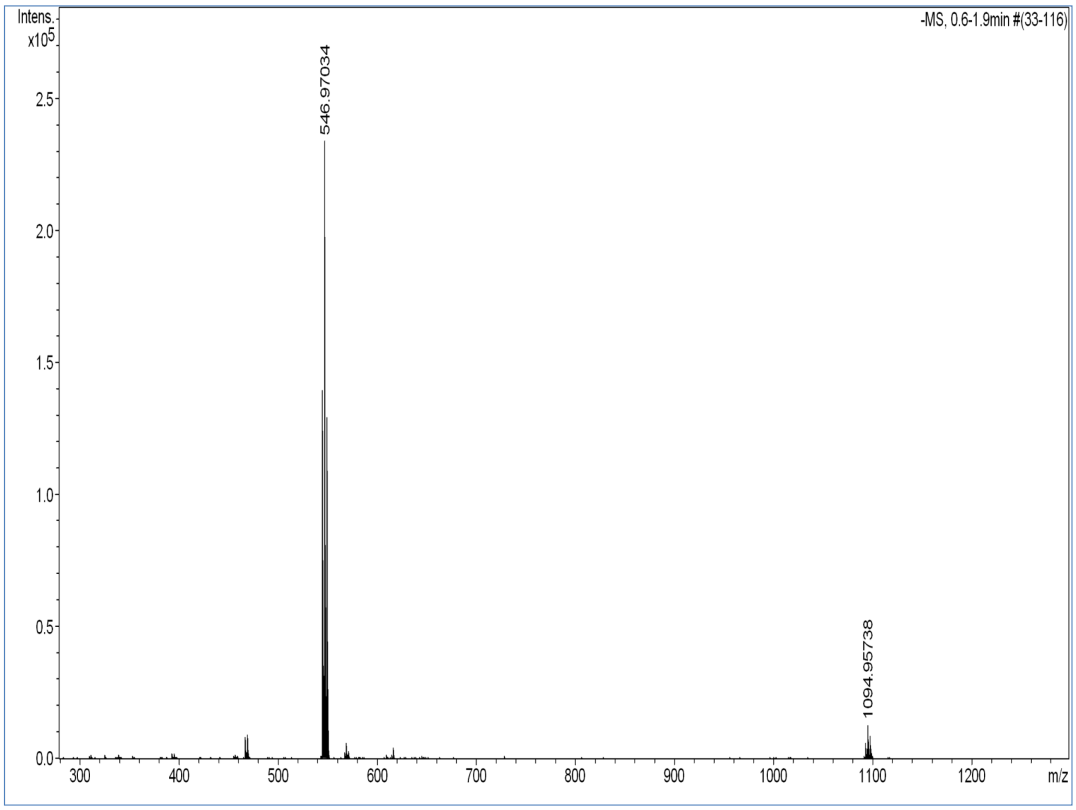

Figure 27: Mass spectrum of compound (±)-**100**

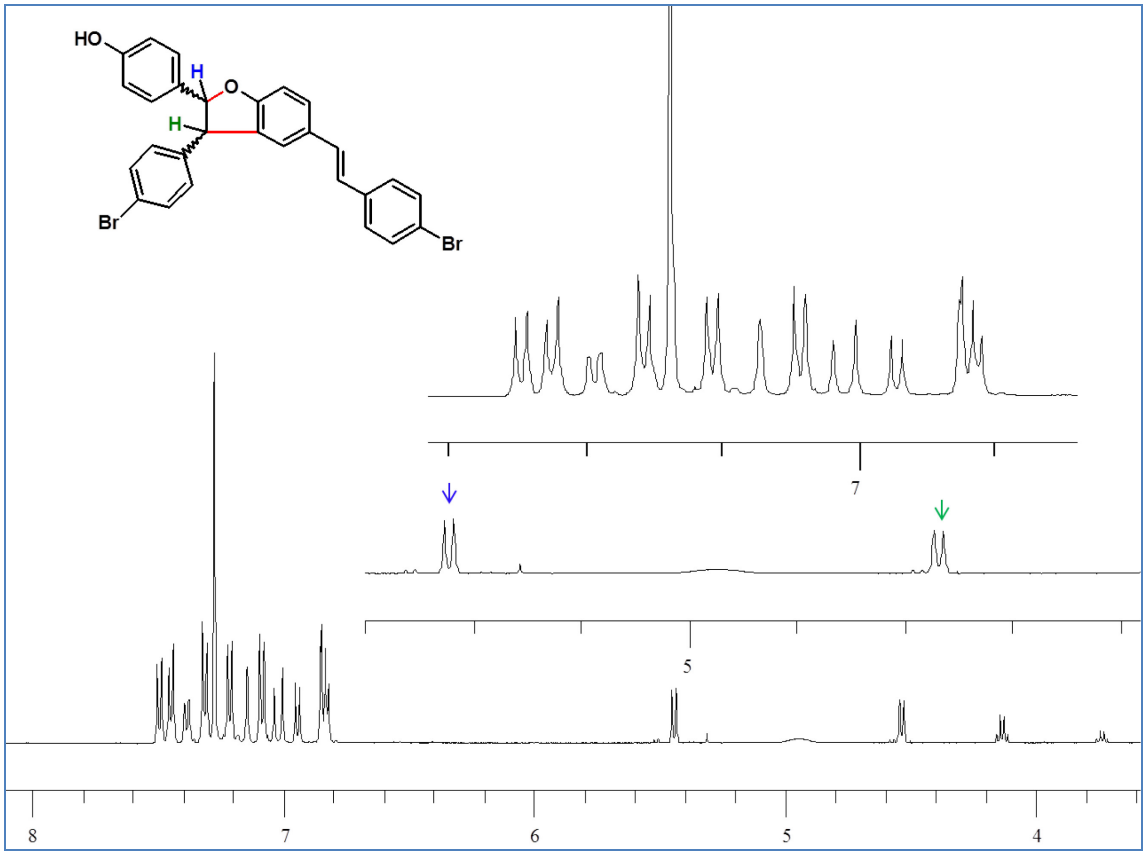

Figure 28: ^{1}H NMR spectrum of compound (±)-**100**

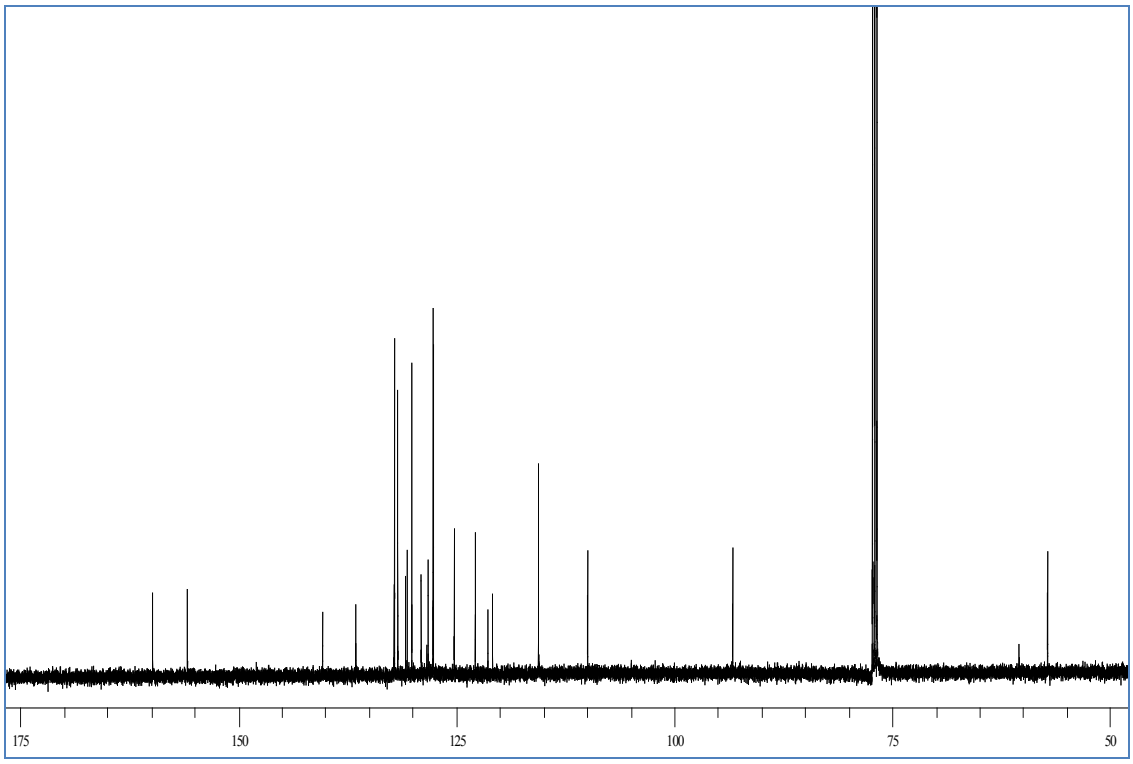

Figure 29: ^{13}C NMR spectrum of compound (±)-**100**

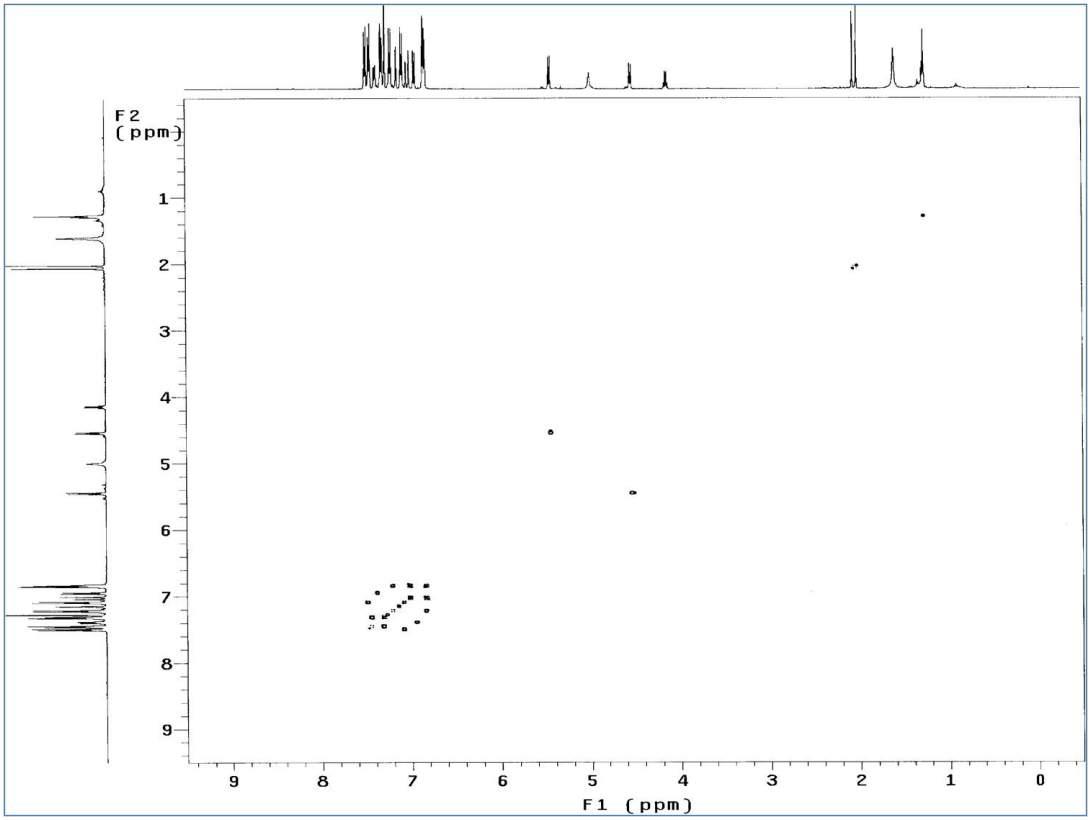

Figure 30: COSY spectrum of compound (±)-**100**

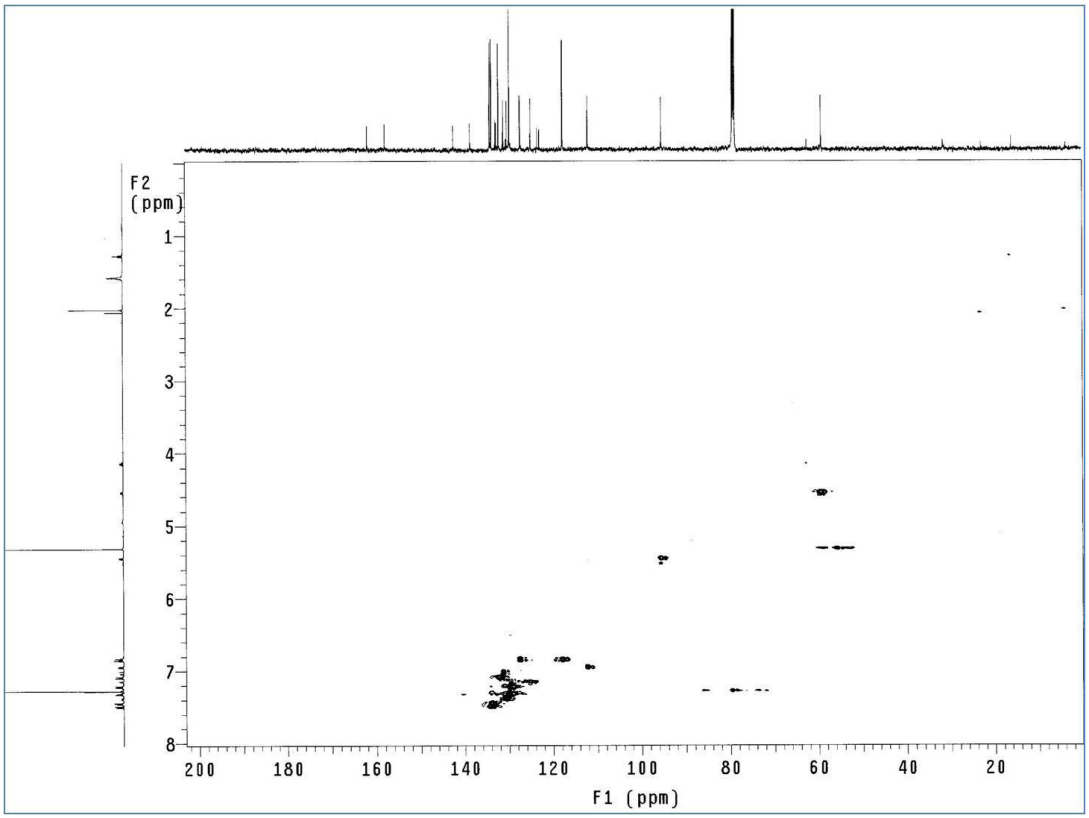

Figure 31: HSQC spectrum of compound (±)-**100**

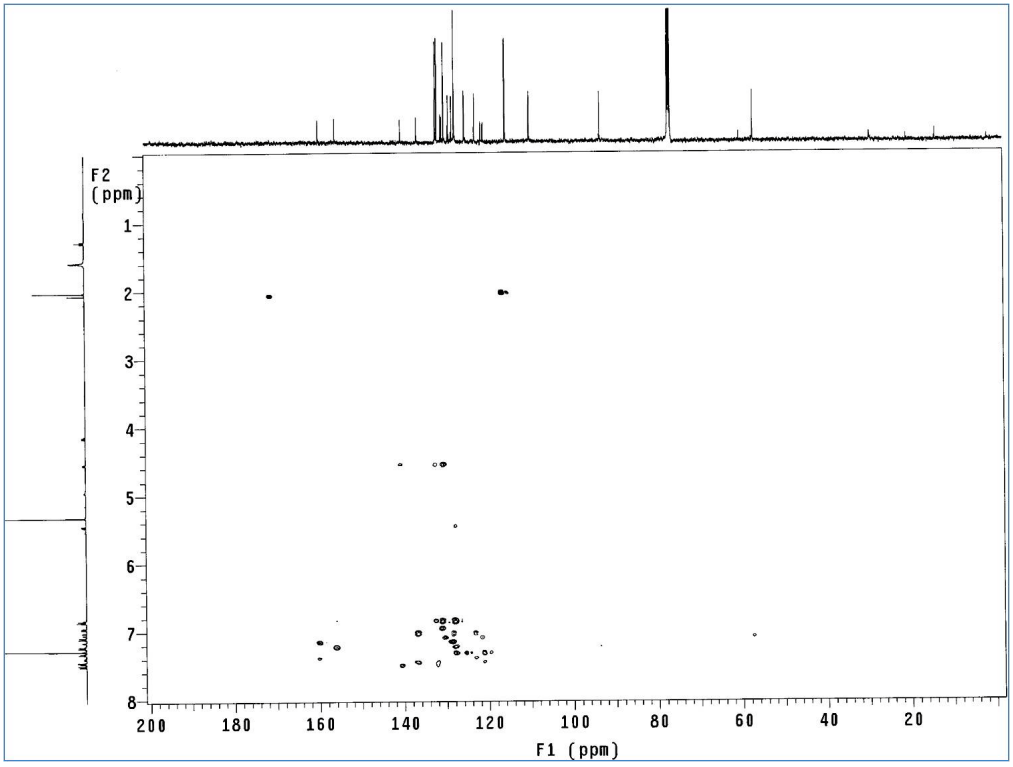

Figure 32: HMBC spectrum of compound (±)-**100**

Table 2: ^{1}H NMR and ^{13}C NMR data of compound (±)-**100**

H	δ_H (mult, J Hz) in $CDCl_3$	C	δ_C in $CDCl_3$
		C-1	130.8
H-2,6	7.21 (d,8.0)	C-2,6	127.6
H-3,5	6.83 (dd,2.5,8.5)	C-3,5	115.5
		C-4	155.8
H-7	5.4 (d,8.75)	C-7	93.3
H-8	4.5 (d,8.75)	C-8	57.1
		C-9	140.3
H-10,14	7.08 (d,8.5)	C-10,14	130.1
H-11,13	7.49 (d,8.5)	C-11,13	131.7
		C-12	121.3
		C-1'	128.24
H-2'	7.38 (d,8.5)	C-2'	128.23
H-3’	6.94 (d,8.0)	C-3'	109.9
		C-4'	159.8
		C-5'	130.6
H-6'	7.14 (s)	C-6'	122.8
H-7'	7.02 (d,16.25)	C-7'	129.0
H-8'	6.83 (d,16.25)	C-8'	125.2
		C-9'	136.5
H-10',14'	7.31 (d,8.0)	C-10',14'	127.6
H-11',13'	7.44 (d,8.5)	C-11',13'	132.0
		C-12'	120.8
4-OH	4.99 (s)		

The ^{13}C NMR spectrum showed 22 signals: the majority of the signals were in the sp^2 region (from δ 159.8 to 109.9 ppm), but two methine signals in the sp^3 region (δ 57.1 and 93.3 ppm) were observed, suggesting the formation of a dihydrobenzofuran ring. In the sp^2 region there are 8 quaternary carbon signals, 11 CH signals. The ^{1}H NMR spectrum of (±)-**100** in the region from δ 7.49 and 6.81 ppm shows almost similarities with the spectra of the previously discussed dihydrobenzofuran neolignan (±)-**99**.

In particular, a COSY (Figure 33) correlation was observed between the two doublet signals at δ 7.21 and 6.83 ppm assigned to a four-proton AA’BB’ system, and between the two doublets at δ 7.08 and 7.49 ppm, assigned to a

four-proton AA'BB' system, another two doublets at δ 7.31 and 7.44 ppm, assigned to a four-proton AA'BB'; these signals indicates that there are three *para* substituted aromatic rings; the ^{13}C chemical shift analysis and HSQC spectrum indicated that one of these rings bear a phenol group, whereas the other two bearing bromo group.

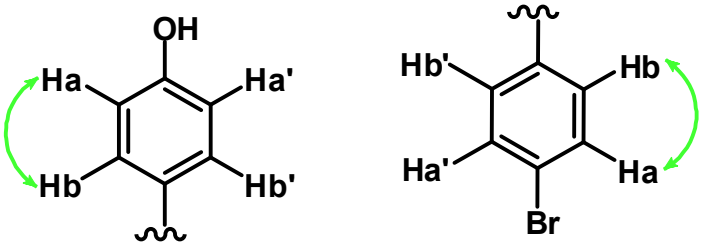

Figure 33

Two doublets at δ = 7.02 and 6.83 ppm (1H each) show a cross-peaks correlation in the COSY spectrum, and may be assigned to a AB system with a large coupling constant (16.25 Hz), clearly due to two *trans* olefinic protons (Figure 34)

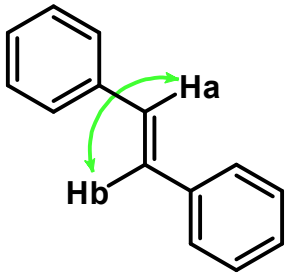

Figure 34

An aromatic AB system δ 7.38 and 6.94 was also evidenced by the COSY experiment; and also a singlet (Hc) was observed at δ 7.14 in proton NMR spectrum. The chemical shift analysis and HSQC and HMBC data, of course aided by the knowledge of the oxidative coupling mechanism (Scheme 28), strongly indicated that this further trisubstituted aromatic ring was joined to the

dihydrobenzofuran ring, whose signals, as cited above, appear as two coupled doublets at δ 4.53 and 5.44

ppm, Figure 35. Finally, a broad singlet at δ 4.98 ppm is present, obviously due to a phenolic OH, because no HSQC correlation is observed for this signal.

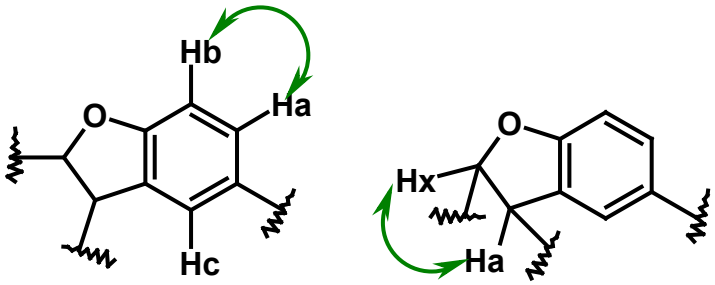

Figure 35

The long-range correlation between H-2,6 at δ 7.21 ppm and C-7 at δ 93.3 ppm, and between H-10,14 at δ 7.08 ppm and C-8 at δ 57.1 ppm allows to establish that the A ring is bonded to C-7 whereas the B ring is bonded to C-8. It is clearly observed the correlation between H-8 at δ 4.53 ppm and C-5' at δ 130.6 ppm confirms the presence of the fused oxygenated five-member ring (Figure 36).

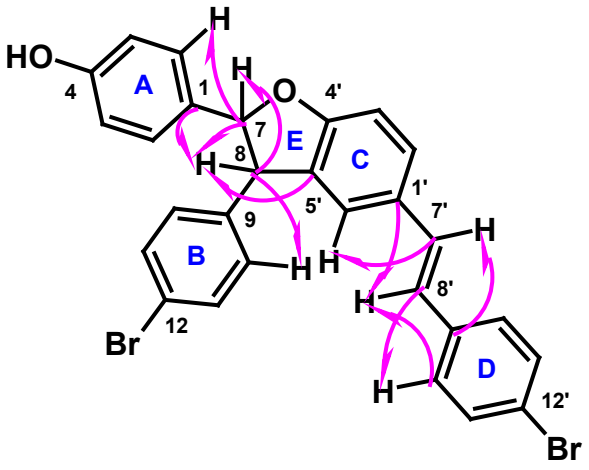

Figure 36: Selected HMBC correlation of compound (±)-**100**

The value of ^{3}J (H-7,H-8) measured from ^{1}H NMR spectrum (8.75 Hz) suggests a predominant conformation with the two H-7 and H-8 protons in a pseudo *trans*-axial arrangement, whereas the ^{3}J (H-7',H-8') is 16.25 Hz, as expected for a double bond with a *trans* configuration. The distinction between the ethylenic protons has been made through the analysis of the C,H long-range correlation found in the HMBC spectrum: the signal of C-7' at δ 129.0 ppm shows a correlation with the proton signal at δ 7.14 ppm, directly bonded to H-6' (i.e.,C-6') whereas the signal due to C-8' at 125.2 ppm is correlated to the proton signal at δ 7.31 ppm, directly bonded to H-10', 14' (i.e., C-10',14'). Figure 36 shows the main selected C, H correlation between the all five rings.

*2.1.2.3 Biomimetic synthesis of stilbenolignan (±)-**101***

Substrate **90** was subjected to oxidation in the presence of LTV or $Mn(OAc)_3$ as mentioned in the below Scheme 23; after the column chromatographic purification racemic mixture **(±)-101** was obtained. The product has been characterized unambiguously by using, mass spectroscopy, 1D and 2D NMR spectroscopy; all spectroscopic data are in agreement with literature data.[28]

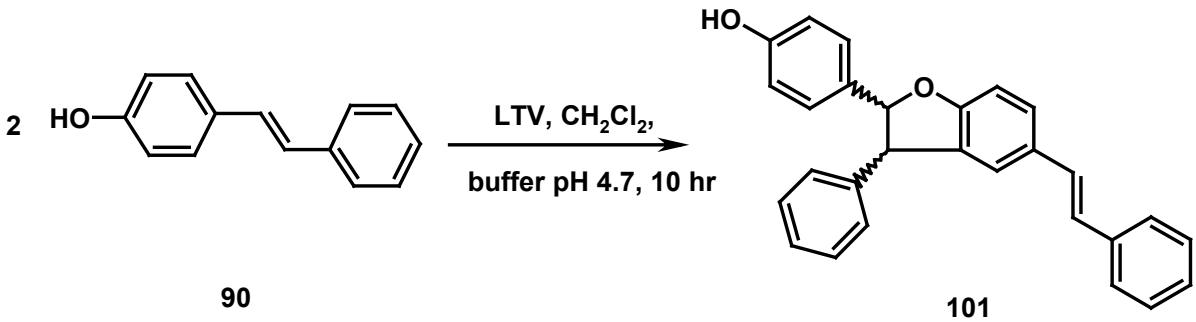

Scheme 23

Mass spectrum, reported in Figure 39, shows a positive ESI-MS peak at *m*/*z* 413.1 $[M+Na]^{+}$ which confirmed the formation of a dimer with molecular formula $C_{28}H_{22}O_2$ The ^{1}H and ^{13}C NMR data (Figures 37 and 38 and Table 3) of (±)-**101**

were in perfect agreement with those reported in the literature. It is worth citing here that in a previously reported enzyme-mediated synthesis of (±)-**101** by Riva *et al*,[29] a lower yield was obtained although longer reaction times were used.

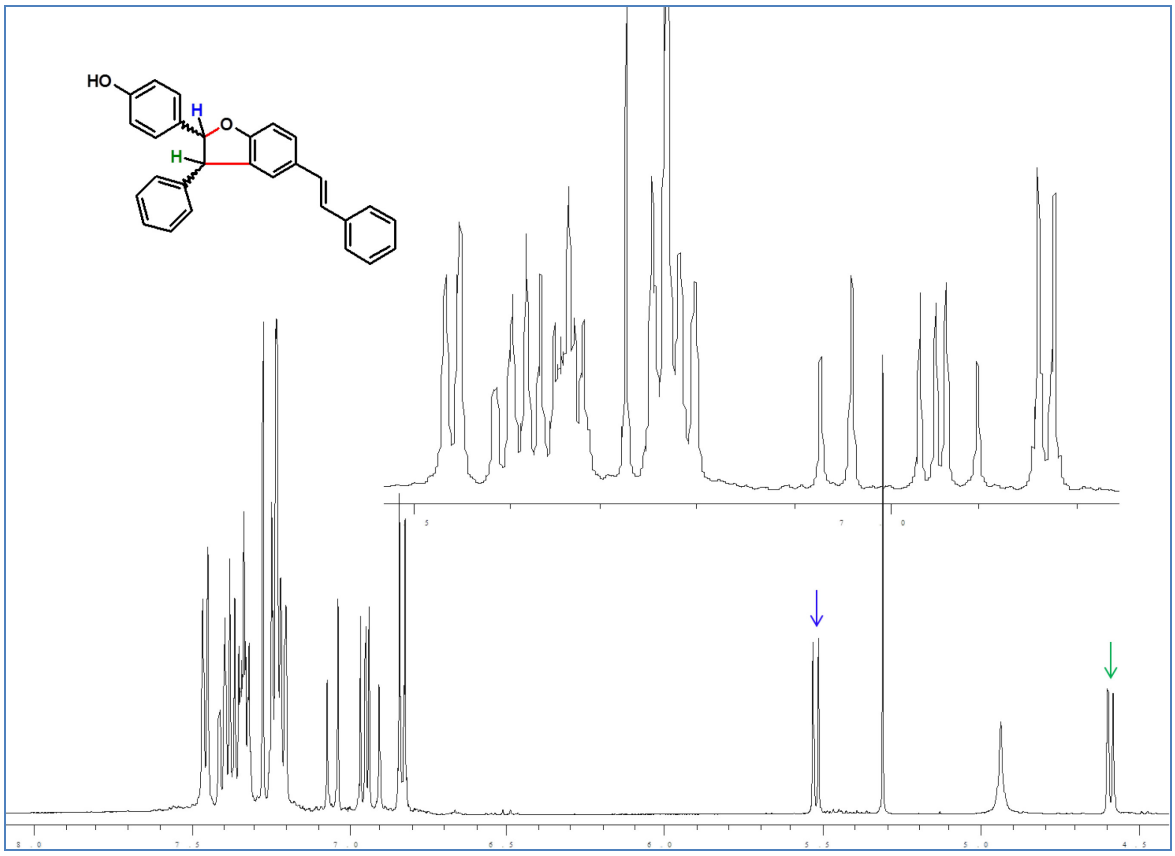

Figure 37: ^{1}H NMR Spectrum of (±)-**101**

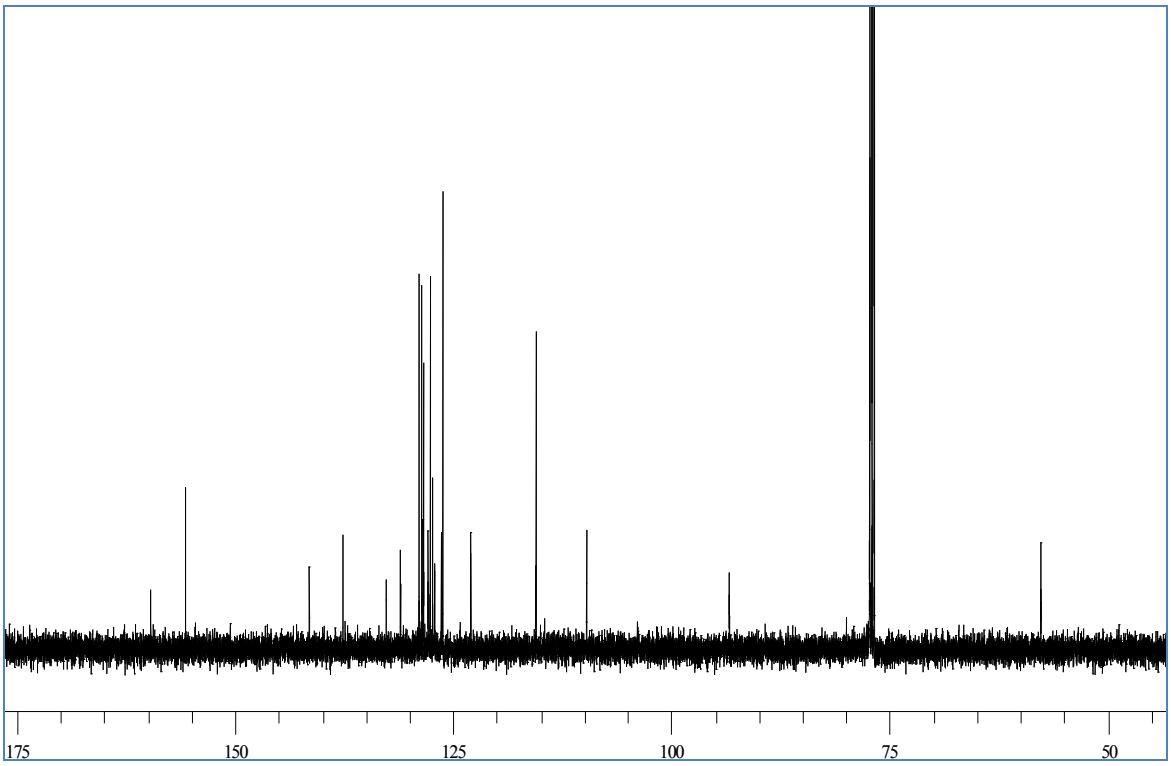

Figure 38: ^{13}C NMR spectrum of (±)-**101**

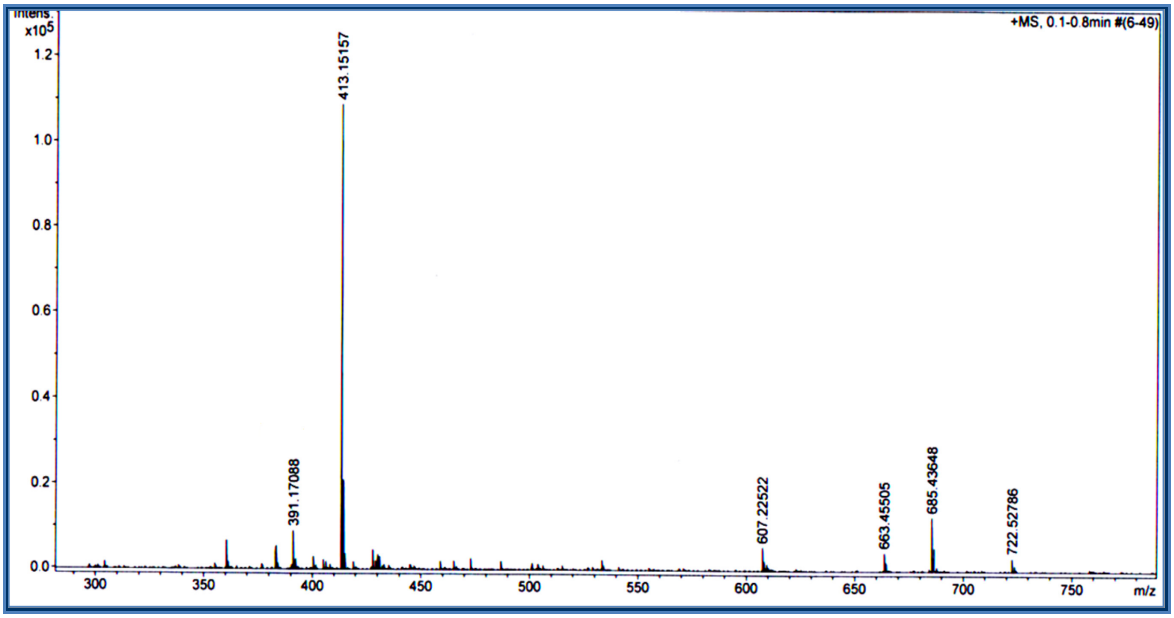

Figure 39: Mass spectrum of (±)-**101**

Table 3: ^{1}H NMR and ^{13}C NMR data of compound (±)-**101**

H ($CDCl_3$)	δH (mult,J Hz)	C ($CDCl_3$)	δC
		C-1	131.08
H-2,6	7.24 (d,8.5, 2H)	C-2,6	128.6
H-3,5	6.82 (d,8.5, 2H)	C-3,5	115.5
		C-4	155.6
H-7	5.52 (d,8.5, 1H)	C-7	93.3
H-8	4.58 (d,8.5, 1H)	C-8	57.6
		C-9	141.5
H-10,14	7.38 (d,7.5, 2H)	C-10,14	128.5
H-11,13	7.22 (m,2H)	C-11,13	128.9
H-12	7.31 (m,1H)	C-12	127.6
		C-1'	131.03
H-2'	7.4 (d,1.5, 1H)	C-2'	128.4
H-3'	6.95 (d,8.0 1H)	C-3'	109.7
		C-4'	159.6
		C-5'	132.6
H-6'	7.19 (s)	C-6'	122.9
H-7'	7.05 (d,16.25, 1H)	C-7'	127.8
H-8'	6.91 (d,16.25, 1H)	C-8'	126.1
		C-9'	137.6
H-10',14'	7.46 (d,7.5, 2H)	C-10',14'	126.3
H-11',13'	7.33 (m, 2H)	C-11',13'	127.3
H-12'	7.21 (m,1H)	C-12'	127.1
4-OH	8.4 (s)		

*2.1.2.4 Biomimetic synthesis of stilbenolignan (±)-**102***

Substrate **91** was subjected to oxidation in the presence of LTV or $Mn(OAc)_3$ as mentioned in the below Scheme 24; after the column chromatographic purification racemic mixture **(±)-102** was obtained. The product has been characterized unambiguously by using, mass spectroscopy, 1D and 2D NMR spectroscopy; all spectroscopic data are in agreement with literature data.[28]

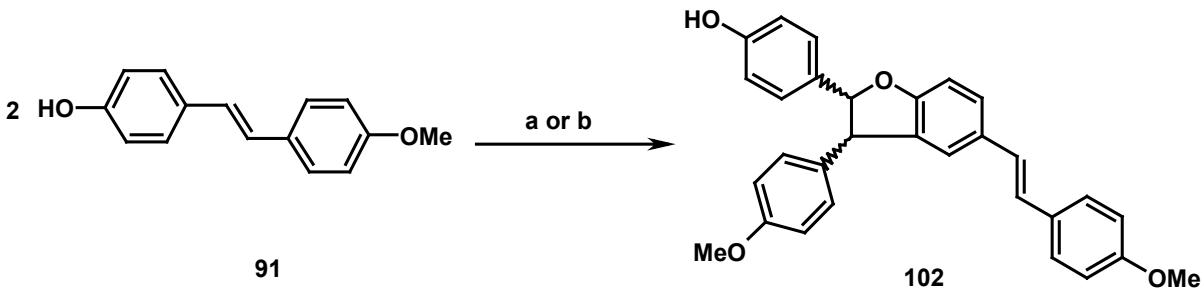

91 102

a. LTV, buffer pH 4.7,EtOAc, 20hr
b. $Mn(OAC)_3$, CH_2Cl_2, 9 hr

Scheme 24

Mass spectrum shows a negative ESI-MS peak at *m*/*z* 449.3 $[M-H]^-$ which confirmed the formation of a dimer with molecular formula $C_{30}H_{26}O_4$ and spectrum is reported in Figure 39. The ^1H and ^{13}C NMR data (Figures 40 and 41, Table 4) of (±)-**102** were in perfect agreement with those reported in the literature. It is worth citing here that in a previously reported enzyme-mediated synthesis of (±)-**102** by Riva *et al*,[29] a lower yield was obtained although longer reaction times were used.

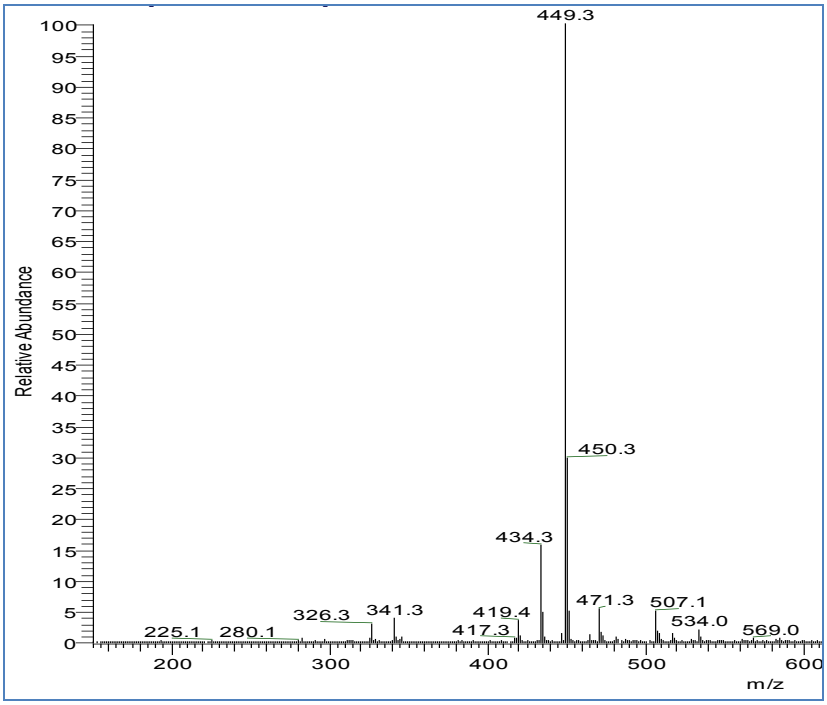

Figure 39.Mass spectrum of **(±)-102**

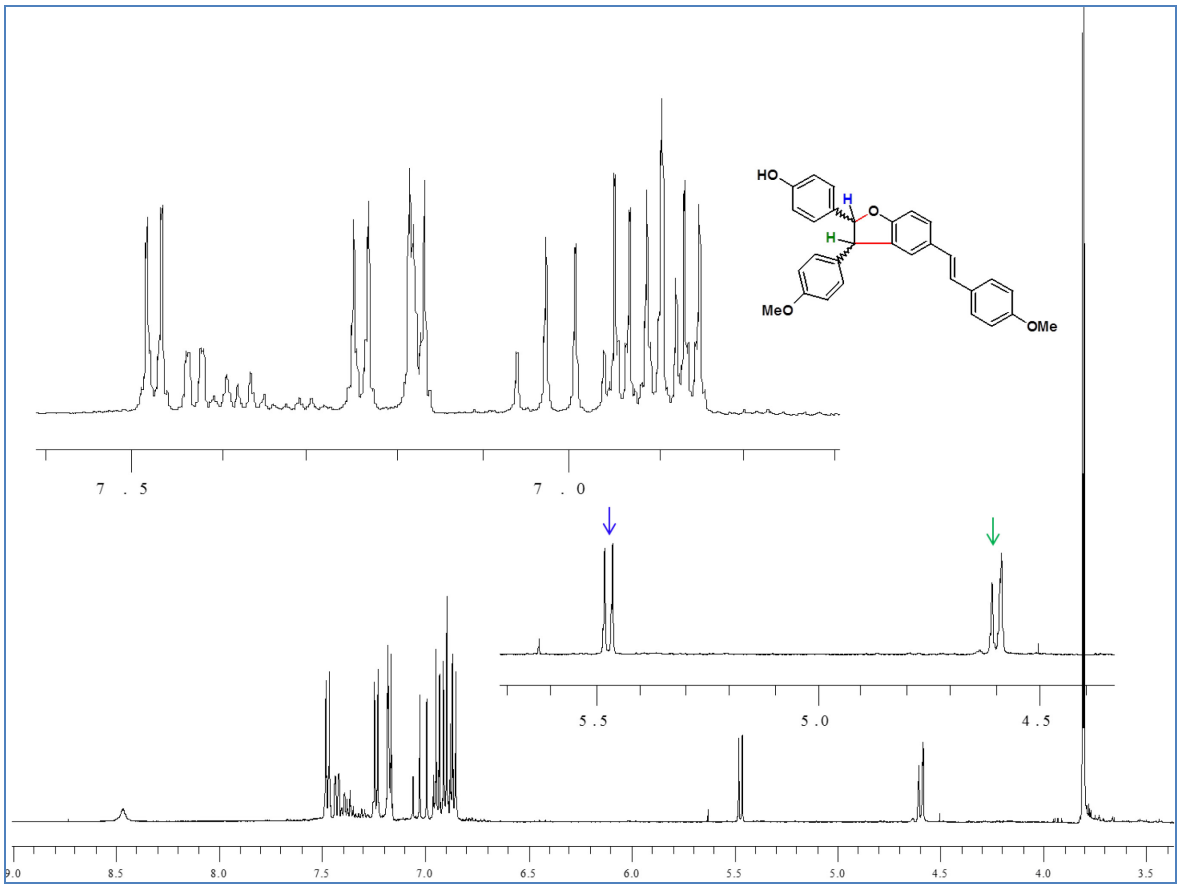

Figure 40: ^{1}H NMR spectrum of (±)**-102**

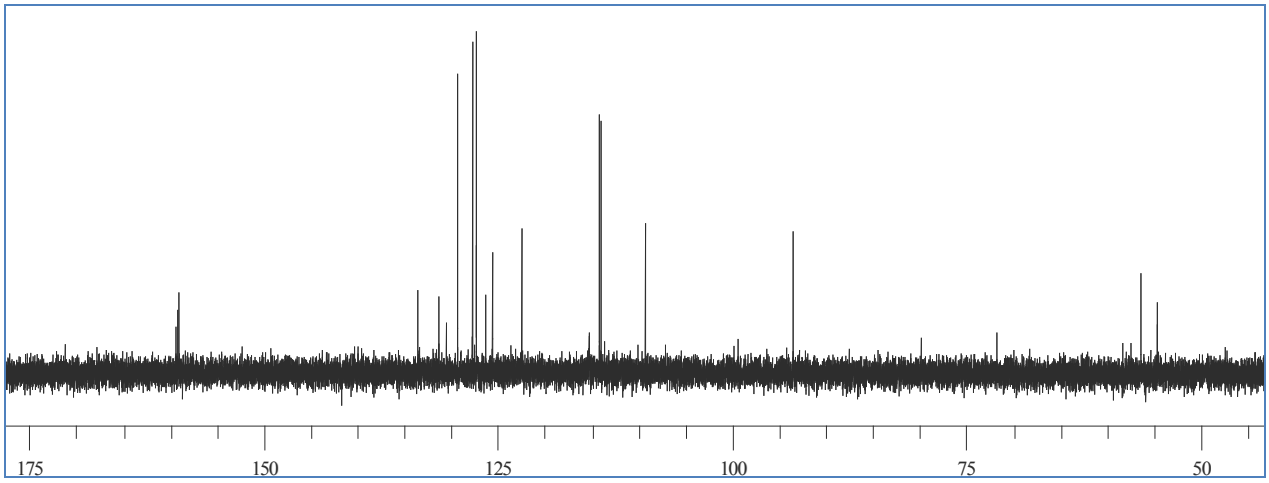

Figure 41: ^{13}C NMR spectrum of (±)**-102**

Table 4: ^{1}H NMR and ^{13}C NMR data of compound (±)-**102**

H	δ_H (mult, J Hz)	C	δ_C
		C-1	129.4
H-2,6	7.11 (d, 8.5)	C-2,6	128.4
H-3,5	6.81 (d, 8.5)	C-3,5	115.4
		C-4	155.7
H-7	5.44 (d, 9.0)	C-7	93.5
H-8	4.51 (d, 9.0)	C-8	55.2
		C-9	133.4
H-10,14	7.2 (d,8)	C-10,14	129.4
H-11,13	6.86 (d,8)	C-11,13	114.2
		C-12	158.8
		C-1'	131.3
H-2'	7.38 (d,8.5)	C-2'	127.4
H-3'	7.36 (d, 8.5)	C-3'	109.6
		C-4'	158.9
		C-5'	132.5
H-6'	7.14 (bs)	C-6'	122.5
H-7'	6.91 (d,15.5)	C-7'	126.4
H-8'	6.86 (d,15.5)	C-8'	125.8
		C-9'	130.5
H-10',14'	7.34 (d, 8.0)	C-10',14'	127.6
H-11',13'	6.89 (d, 8.0)	C-11',13'	114.2
		C-12'	159.3
12-OCH_3	3.81 (s)	12-OCH_3	55.2
12'-OCH_3	3.80 (s)	12'-OCH_3	56.9
4-OH	8.45 (s)		

*2.1.2.5 Biomimetic synthesis of stilbenolignan (±)-**103***

Substrate **92** was subjected to oxidation in the presence of $Mn(OAc)_3$ as mentioned in the below Scheme 25.

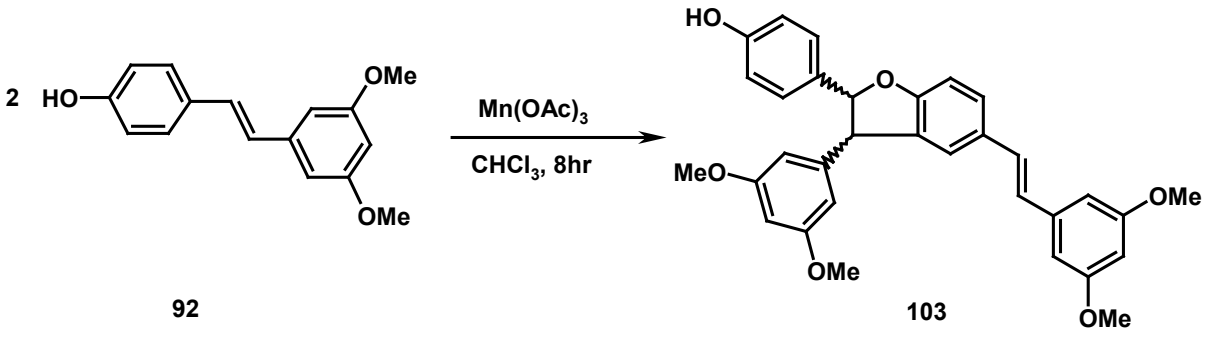

Scheme 25

After the column chromatographic purification racemic mixture **(±)-103** was obtained. The dimer **(±)-103**, a previously reported compound, was characterized by ^{1}H NMR (Figure 42 and Table 5), which is in agreement with reported in the literature.[36]

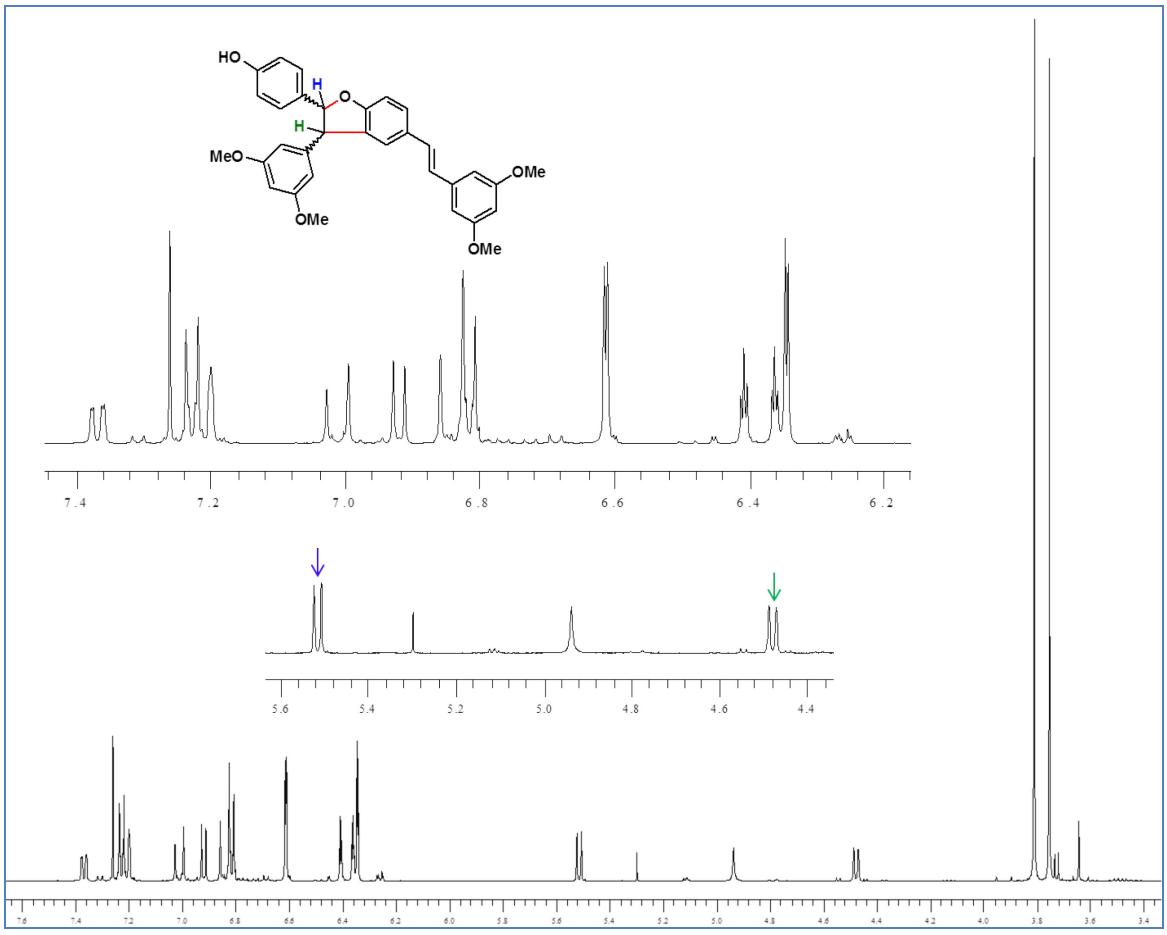

Figure 42: ^{1}H NMR spectrum of **(±)-103**

Table 5: ^{1}H NMR data of **(±)-103**

H	δ_H (mult, J Hz) in $CDCl_3$
H-2,6	7.22 (d, 8.5,)
H-3,5	6.81 (d, 8.5)
H-7	5.51 (d, 8.5)
H-8	4.47 (d, 8.5)
H-10,14	6.34 (d, 2.5)
H-12	6.40 (t, 2.5)
H-2'	7.36 (dd, 8.5,1.5)
H-3'	6.91 (d, 8.5)
H-6'	7.19 (d, 1.5)
H-7'	7.01 (d,16.5)
H-8'	6.84 (d,16.5)
H-10',14'	6.61 (d, 2.5)
H-12'	6.36 (t, 2.5)
11,13-OCH_3	3.81 (s)
11',13'-OCH_3	3.75 (s)
4-OH	4.9 (s)

*2.1.2.6 Biomimetic synthesis of stilbenolignan (±)-**104***

Substrate **95** was subjected to oxidation in the presence of LTV as mentioned in the below Scheme 26. After the column chromatographic purification racemic mixture **(±)-104** was obtained and a spectroscopic characterization was carried out. The ^{1}H and ^{13}C NMR data (Figures 43 and 44, Table 6) of (±)-**104** were in perfect agreement with those reported in the literature.[29]

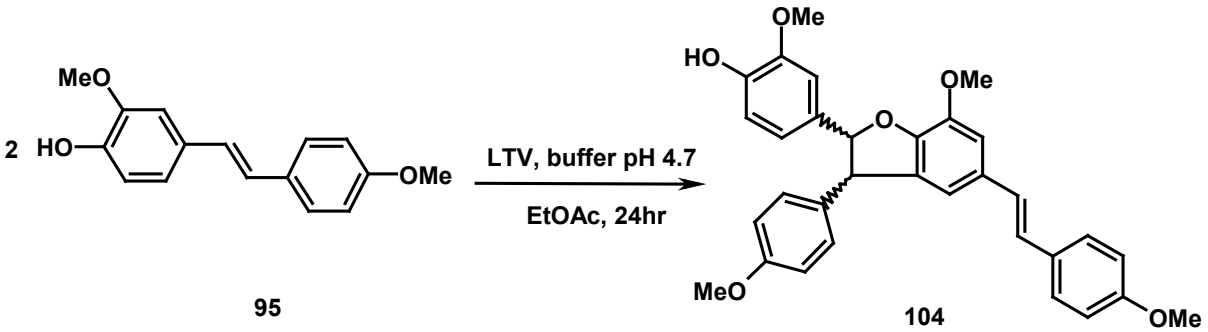

95 104

Scheme 26

Table 6: ^{1}H NMR and ^{13}C NMR data of (±)-**104**

H	δ_H (mult, J Hz) in $CDCl_3$	C	δ_C in $CDCl_3$
		C-1	130.3
H-2	6.95 (bs)	C-2	119.7
		C-3	146.6
		C-4	145.7
H-5	6.74 (bs)	C-5	115.3
H-6	6.74 (bs)	C-6	119.7
H-7	5.42 (d, 9.0)	C-7	94.5
H-8	4.68 (d, 9.0)	C-8	57.3
		C-9	133.1
H-10,14	7.45 (d, 8.5)	C-10,14	129.5
H-11,13	6.89 (d, 8.5)	C-11,13	114.2
		C-12	158.8
		C-1'	132.0
H-2'	7.13 (bs)	C-2'	108.7
		C-3'	144.4
		C-4'	147.0
		C-5'	132.1
H-6'	6.69 (bs)	C-6'	109.8
H-7'	6.99 (s)	C-7'	126.6
H-8'	6.99 (s)	C-8'	126.2
		C-9'	130.3
H-10',14'	7.14 (d, 8.5)	C-10',14'	127.3
H-11',13'	6.91 (d, 8.5)	C-11',13'	114.1
		C-12'	159.0
3-OCH_3	3.74 (s)	3-OCH_3	56.0
12-OCH_3	3.74 (s)	12-OCH_3	56.0
3'-OCH_3	3.87 (s)	3'-OCH_3	55.2
12'-OCH_3	3.75 (s)	12'-OCH_3	55.2
4-OH	8.45 (s)		

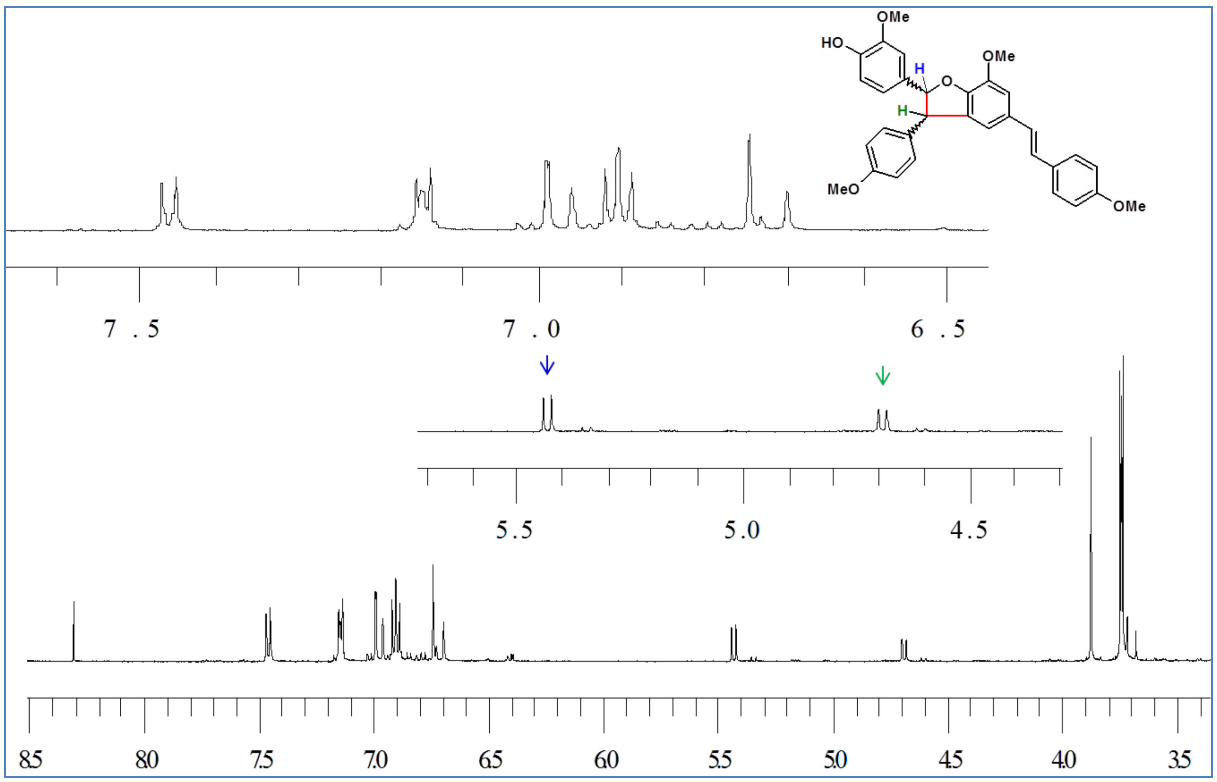

Figure 43: ^{1}H NMR spectrum of **(±)-104**

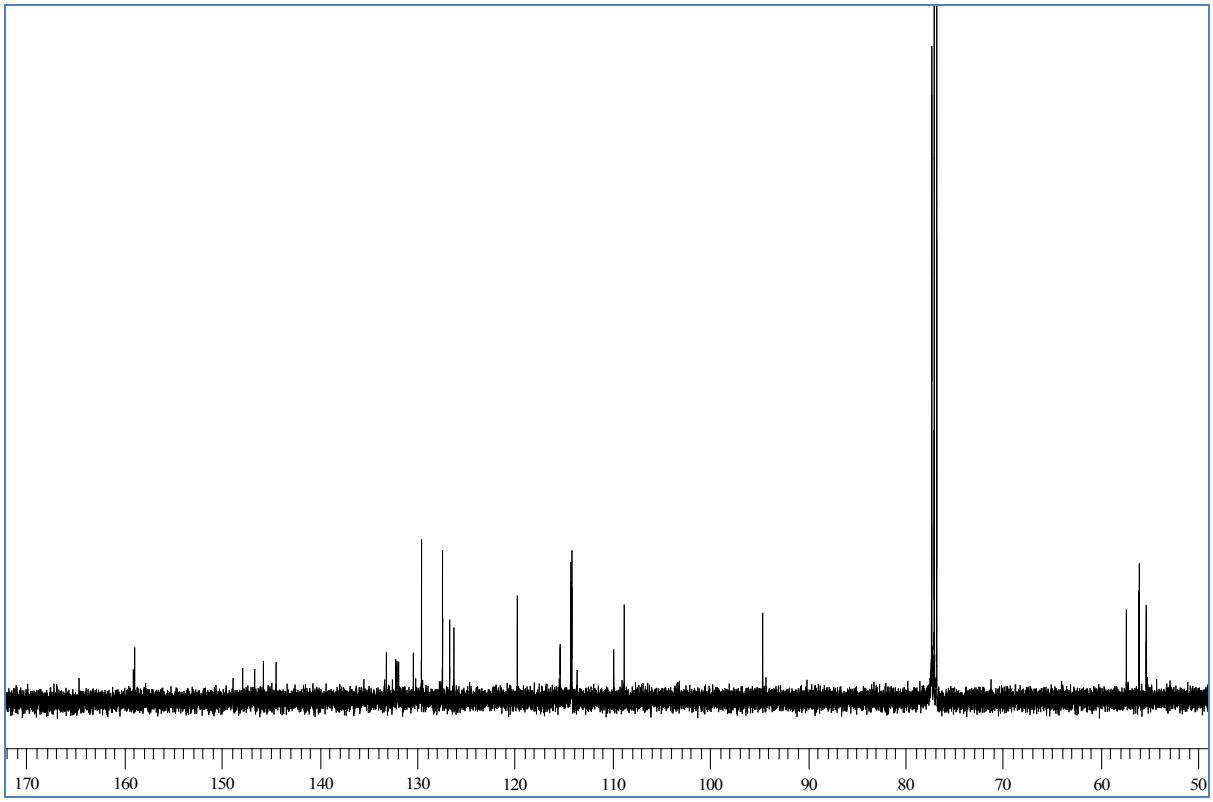

Figure 44: ^{13}C NMR spectrum of **(±)-104**

*2.1.2.7 Biomimetic synthesis of stilbenolignan (±)-**105***

Compound **96** was used as substrate with the aim to obtain the previously unreported dimer (±)-**105**. The substrate was stirred in EtOAc for 10 hrs at room temperature in the presence of LTV enzyme and buffer pH 4.7 as reported in Scheme 27.

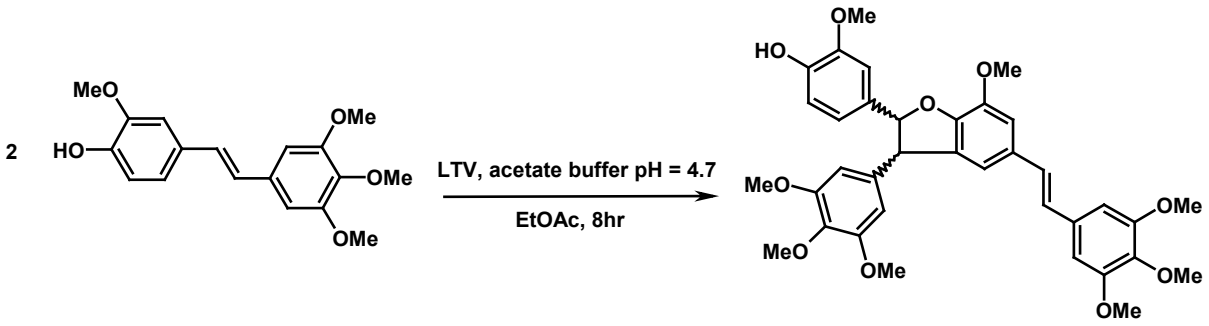

96 105

Scheme 26

After a TLC check, three spots were observed. The main product (±)-**105** was separated by silica-gel column chromatography. Mass spectrum shows peak at *m/z* 629.2 $[M-H]^-$ (Figure 45) which confirmed the formation of a dimer and gives molecular formula $C_{36}H_{38}O_{10}$. The ^1H, ^{13}C, COSY, HSQC and HMBC NMR spectra are reported in Figure 46, 47, 48, 49 and 50, respectively, and ^1H, ^{13}C data are reported in Table 7.

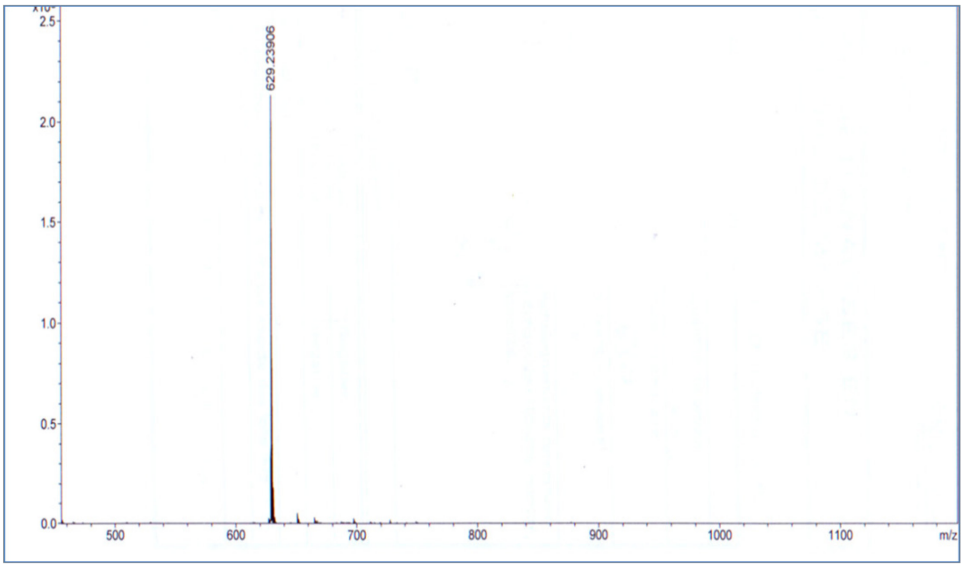

Figure 45: Mass spectrum of compound (±)-**105**

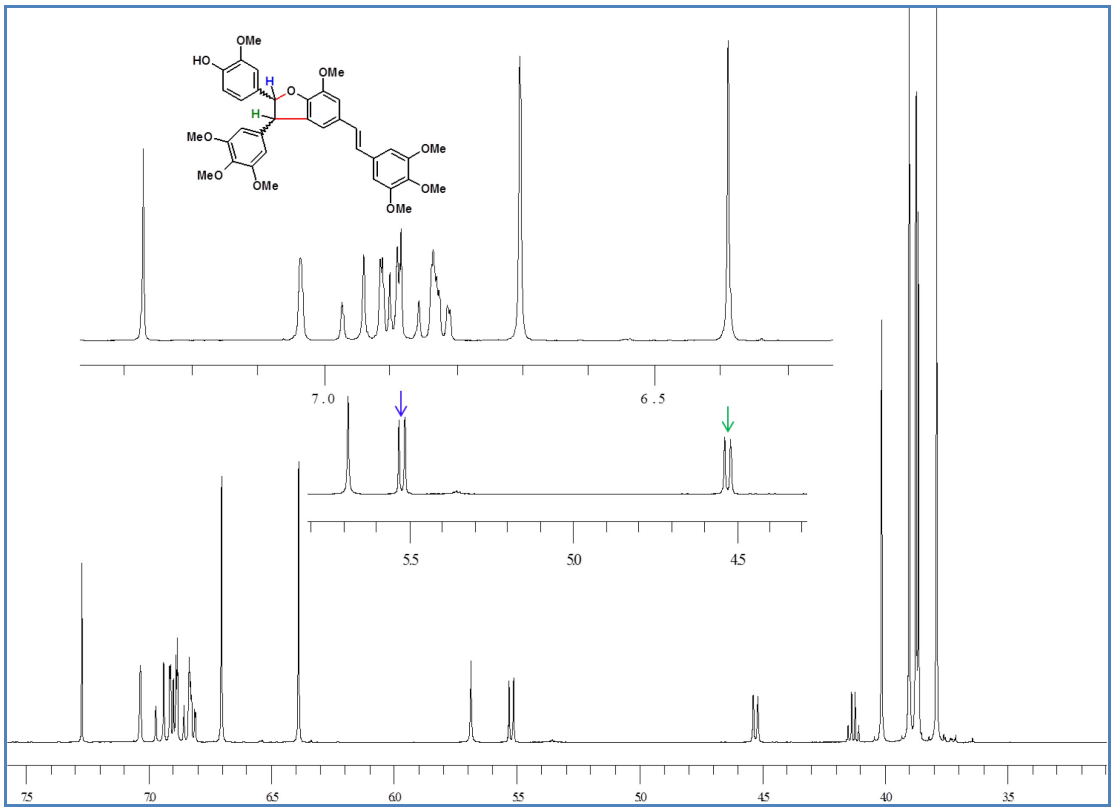

Figure 46: ^{1}H NMR spectrum of compound (±)-**105**

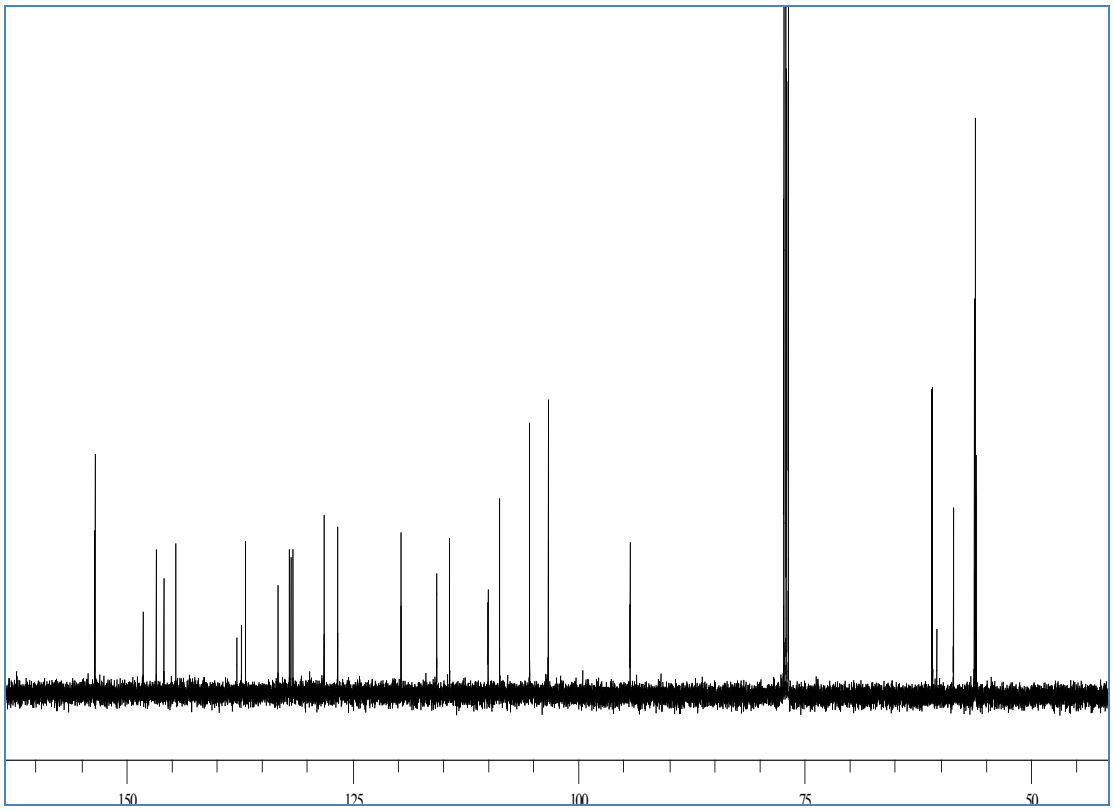

Figure 47: ^{13}C NMR spectrum of compound (±)-**105**

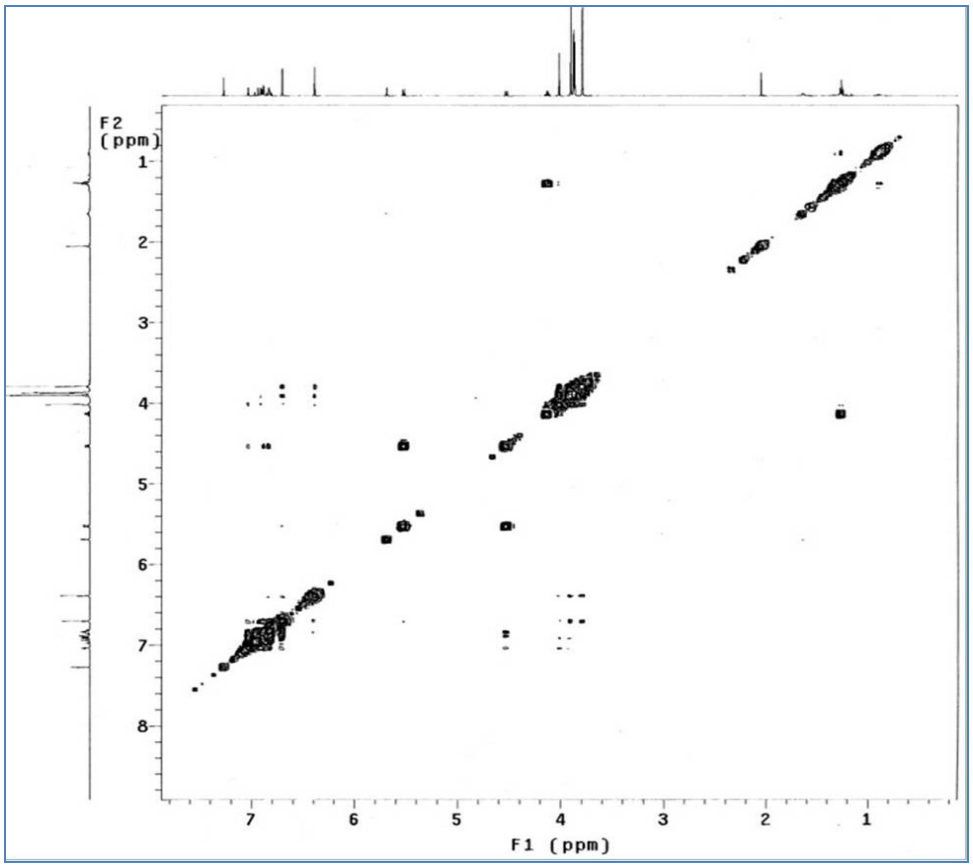

Figure 48: COSY spectrum of compound (±)-**105**

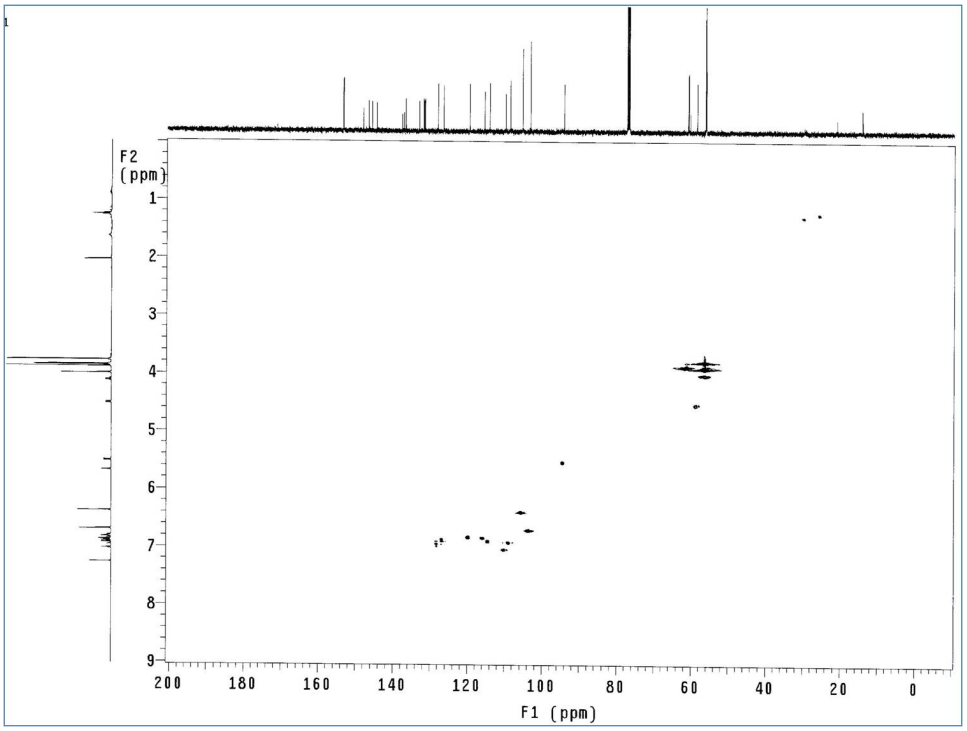

Figure 49: HSQC spectrum of compound (±)-**105**

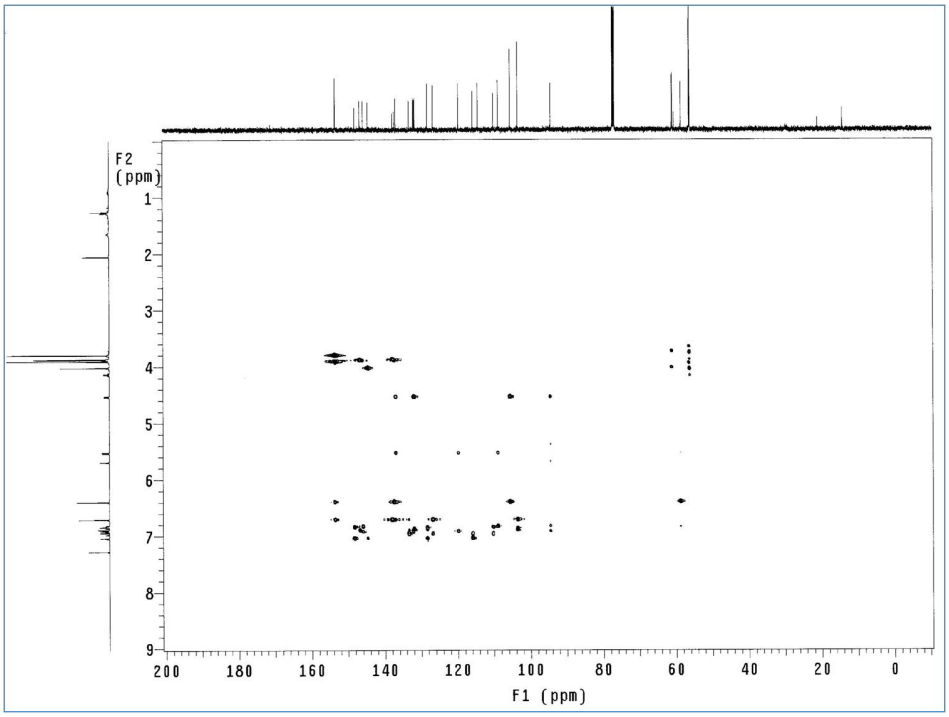

Figure 50: HMBC spectrum of compound (±)-**105**

Table 7: ^{1}H and ^{13}C NMR data of (±)-**105**

C	**δ_C in $CDCl_3$**	**H**	**δ_H (mult, J Hz) in $CDCl_3$**
C-1	131.9		
C-2	119.6	H-2	6.80 (d,1.5)
C-3	148.1		
C-4	145.8		
C-5	114.2	H-5	6.88 (d, 8.0)
C-6	115.6	H-6	6.82 (dd, 8.0,1.5)
C-7	94.2	H-7	5.52 (d, 9.25)
C-8	58.5	H-8	4.52 (d, 9.25)
C-9	131.7		
C-10,14	105.4	H-10,14	6.38 (s)
C-11,13	153.5		
C-12	137.2		
C-1'	133.2		
C-2'	109.9	H-2'	7.03 (s)
C-3'	144.5		
C-4'	146.6		
C-5'	136.8		
C-6'	108.7	H-6'	6.90 (d, 2.0)
C-7'	128.2	H-7'	6.95 (d,16.0)
C-8'	126.6	H-8'	6.86 (d,16.0)
C-9'	131.5		
C-10',14'	103.3	H-10',14'	6.70 (s)
C-11',13'	153.4	H-11',13'	
C-12'	137.7		
3-OCH_3	56.01	3-OCH_3	3.874 (s)
11,13-OCH_3	56.1	11,13-OCH_3	3.78 (s)
12-OCH_3	60.9	12-OCH_3	3.86 (s)
3'-OCH_3	56.2	3'-OCH_3	4.01 (s)
11',13'-OCH_3	56.05	11',13'-OCH_3	3.90 (s)
12'-OCH_3	60.8	12'-OCH_3	3.872 (s)

The ^{13}C NMR spectrum shows 30 signals: the majority of the signals were in the sp^2 region (from 153.5 to 103.3 ppm): 11 quaternary carbon signals and 9 CH signals; two methine signals in the sp^3 region (58.5 and 94.2 ppm) were also observed, suggesting the formation of a dihydrobenzofuran ring. In upperfield of the spectra there are six O$\underline{C}H_3$ signals observed at 60.9, 60.8, 56.2, 56.1, 56.05, 56.01 ppm.

On the basis of the knowledge of radical dimerization mechanism from previous studies, and HSQC study with ^1H and ^{13}C NMR spectroscopy it is possible to assign protons (i.e., H-2 at δ 6.80, H-5 at δ 6.88 and H-6 at δ 6.82) on A ring. ^{13}C NMR and HSQC spectrum shows two *para* substituted O$\underline{C}H_3$ signals at δ 60.9 ppm and δ 60.8 ppm of 12 and 12' O$\underline{C}H_3$ respectively of B and D ring. These signals indicate that there are two *para* and *meta* substituted aromatic rings and one *meta* substituted aromatic ring; the ^{13}C chemical shift analysis and HSQC, HMBC spectrum indicated that one of these rings bear a phenol group and which is *meta* substituted aromatic ring (A), whereas the other two bearing *para* and *meta* substituted aromatic rings (B&D).

The long-range correlation between C-2 at δ 119.6 ppm and H-7 at δ 5.52 ppm, and between C-10,14 at δ 105.4 ppm and H-8 at δ 4.52 ppm allows to establish that the A ring is bonded to C-7 whereas the B ring is bonded to C-8 (Figure 51). It is clearely observed the correlation between C-5' at δ 136.8 and H-7,H-8 at δ 4.52, δ 5.52 ppm confirms the presence of the fused oxygenated five-member ring (E). The correlation between a doublet H-7 at δ 5.52 and H-8 at δ 4.52 indicates two *trans* axial protons, the COSY spectra also corroborate the correlation between H-7 and H-8 protons (Figure 52).

The value of ^3J (H-7,H-8) measured from ^1H NMR spectrum (9.25 Hz) suggests a predominant conformation with the two H-7 and H-8 protons in a pseudo

trans-axial arrangement, whereas the ^{3}J (H-7',H-8') is 16.0 Hz, as expected for a double bond with a *trans* configuration.

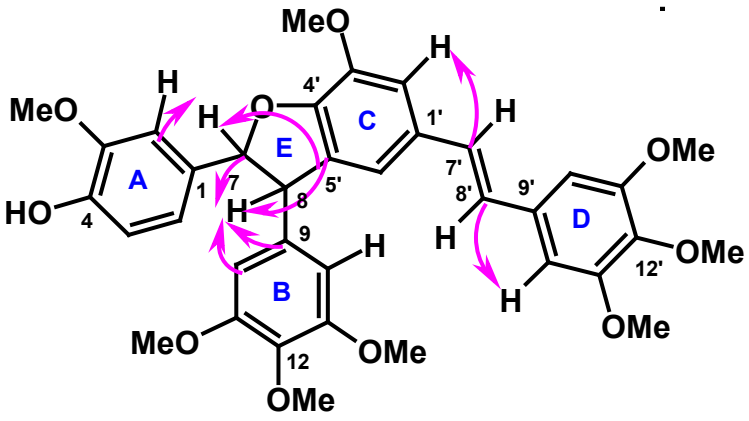

Figure 51: Selected HMBC correlation of (±)-**105**

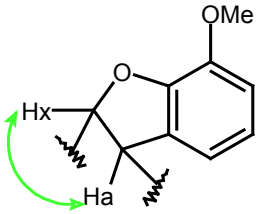

Figure 52

The distinction between the ethylenic protons has been made through the analysis of the C,H long-range correlation found in the HMBC spectrum: the signal of C-7' at δ 128.2 ppm shows a correlation with the proton signal at δ 7.03 ppm, directly bonded to H-2' (i.e.,C-2') whereas the signal due to C-8' at 126.6 ppm is correlated to the proton signal at δ 6.70 ppm, directly bonded to H-10', 14' (i.e., C-10',14'). Figure 51 shows main selected C, H correlation between the all five rings.

In particular, a NOESY correlation was observed between a singlet signal at δ 6.38 having a correlation with singlet signal at δ 3.78 (-OC$\underline{H}_3$), and another singlet signal at δ 6.70 having a correlation with singlet signal at δ 3.90 (-OC$\underline{H}_3$), assigned to twelve protons of OC$\underline{H}_3$ and four protons A2 system of B and D aromatic ring (Figure 53), and one more correlation was observed between the one singlet signal at δ 7.03 having a correlation with a singlet

signal at δ 4.01 assigned to three protons of OCH_3 and one proton of H-2' (ie., C-2') of D ring (Figure 53).

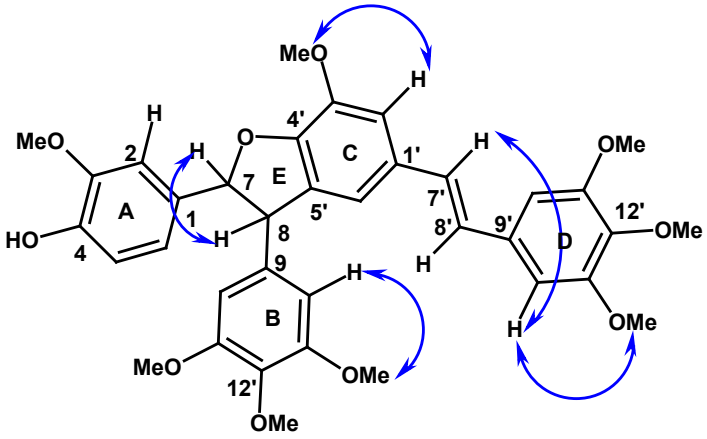

Figure 53: Selected 2D NOESY correlation of compound (±)-**105**

*2.1.2.8 Biomimetic synthesis of stilbenolignan (±)-**106***

Compound **98** was used as substrate with the aim to obtain the previously unreported dimer (±)-**106**. The substrate was stirred in EtOAc for 10 hrs at room temperature in the presence of LTV enzyme and buffer pH 4.7 as reported in Scheme 28.

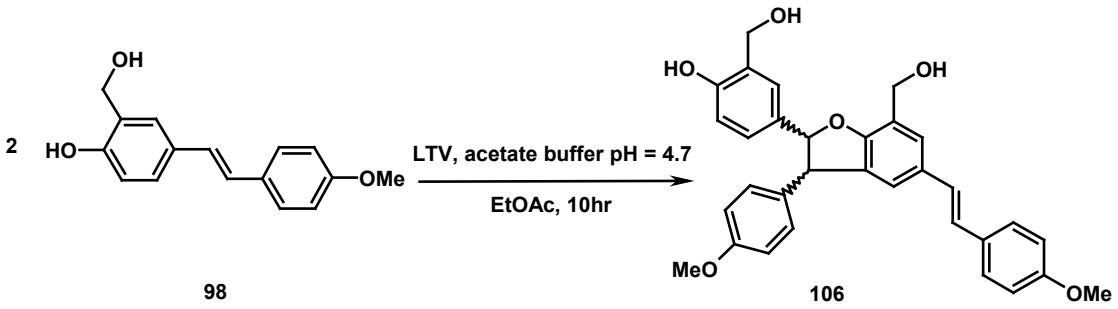

Scheme 28

After a TLC check, three spots were observed. The main product (±)-**106** was separated by silica-gel column chromatography. The positive ESI mass spectrum, reported in Figure 54, showed a peak at *m*/*z* 533.1 $[M+Na]^+$ which

confirms the formation of dimer and gives its molecular formula $C_{32}H_{30}O_6$. The ^1H NMR spectrum is reported in Figure 55.

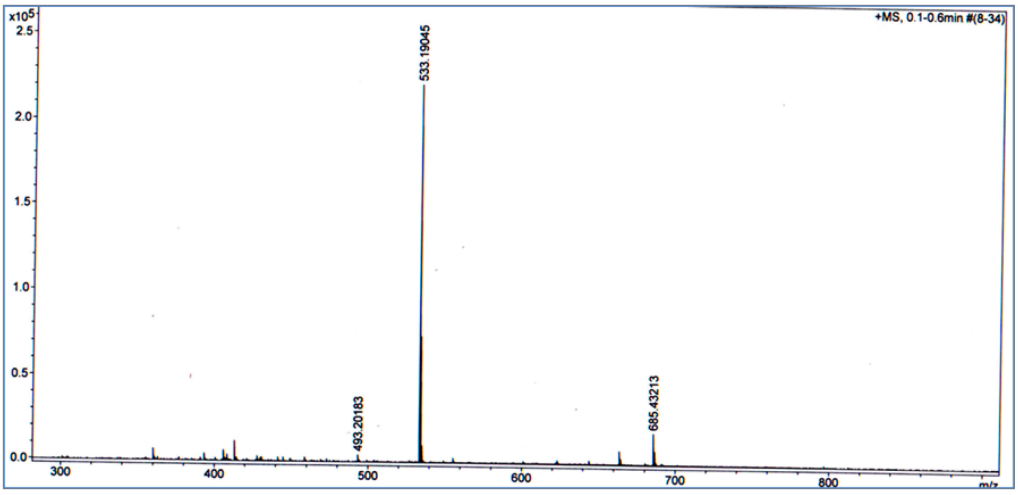

Figure 54: Mass spectrum of (±)**-106**

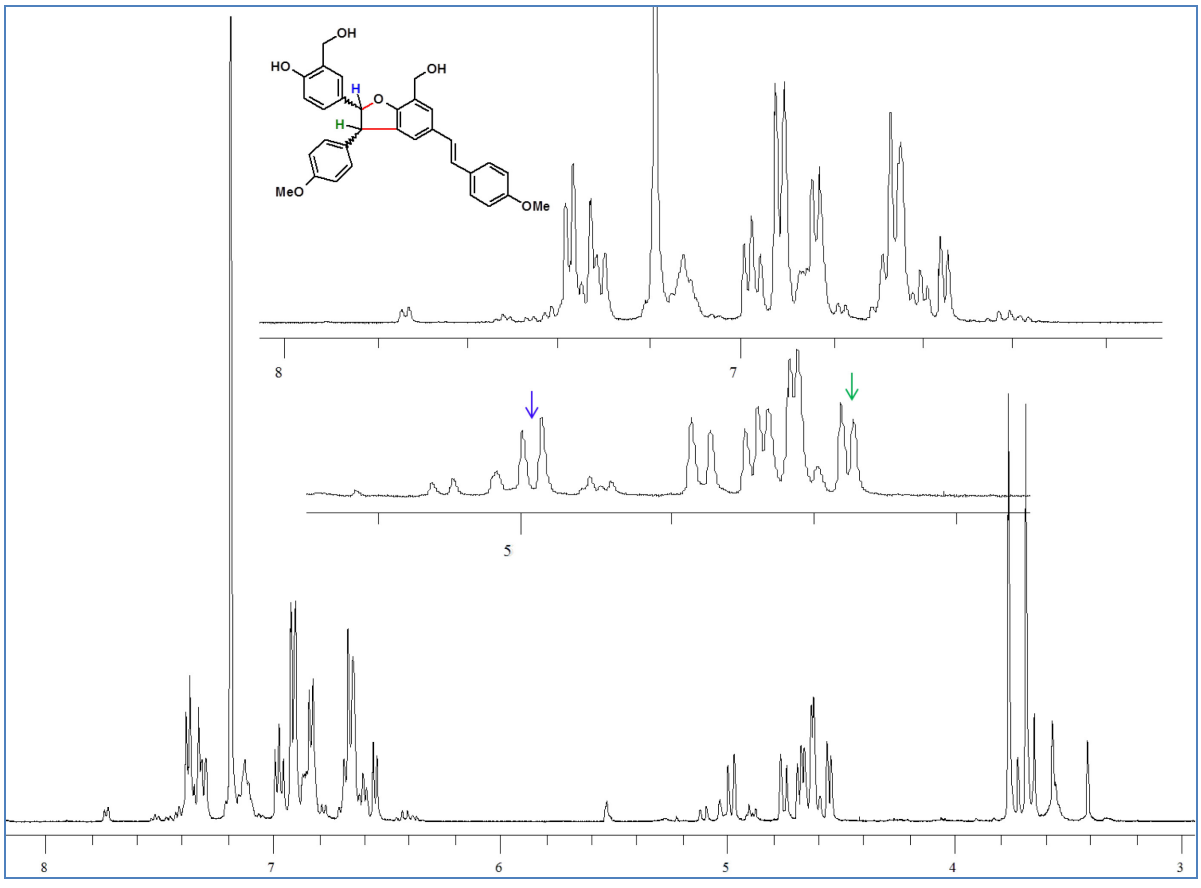

Figure 55: ^1H NMR of compound (±)**-106**

The ^{1}H NMR spectrum shows two singlets (six protons) at δ = 3.76 and δ = 3.68 due to 12-OMe and 12'-OMe and two doublets (AB system) at δ = 7.34 and δ = 6.62, with a large coupling constant of 17.0 Hz, due two *trans* olefinic protons (H-7' and H-8'). Are also present two *trans* hydrogens at δ = 4.56 and δ = 4.97 (H-7 and H-8, $J_{7,8}$ = 8.5 Hz) due the dihydrobenzofuran cycle, like other dimer of the stilbenes and one multiplet at δ = 4.65 is due to four hydrogens of H-15 and H-15'. Are visible in the aromatic region four doublets at δ = 6.84, δ = 7.38, δ = 6.67 and δ = 6.92 for eight protons due at two AA'BB' (H-10,14 and H-10',14',H-11,13 and H-11'-13') .. One singlet at δ=7.32 due to H-2 proton, two broad singlets at δ = 6.97 and δ = 7.29 due to two meta position protons H-2' and H-6'. One doublet at δ = 6.55 due to H-5 hydrogen and a multiplet at δ=7.12 due to H-6.

2.1.3 Reaction Mechanism of Biomimetic synthesis of stilbenolignans

It is known that during the course of oxidative coupling of phenols, phenoxyl radicals are generated as intermediates. In the case of above stilbenes, the formed radical has five mesomeric forms, three of which, designated as **107**, **108**, and **109**, are relevant to the coupling reactions (Scheme 29). As a result, different coupling modes for the mesomers are possible (for instance **109**-**109**, **109**-**108**, **109**-**107**, **108**-**108**, **108**-**107**, and **107**-**107**), leading to complex products. The major product was reported to be **109**-**108** linked compound.[84] This is verified by our above experimental results. The chance of **109**-**109** coupling could be increased if the **109**-**108** coupling is blocked by another substituent at the 5 position of the phenyl ring.

On the basis of the results obtained, a mechanism for the synthesis of the dihydrobenzofuran dimers can be proposed. Mechanism of formation of free radicals from laccase enzyme was reported in introduction section 1.2. The

dimeric structures indicate that the oxidation reactions took place at the 4-OH or 4'-OH position of the hydroxystilbenic moieties. In turn, the formed phenoxy radicals could delocalize themselves as reported in Scheme 30.

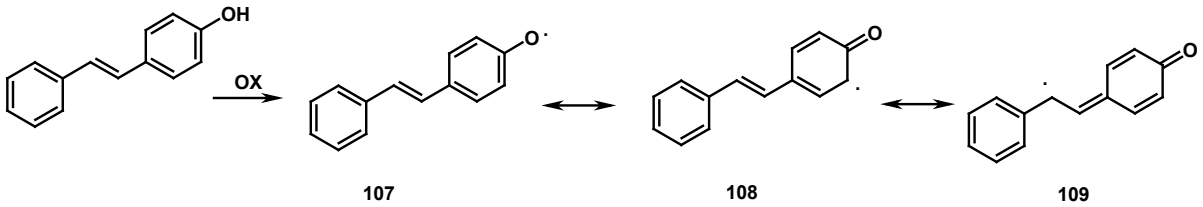

Scheme 29

Successively, the coupling of one radical **108** and one radical **109**, followed by tautomeric rearrangement and intramolecular nucleophilic attack to the intermediate quinone, gave the dihydrobenzofuran dimers (Scheme 30).

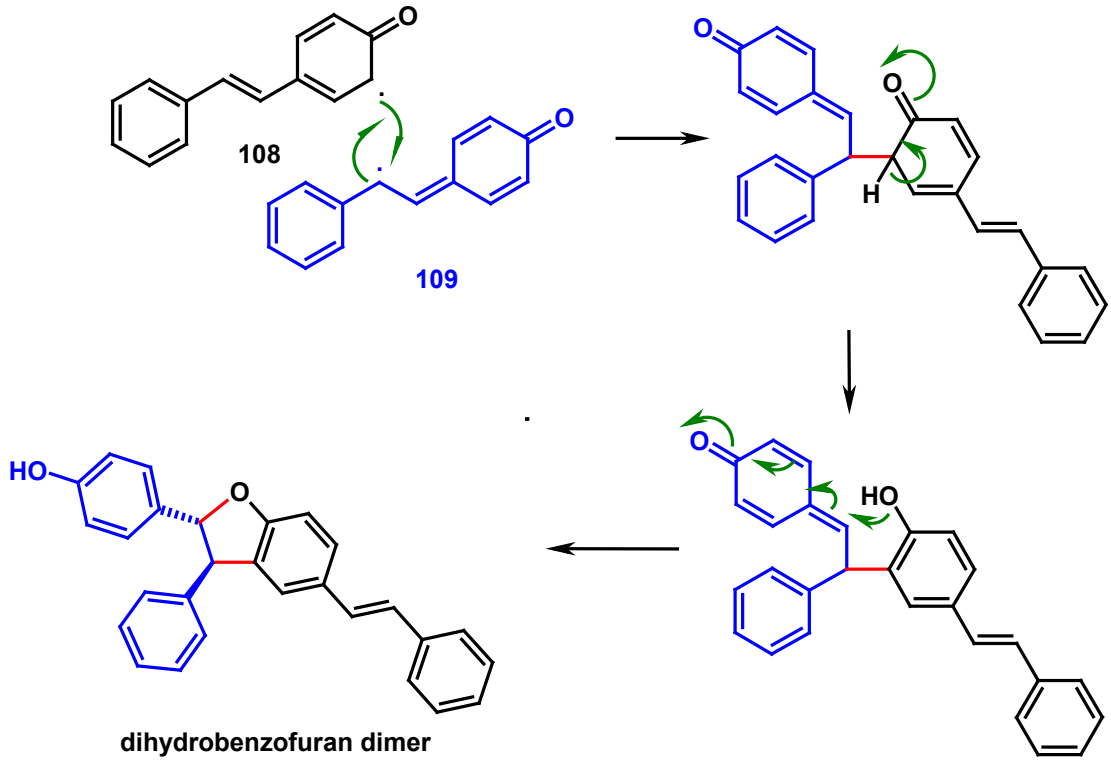

Scheme 30

An interesting aspect of this reaction is that only a racemic mixture is obtained, at least in detectable amounts, although in principle four stereoisomers are theoretically possible. That is, the racemate with a *trans* disposition of the

substituents on the dihydrobenzofuran ring is by far the main product of the reaction. This is established on the basis of the coupling constant value of the two *trans* hydrogens at C-7 and C-8 on the dihydrobenzofuran cycle ($J_{7,8}$ = 8.5 Hz), and it is in agreement with all previous literature references on dihydrobenzofuran neolignans obtained by synthesis. A plausible explanation of the preferred formation of the *trans* couple is that the less hindered transition state leading to the *trans* enantiomers is largely favoured on the basis of its formation enthalpy (ΔH_f). This is corroborated by recent data C.Tringali *et al* referred to the oxidative coupling of caffeic acid esters to give benzoxanthene and aryldihydronaphtalene lignans. In this work it is calculated the ΔH_f values for the possible transitions states originating from the quinone methide intermediate; calculations clearly indicate that the 6-7'-ct TS (see Figure 56), leading to the *trans* aryldihydronaphtalene racemate, is by far as the most stable transisiton state (36.54% Boltzmann distribution *versus* 0.04 – 0.51% for the other aryldihydronaphtalene TS).

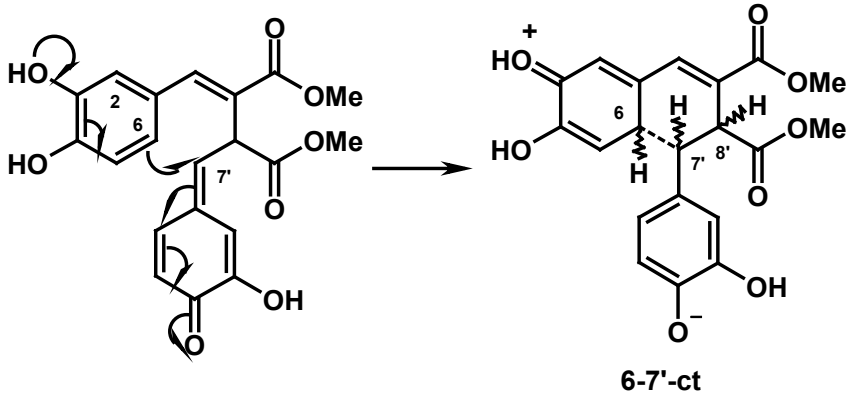

Figure 56

On the basis of our results, reactions carried out in ethyl acetate, dichloromethane, and chloroform show some common characteristics. Quite large amounts of starting material were recovered untransformed, especially in

dichloromethane and chloroform. We observed more than six products on TLC while the reaction was carried out in chloroform. With ethyl acetate solvent, the starting material was recovered in a comparatively low yield, even though ethyl acetate is much better solvent in terms of solubility of starting material and with this solvent only three to four products were observed on TLC by enzyme mediated reactions. Interestingly in metal mediated $Mn(OAc)_3$ reactions, solvents like dichloromethane and chloroform gives better results comparatively ethyl acetate. In summary, ethyl acetate is appear to be good solvent for generating dihydrobenzofuran dimers from our stilbenes in enzyme mediated reactions. Chloroform and dichloromethane appear to be the best solvents for generating dihydrobenzofuran dimers from our stilbene im metal mediated reactions.

From our results it was also observed that 67% of yield in the enzyme catalyzed reaction of monomer **94** gives dimer (±)-**104** (Scheme 25). In monomer **94**, position 3 radical was blocked by $-OCH_3$ function and this increases the rate of coupling chance of position 5 (**108**) radical coupling with β (**109**) radical. Whereas dimers (±)-**(99**-**103**) obtained in 10-30% of yield due to unblocking of position 3 in respective monomers. Although, monomers **83** and **86** give very low yield due to free ethylene function and more electronegative bromine function respectively.

2.1.4 Antiproliferative activity and absolute configuration of stilbenolignans

2.1.4.1 Antiproliferative activity of the racemic stilbenolignans

The racemic mixtures (±)-**99**-**105** were submitted to bioassays for antiproliferative activity towards SW-480 colon carcinoma cells; the results are reported in graph 2; in this phase of work all racemic mixtures were tested to

calculate the value of IC_{50} expressed in μM. The most active compounds are (±)-**99** (IC_{50} = 22.3 μM), (±)-**100** (IC_{50} = 30.7 μM), (±)-**101** (IC_{50} = 22.5 μM), (±)-**102** (IC_{50} = 33.4 μM), and (±)-**103** (IC_{50} = 27.8 μM). Compounds (±)-**104** and (±)-**105** bearing resulted not active (IC_{50} > 100 μM).

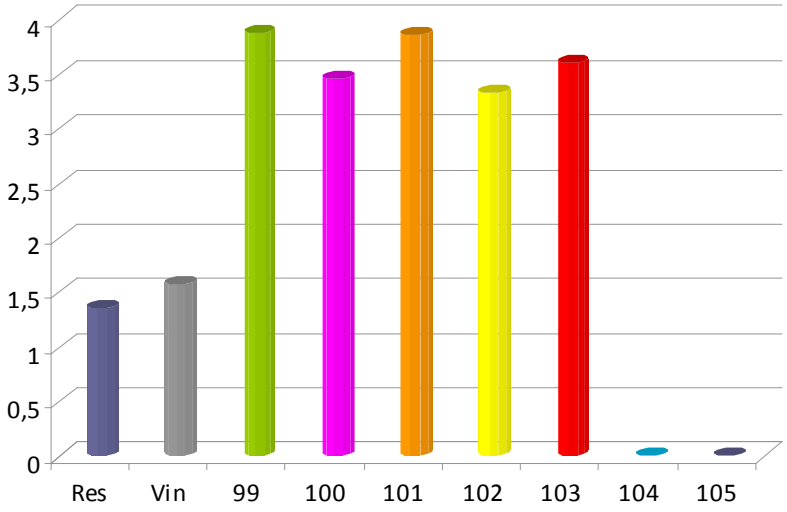

Graph 2

2.1.4.2 Chiral resolution of the active racemates and absolute configuration of the enantiomers

The active racemates (±)-**99**-**103**, were subjected to chiral HPLC in order to separate the pure enantiomers, evaluate their antiproliferative activity and possibly establish structure activity relationships.

In Figure 57 the HPLC profile of the racemate (±)-**99** is reported: the mixture was resolved on Chiralpak IA column using as hexane:iso-propanol, 50:50. We have separated quantitatively the two enantiomers; the first enantiomer (retention time 12.0 min) was indicated as **99A** and the second (with retention time 14.0 min) was indicated as **99B**. The Circular Dicroism (CD) spectra were run on samples of the pure enantiomers; in Figure 58 the CD spectra of compounds **99A** and **99B** are reported.

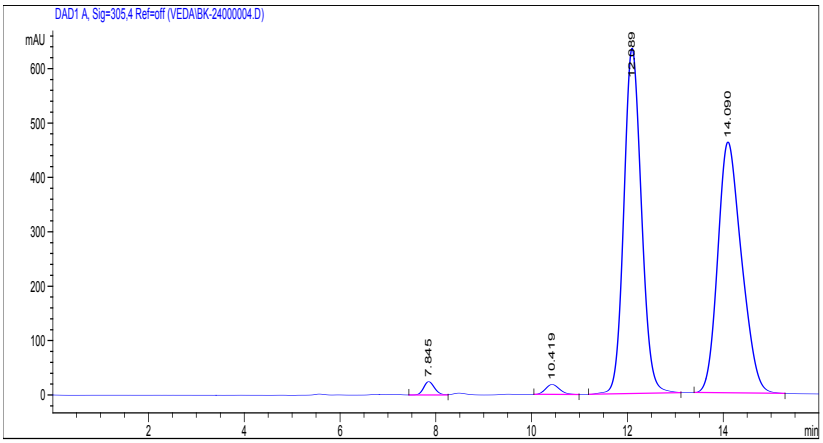

Figure 57: HPLC profile of the racemate (±)-**99**

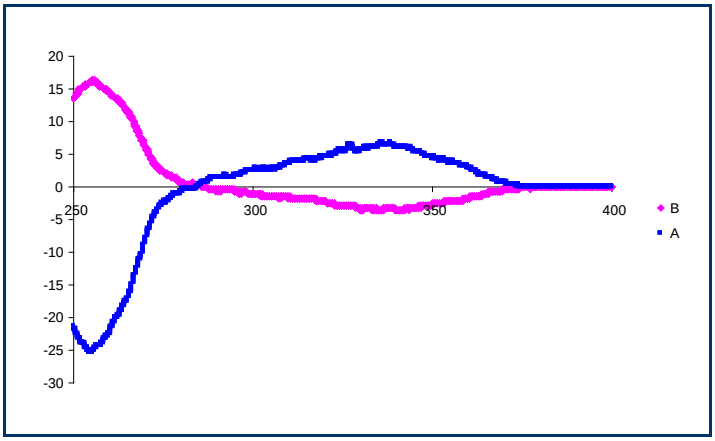

Figure 58: CD spectra of compounds **99A** and **99B**

The absolute configuration of the enantiomers **99A** and **99B** was determined through a comparison of their CD spectra with the CD spectra of (-)-ε-viniferin, a compound with a similar chromophore and with a known absolute configuration[85]; to the firstly eluted enantiomer **99A** the 7*R*,8*R*-configuration was assigned and consequently the secondly eluted enantiomer **99B** has a 7*S*,8*S*-configuration.

A chiral HPLC analysis confirmed that (±)-**100** is, as expected, a racemic mixture of the (7*S*,8*S*)- and (7*R*,8*R*)-enantiomers; in Figure 59 is reported the HPLC profile obtained on Chiralpak IA column using as hexane:iso-propanol, 50:50. We have separated quantitatively the two enantiomers; the first enantiomer (retention time 10.4 min) was indicated as **100A** and the second (with retention time12.5 min) was indicated as **100B**.

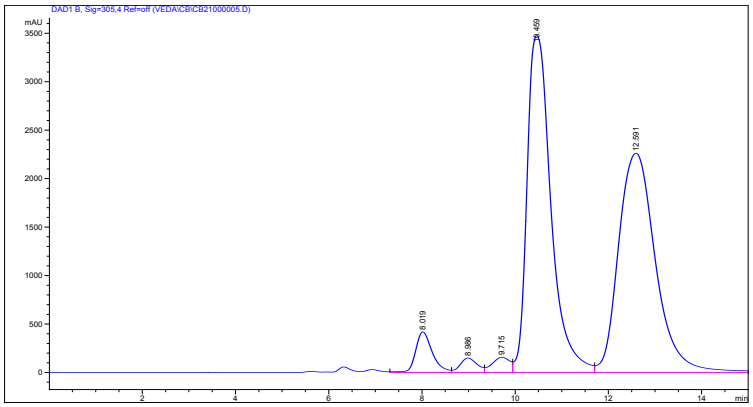

Figure 59: HPLC profile of the racemate (±)-**100.**

The pure enantiomers were subjected to CD spectra; in Figure 60 are reported the spectra of compounds **100A** and **100B**

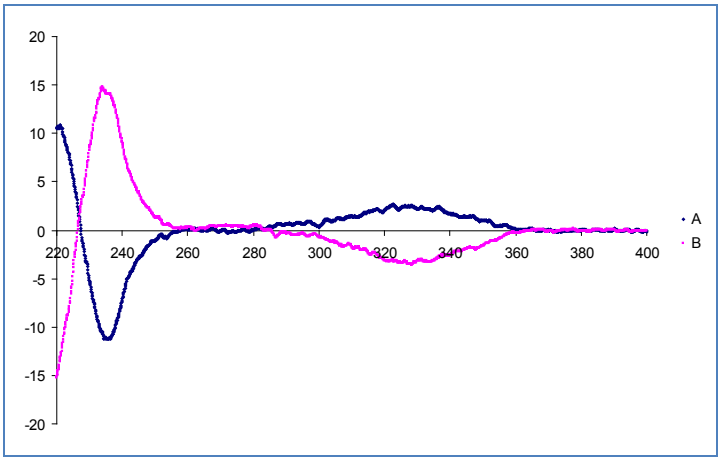

Figure 60: CD spectra of compounds **100A** and **100B**

The absolute configuration of the enantiomers **100A** and **100B** was determined through a methodology reported before; to the firstly eluted enantiomer **100A** the 7*R*,8*R*-configuration was assigned and consequently the secondly eluted enantiomer **100B** has a 7*S*,8S-configuration.

A chiral HPLC analysis confirmed that (±)-**101** is, as expected, a racemic mixture of the (7*S*,8*S*)- and (7*R*,8*R*)-enantiomers; in Figure 61 is reported the HPLC profile obtained on Chiralpak IA column using as hexane:iso-propanol, 10:90. We have separated quantitatively the two enantiomers; the first enantiomer (retention time 14.3 min) was indicated as **101A** and the second (with retention time 18.1 min) was indicated as **101B**.

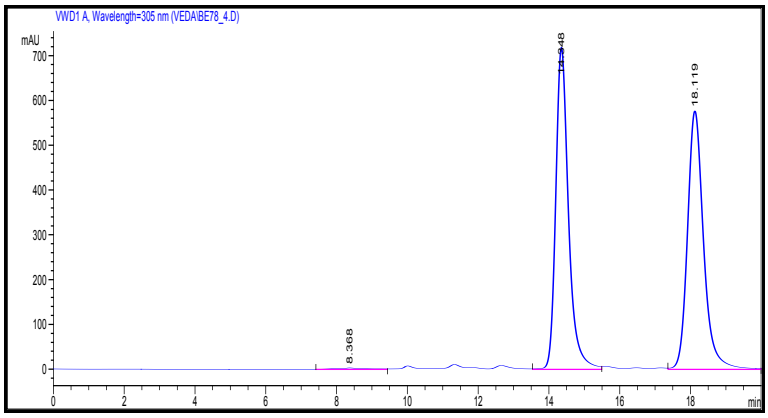

Figure 61: HPLC profile of the racemate (±)-**101**

The pure enantiomers were subjected to Circular Dicroism (CD) spectra; in Figure 62 are reported the spectra of compounds **101A** and **101B**

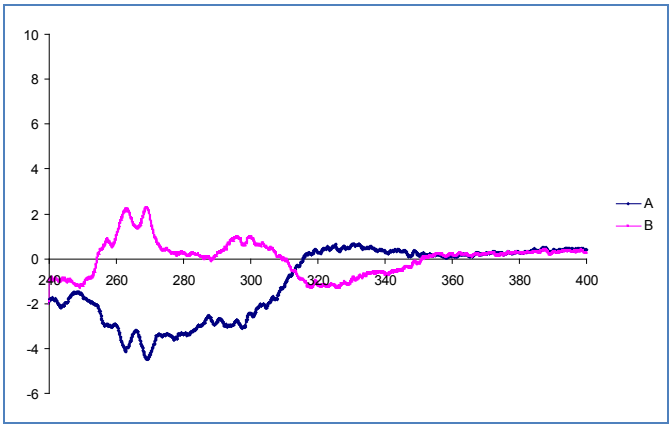

Figure 62: CD spectra of compounds **101A** and **101B**

The absolute configuration of the enantiomers **101A** and **101B** was determined through a methodology reported before; to the firstly eluted enantiomer **101A** the 7S,8*S*-configuration was assigned and consequently the secondly eluted enantiomer **101B** has a 7*R*,8R-configuration.

A chiral HPLC analysis confirmed that (±)-**102** is, as expected, a racemic mixture of the (7*S*,8*S*)- and (7*R*,8*R*)-enantiomers; in Figure 63 is reported the HPLC profile obtained on Chiralpak IA column using as hexane:iso-propanol, 70:30. We have separated quantitatively the two enantiomers; the first enantiomer (retention time 21.0 min) was indicated as **102A** and the second (with retention time 25.1min) was indicated as **102B**.

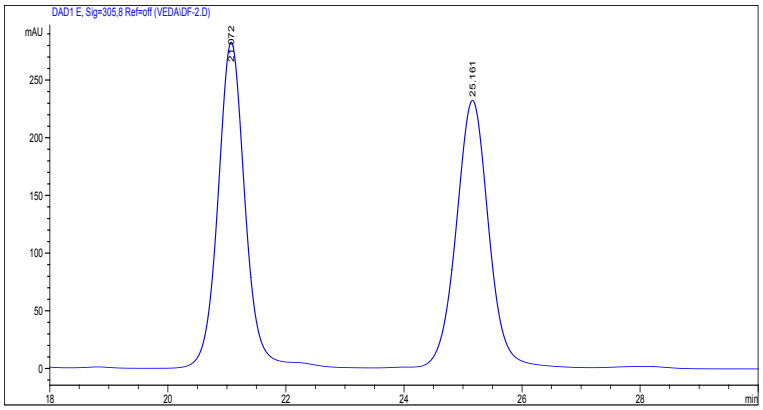

Figure 63: HPLC profile of the racemate (±)-**102**

The pure enantiomers were subjected to Circular Dicroism (CD) spectra; in Figure 64 are reported the spectra of compounds **102A** and **102B**

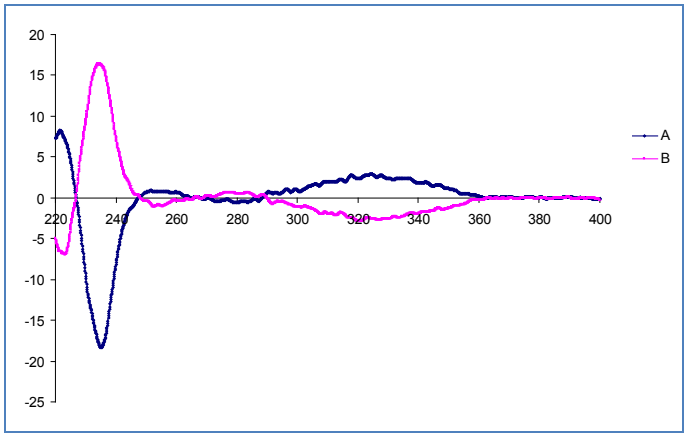

Figure 64: CD spectra of compounds **102A** and **102B.**

The absolute configuration of the enantiomers **102A** and **102B** was determined through a methodology reported before; to the firstly eluted enantiomer **102A** the 7*R*,8*R*-configuration was assigned and consequently the secondly eluted enantiomer **102B** has a 7*S*,8*S*-configuration.

A chiral HPLC analysis confirmed that (±)-**103** is, as expected, a racemic mixture of the (7*S*,8*S*)- and (7*R*,8*R*)-enantiomers; In Figure 65 is reported the HPLC profile obtained on Chiralpak IA column using as hexane:iso-propanol, 40:60. We have separated quantitatively the two enantiomers; the first enantiomer (retention time 13.4 min) was indicated as **103A** and the second (with retention time 16.0 min) was indicated as **103B**.

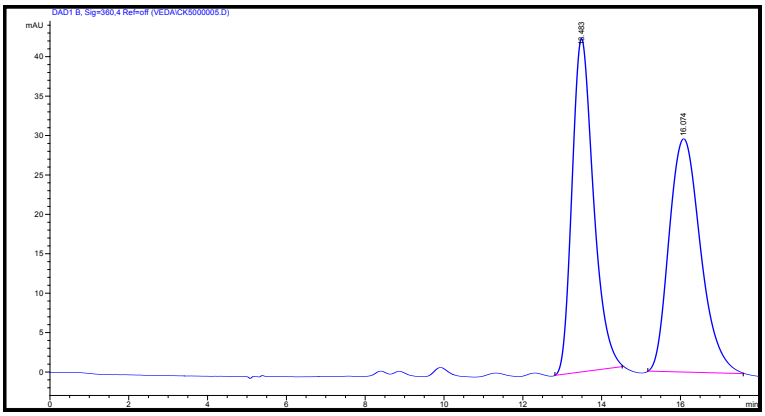

Figure 65: HPLC profile of the racemate (±)-**103**

The pure enantiomers were subjected to Circular Dicroism (CD) spectra; in Figure 66 are reported the spectra of compounds **103A** and **103B**; on the basis of the sign of the CD spectrum, we can now more precisely indicate these enantiomers as 7*R*,8*R*-**103** (corresponding to **103A**) and 7*S*,8*S*-**103** (corresponding to **103B**).

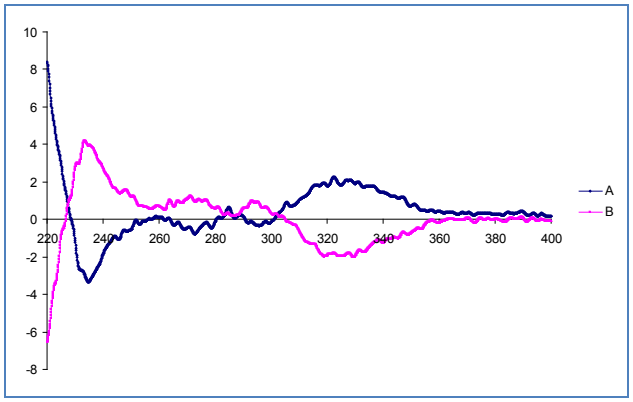

Figure 66: CD spectra of compounds **103A** and **103B**

2.1.4.3 Antiproliferative activity of pure stilbenolignans and SAR

The pure enantiomers were submitted to bioassays for antiproliferative activity towards SW-480 colon carcinoma cells; the results are reported in Table 8 and Graph 3.

Table 8: Antiproliferative activities toward SW480 human colorectal cells

Compounds	IC_{50} (μM) ± SD*
7*R*,8*R*-**99**	20.0 ± 0.4
7*S*,8*S*-**99**	22.5 ± 0.7
7*R*,8*R*-**100**	21.0 ± 0.4
7*S*,8*S*-**100**	35.0 ± 0.8
7*R*,8*R*-**101**	88.1 ± 2.1
7*S*,8*S*-**101**	22.5 ± 0.8
7*R*,8*R*-**102**	73.4 ± 2.3
7*S*,8*S*-**102**	19.9 ± 0.6
7*R*,8*R*-**103**	43.8 ± 1.5
7*S*,8*S*-**103**	24.9 ± 0.9

*IC_{50} calculated after 48 h of treatment; values are the mean (±SD) of three experiments

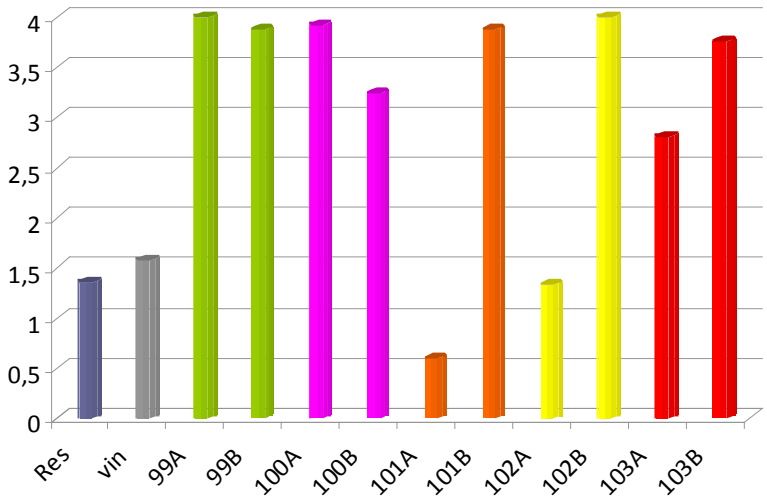

Graph 3

In addition to these data, previous experiments carried out in France and not reported here showed that the OH group in position 4 is of critical importance; when it is replaced with an acetoxy group the activity is lost. In addition, looking to the structures of the two inactive racemates (±)-**104** and (±)-**105** in comparison with those of the five active dimers, it is evident that the presence

of a methoxy function in *ortho* position to the C-4 hydroxy group causes a dramatic reduction of activity. This is of clear evidence from comparison of (±)-**104** with (±)-**102A**. Both these observations points to a probable role of the 4-phenoxy moiety in the interaction with a key enzyme/receptor involved in the control of SW-480 cell growth. Further observations on the structure-activity relationship (SAR) based on the antiproliferative activity data of the pure enantiomers do not lead to simple conclusions: in fact, the most active enantiomers have in three cases the 7*S*,8*S* configuration (namely **101B**, **102B**, and **103B**) and in two cases the 7*R*,8*R* configuration (namely **99A** and **100A**): in addition, the enantiomers 7*R*,8*R*-**99** and 7*S*,8*S* -**99** show comparable IC_{50} values (see Table 8). Interestingly, in two cases, namely **101** and **102** a significant difference is observed between the two enantiomers (see Table 8); this suggests that, at least in some cases, the configuration of the stereogenic centers could have a role.

In conclusion, the following considerations can be made as a basis for possible future studies on these stilbenolignans:

a) all the active dimers results significantly more potent that the reference natural compounds resveratrol (**1**) and ε-viniferin (**24**). This suggest that in addition to a 4-phenoxy function, other structural requirements and probably an higher lipophilic character are necessary for higher activity;
b) the number and position of substituents on the second ring (that not bearing an oxygenated group in C-4) may significantly influence the activity;
c) the configuration of the stereogenic centers may have a role in the activity, at least for dimers where other factors (diffusion, membrane permeability, metabolic stability) result less important.

2.2 Biomimetic synthesis of benzo[*k,l*]xanthene lignans

As reported in the Introduction, Prof. Tringali's group have employed MnO_2 or $Mn(OAc)_3$ as oxidative agents in biomimetic coupling reactions of caffeic acid phenethyl ester (CAPE), according to Scheme 7. This allowed to obtain the new benzo[*k,l*]xanthene lignan **46**, belonging to a rare group of natural products; this compound resulted active toward both on SW480 colon carcinoma (IC_{50} = 2.57 μM) and HepG2 (hepatoblastoma) cancer cells (IC_{50} = 4.76 μM) and is able to interact with DNA both as intercalating agent and minor groove binder. Based on these promising biological properties we attempted to synthesize new benzo[k,l]xanthene lignanamides by oxidative coupling of caffeic amides. To obtain further benzo[*k,l*]xanthene lignans we have synthesized caffeic amides as monomers to be subjected to dimerization (oxidative coupling) in the presence of $Mn(OAc)_3$ as oxidant. The aim of this project is to obtain a library of benzo[*k,l*]xanthene lignanamides to be evaluated for their DNA-interacting and antiproliferative activity.

2.2.1 Synthesis of benzo[*k,l*]xanthene **112**

*2.2.1.1. Step1. Preparation of amide **111***

As first attempt to the direct synthesis of the amide, we used caffeic acid (**7**) and tyramine (**110**) with DMF as primary solvent and dichloromethane as secondary solvent. The complete reaction was carried out in basic conditions; employing triethylamine (TEA) is a base and dicyclohexylcarbodiimide (DCC) as coupling agent.[86] In these conditions we obtained the caffeic *N*-acylurea as major component. (This work is discussed in section 2.3 in detail)

Various attempts to obtain the planned caffeoyl amide were unsuccessful, and only after several modifications of the reaction conditions we could prepare the desired caffeoyl tyramide (**110**) through the protocol reported in Scheme 31,

where the amidation of caffeic acid with tyramine was carried out with good yield (70%) in the presence of BOP reagent with basic NEt_3 condition. The reaction was carried out at 0 ^oC during the first 30 min, in the course of addition of BOP reagent in CH_2Cl_2 solution, and subsequently stirred at room temperature for 24 hrs. Caffeic amide **111** was obtained by column chromatographic purification. The ^1H and ^{13}C NMR spectra are in agreement with reported literature[87] data and reported in Figure 67 and 68.

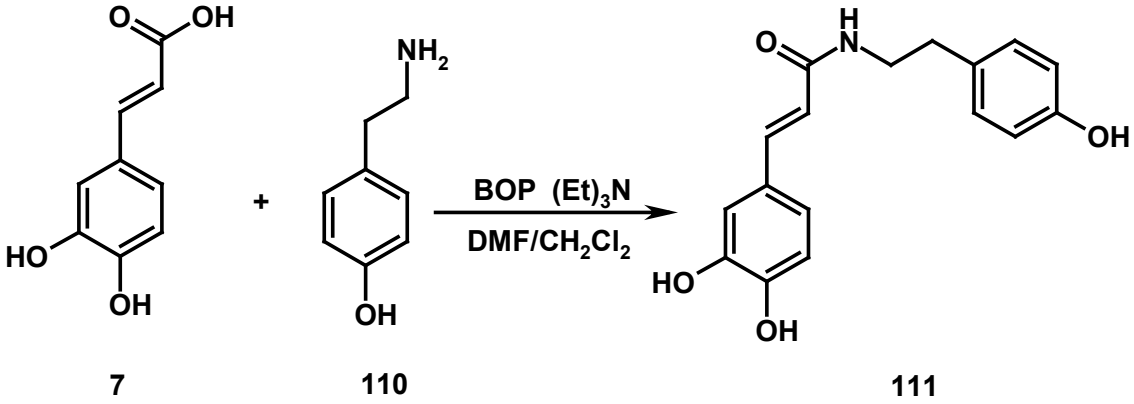

7 110 111

Scheme 31

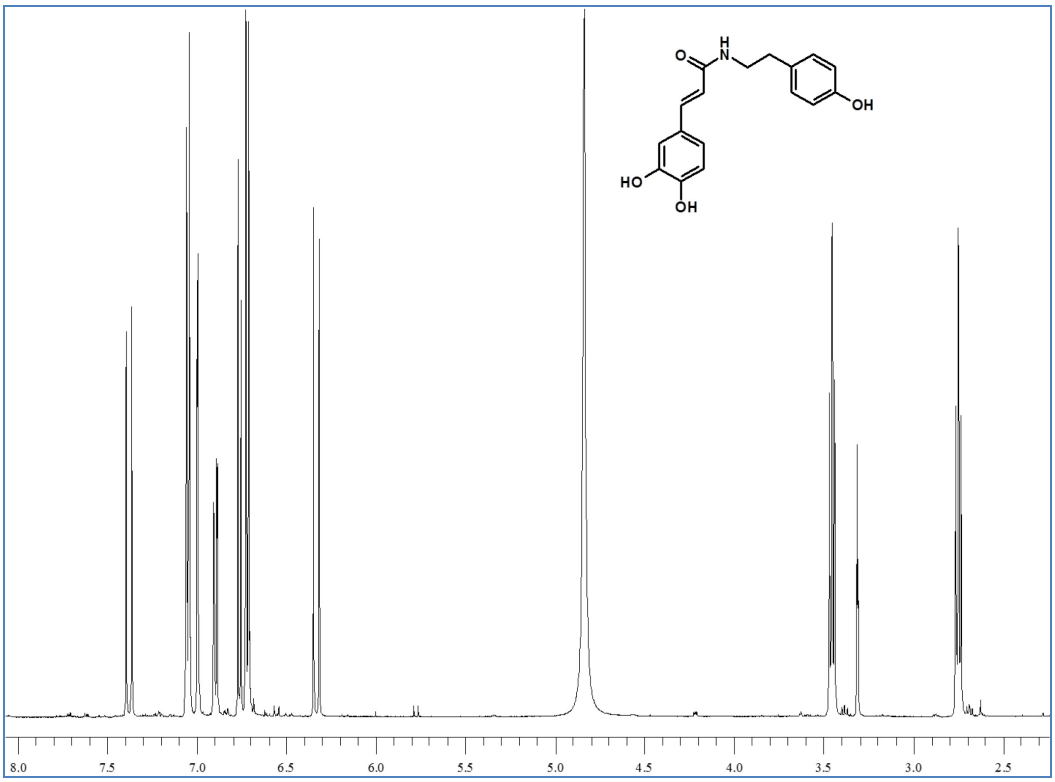

Figure 67: ^1H NMR of compound **111**

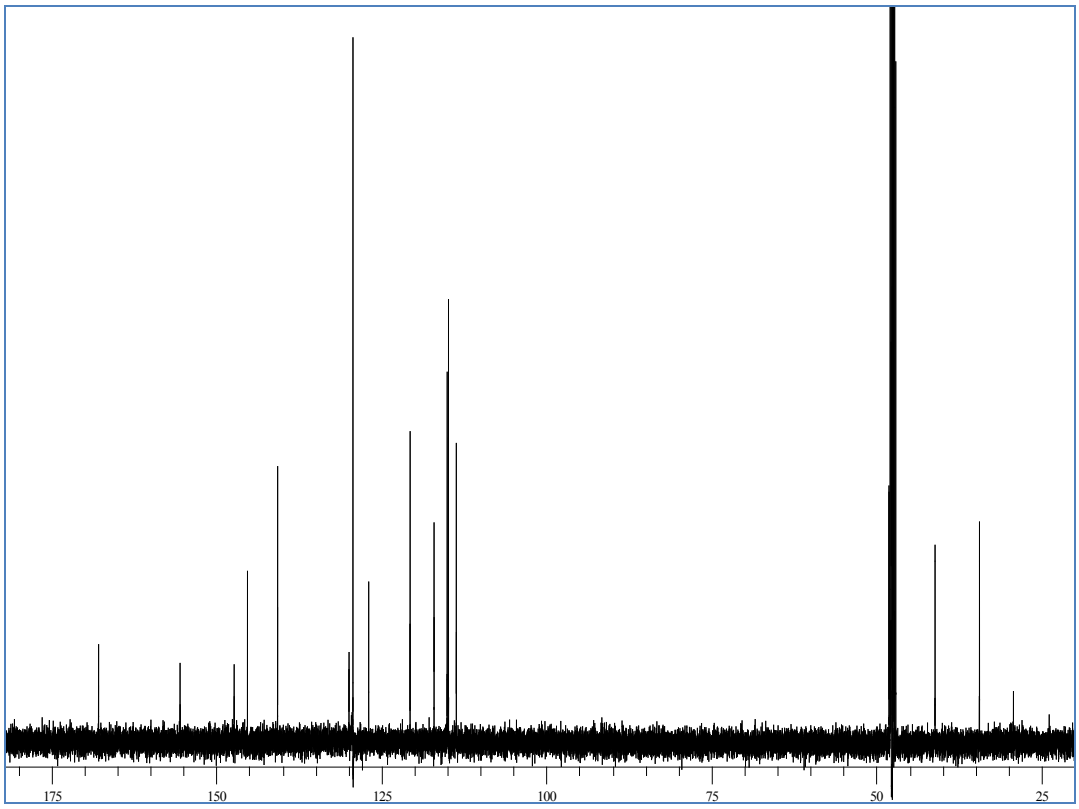

Figure 68: ^{13}C NMR of compound **111**

*2.2.1.2 Step2. Preparation of compound **112***

Since **111** is poorly soluble in non-polar, low dielectric constant solvents like $CHCl_3$ and CH_2Cl_2 it was not possible to carry out the coupling reaction in the same conditions used for compound **9**,[49] so we tried to carry out the reaction in various solvents, namely: DMF, DMF:$CHCl_3$, MeOH:$CHCl_3$, Pyridine:$CHCl_3$ or EtOH. The best conditions were obtained with $Mn(OAc)_3$ in DMF:$CHCl_3$ or in EtOH, and the product was recovered with 20% and 30% yield, respectively (Scheme 32).

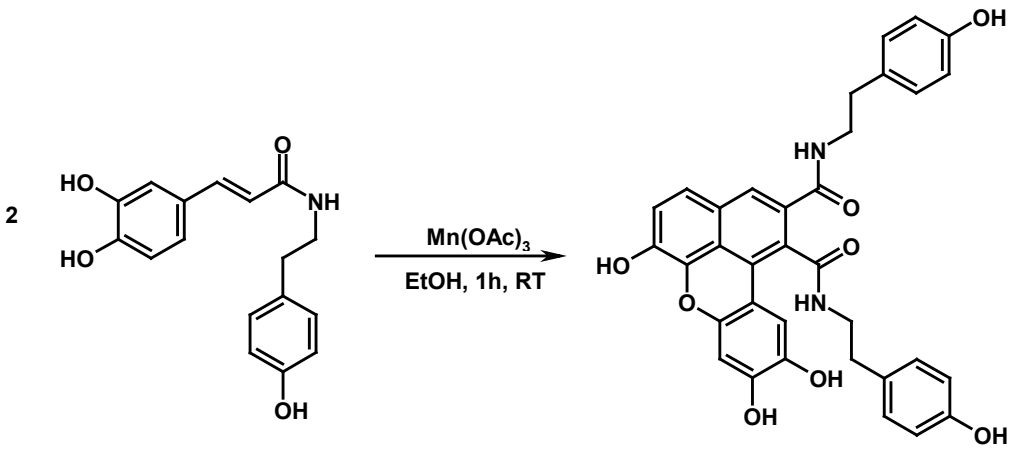

111 112

Scheme 32

The structure of this product has not been previously reported, so we employed Mass spectrum, reported in Figure 69, shows a negative ESI-MS peak at *m*/*z* 591.3 $[M-H]^-$ confirms the formation of dimer with molecular formula$C_{34}H_{28}N_2O_8$; the ^1H and ^{13}C NMR to assign proton signals on the basis of previously established structure **46**; the ^1H, ^{13}C NMR (Table 9), COSY and HSQC spectra are reported in Figure 70, 71, 72 and 73 respectively .

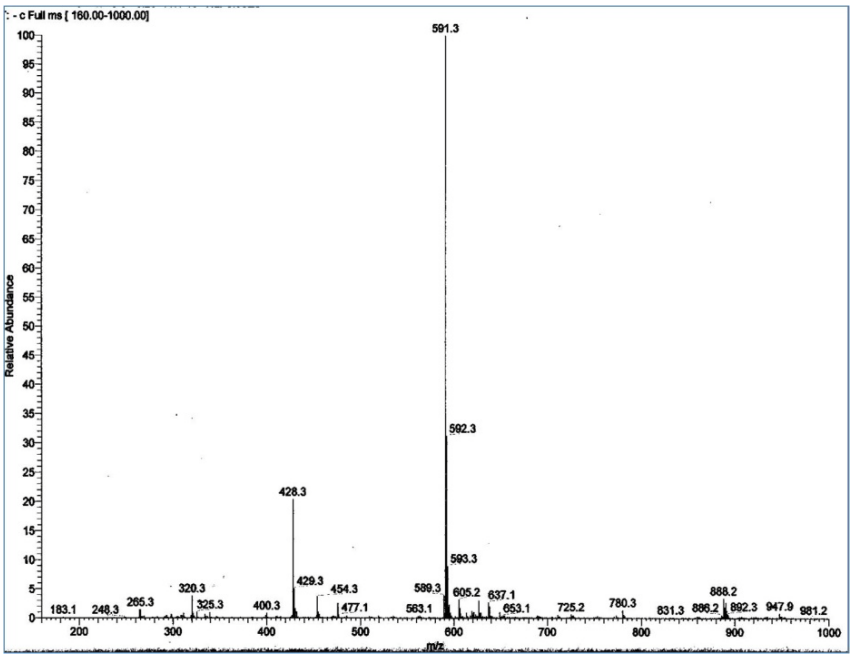

Figure 69: Mass spectra of **112**

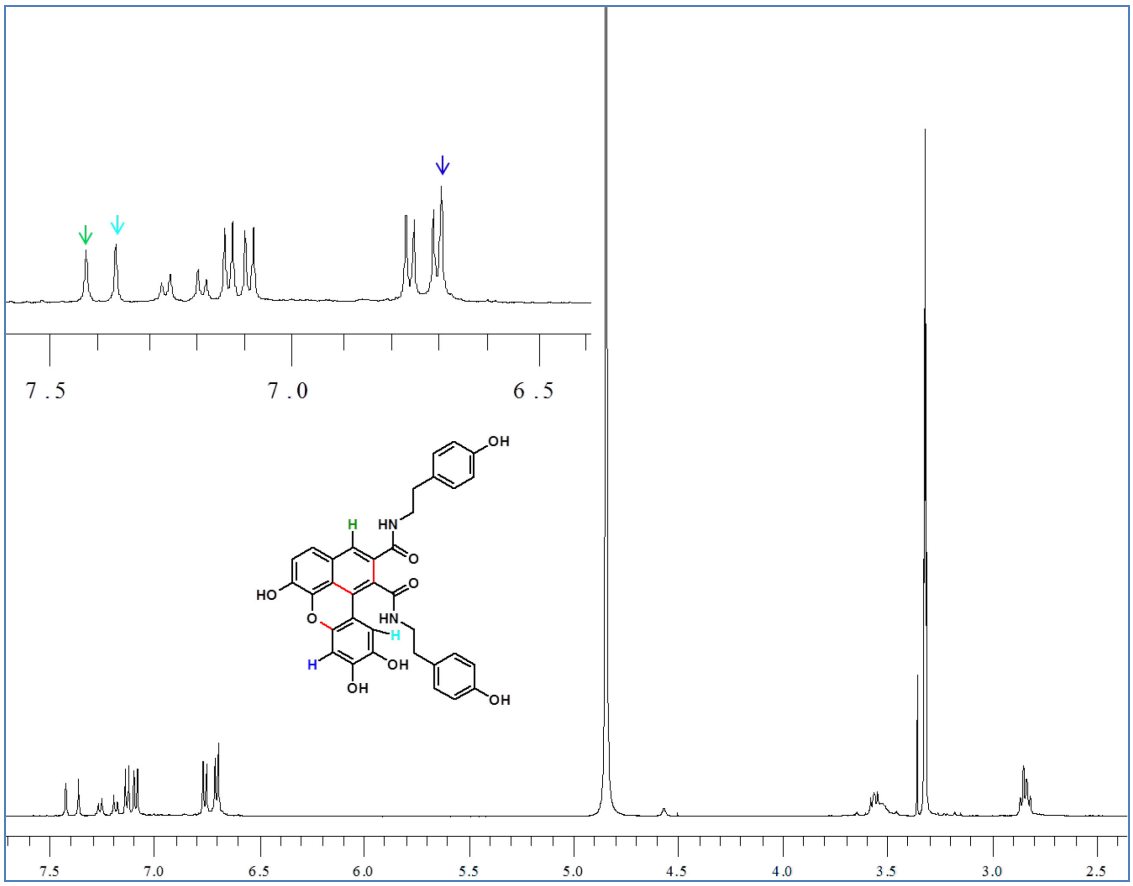

Figure 70: ^{1}H NMR spectrum of **112**

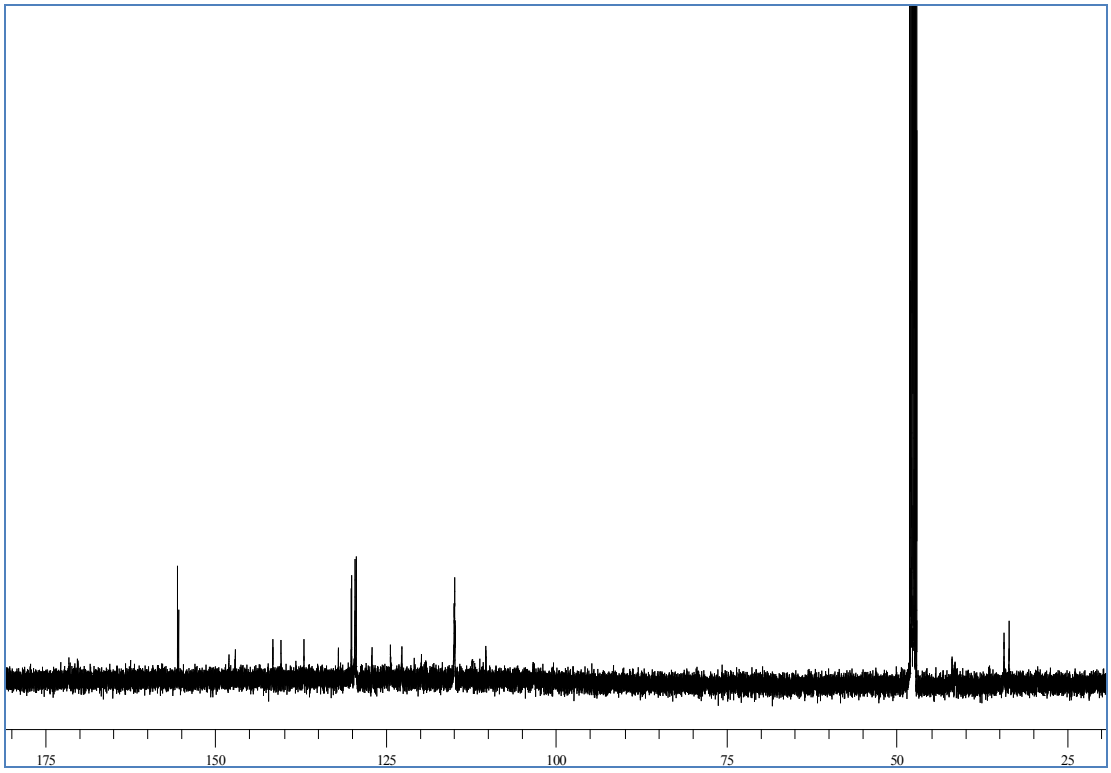

Figure 71: ^{13}C NMR spectrum of **112**

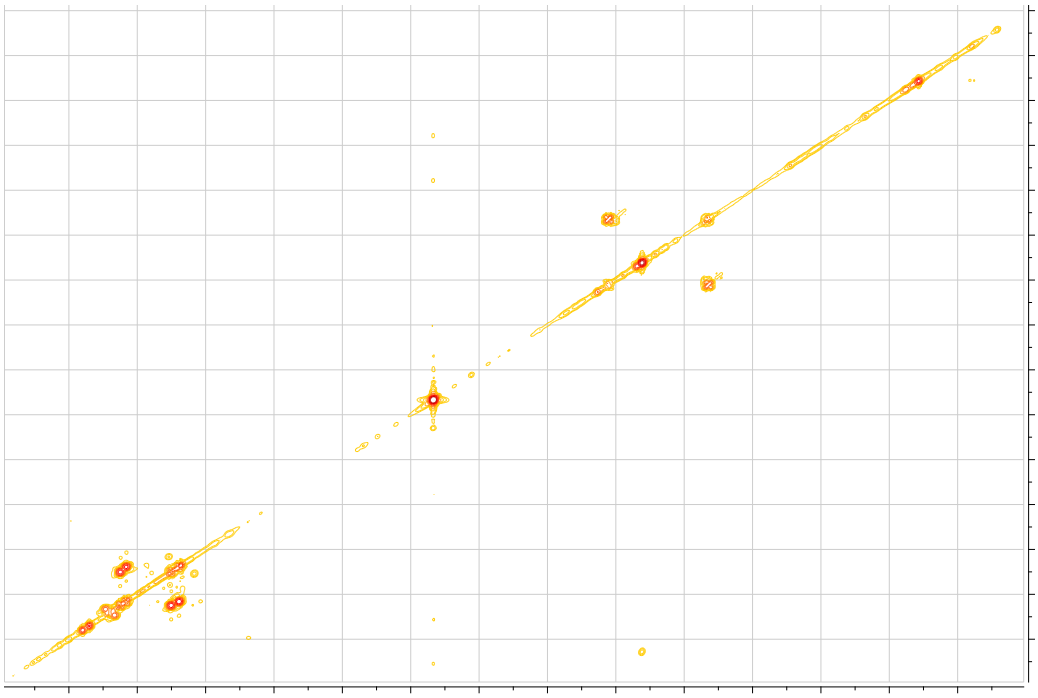

Figure 72: COSY spectrum of **112**

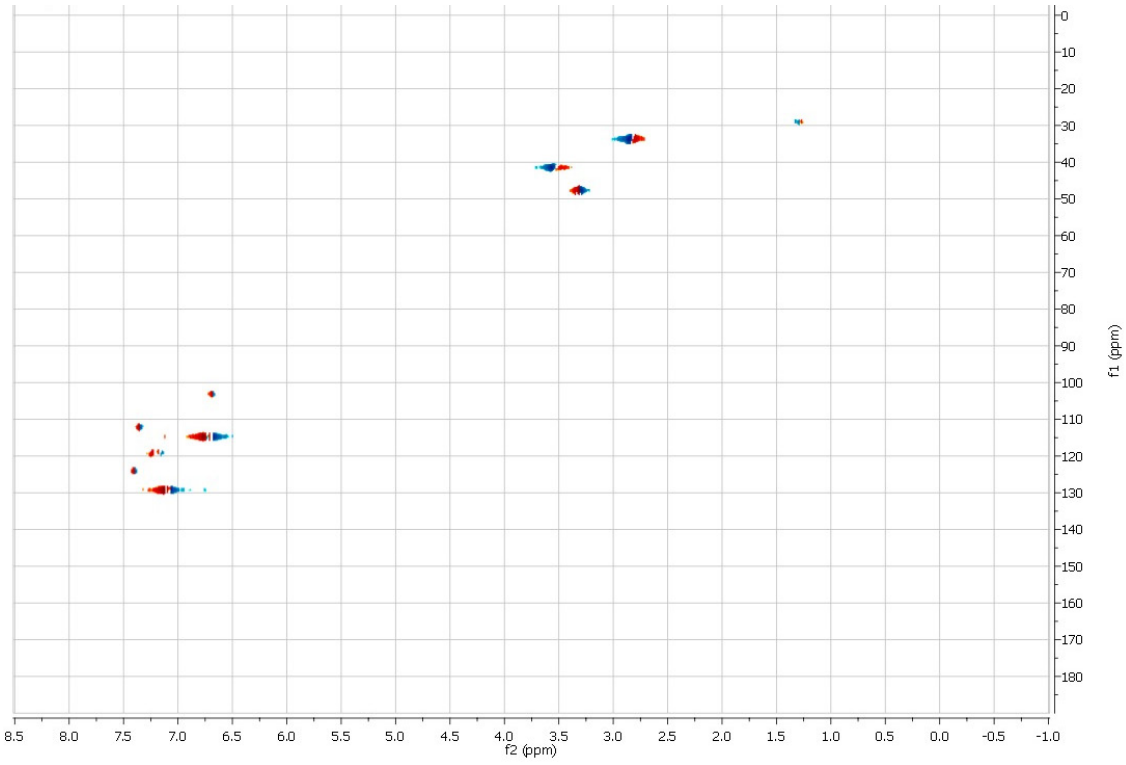

Figure 73: HSQC spectrum of **112**

Table 9: ^{1}H NMR and ^{13}C NMR data of compound **112**

H	δH (mult, J Hz, nH) in CD_3OD	C	δC in CD_3OD
		C-1	131.9
		C-2	122.6
		C-3	129.9
H-4	7.42 (s, 1H)	C-4	124.19
H-5	7.26 (d, 8.5, 1H)	C-5	124.2
H-6	7.19 (d, 8.5, 1H)	C-6	119.7
		C-7	141.5
		C-8	136.9
		C-9	119.0
		C-10	127.0
		C-1’	112.2
		C-2’	148.0
H-3’	6.69 (bs, 1H)	C-3’	103.3
		C-4'	147.0
		C-5'	140.3
H-6’	7.36 (s, 1H)	C-6'	110.2
		C-1''	129.4
H-(2-6)’’	7.08 (d, 8.7, 2H)	C-2’’,6’’	129.3
H-(3-5)’’	6.70 (d, 8.0, 2H)	C-3’’,5’’	114.8
		C-4’’	155.5
H-7’’	3.55 (t, 7.5, 2H)[#]	C-7’’	41.4
H-8’’	2.82 (q, 7.5, 2H)	C-8’’	33.5
		C-9’’	171.4
		C-1’’’	129.4
H-(2-6)’’’	7.13 (d, 8.7, 2H)	C-2’’’,6’’’	129.3
H-(3-5)’’’	6.75 (d, 8.0, 2H)	C-3’’’,5’’’	114.8
		C-4’’’	155.3
H-7’’’	3.55 (t, 7,5, 2H) [#]	C-7’’’	41.8
H-8’’’	2.82 (q, 7.5, 2H)	C-8’’’	33.2
		C-9'''	170.2

[#] overlapped with broad signall due to OH group

The ^{13}C NMR spectrum shows 26 signals: the majority of the signals were in the sp^2 region (from δ 171.4 to 103.3 ppm) and four aliphatic carbon signals in the upper field region of the spectra (δ, 33.2, 33.5, 41.4, and 41.8). In the sp^2 region there are 14 quaternary carbon signals and 8 CH signals, in particular there are two signals due to two carbonyl carbons (171.4 and 170.2 ppm) and

seven signals at 155.5, 155.3, 148.0, 147.0, 141.5, 140.3, 136.9 ppm due to oxygenated carbon sp^2. Remaining all aromatic signals are comparable with similar dimer **50**.

^{1}H NMR suggest the absence of large coupling constant two *trans* olefinic protons (α,β-unsaturated), refers that formation of a dimer which is not belongs to dihydrobenzofuran neolignans such as (±)-**52**. The ^{1}H NMR spectrum of **112** in the region from δ 7.42 and 6.69 ppm shows clear similarities with the spectra of the previously discussed benzo[*k,l*]xanthene **50** lignan. Both spectra showed part of the signals attributable to two not equivalent hydroxyphenethyl moieties; in fact there are four doublets at δ = 7.08 and 7.13, J = 8.75 Hz and δ = 6.70 and 6.75, J = 8.0 (eight aromatic AA'BB' protons) due to two hydroxyphenethyl moiety. In addition there are two doublet for proton H-5 (7.26, J = 8.5 Hz) and H-6 (7.19, J = 8.5 Hz) and three singlets (7.42, 7.36, 6.69 ppm this latter partially overlapped with doublet at 6.70 ppm) due to H-4, H-3', H-6' protons. Remaining upper field triplets are due to eight protons at δ = 2.83 and δ = 3.50. COSY correlation was observed between the two doublet signals at δ 7.26 and 7.19 ppm assigned to a two-proton AB system in ring A (Figure 74). In ring E and F two signals are observed of AA'BB' protons with doublet at δ 7.08 is correlated with 6.70 ppm and at δ 7.13 is correlated with 6.75 ppm of two tyramine rings. In COSY spectrum it was also observed that correlation between two quartet at δ 2.82 and at δ 3.55 ppm which are assigned to two -CH_2CH_2- group.The ^{13}CNMR chemical shift analysis and HSQC, HMBC spectrum indicated that three carbons of one ring connected to three oxygen atoms (D ring) and two carbons of another ring connected to two oxygen atoms (A ring).

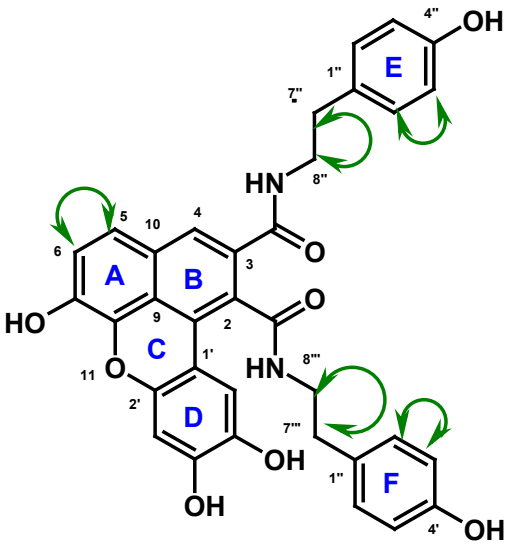

Figure 74: COSY correlation of **112**

2.2.2 Synthesis of benzo[*k,l*]xanthene **115**

*2.2.2.1. Step1. Preparation of amide **114***

Caffeic acid **7** was coupled with diethyl amine **113** in the presence of benzotriazole-1-yl-oxy-tris-(dimethylamino)-phosphonium hexafluorophosphate (BOP reagent) as coupling agent and triethylamine as base with DMF/CH_2Cl_2 as solvent (Scheme 33).

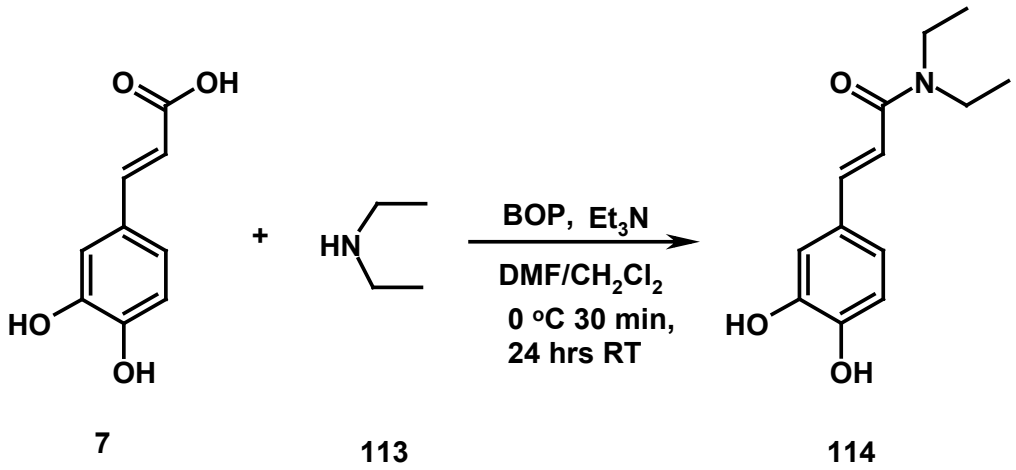

7 113 114

Scheme 33

The reaction was carried out at 0 ^oC during the first 30 min, in the course of addition of BOP reagent in CH_2Cl_2 solution, and subsequently stirred at room temperature for 24 hrs. Caffeic amide **114** was obtained by column

chromatographic purification. The ^{1}H and ^{13}C NMR spectra are in agreement with reported literature data.[88]

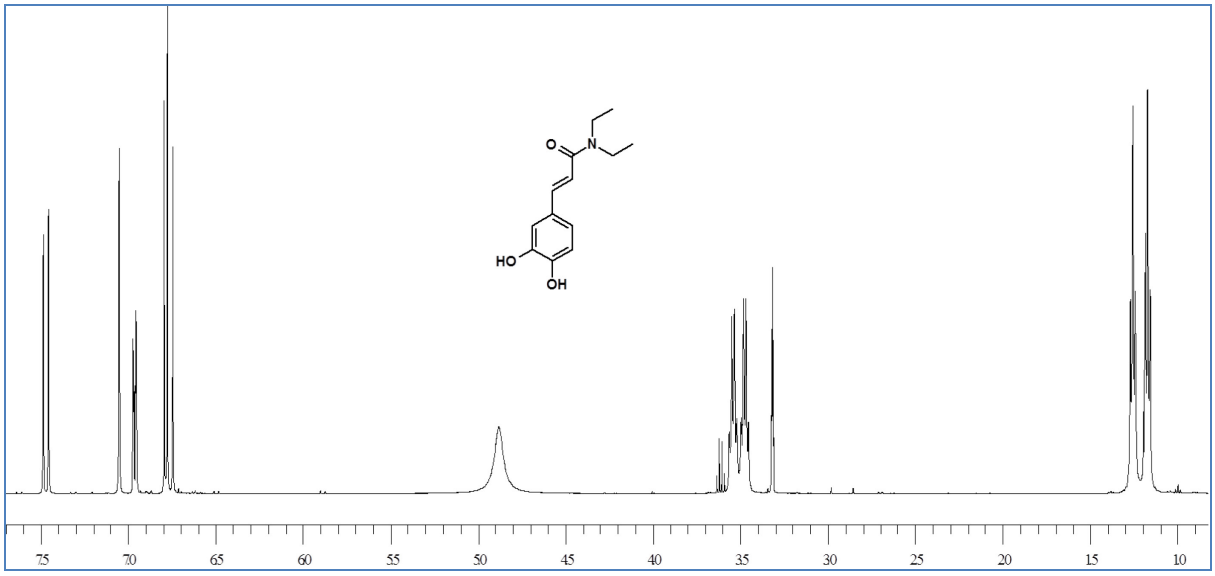

Figure 75: ^{1}H NMR spectrum of **114**

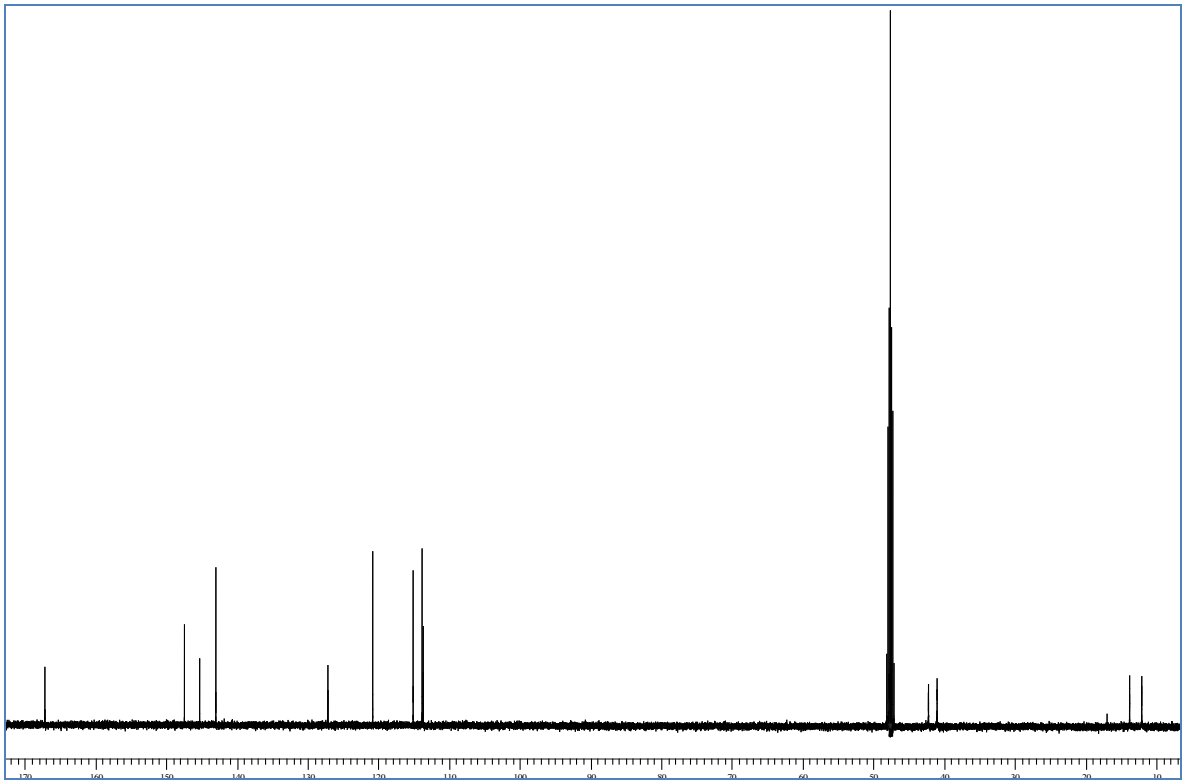

Figure 76: ^{13}C NMR spectrum of **114**

*2.2.2.2 Step2. Preparation of compound **115***

Caffeic amide **114** was subjected to dimerization in the presence of $Mn(OAc)_3$ with CH_2Cl_2 solvent: in these conditions, very poor conversion of substrate into product was observed, probably due to scarce solubility of the starting material in CH_2Cl_2. So, the same reaction was carried out in EtOH solvent (Scheme 34); this reaction gave complete conversion of substrate into products within one hour. By increasing the reaction time we observed more polar spots on TLC. The dimer **115**, followed under 366 nm UV light as highly greenish fluorescent compound, was obtained by silica gel column chromatography.

The structure of the dimer **115** has not been previously reported, so we employed both mono and two-dimensional NMR methods (COSY, HSQC and HMBC) to establish the structure and achieve a complete assignment of all the NMR signals independently from previously reported data. The ^{1}H and ^{13}C NMR spectra are reported in Figure 77 and 78 , respectively, and (Table 10); assignments were aided by the careful analysis of COSY, HSQC and HMBC spectra, reported in Figure 79, 80 and 81 respectively.

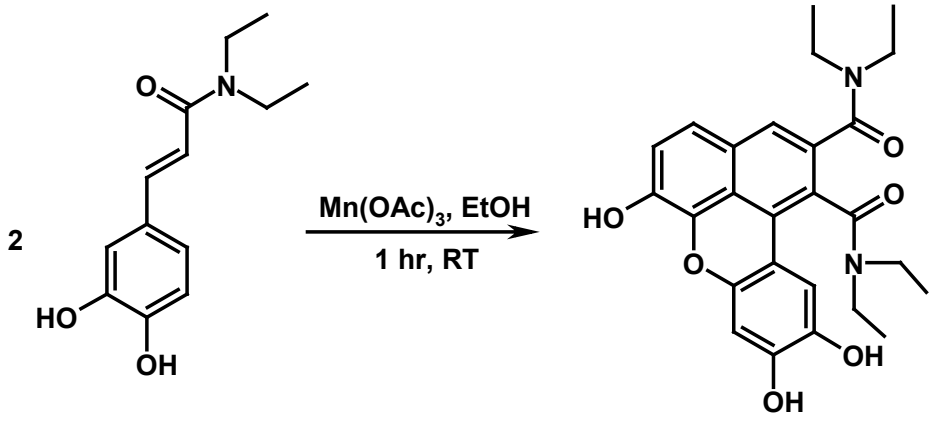

Scheme 34

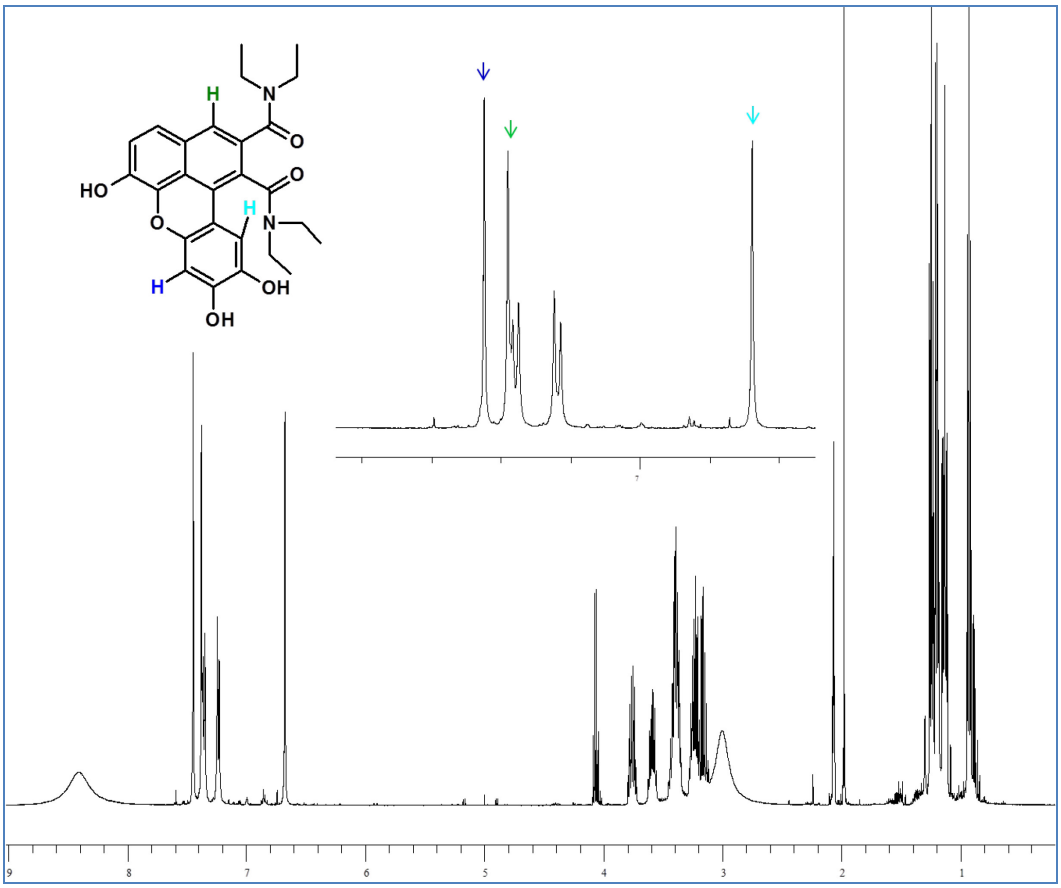

Figure 77: ^{1}H NMR spectrum of **115**

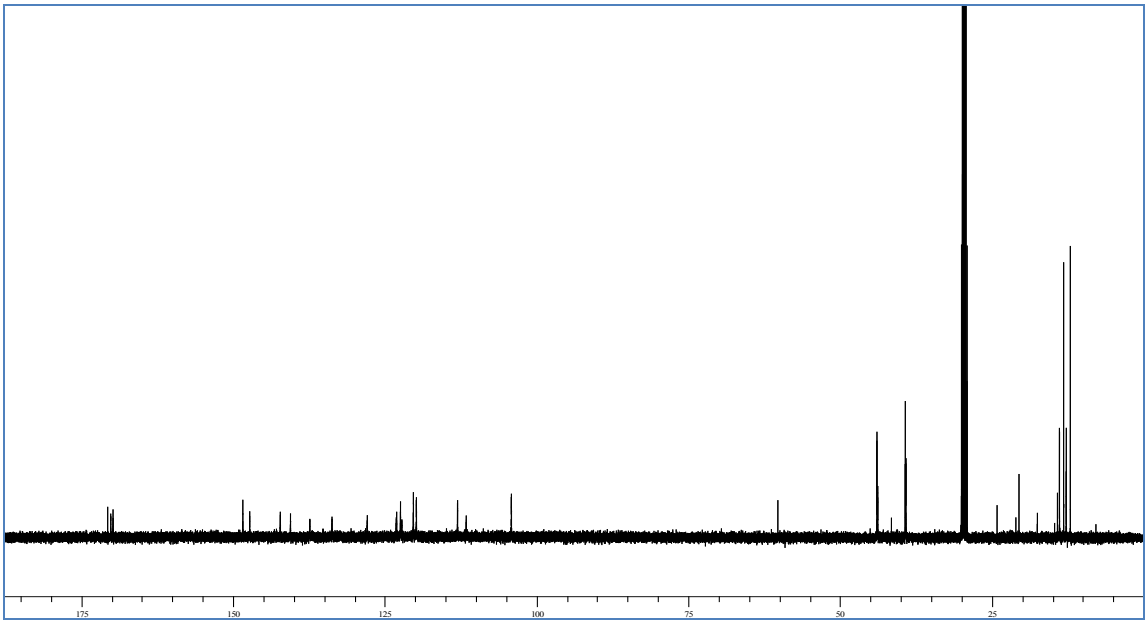

Figure 78: ^{13}C NMR spectrum of **115**

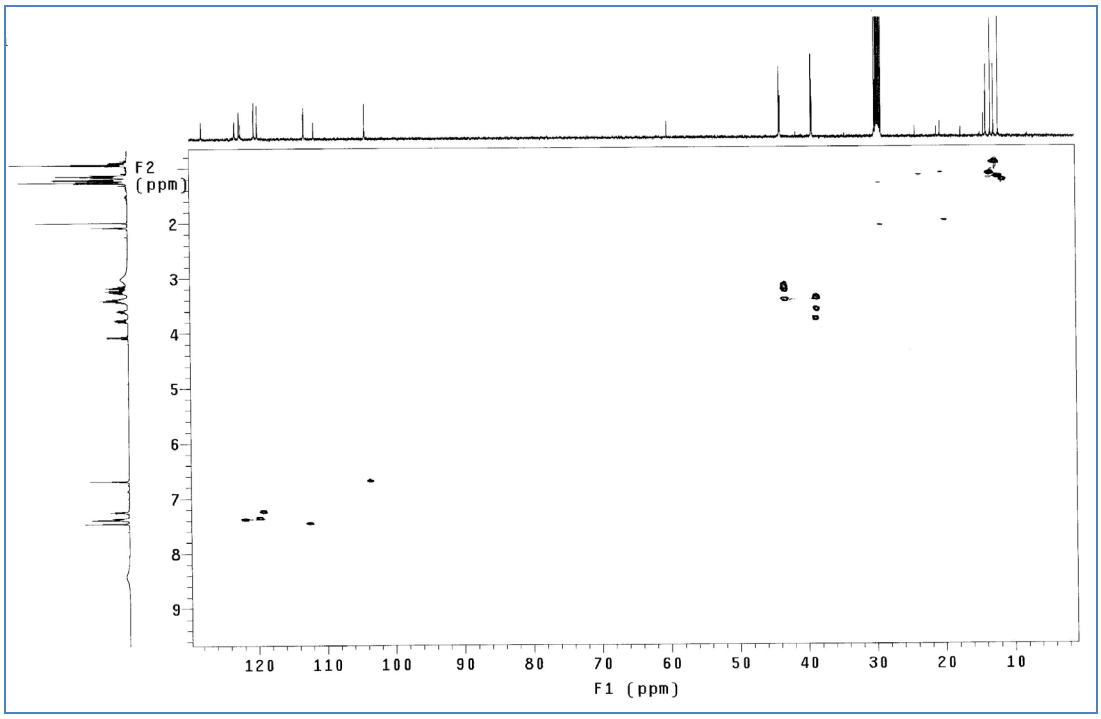

Figure 80: HSQC spectrum of compound **115**

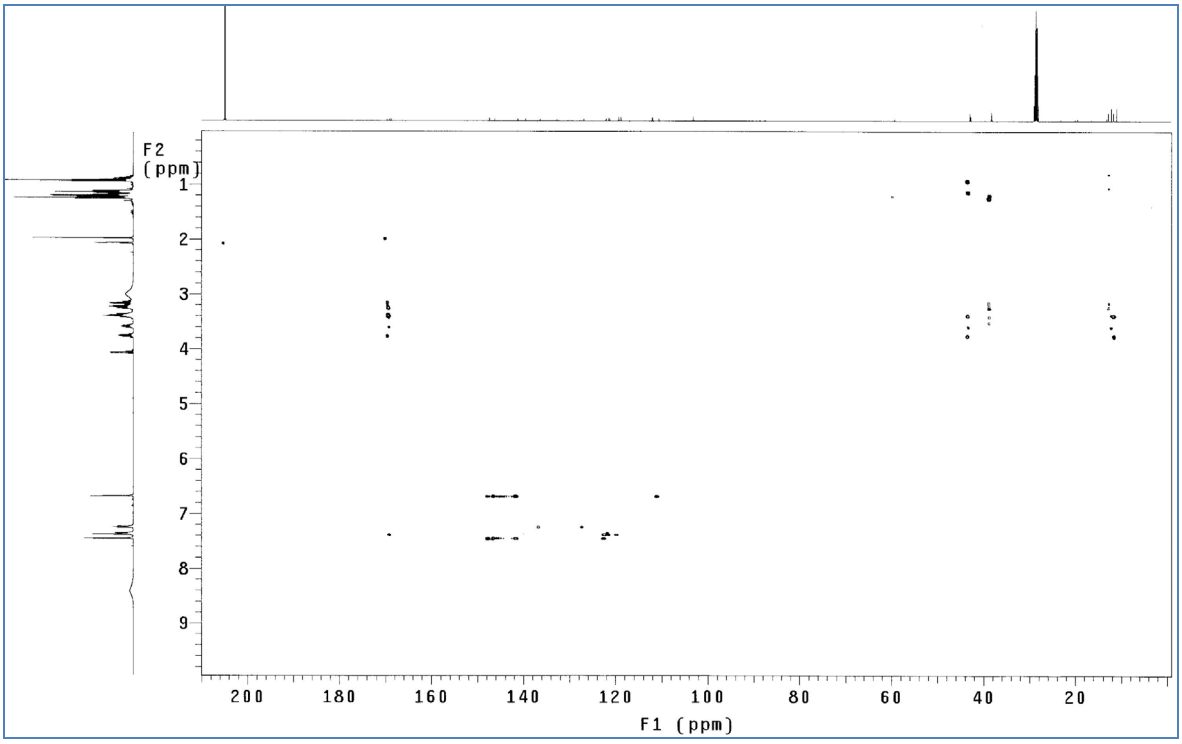

Figure 81: HMBC spectrum of compound **115**

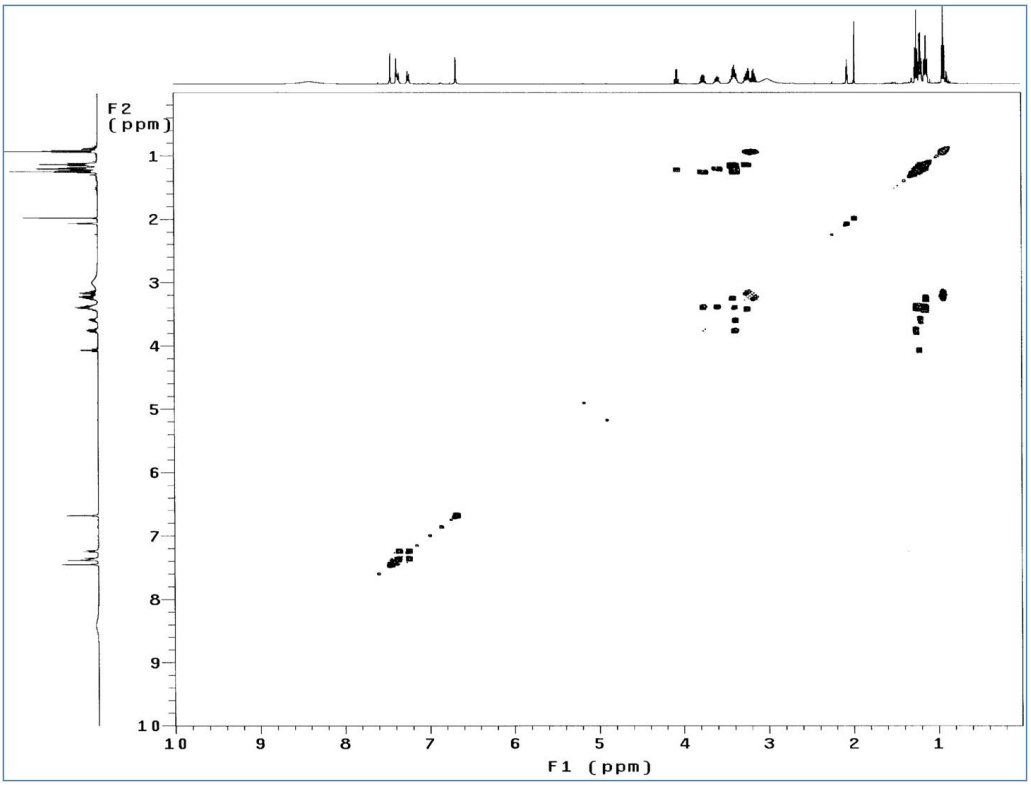

Figure 79: COSY spectrum of compound **115**

Table 10: ^{1}H and ^{13}C NMR spectral data of compound **115**

C	δ_C in Acetone-D_6	H	δ_H (mult, JHz) in Acetone-d_6
C-1	123.1		
C-2	133.7		
C-3	123.0		
C-4	122.4	H-4	7.37 (s, 1H)
C-5	120.3	H-5	7.34 (d,9.5, 1H)
C-6	119.8	H-6	7.24 (d,8.5, 1H)
C-7	140.5		
C-8	137.3		
C-9	122.2		
C-10	127.9		
C-1’	111.6		
C-2’	142.2		
C-3’	104.1	H-3’	6.67 (s, 1H)
C-4'	148.4		
C-5'	147.2		
C-6'	113.0	H-6’	7.44 (s, 1H)
C-1''	39.2	H-1’’	3.76 (m, 2H)
C-2’’	12.7	H-2’’	1.13 (t, 7.0, 3H)
C-3’’	43.8	H-3’’	3.40 (m, 2H)
C-4’’	13.8	H-4’’	1.24 (t, 7.0, 3H)
C-1’’’	39.1	H-1’’’	3.58 (m, 2H)
C-2’’’	13.2	H-2’’’	1.19 (t, 7.0, 3H)
C-3’’’	43.9	H-3’’’	3.23 (m, 2H)
C-4’’’	12.0	H-4’’’	0.92 (t, 7.0, 3H)
C-9’	169.7		
C-9’’	170.1		
		OH	8.41 (bs)
		OH	3.01 (bs)

The ^{13}C NMR spectrum showed 26 signals: the majority of the signals were in the sp^2 region (from 170.0 to 104.1 ppm), but eight ethyl signals in the upper field region of the spectra (43.9 to 12.0 ppm) were observed, suggesting the formation of a dimer. In the sp^2 region there are 13 quaternary carbon signals, 5 CH signals were observed suggest that loss of hydrogen from one caffeic acid ring moiety. ^1H NMR suggest the absence of large coupling constant two *trans* olefinic protons, refers that formation of a dimer which is not belongs to dihydrobenzofuran neolignan such as (±)-**52**.

The ^1H NMR spectrum of **115** in the region from 7.44 and 6.67 ppm shows clear similarities with the spectra of the previously discussed benzoxanthene (**112**) lignans with the absence of tyramine ring moiety. And ^{13}C shows two carbonyl carbons at δ 169.7 and 170.0 in complete lower field of the spectra, which suggested that obtained product is dimer. For the complete structural elucidation was made on the basis of 1D and 2D NMR spectra as following below.

COSY correlation was observed between the two doublet signals at δ = 7.24 and 7.34 ppm assigned to a two-proton AB system (Figure 82a). Between the four multiplet and four triplets of aliphatic chains integrated to twenty protons in upper field of the spectra are observed in COSY correlation (Figure 82b). The ^{13}C NMR chemical shift analysis and HSQC, HMBC spectrum indicated that three carbons of one ring connected to three oxygen atoms (D ring) and two carbons of another ring connected to two oxygen atoms (A ring).

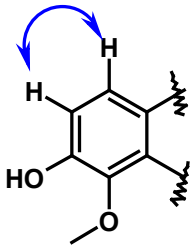

Figure 82 a

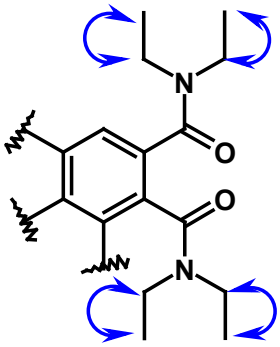

Figure 82 b

In ^{1}H NMR spectra three singlet were observed in low field region and are integrated to three hydrogens, with the help of HSQC and HMBC (Figure 83) correlation these hydrogens are assigned to H-4 at δ = 7.37 which is correlated to carbon C-4 at δ = 122.4 in ring B, and H-3', H-6' at δ 6.67, 7.44 which are correlated to C-3', C-6' at δ 104.1, 113.0 carbons respectively in ring D. It was also observed clear correlation of carbon to hydrogen in ring D, C-1', C-2', C-4', C-5' to H-3', and C-4', C-5', C-2', C-1 to H-6'. Similarly in ring A, C-10, C-8, C-7, to H-6, and C-10, C-4 to H-5 shows A ring is fused with B ring. Very small although visible correlation of C-3, C-9' to H-4 gives the carbonyl function fused to ring B. And C-9', C-9'' to -CH_2CH_3 chains correlations shows the connection between benzoxanthene scheleton and aliphatic pendant. Figure 83 shows the selected HMBC correlation of dimer benzo[*k,l*]xanthene lignan **115**.

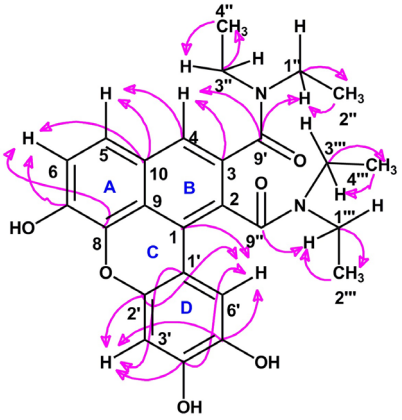

Figure 83: Selected HMBC correlation of **115**

2.2.3 Synthesis of benzo[*k,l*]xanthene **118**

*2.2.3.1 Step 1. Preparation of amide **117***

Caffeic acid **7** was coupled with *n*-butyl amine **116** in the presence of BOP reagent as coupling agent and triethylamine as base with DMF and CH_2Cl_2 solvent system (Scheme 35). The reaction was carried out in 0 ^oC for first 30 min in the course of addition of BOP reagent which is solubilised in CH_2Cl_2 and subsequently stirred at room temperature for 24 hrs. A secondary caffeic amide **117** was obtained by column chromatographic purification.

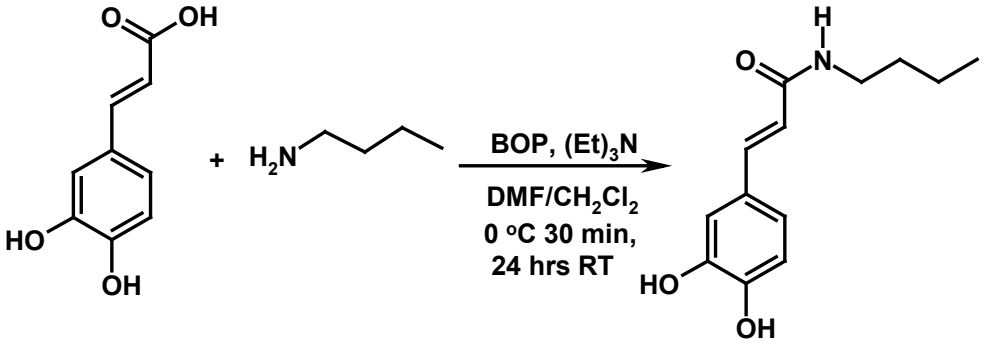

7 **116** **117**

Scheme 35

The complete characterization of the compound **117** has been carried out by ^1H NMR and ^{13}C NMR spectroscopy. ^1H NMR (Figure 84) suggests that in the low field there are five signals, which have integrated to five hydrogens. Two doublet signals at δ 7.40 and 6.38 with large coupling constant 15.75 Hz gives two olefinic α,β-unsaturated hydrogens, and reaming three signals integrated to three hydrogens, one is double of doublet at δ 6.89 with coupling constants 8.5 and 2.0 Hz, and other two hydrogens are doublets with coupling constant 8.5 and 2.0 Hz at δ 7.01 and 6.77 respectively (caffeic ring moiety). One broad singlet, which is integrated to three hydrogens: one amide (-NH) and two hydroxy (-OH) functions, was observed at δ 4.89. In the upper field was observed a triplet at δ 0.94 (J = 7.5 Hz), which is integrated to three hydrogens

assign to –C<u>H</u>$_3$ function of butyl chain. Reaming three signals at δ 3.26 (t), δ 1.50 (p) and δ 1.40 (sex) in upper field of the spectra are integrated to six hydrogens which are assign to -C<u>H</u>$_2$ function of butyl chain. ^{13}C NMR (Figure 85) shows 13 signals in particular 9 signals are in sp^2 region (from at δ 169.2 to δ 115.0) and four signal (40.2, 32.5, 21.1 and 14.0 ppm) in are in sp^3 region. These latter have been assigned to butyl chain carbons (-<u>C</u>H$_2$-<u>C</u>H$_2$-<u>C</u>H$_2$-<u>C</u>H$_3$) and the signal at δ 169.2 has been assigned to carbonyl carbon (<u>C</u>=O), the remaing signals are due to aromatic ring and double bond (caffeic moiety).

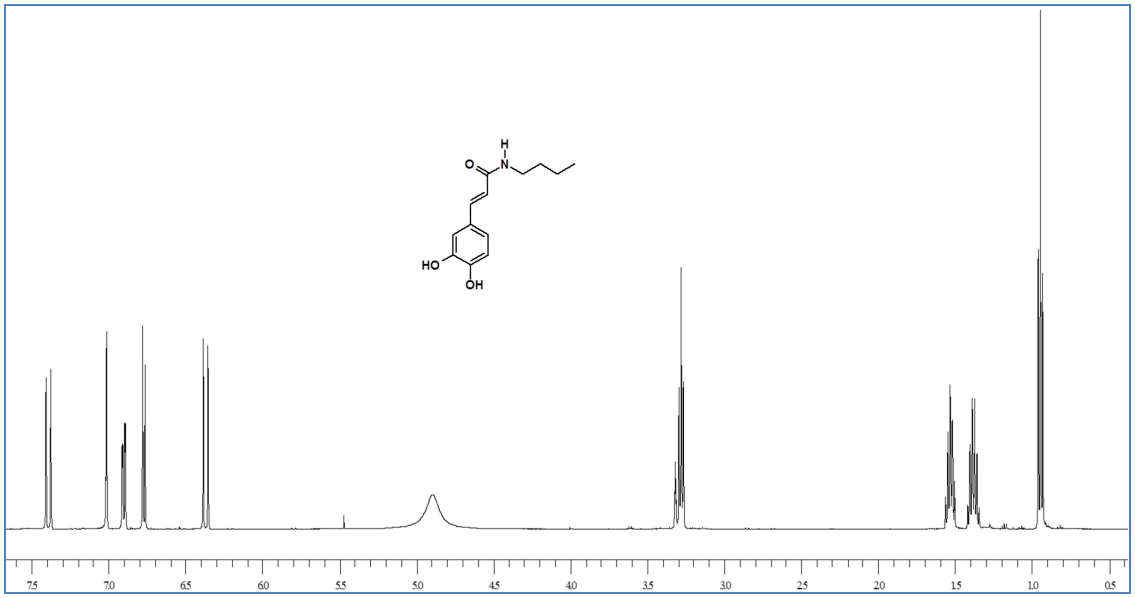

Figure 84: ^{1}H NMR spectra of compound **117**

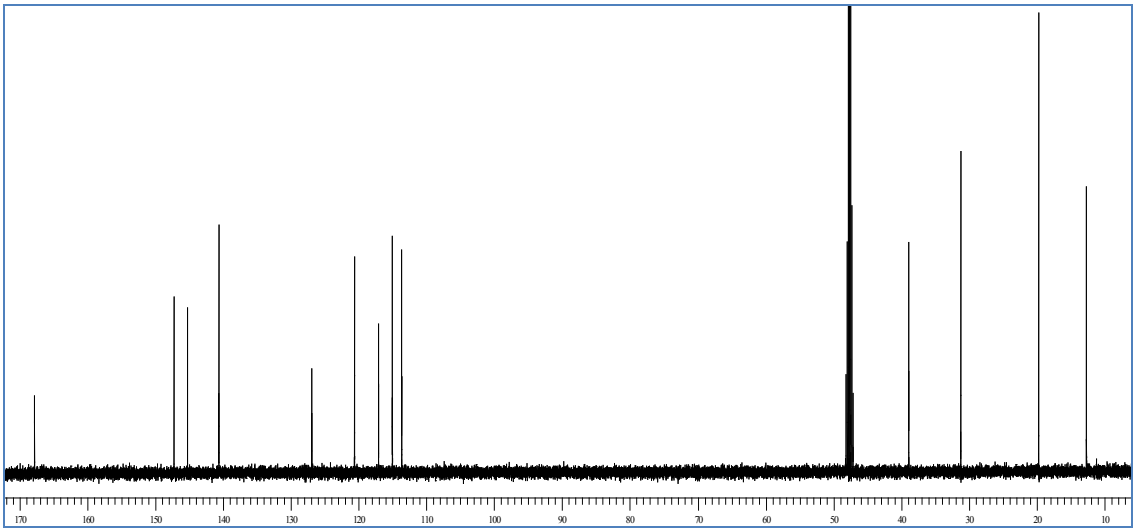

Figure 85: ^{13}C NMR spectra of compound **117**

*2.2.3.2 Step2. Preparation of compound **118***

Secondary caffeic amide **117** was subjected to dimerization in the presence of $Mn(OAc)_3$ in EtOH solvent (Scheme 36), this reaction gives complete conversion of substrate in to products within one hour. By increasing the reaction time we observed more polar spots on TLC. The dimer **118** is highly greenish fluorescent (under 366 nm UV light) compound obtained by silica gel column chromatography.

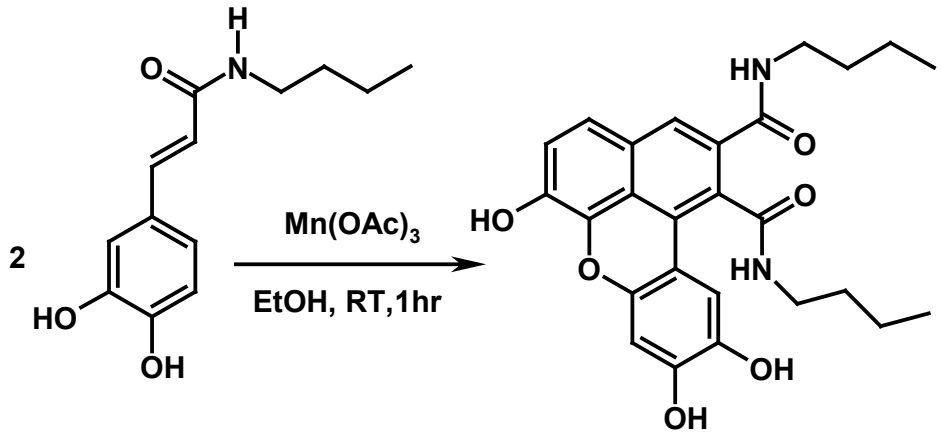

117 **118**

Scheme 36

The structure of this product has not been previously reported, so we employed ^{1}H and ^{13}C NMR to assign proton signals on the basis of previously established structure **115**; the ^{1}H, ^{13}C NMR and HMBC spectra are reported in Figure 86, 87 and 88 respectively and ^{1}H,^{13}C data are reported in Table 11.

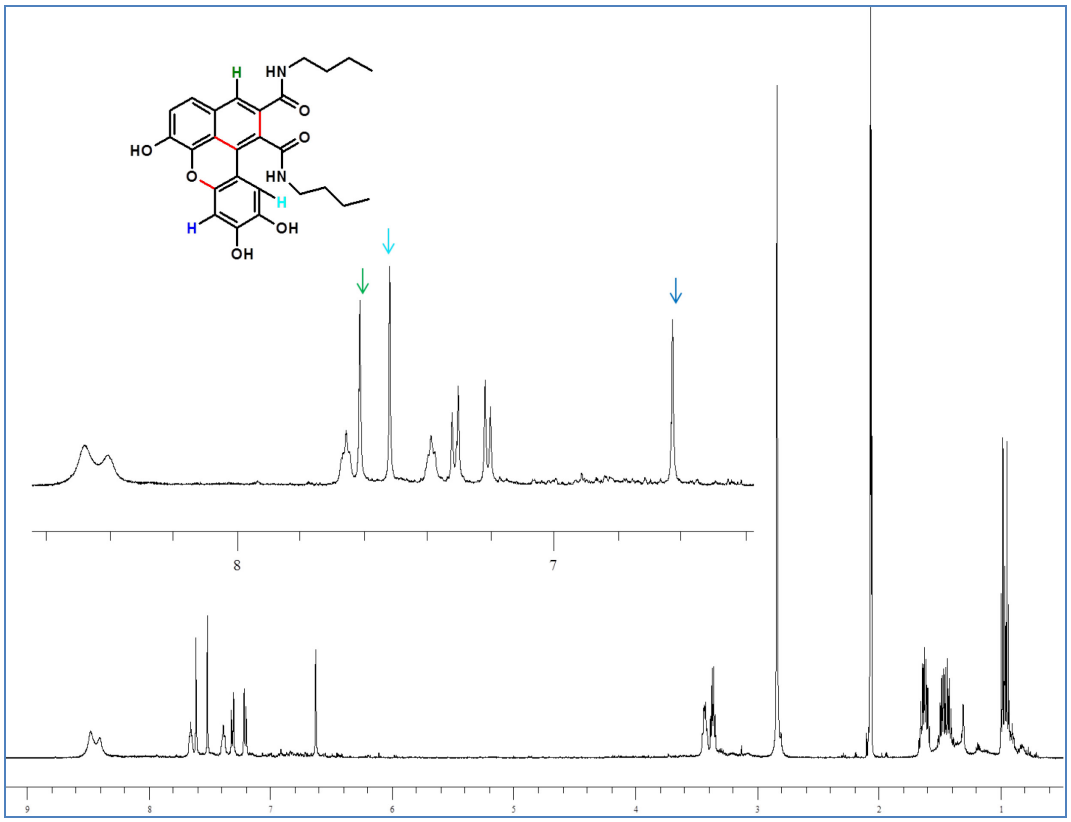

Figure 86: ^{1}H NMR spectrum of compound **118**

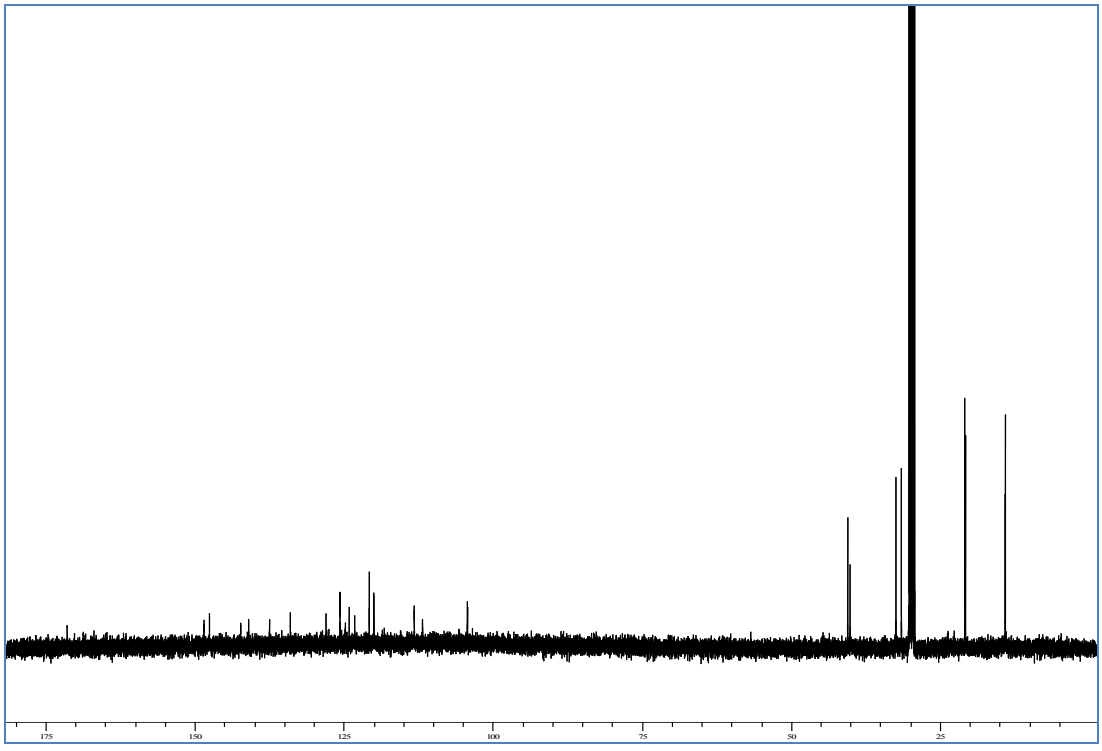

Figure 87: ^{13}CNMR spectrum of compound **118**

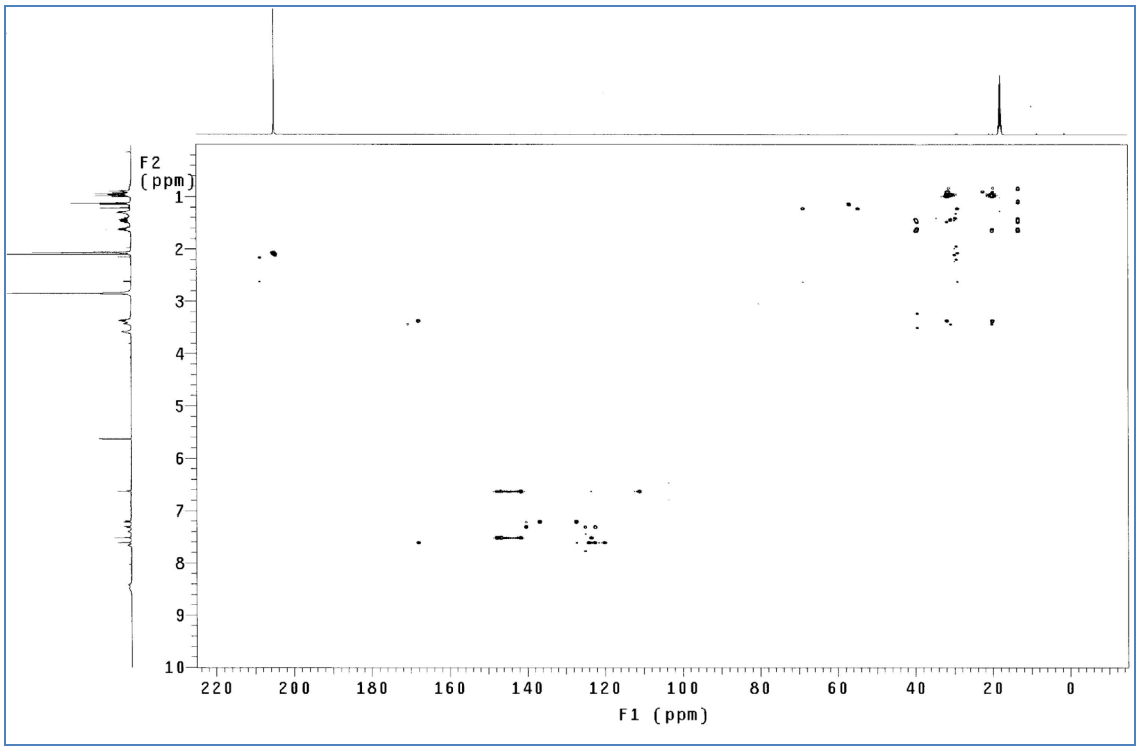

Figure 88: HMBC spectrum of compound **118**

Table 11: ^{1}H and ^{13}C NMR data of compound **118**

C	δ_C in Acetone-d_6	H	δ_H (mult, J Hz) in Acetone-d_6
C-1	124.1		
C-2	133.9		
C-3	124.7		
C-4	125.6	H-4	7.61(s)
C-5	120.7	H-5	7.30 (d,8.0)
C-6	119.9	H-6	7.21 (d,8.0)
C-7	140.9		
C-8	137.4		
C-9	123.1		
C-10	127.9		
C-1’	111.7		
C-2’	142.3		
C-3’	104.2	H-3’	6.62 (s)
C-4'	148.4		
C-5'	147.5		
C-6'	113.1	H-6’	7.51 (s)
C-1''	40.4	H-1’’	3.38 (q, 6.0)
C-2’’	32.4	H-2’’	1.62 (m)
C-3’’	20.8	H-3’’	1.46 (m)
C-4’’	14.0	H-4’’	0.94 (m)
C-1’’’	40.0	H-1’’’	3.43 (q, 6.0)
C-2’’’	31.4	H-2’’’	1.62 (m)
C-3’’’	20.7	H-3’’’	1.46 (m)
C-4’’’	14.0	H-4’’’	0.94 (m)
C-9’	168.6		
C-9’’	171.4		
		OH	8.48 (bs)*
		OH	8.40 (bs)*
		NH	7.65 (t, 6.0)
		NH	7.38 (t, 6.0)

Partially overlapped*

The ^{13}C NMR spectrum shows 25 signals (one signal at δ 14.0 for 2C, -$\underline{C}H_3$ in butyl chain): the majority of the signals were in the sp^2 region (from δ 171.4 to 104.2 ppm), only seven butyl carbon signals in the upper field region of the spectra (from 40.4 to 14.0 ppm) were observed. In the sp^2 region there are 13 quaternary carbon signals, 5 CH signals were observed suggest that loss of hydrogen from one caffeic acid ring moiety. ^1H NMR suggest the absence of large coupling constant two *trans* olefinic protons (α,β-unsaturated), refers that formation of a dimer which is not belongs to dihydrobenzofuran neolignan such as (±)-**52**.

The ^1H NMR spectrum of **118** in the region from δ 7.61 and 6.62 ppm shows clear similarities with the spectra of the previously discussed benzo[*k,l*]xanthene **115** lignans. We observed two broad triplets at δ 7.65, 7.38 due two hydrogens which have been assign to two –N$\underline{H}$ groups; also we observed two partially overlapped broad singlets at δ 8.4 and 8.40 (three protons), which have been assign to three hydroxy functions. Remaining five signals, two doublets (7.30 and 7.20 ppm) and three singlets (7.61, 7.51 and 6.62 ppm) are typical signals of benzo[*k,l*]xanthene core. The comparison of ^{13}C NMR of the monomer **117** and product **118**, clearly indicated that **118** is a dimer derived from **117**; in fact the spectrum of **117** shows 13 carbon signals whereas **118** shows 25 carbon signals; in particular two signals (168.6 and 171.4 ppm) are due two carbonyl groups derived from two different caffeic amide monomers

The ^{13}C chemical shift analysis, HSQC and HMBC spectrum indicated that three carbons of one ring connected to three oxygen atoms (D ring) and two carbons of another ring connected to two oxygen atoms (A ring). As mentioned above in the lower field region of ^1H NMR spectrum three singlet were

observed,, with the help of HSQC and HMBC spectra these hydrogens are assigned to H-4, H-3' and H-6'; in particular H-4 at δ = 7.61 is correlated to carbon C-4 at δ = 125.6 in ring B, H-3', at δ 6.62 and H-6' at δ 7.51 are correlated to C-3', C-6' at δ 104.2, 113.1 respectively in ring D. It was also observed clear correlation between C-1', C-2', C-4', C-5'and H-3', C-4', C-5', C-1 and H-6' (ring D), the correlations between C-10, C-8,and H-6, C-9,C-10, C-4 and H-5 shows that A ring is fused with B ring. The correlation of C-9, C-5,C-3, C-9' and H-4 confirm the ring A and carbonyl function fused to ring B. And C-9'' to N-H correlation shows the connection between amide and caronyl. Figure 89 shows the selected HMBC correlation of dimer benzo[*k,l*]xanthene lignan **118**.

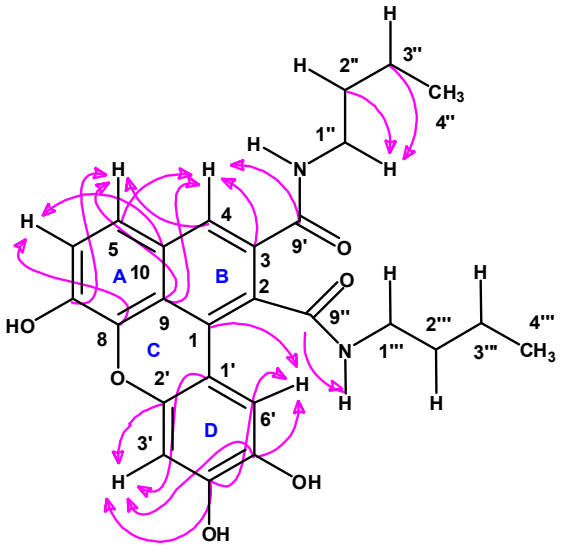

Figure 89: Main selected HMBC correlation of compound **118**

2.2.4 Synthesis of benzo[*k,l*]xanthene **121**

*2.2.4.1 Step1. Preparation of amide **120***

Caffeic acid **7** was coupled with dicyclohexylamine **119** in the presence of BOP reagent as coupling agent and triethylamine as base with DMF and CH_2Cl_2 solvent system (Scheme 37). The reaction was carried out in 0 ^oC for first 30 min in the course of addition of BOP reagent which is solubilised in CH_2Cl_2 and

subsequently stirred at room temperature for 24 hrs. A tertiary caffeic amide **120** is obtained by the column chromatographic purification.

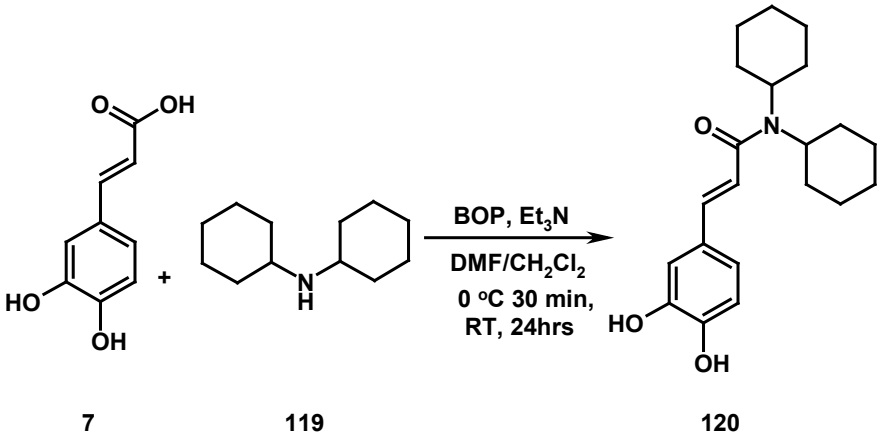

7 **119** **120**

Scheme 37

The characterization of the compound **120** has been carried out by ^{1}H NMR and ^{13}C NMR spectroscopy. ^{1}H NMR suggests that in the lower field region there are five signals, integrantig for five hydrogens. Two doublet signals at δ 7.28 and 6.73 with large coupling constant 15.5 Hz gives two olefinic α,β-unsaturated hydrogens, and reaming three signals, one is double of doublet at δ 6.92 with coupling constant 8.0 and 2.0 Hz, and other two doublets with coupling constant 8.5 and 2.0 Hz at δ 7.02 and 6.78 respectively to assign caffeic ring moiety. In upper field of the spectra a set of multiplet were observed, which have been overlapped each other and assigned to hexane ring moiety integrated to 22 hydrogens. ^{1}H and ^{13}C NMR spectra are reported in Figure 90 and 91.

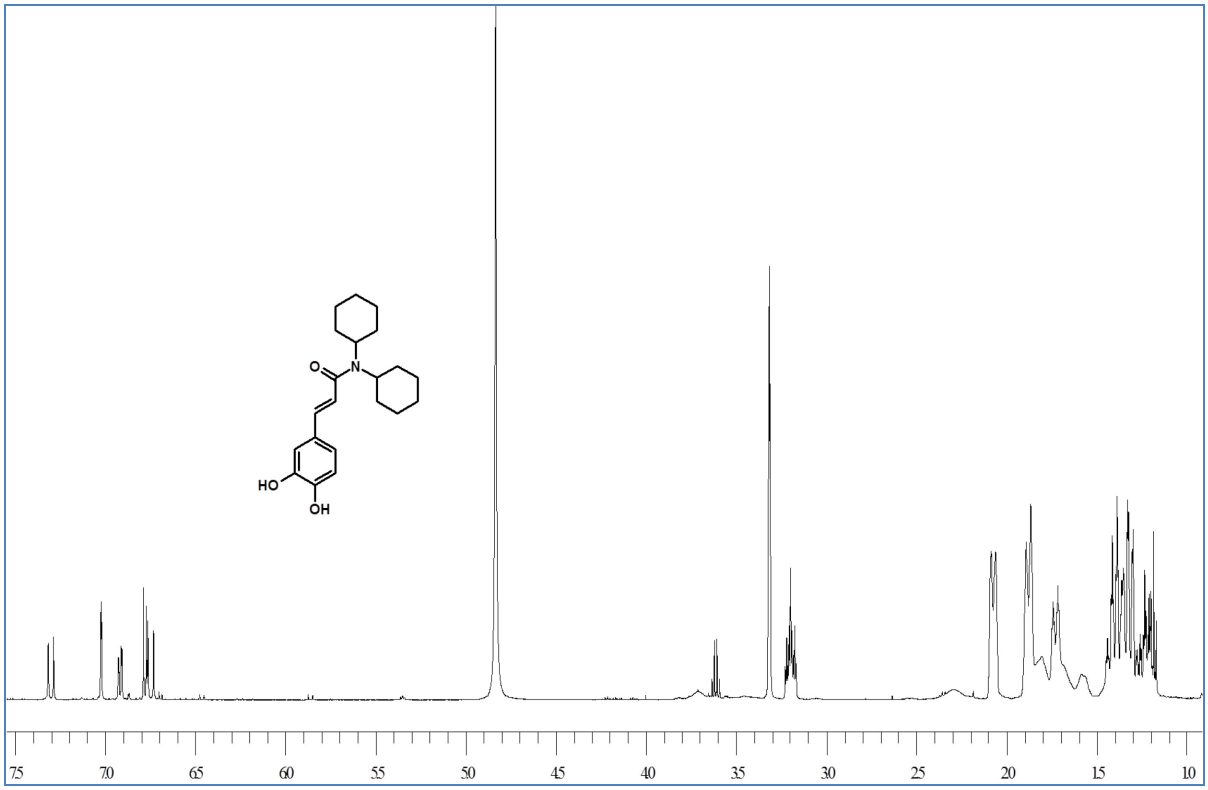

Figure 90: ^{1}H NMR spectrum of compound **120**

The ^{13}C NMR spectrum of **120** shows 13 signals: nine signals were observed in sp^2 region from (169.3 to δ 114.8) and four signal in upper field (from 54.6 to 25.4 ppm); these latter are assignable to cyclohexyl rings and the signal at δ 169.4 has been assigned to carbonyl carbon (C=O), the remaing signals are due to aromatic ring and double bond (caffeic moiety).

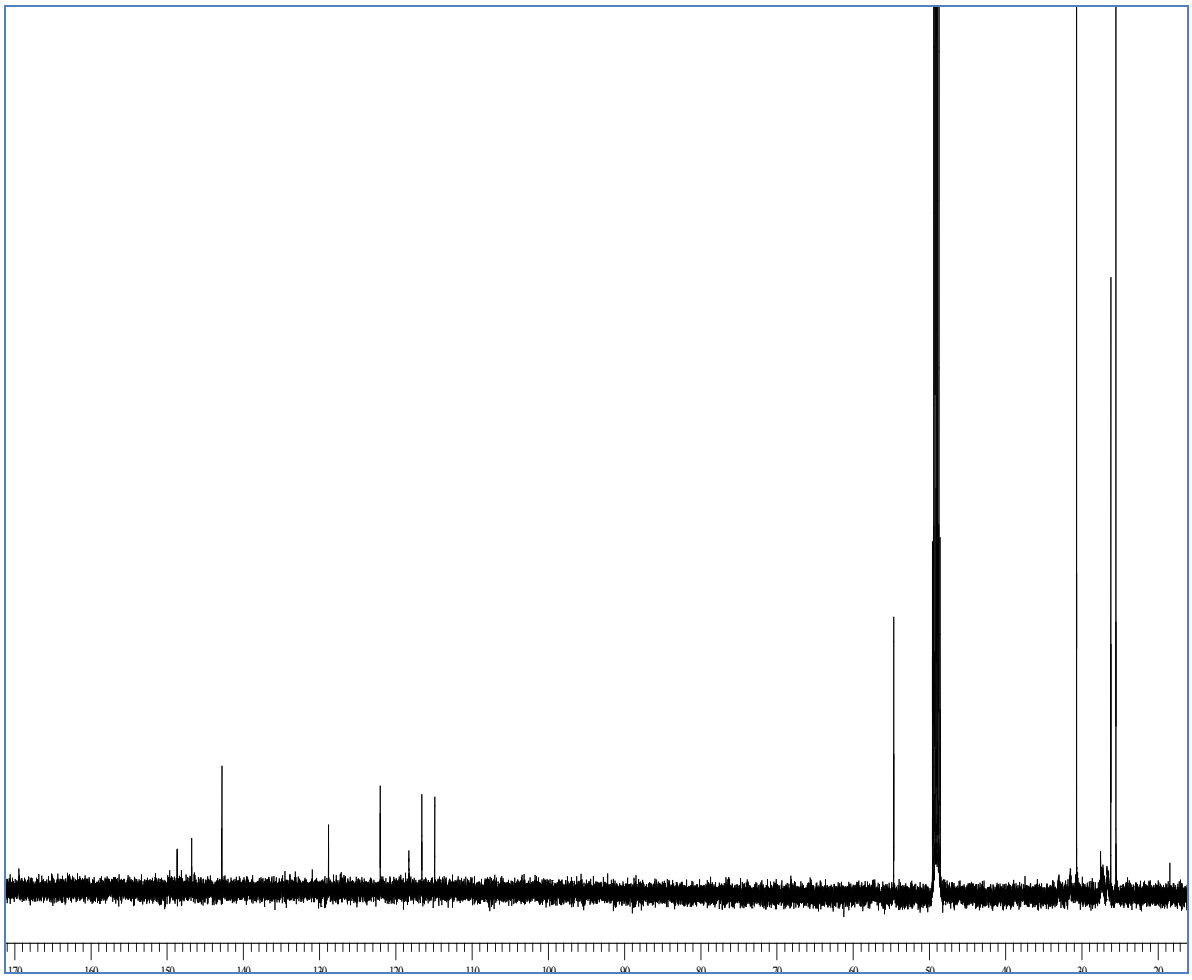

Figure 91: ^{13}C NMR spectrum of compound **120**

*2.2.4.2 Step2. preparation of compound **121***

Tertiary caffeic amide **120** was subjected to dimerization in the presence of $Mn(OAc)_3$ in EtOH solvent (Scheme 38), this reaction gives complete conversion of substrate in to products within one hour. By increasing the reaction time we observed more polar spots on TLC. The dimer **121** is highly bluish fluorescent (under 366 nm UV light) compound obtained by column chromatographic purification. The ^1H and COSY NMR spectra are reported in Figure 92 and 93.

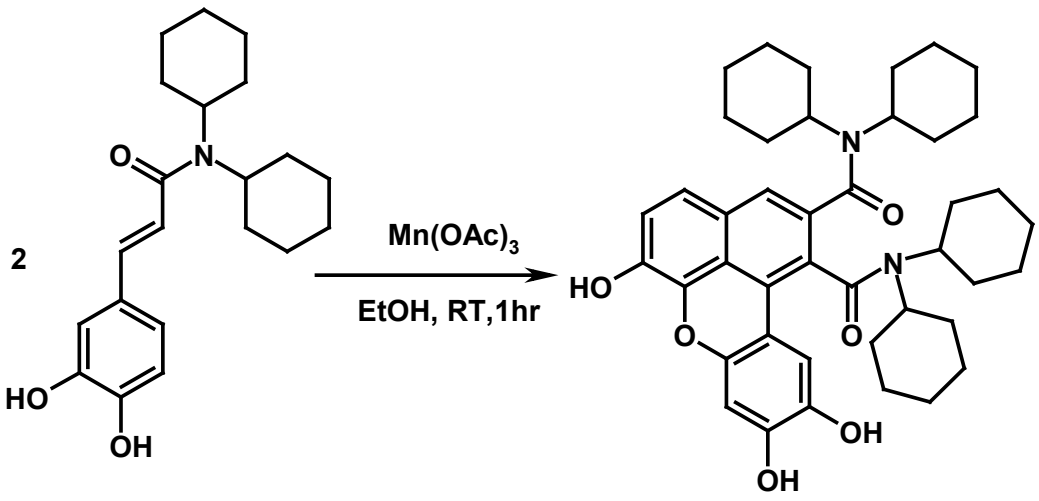

Scheme 38

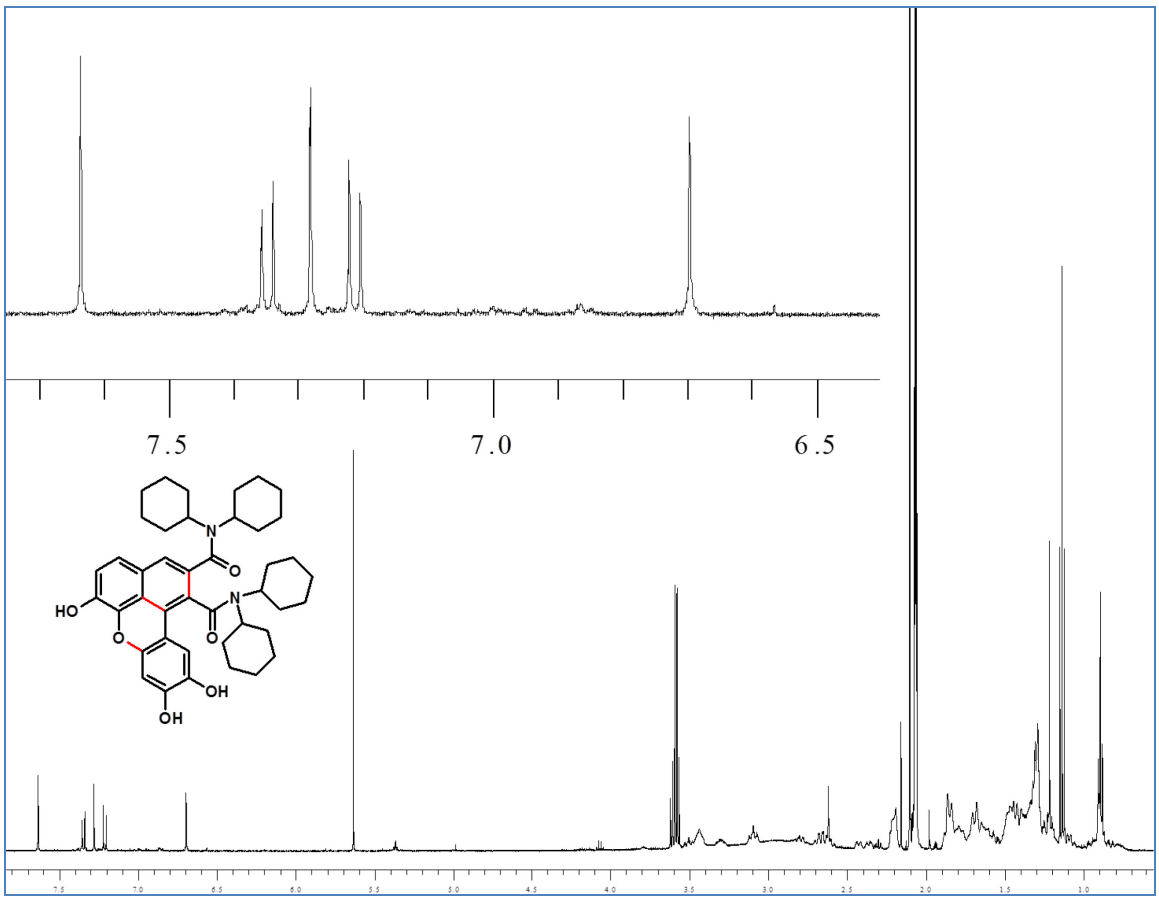

Figure 92: ^{1}H NMR spectra of compound **121**

The structure of this product has not been previously reported, so we employed ^{1}H NMR to assign proton signals on the basis of previously established benzo[*k,l*]xanthene structure **118**; ^{1}H NMR suggest the absence of large

coupling constant two *trans* olefinic protons (α,β-unsaturated), refers that formation of a dimer which is not belongs to dihydrobenzofuran neolignan such as (±)-**52**. The ^{1}H NMR spectrum of **121** in the region from δ 7.63 and 6.69 ppm shows clear similarities with the spectra of the previously discussed benzo[*k,l*]xanthene**s**. In lower field region there are five signals, two of them are doublets and three are singlets.

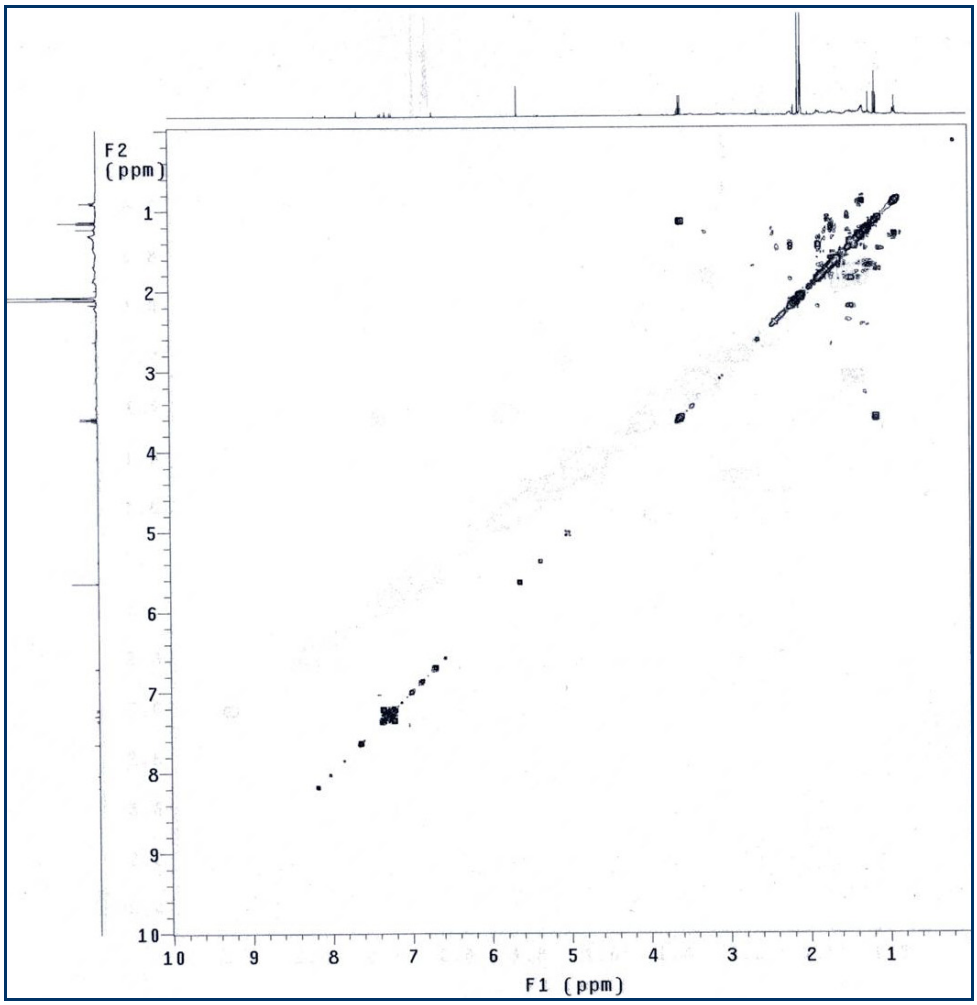

Figure 93: HMBC spectrum of compound **121**

A COSY spectrum shows the correlation between two doublets in lower field region and correlation of cyclohexyl ring hydrogens. Due to the low amount of **121** available was not possible to record the spectra of ^{13}C and 2D-NMR, we intend to repeat the synthesis in order to obtain a larger amount to perform the experiments needed to unambiguously assign all the signals

2.2.5 Synthesis of benzo[*k,l*]xanthene **124**

*2.2.5.1 Step1. Preparation of amide **123***

Caffeic acid **7** was coupled with benzyl amine **122** in the presence of BOP reagent as coupling agent and triethylamine as base with DMF and CH_2Cl_2 solvent system (Scheme 38). The reaction was carried out in 0 ^oC for first 30 min in the course of addition of BOP reagent which is solubilised in CH_2Cl_2 and subsequently stirred at room temperature for 24 hrs. The monomer **123** was obtained after column chromatographic purification. The complete characterization of the compound **123** has been carried out by ^1H and ^{13}C NMR spectroscopy. ^1H and ^{13}C NMR spectra are reported in Figure 94 and 95.

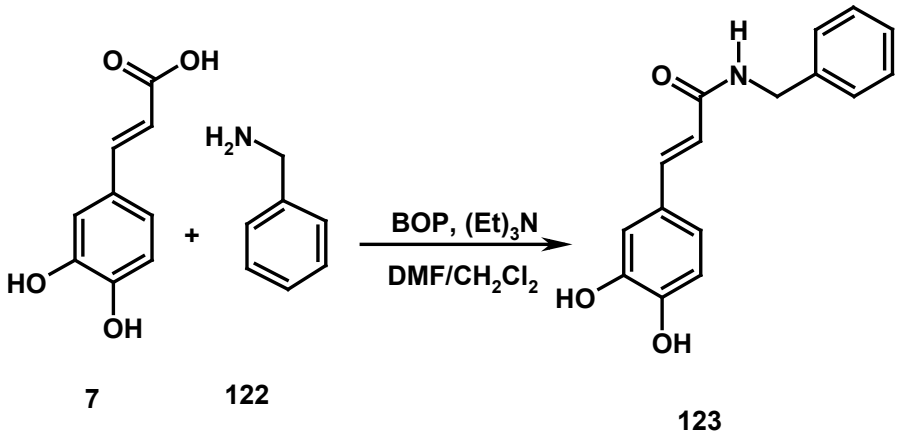

7 **122** **123**

Scheme 39

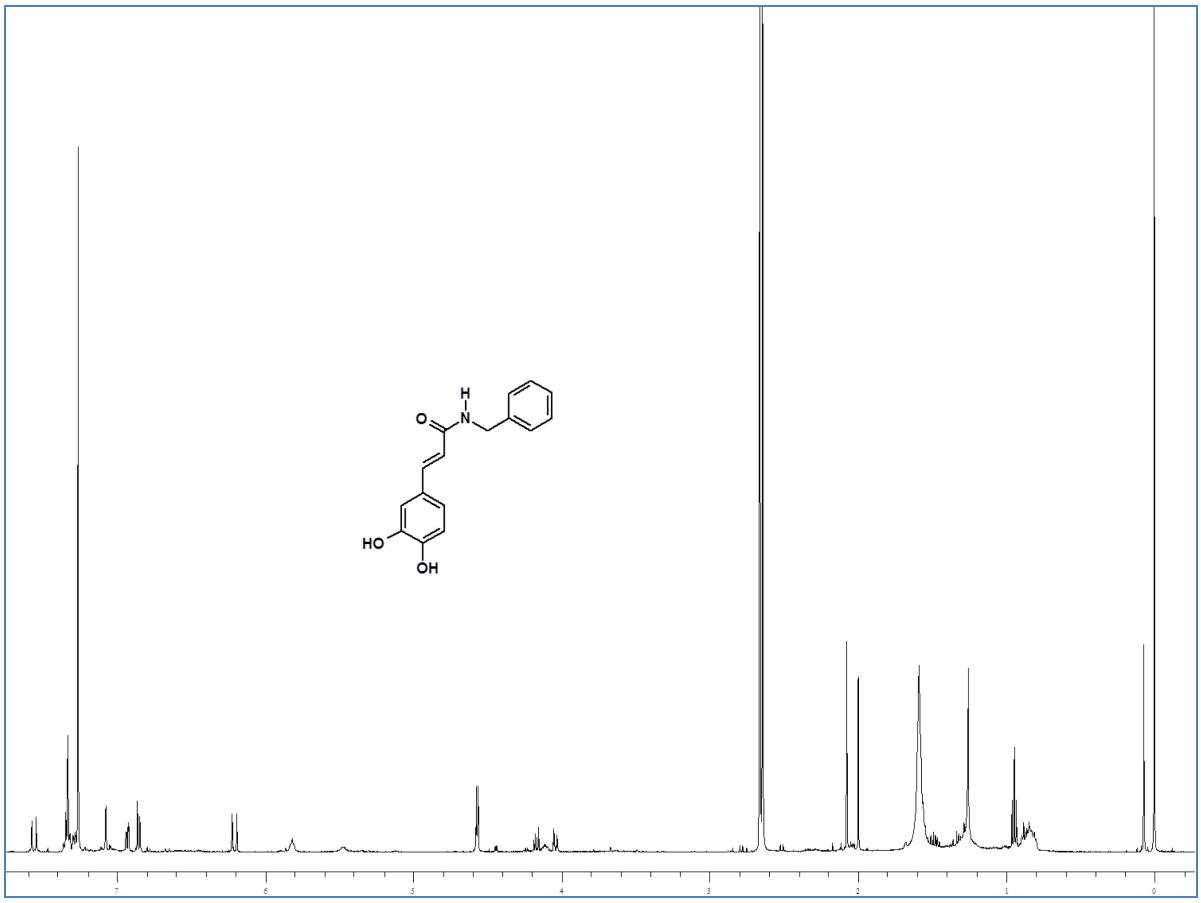

Figure 94: ^{1}H NMR spectrum of compound **123**

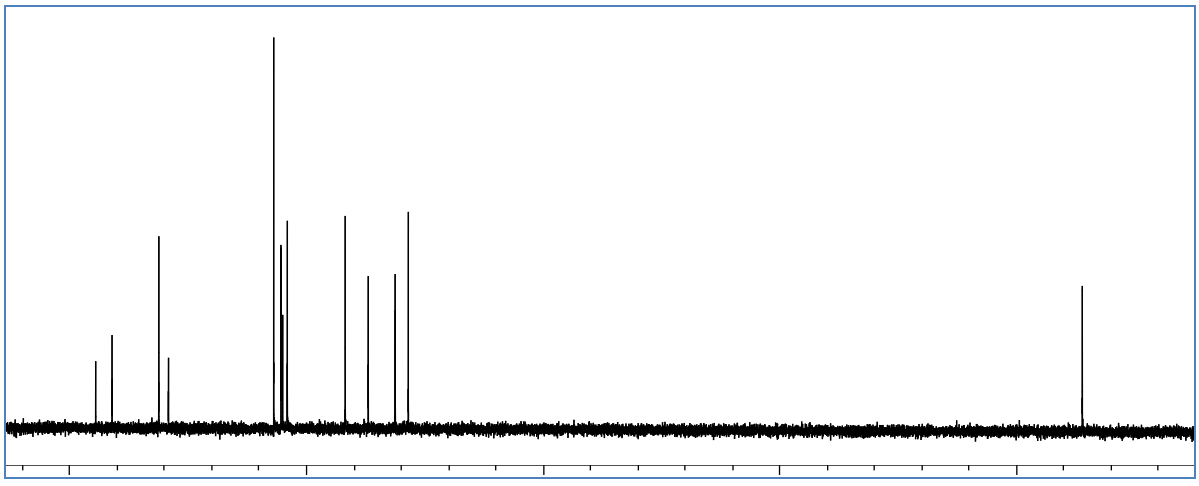

Figure 95: ^{13}C NMR spectrum of compound **123**

^{1}H NMR suggests that in the lower field region there are five signals, which have integrated to ten hydrogens. Two doublet signals at δ 7.46 and 6.44 with large coupling constant 15.5 Hz gives two olefinic α,β-unsaturated hydrogens,

and reaming lower field signals, one is singlet at δ 7.07, and other two doublets with coupling constant 8.0 and 8.5 Hz at δ 6.92 and 6.78 respectively to assign caffeic ring moiety hydrogens. And one multiplet was observed at δ 7.22-7.30 is assignable to benzyl ring. In the ^{13}C NMR of **123** there are 14 signals: in which 13 signals in sp^2 region from at δ 166.7 to δ 114.5 and one signal in upper field of the spectra. One carbon in lower field of the spectra at δ 166.7 is assignable for carbonyl carbon (C=O).

*2.2.5.2 Step2. preparation of compound **124***

Secondary caffeic amide **123** was subjected to dimerization in the presence of $Mn(OAc)_3$ in $CHCl_3$ solvent (Scheme 40), this reaction gives complete conversion of substrate in to products within five hours. The dimer **124** is highly fluorescent (under 366 nm UV light) compound obtained by column chromatographic purification.

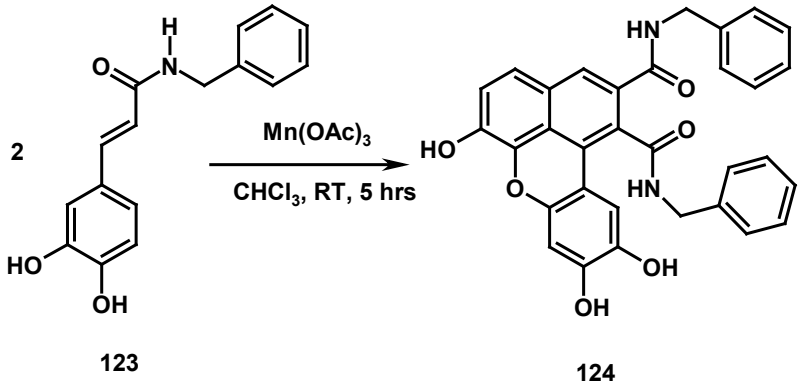

123 124

Scheme 40

At moment the characterization of the compound **124** is in progress

2.2.5 Reaction mechanism of formation of benzo[*k,l*]xanthene

Recently C.Tringali *et al* illustrated the mechanism for the formation of benzo[*kl*]xanthene lignan **50**; in this thesis work we are proposing the similar mechanism which is proposed by C.Tringali group (see Scheme 41). The

benzo[*kl*]xanthene could originate by the 8-8' coupling, generating the quinone methide intermediate **A** whose tautomer **B** undergoes an intramolecular cyclization; two further oxidative steps on **C** originate in sequence the intermediates **D** and **E**: this latter undergoes a further cyclization step as nucleophilic attack of the 3-OH to the position 5' of the quinone methide moiety, giving rise to the intermediate **F** which is then converted by tautomerism into the final products benzo[*kl*]xanthene.

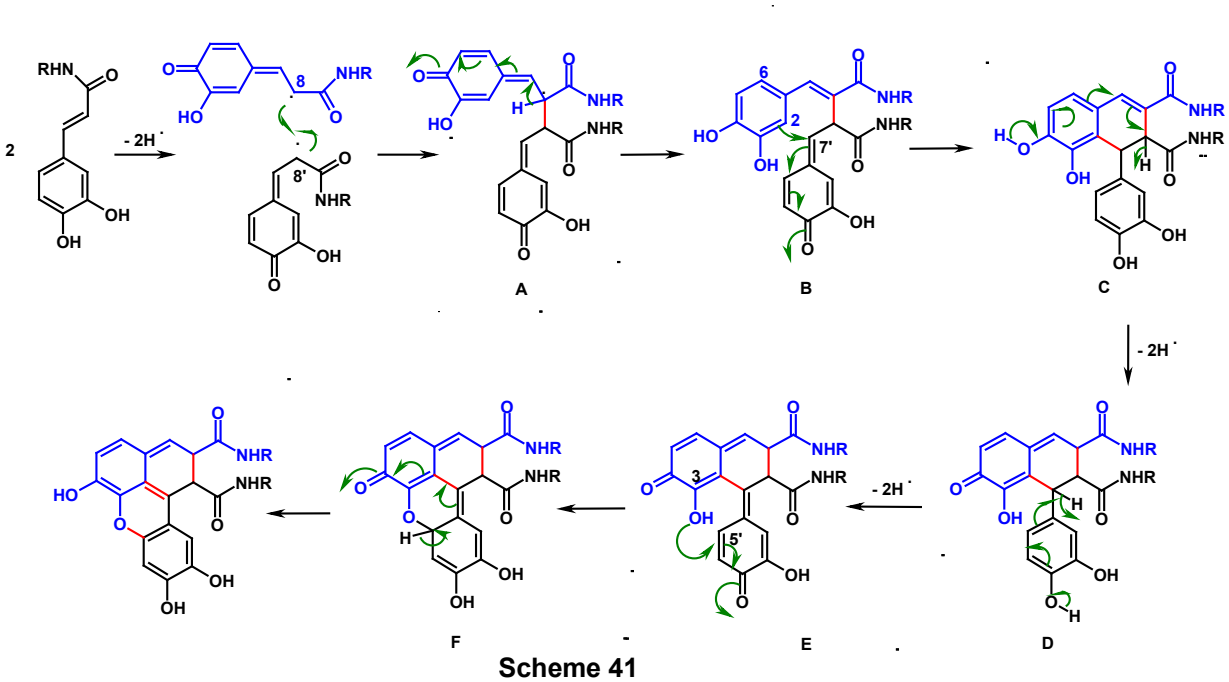

Scheme 41

2.3 Synthesis of caffeic hydantoins

As mentioned above (in section 2.2, before synthesis of caffeoyl tyramine), during the synthesis of caffeoyl amide monomers we observed the formation of *N*-acylurea **125** as major product of the coupling reaction of caffeic acid (**7**) and tyramine (**110**) with dicyclohexylcarbodiimide (DCC) in presence of Et_3N as base (See Scheme 42).

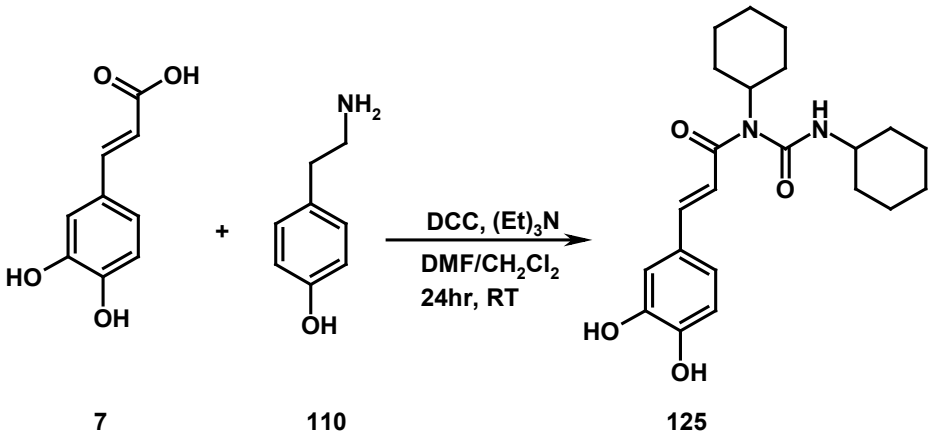

7 110 125

Scheme 42

For a better understanding of the formation of **125** it is useful to resume the mechanism of DCC (**126**) activation, which is complex and depending on the solvent; for the sake of clarity we reported here this mechanism applied to the reaction of **7** with DCC (Scheme 43). It starts by a proton transfer, followed by addition of the carboxylate to form the *O*-acylisourea **127**. This is the most reactive specie that can attack the amino component to give the corresponding amide. However, the *O*-acylisourea can undergo a rearrangement to give the *N*-acylurea (**125**), which is not reactive.[89] If activation is carried out in a solvent of low dielectric constant such as $CHCl_3$ or CH_2Cl_2, the formation of *O*-acylisourea occurs instantaneously, which is absent of a nucleophile or base and can be stable for many hours. However, if the activation is carried out in a more polar solvent such as DMF, no immediate reaction can be detected.

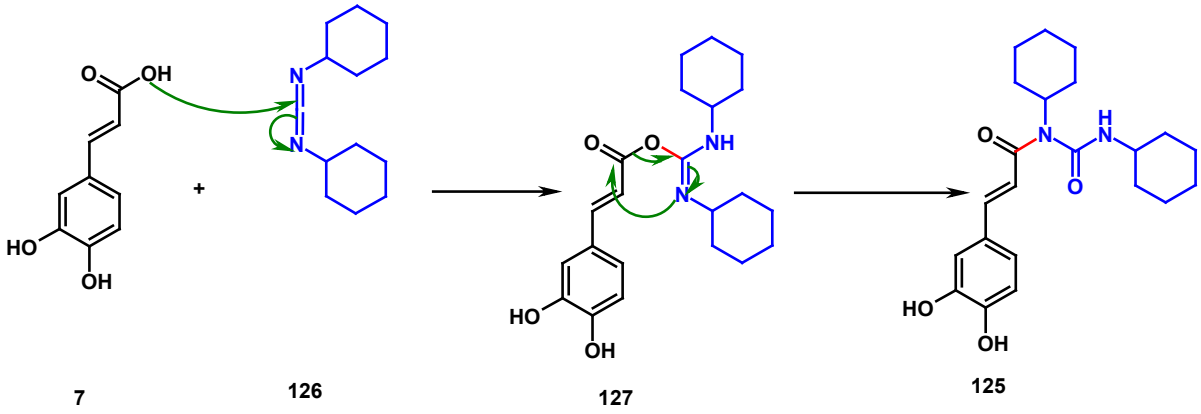

Scheme 43

We tried to exploit this unexpected product **125** as starting material for the preparation of previously unreported dimers through an enzyme-mediated oxidative coupling; promising results were obtained with Laccase from *Trametes versicolor* (LTV), we have now optimized the synthesis of **125**, according to Scheme 44; then we carried out the enzyme-mediated reaction (Scheme 45) with the aim to establish the structure of the product. As detailed below, this reaction afforded an unexpected product **128**, which was submitted to spectral analysis and established as a hydantoin-related compound. A further reaction was carried out with a different laccase, namely Laccase from *Pleurotus ostreatus* (LPO).

As mentioned in introduction, literature survey suggests that hydantoins have been widely used in biological screenings resulting in numerous pharmaceutical applications.[69-75] Thus, we dedicated some efforts to understand the mechanism of this reaction which represent a synthetic methodology of possible interest in 'green chemistry'; in fact, enzymatic syntheses require mild conditions and avoid the use of toxic reagents/catalysts and the production of dangerous waste products.[90]

2.3.1. Enzymatic synthesis of caffeic hydantoin 128

*2.3.1.1 Step 1. Synthesis of caffeic N,N'-dicyclohexylurea **125***

We used caffeic acid **7** as starting material for the synthesis of caffeic acid *N*-acylurea **125** in the presence of DCC and *N*-ethyldiisopropylamine as base; CH_3CN was used as solvent (Scheme 44). The reaction was maintained at 0 ^oC during addition of DCC (30 min) and subsequently stirred at room temperature for 24 hr. The *N*-acylurea **125** was obtained by column chromatography purification in better yield (42%) than that obtained during the unexpected product in Scheme 42.

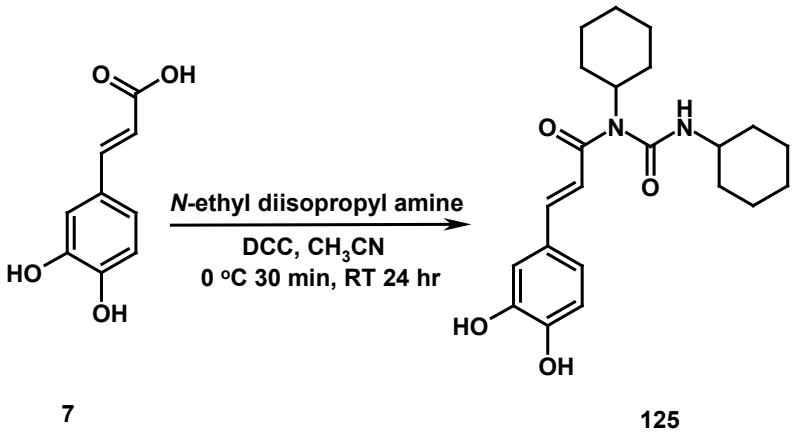

7 **125**

Scheme 44

The structure of **125** has not been previously reported, so we run both ^1H and ^{13}C NMR spectra; the Mass spec, ^1H and ^{13}C NMR spectra are reported in Figure 96, 97 and 98, respectively. The mass spectrum shows a peak at *m/z* 385.3 $[M-H]^-$ supporting the expected structure of *N,N'*-dicyclohexylurea product incorporating two *N*-cyclohexyl moieties with molecular formula $C_{22}H_{30}N_2O_4$.

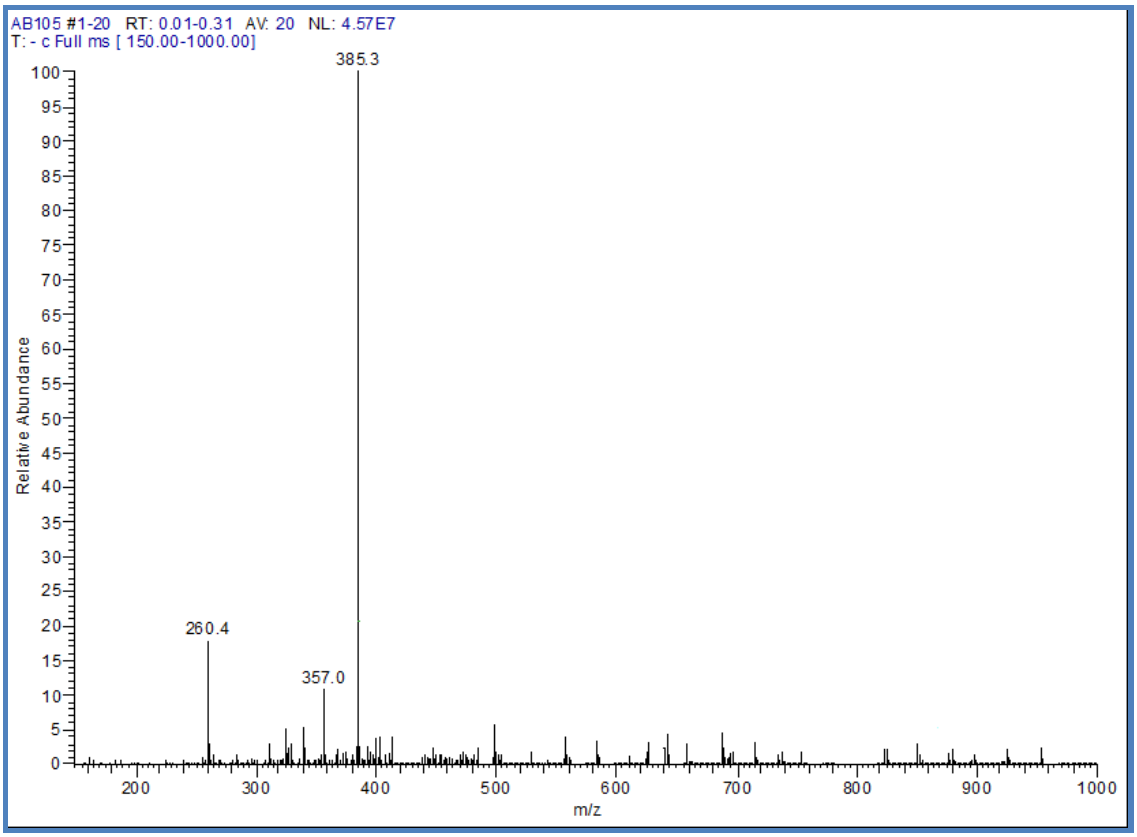

Figure 96: Mass spectrum of **125**

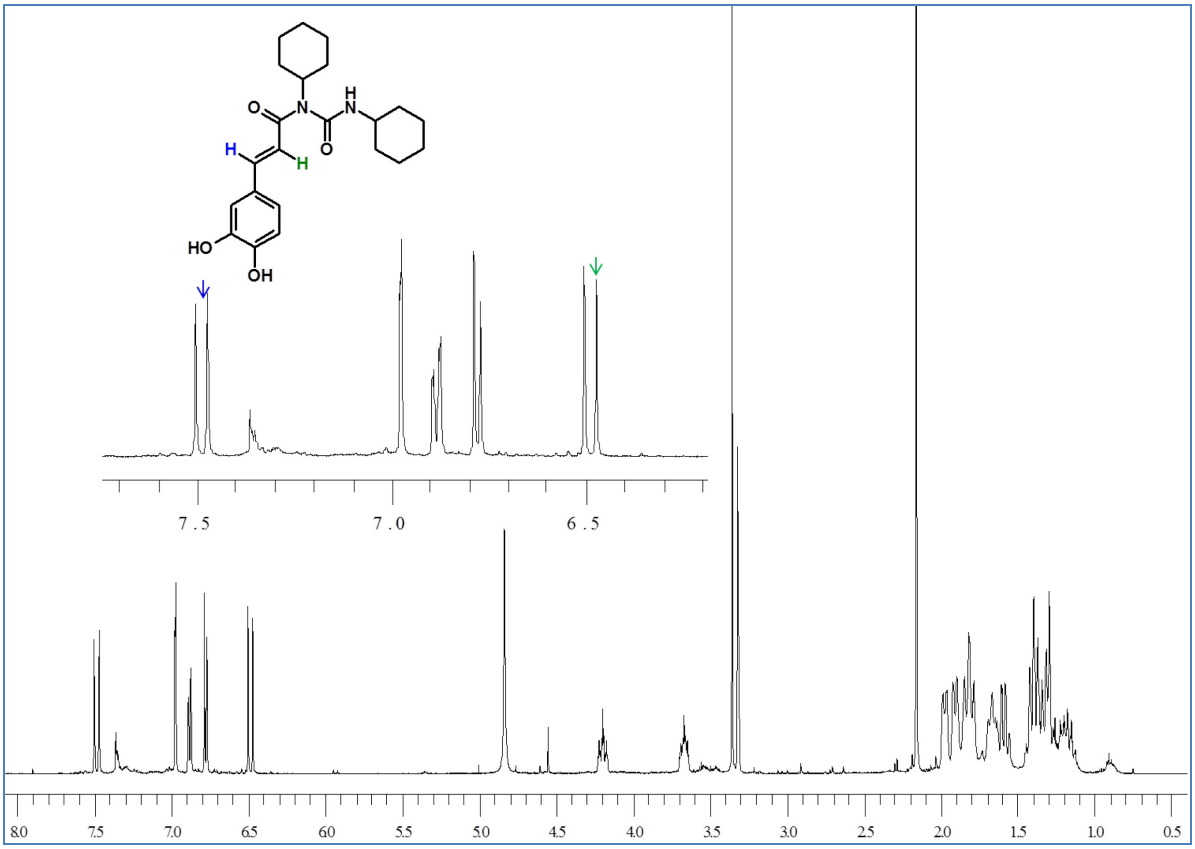

Figure 97: ^{1}H NMR spectrum of **125**

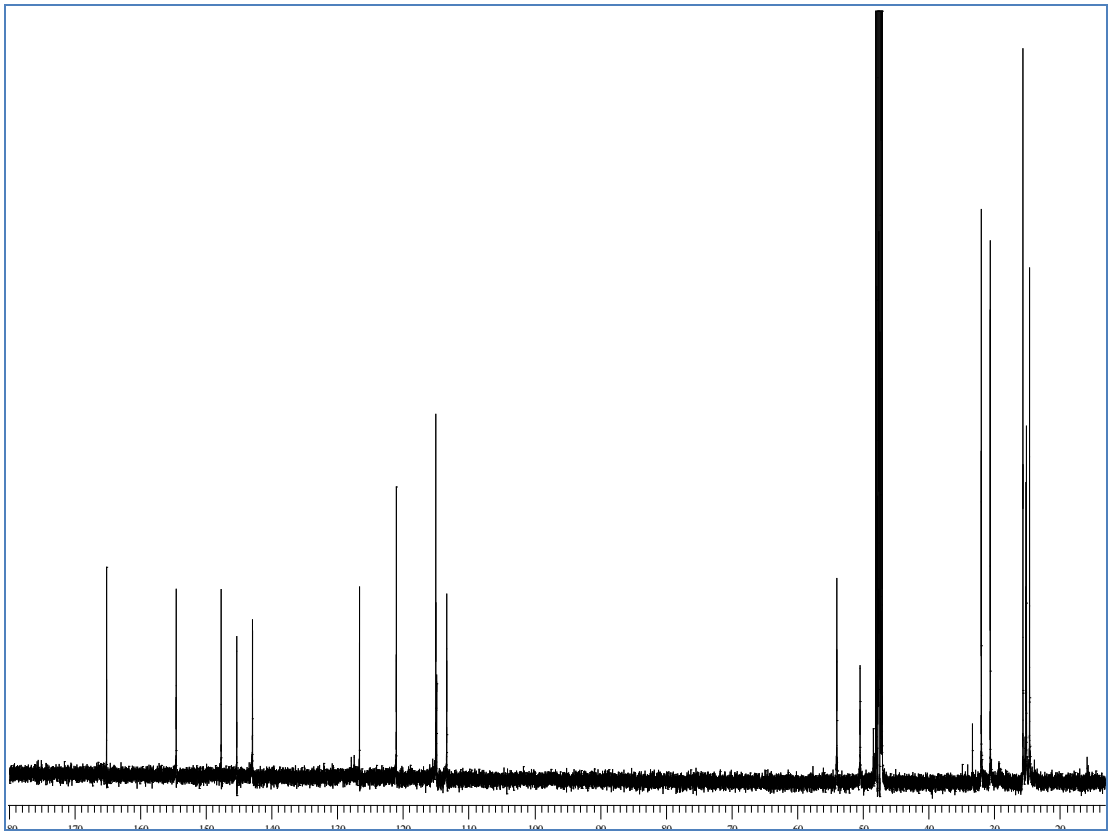

Figure 98: ^{13}C NMR spectrum of **125**

In the complete upper field region of ^{1}H NMR spectrum, multiplet signals were observed due to two cyclohexane ring, which have integrated to 20 protons: in lower field of the spectrum two doublet signals at δ 7.46 and 6.46 with large coupling constant 15.5 Hz due two olefinic α,β-unsaturated protons, and reaming three signals (δ 6.77, 6.87, 6.97, ppm) integrated each for one protons due to caffeic ring moiety. In upper field of the spectrum one multiplet at δ 4.19 and another multiplet at δ 3.66 were observed and integrated each to one proton, which are assigned to–C<u>H</u> of cyclohexane ring. In the ^{13}C NMR spectrum of **125** there are 18 signals: in upper field region eight signals were observed at δ 54.0 to 25.2 ppm due to two cyclohexyl ring; in the lower field region ten signals were observed at δ 165.2 to 113.4, two of them δ 165.2 and δ 154.6 are assignable for carbonyl carbons (<u>C</u>=O), the other eight signals six for aromatic ring and two for a double bond (olefinic carbons) could easily assignable to caffeic moiety.

*2.3.1.2 Step 2. Enzymatic conversion of **125** to caffeic hydantoin **128***

The substrate **125** in the presence of LTV enzyme and biphasic solvent system such as EtOAc, acetate buffer pH 4.7 at room temperature for 24 hr gives compound **128** about 68% yield. The same reaction was carried out in distilled water instead of buffer pH 4.7, this reaction gives about 65% yield with in 2 hrs. In our enzyme screening reaction, substrate **125** in the presence of LPO enzyme and biphasic solvent system such as EtOAc, distilled water in room temperature for 2 hr gives about 60% yield after column purification.

The complete spectroscopic characterization of the product **128** was carried out on a carefully purified sample. The positive ESI mass spectrum, reported in Figure 99, showed a peak at *m*/*z* 385.2 $[M+H]^+$ and a peak at *m*/*z* 407.2 which was interpreted as $[M+Na]^+$; the negative ESI mass spectrum showed a molecular ion of 383 $[M-H]^-$. Both data show the loss of two hydrogens from substrate.

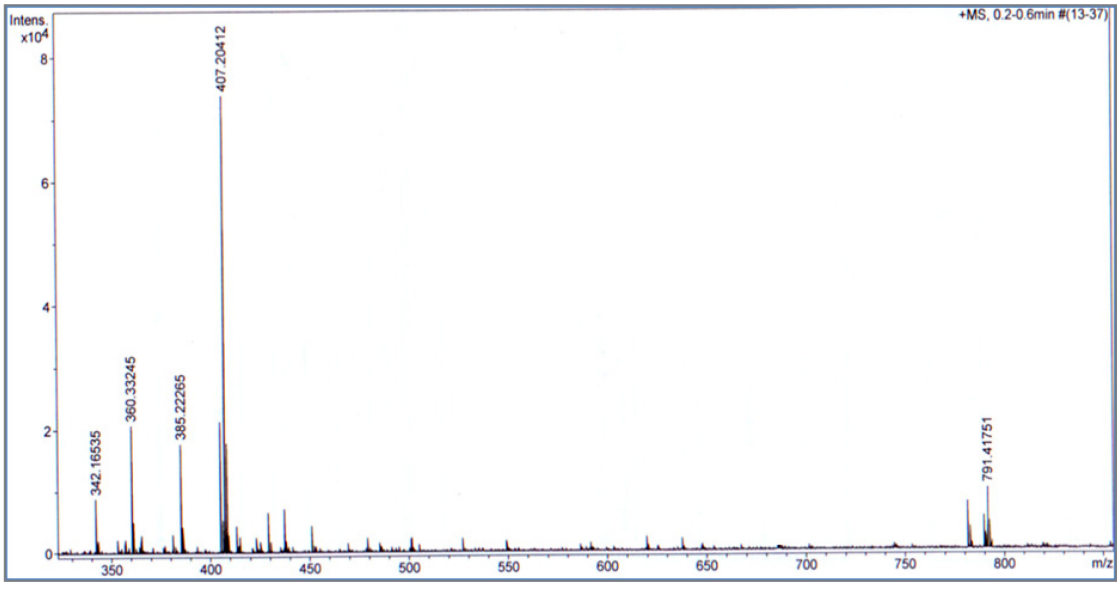

Figure 99: Mass spectrum of compound **128**

This mass analysis allowed us to determine that its molecular formula was $C_{22}H_{28}N_2O_4$. The loss of two units is due a new degree of unsaturation which could reasonably attribute to new cycle; this is confirmed by ^{1}H NMR,^{13}C NMR,

COSY, NOESY, HMBC, and HSQC spectra (reported in Figure 100, 101, 102, 103, 104 and 105 , respectively, and Table 12). The ^{1}H NMR spectrum don't show a significant modification of the caffeic acid substructures except for olefinic protons, only one singlet was observed at δ 6.35.

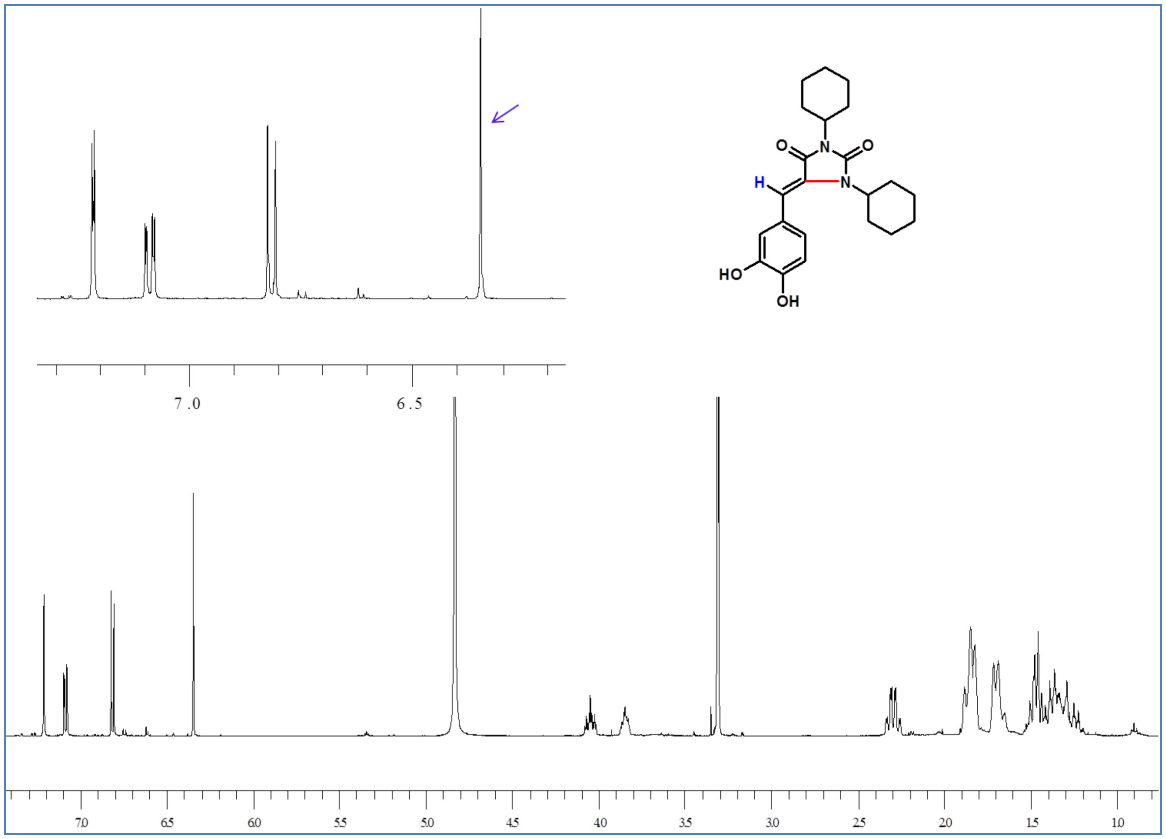

Figure 100: ^{1}H NMR spectrum of compound **128**

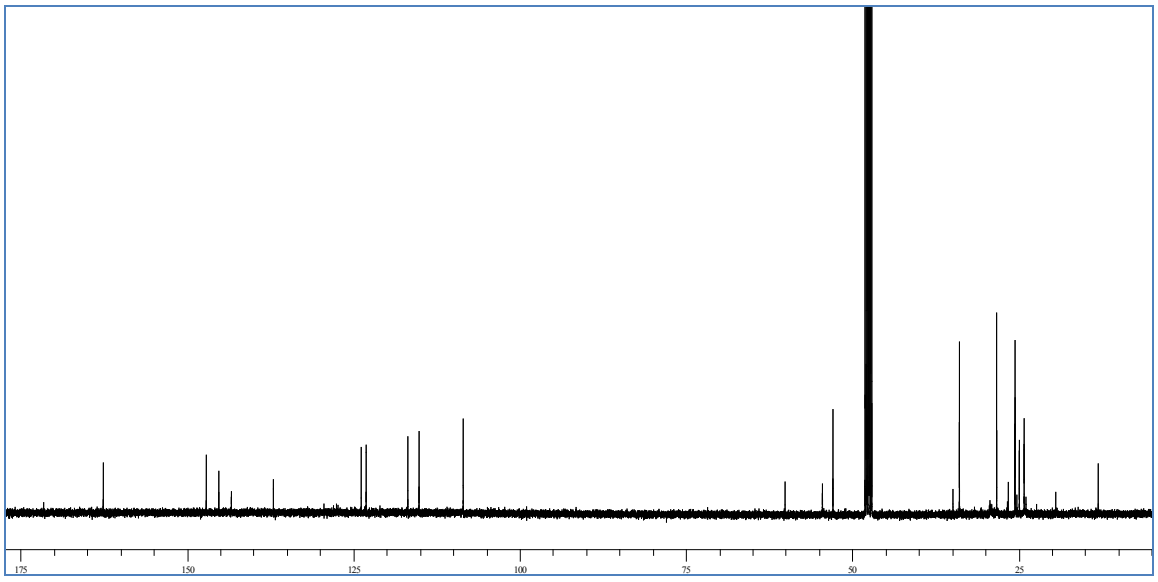

Figure 101: ^{13}C NMR spectrum of compound **128**

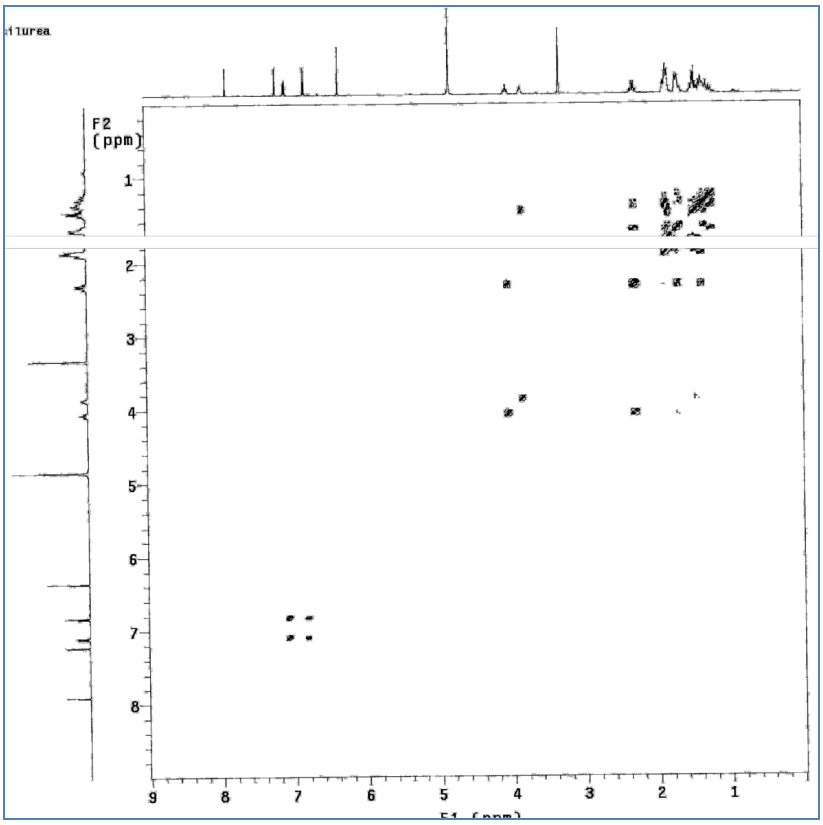

Figure 102: COSY spectrum of compound **128**

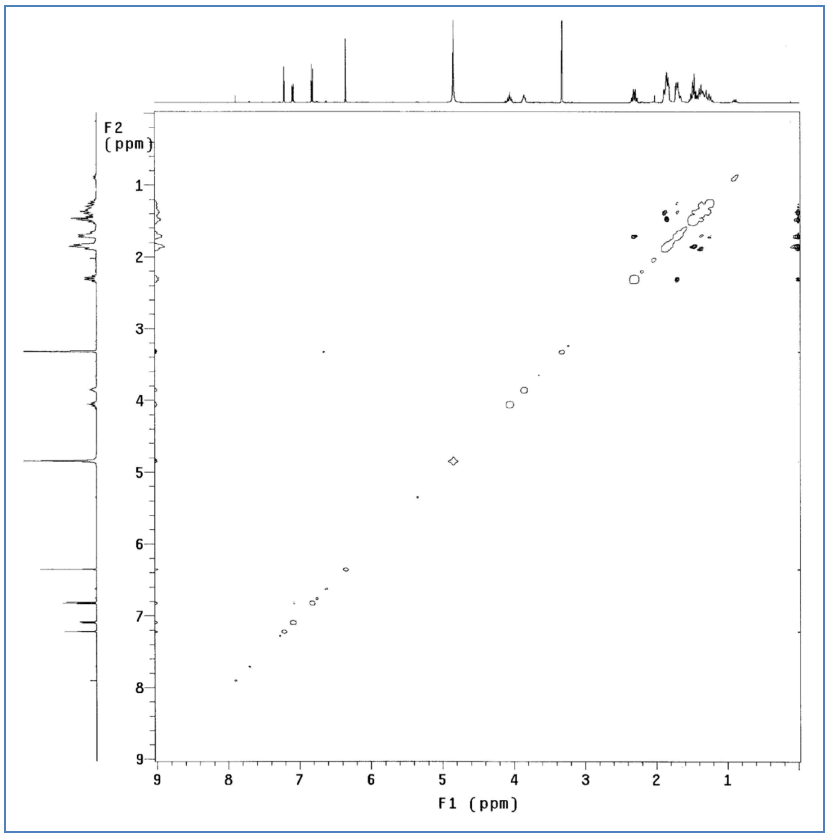

Figure 103: NOESY spectrum of compound **128**

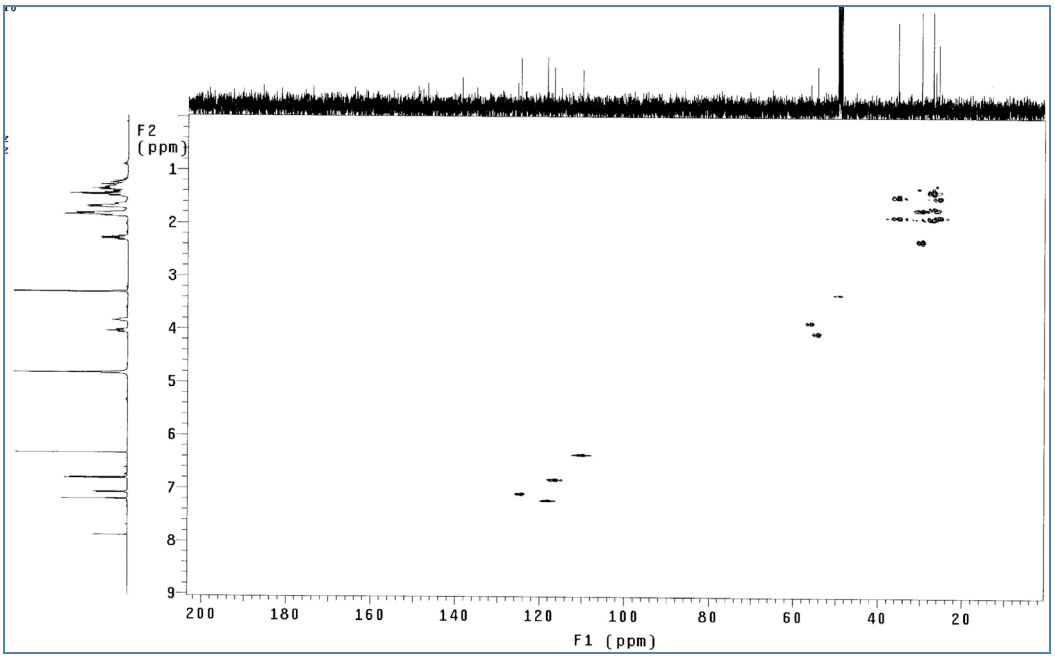

Figure 104: HSQC spectrum of compound **128**

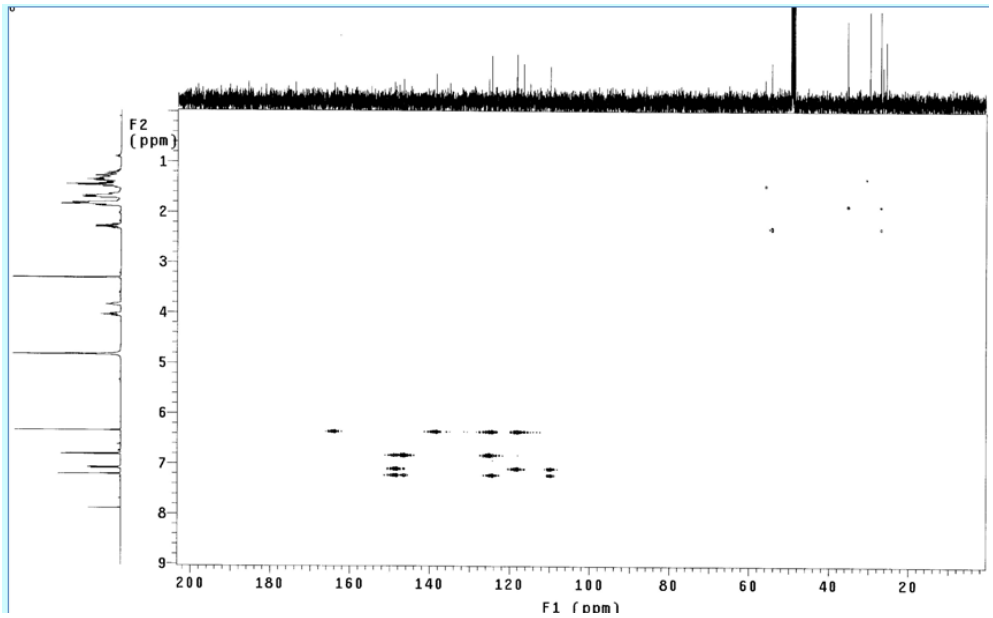

Figure 105: HMBC spectrum of compound **128**

Table 12: ^{1}H and ^{13}C NMR data of compound **128**

C	δ_C in $CDCl_3$	δ_H (mult, J Hz) in CD_3OD	COSY	HMBC
C-1	138.5			H-7
C-2	118.2	7.21 (d, 2.0)		H-7,H-6
C-3	146.6			H-5
C-4	148.5			H-6
C-5	116.5	6.82 (d, 8.5)	H-6	
C-6	124.5	7.08 (dd, 8.5, 2.0)	H-5	H-2,H-5,H-7
C-7	109.9	6.35 (s)		H-6
C-8	125.2			H-7
C-9	144.7			H-7,H-11
C-10	164.0			
C-11	54.3	4.05 (m)	H-12	
C-12,12’	35.2	2.29 (m)	H-11,13	
C-13,13’	29.7	1.70 (m)	H-12	
C-14	26.9	1.34 (m)		
C-15	55.9	3.84 (m)		
C-16,16’	27.5	2.19 (m)		
C-17,17’	26.3	1.70 (m)		
C-18	25.5	1.31 (m)		

The ^{13}C NMR spectrum of **128** was in part similar to that of the starting material **125**; in particular, it showed 18 signals: eight signals attributable to a cyclohexane ring appeared in the upper field region of the spectra (δ 54.3 to 25.5 ppm); ten signals were in the sp^2 region due at 6 quaternary carbon (at δ 164.0, 148.5, 146.6, 144.7 138.5,125.2, ppm) and 4 CH (at δ 109.9, 118.2, 116.5, 124.5 ppm) unlike the spectrum of **125** shows that 5 CH.

On the basis of these data is possible imagine that the compound **32** underwent a cyclization, the nitrogen atom might give a reaction of aza-Michael or anti-aza-Michael to give **128A** or **128B** respectively, with the formation of a cycle 5 or 6 terms.

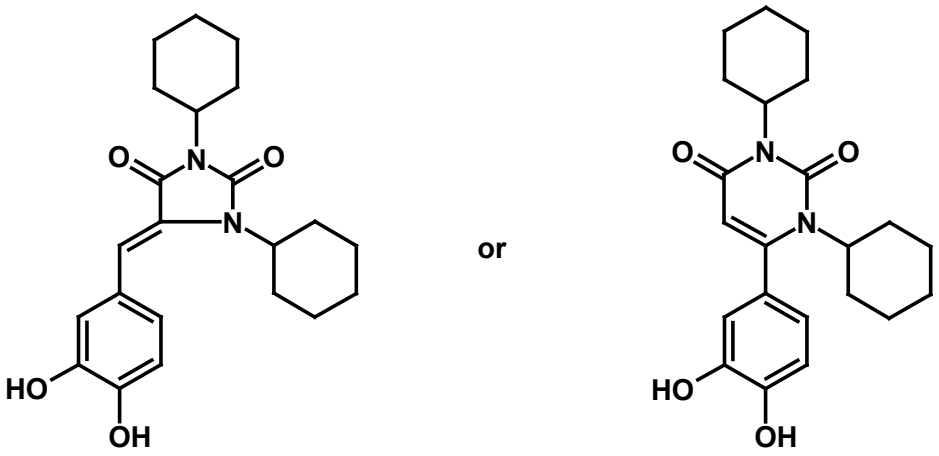

128A **128B**

To establish the correct structure the compound was analyzed through 2D-NMR method. In Figure 102 is reported the COSY spectrum and Figure 106 shows its correlation: a correlation was observed between the two doublet signals at δ 6.82 and 7.08 ppm assigned to two-proton AB system (Figure 106) in ring A. Other correlations were observed for the signals of cyclohexane ring C, ie H-11 at δ 4.05 to H-12 at δ 2.29, and H-12 at δ 2.29 to H-13 at δ 1.70 (Figure 106).

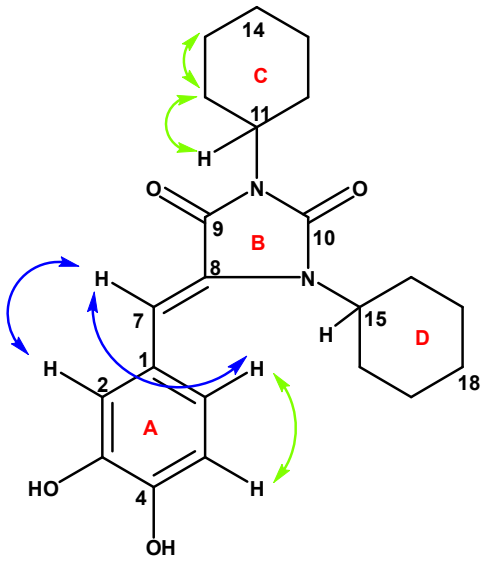

Figure 106: COSY (green arrows) and NOESY (blue arrows) correlation of compound **128A**

In Figure 105 is reported the HMBC spectrum and Figure 107 shows its correlation; correlations were observed between C-1, C-2, C-6, C-8, and C-9 (δ 138.5, 118.2, 124.5 125.2, and 164.0 respectively) to H-7 at δ 6.35. The six membered cyclic ring could be excluded on the basis of some HMBC correlations (for instance between the C-6, C-2 atoms at δ 124.5 and 118.2 respectively with the proton H-7 at δ 6.35, this correlation should be a 4J. Main selected HBMC correlations are shown in Figure 107.

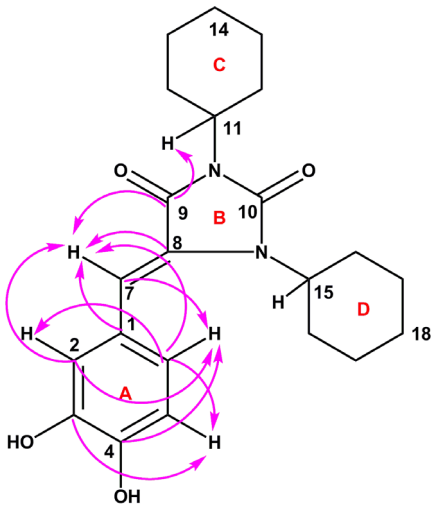

Figure 107: Selected HMBC correlation of compound **128A**

Based on these considerations, the most plausible structure is the **128A**; for this latter is possible write two alternative structures **128AA** and **128AB** which differ for the configuration of double bond. To define the configuration *E* or *Z* double bond, we used for 1D-NOEDs spectra reported in Figures 108 A, B, C.

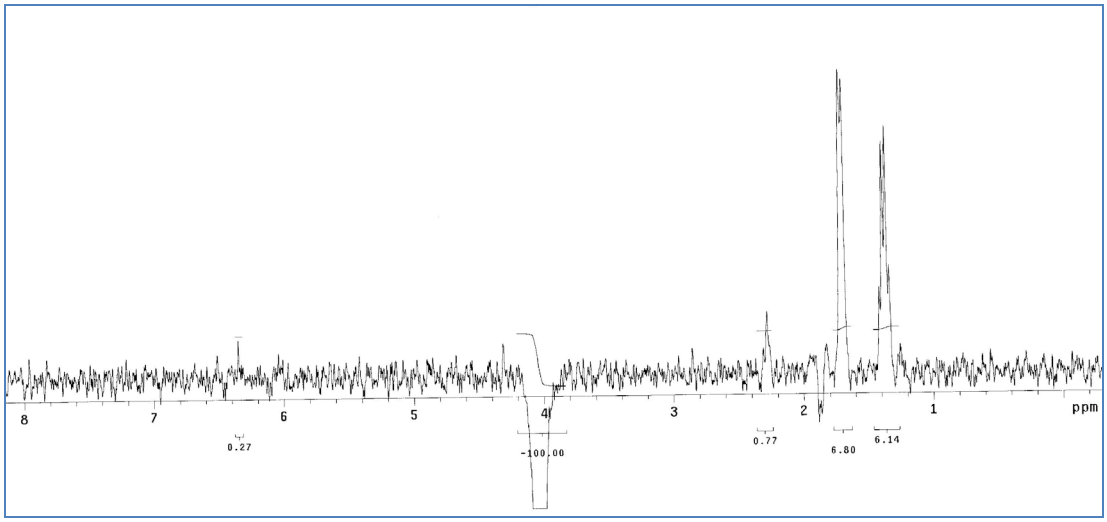

Figure 108A: 1D NOEDs spectrum of compound **128A**

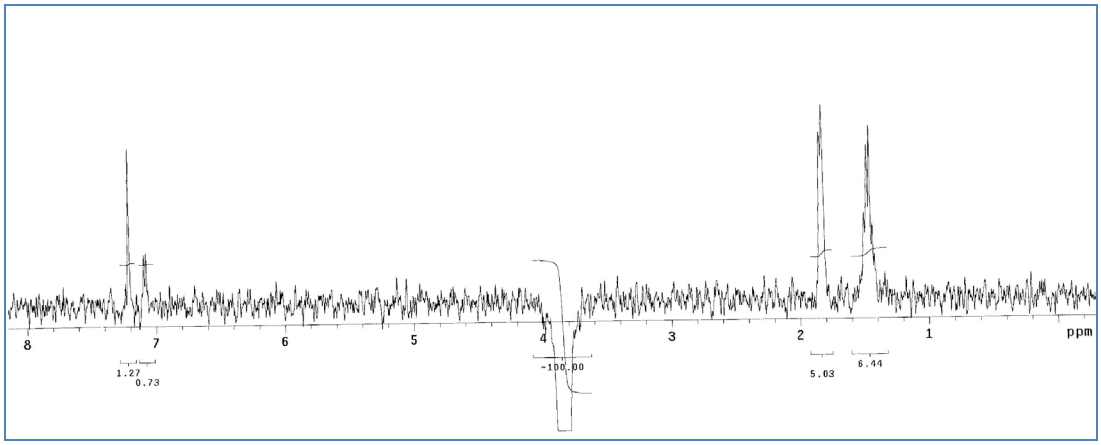

Figure 108B: 1D NOEDs spectrum of compound **128A**

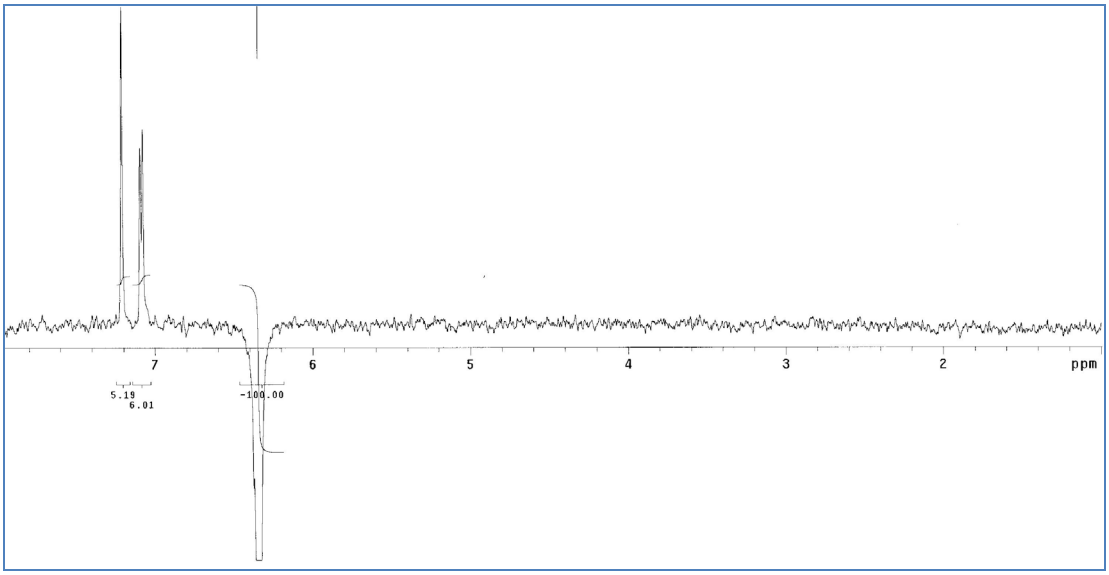

Figure 108C: 1D NOEDs spectrum of compound **128A**

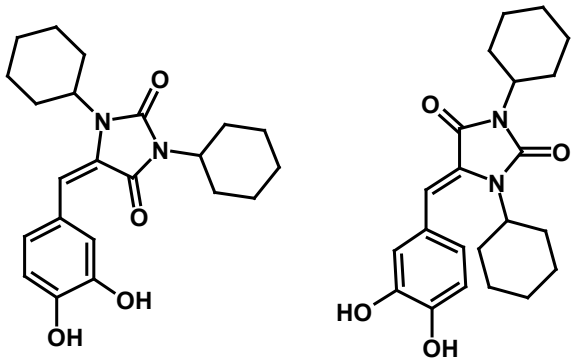

128AA **128AB**

It was observed that correlation between (Figure 108 A) the signals at δ 4.07 (H-11) and at δ 6.35 (H-7), which shows the connection between olefinic hydrogen and DCC moiety. Two correlations were observed from H-7 at δ 6.35 to H-2 and H-6 at δ 7.21, 7.08 respectively. This shows, caffeic moiety is connected to olefinic single proton. And also the correlation between H-15 at δ 3.84 to H-2 and H-6 at 7.21, 7.08 respectively, shows the formation of heterocyclic ring B. The key Noe correlations are reported in Figure 109 Based on these considerations, the most plausible structure is the **128AB**. Our theoretical study also corroborates the same hypothesis, which is discussed in section 2.3.4.

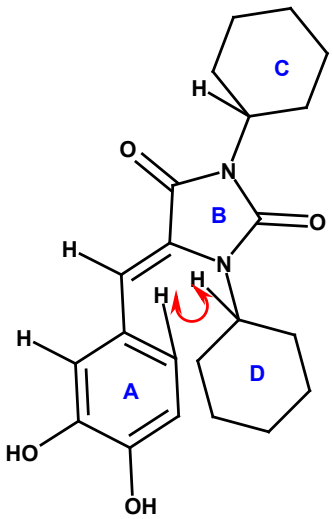

128AB

Figure 109: Selected NOE correlation of compound **128AB**

2.3.2 Enzymatic synthesis of caffeic hydantoin 130

To confirm that this methodology allows obtaining other hydantoins in mild conditions, one further enzyme-mediated synthesis was carried employing a different carbodiimide. In particular we synthesized the *N*-isopropylurea **129** and than hydantoin **130** (Schemes 45 and 46)

*2.3.2.1 Step1. Synthesis of caffeic N,N'-diisopropylurea **129***

For the synthesis of caffeic *N*-isopropylurea **129** we used caffeic acid **7** as starting material in the presence of DIC and *N*-ethyldiisopropylamine as base (Scheme 45). The reaction was carried in the best conditions previously found for the synthesis of **125**; the product **129** was obtained by column chromatography purification (yield 52%).

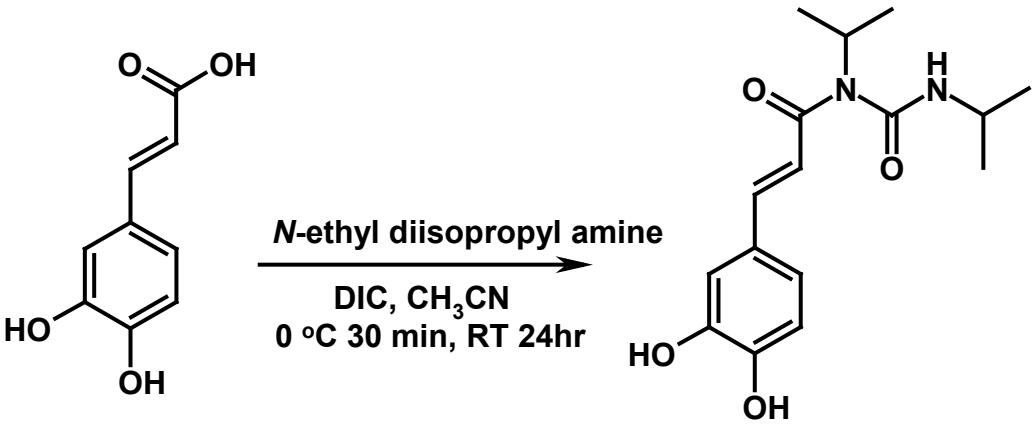

7 **129**

Scheme 45

The structure of **129** has not been previously reported, so we run both ^{1}H and ^{13}C NMR spectra; the ^{1}H and ^{13}C NMR spectra are reported in Figure 110 and 111, respectively. The mass spectrum shows a peak at *m/z* 305 $[M-H]^-$ (spectrum is not reported), supporting the expected structure of *N,N'*-diisopropylurea product incorporating two *N*-isopropyl moieties .

The ^{1}H NMR and ^{13}C NMR spectra are similar to those of the previously reported compound **125**, thus corroborating the hypothesis of the expected structure **129**. In fact, in the upper field of ^{1}H NMR spectrum there are seven signals, which have integrated to eight protons: a broad singlet at δ 4.87 (two protons) assigned to two group –OH, one doublet at δ 7.59 (with coupling constant 6.5 Hz) assigned to –N<u>H</u> function, two doublet signals at δ 7.46 and 6.62 with large coupling constant 15.25 Hz due two olefinic α,β-unsaturated protons, and reaming three signals (δ 6.86, 6.97, 7.11 ppm) integrated each for one proton due caffeic ring moiety. In low field region of the spectrum a heptet at δ 4.55 and an octet at δ 4.03 were observed and integrated each to one protons, which are assigned to isopropyl chain –C<u>H</u> of isopropyl chain, remaining two doublets with coupling constant 6.5 Hz at at δ 1.31 and 1.25, integrated to twelve hydrogens assigned to isopropyl chain $–CH_3$ function. In the ^{13}C NMR spectrum of **129** there are 14 signals: in upper field were observed 4 signals at 46.86, 43.5, 22.28 and 20.72 ppm for two CH and four CH_3; in the lower field (δ 165.5 to δ 114.6) were observed 10 signals, two of these (δ 165.2 and δ 154.6) are assignable for carbonyl carbons (<u>C</u>=O), the other eight signal (six for aromatic ring and two for a double bond (olefinic carbons) could easily assignable to caffeic moiety.

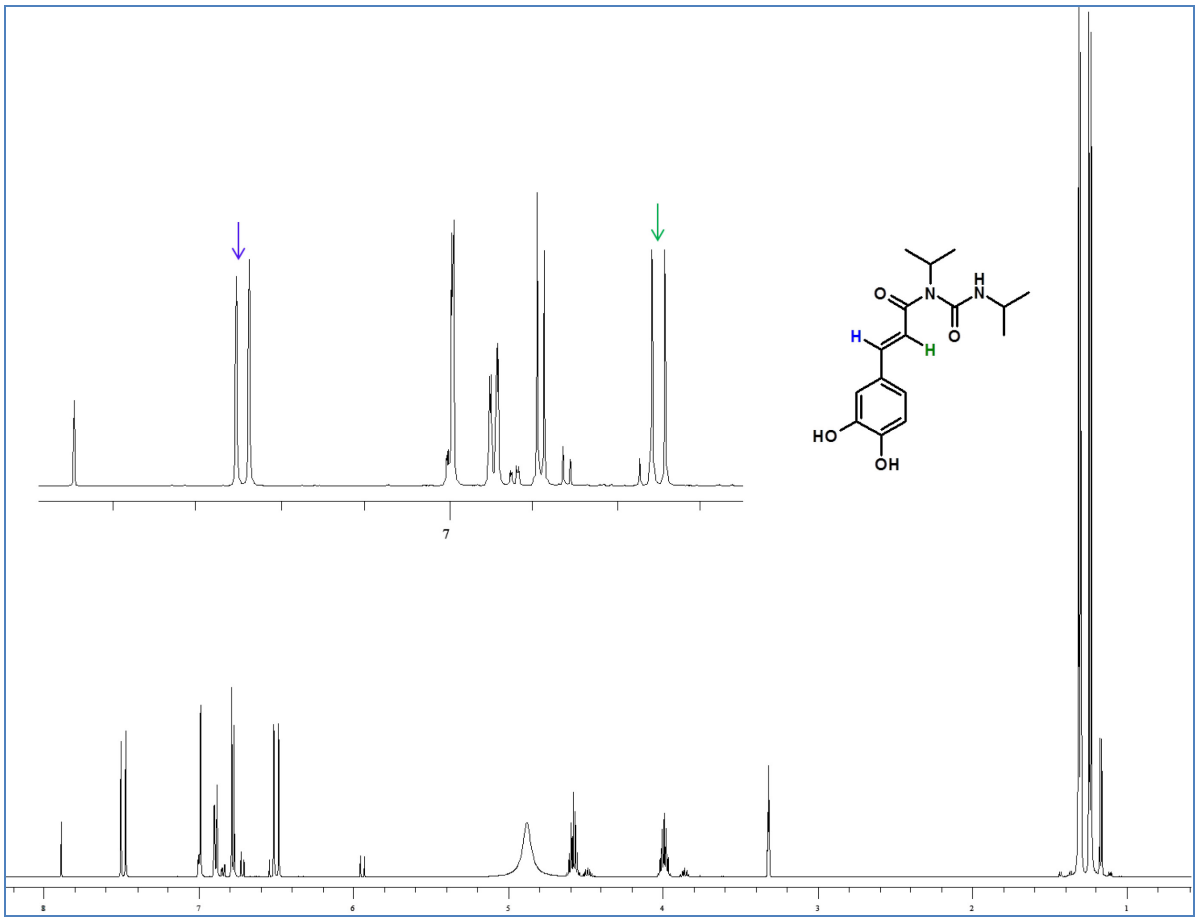

Figure 110: ^{1}H NMR spectrum of compound **129**

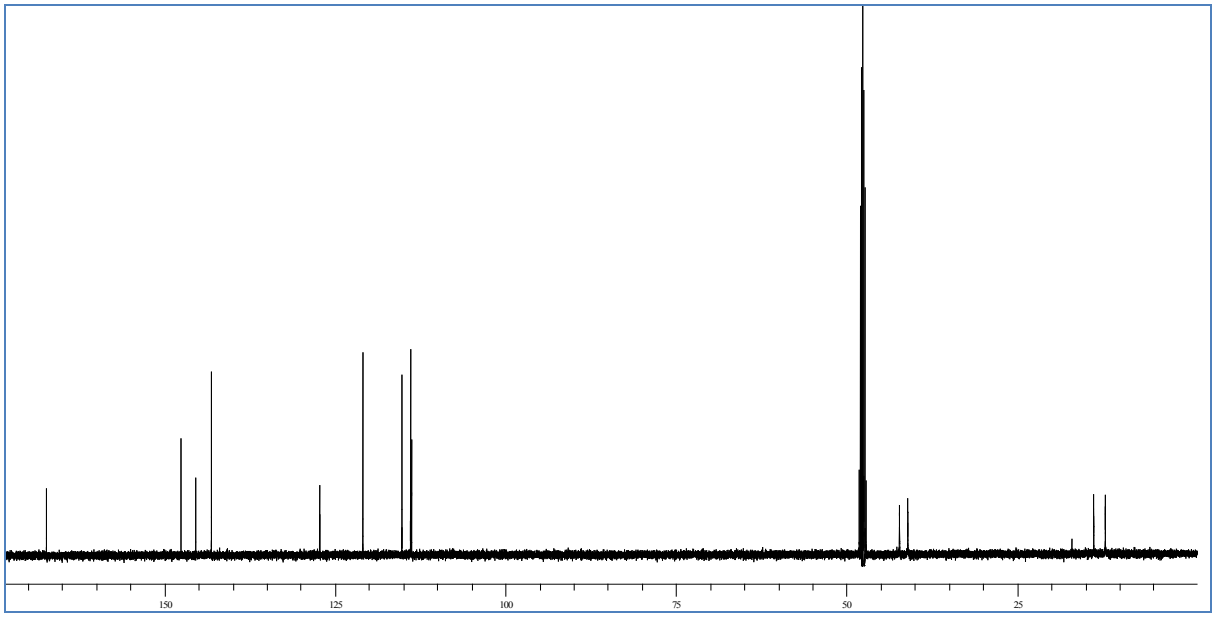

Figure 111: ^{13}C NMR spectrum of compound **129**

*2.3.2.2. Step 2. Enzymatic conversion of **129** to caffeic hydantoin **130***

The caffeic *N*-isopropylurea **129** was maintained in the presence of LTV enzyme for 24 hrs, as reported in Scheme 46, and afforded caffeic hydantoin **130** in 52% yield.

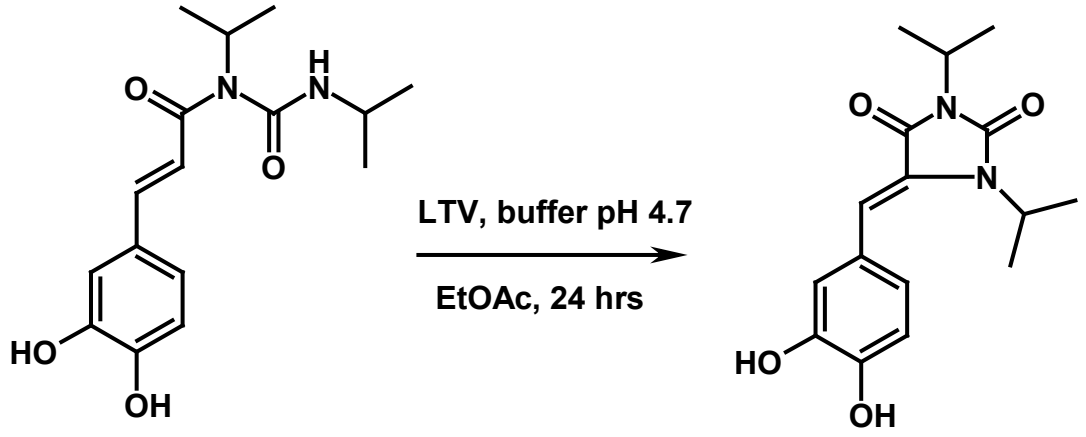

129 **130**

Scheme 46

After chromatographic purification, a complete spectroscopic characterization of the product **130** was carried out. The structure of this product has not been previously reported, so we employed both mono and two-dimensional NMR methods (COSY, NOESY, HMBC and HSQC) to assign all the signals.

The MS spectrum gave a $[M-H]^-$ ion at 303 *m/z* (spectrum not reported), supporting the expected structure of a hydantoin-related product incorporating two *N*-isopropyl moieties. The ^1H and ^{13}C NMR spectra are reported in Figure 112 and 113, respectively, and Table 13; assignments were aided by the careful analysis of COSY, HSQC and HMBC spectra, reported in Figure 114, 115, and 116 respectively.

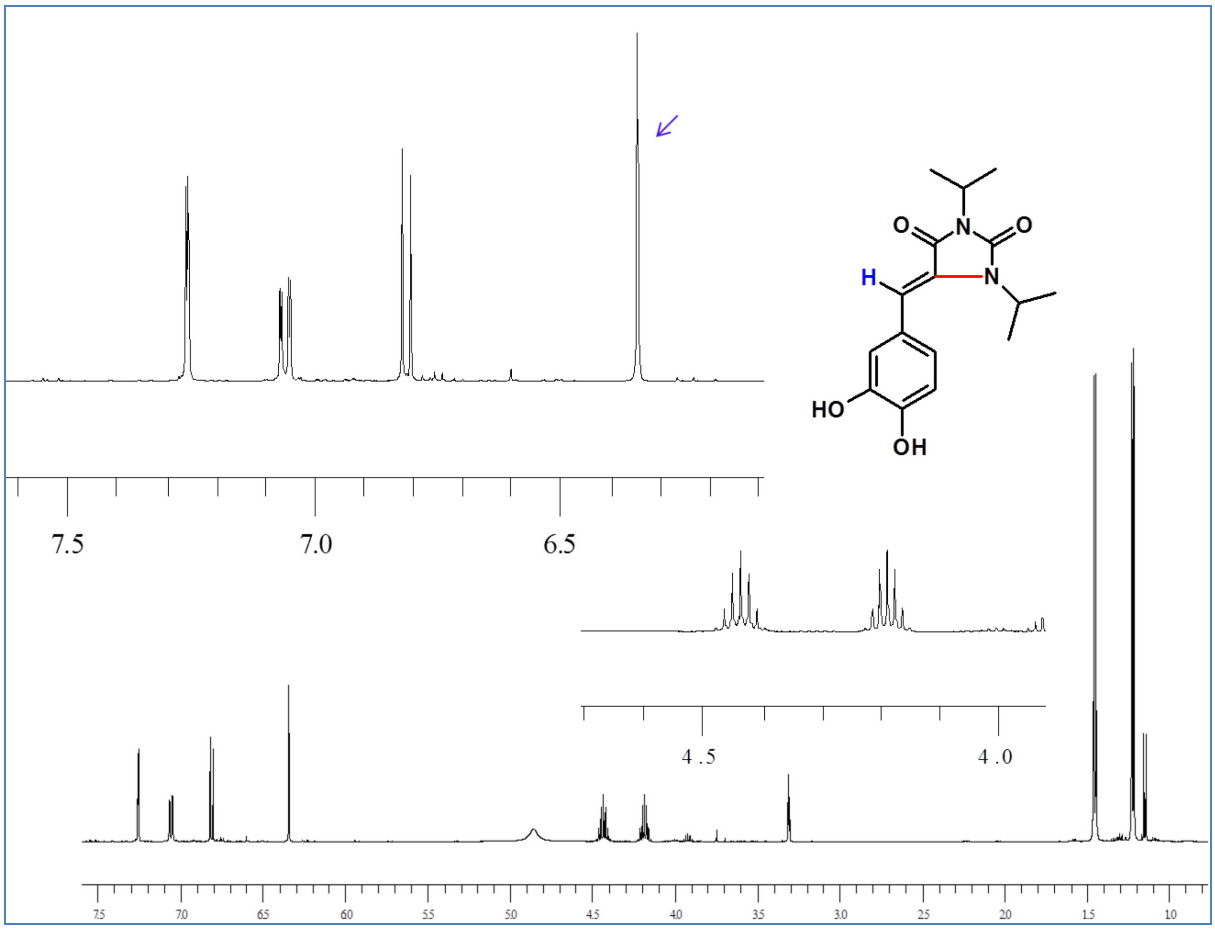

Figure 112: ^{1}H NMR spectrum of compound **130**

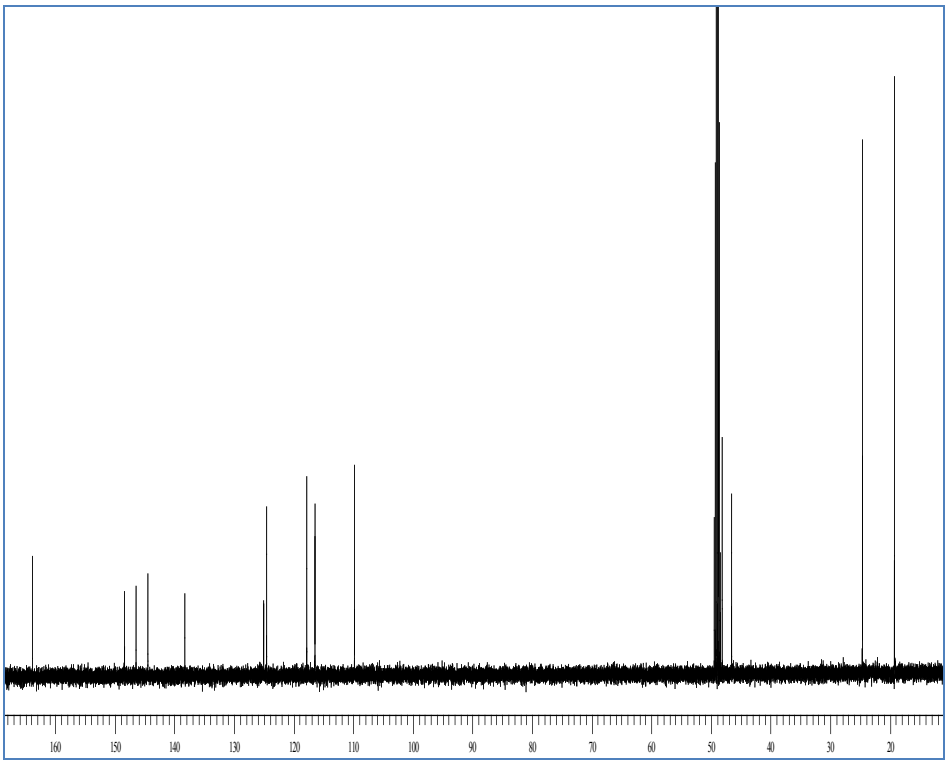

Figure 113: ^{13}C NMR spectrum of compound **130**

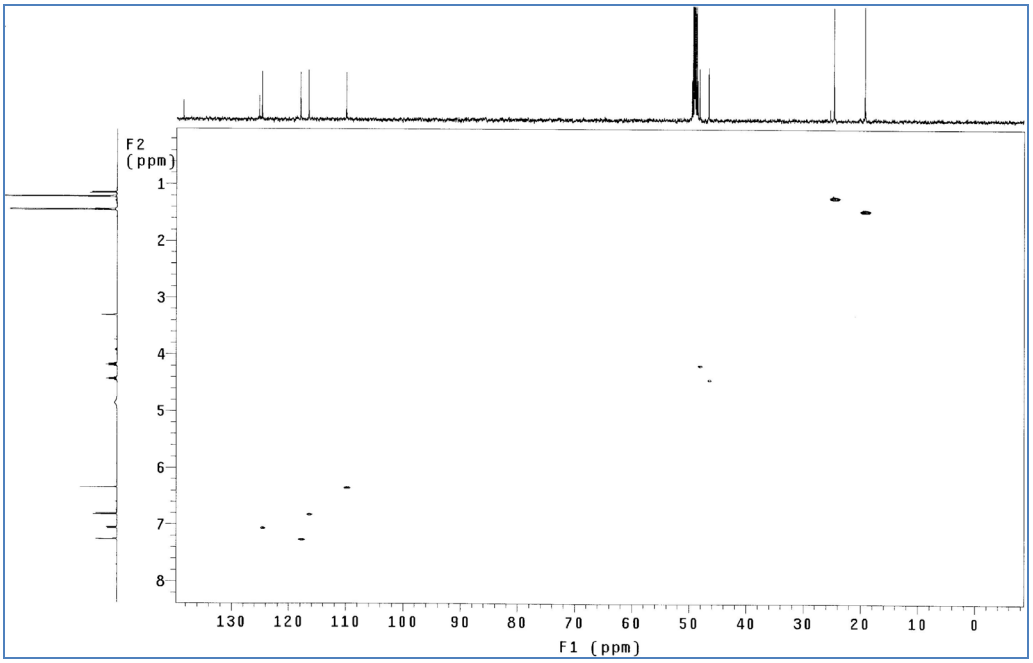

Figure 115: HSQC spectrum of compound **130**

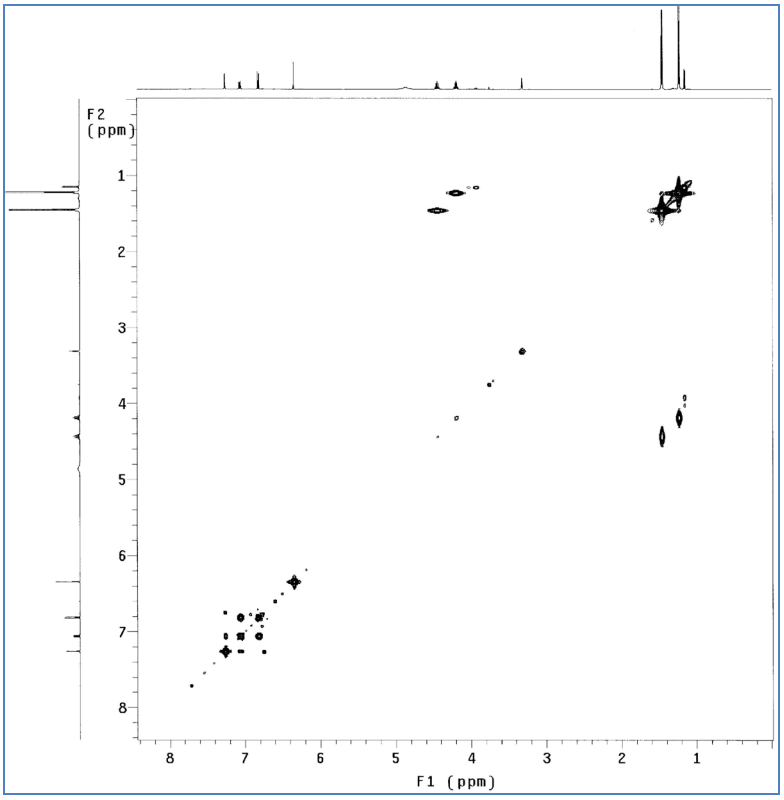

Figure 114: COSY spectrum of compound **130**

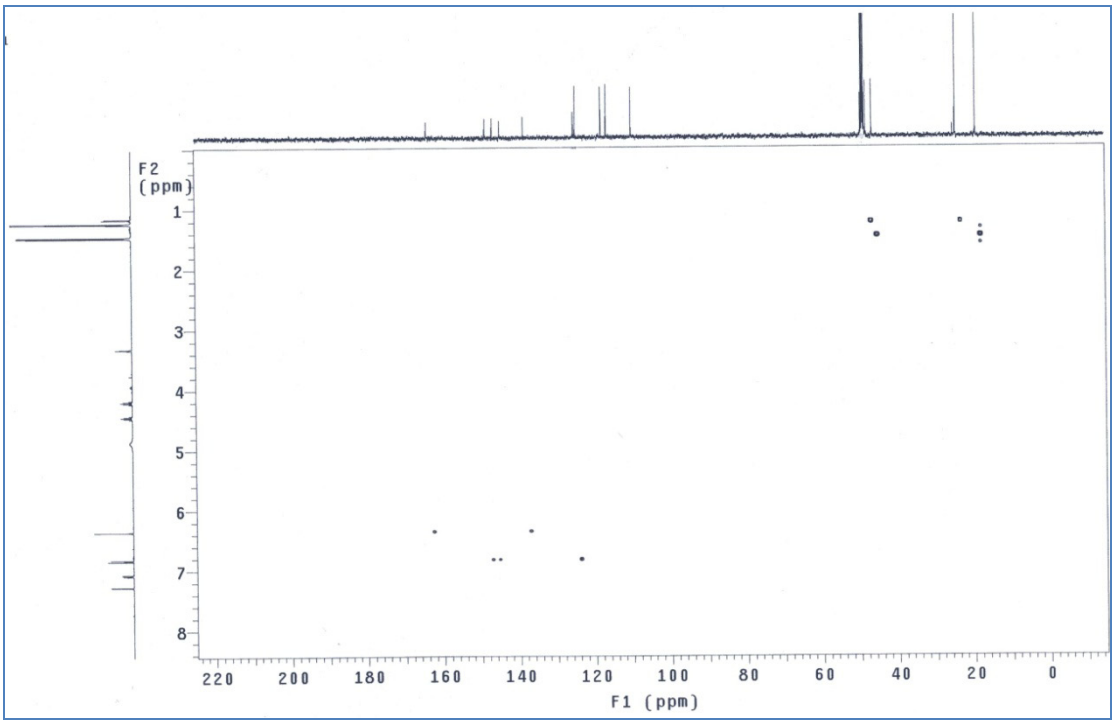

Figure 116: HMBC spectrum of compound **130**

Table13: ^{1}H and ^{13}C NMR data of compound **130**

C	δ_C in CD_3OD	H	δ_H (mult, J Hz) in CD_3OD
C-1	125.1		
C-2	117.9	H-2	7.26 (d,2.0)
C-3	146.6		
C-4	148.5		
C-5	116.5	H-5	6.81 (d,8.5)
C-6	124.6	H-6	7.06 (dd, 8.5, 2.0)
C-7	109.9	H-7	6.35 (s)
C-8	138.4		
C-9	163.9		
C-10	144.6		
C-11	46.5	H-11	4.44 (m)
C-12,12'	19.2	H-12,12'	1.45 (d,6.5)
C-13	48.1	H-13	4.19 (m)
C-14,14'	24.6	H-14,14'	1.22 (d,6.5)
		OH-3,4	4.87 (s)

The ^{13}C NMR spectrum showed 14 signals: the majority of signals were in the sp^2 region (from δ 163.9 to 109.9 ppm), but four signals (isopropyl chain) in the upper field region of the spectra (δ 46.5 to 24.6 ppm) were observed. In the sp^2

region there are 6 quaternary carbon signals and 4 CH. In those two signals at δ 144.6 and δ 164.0 assign to two carbonyl carbons C-10 and C-9 respectively. The ^{1}H NMR spectrum of **130** in the region from 7.26 and 6.35 ppm shows clear similarities with the spectra of the substrate **129**, except two olefinic protons in fact one singlet was observed at δ 6.35 instead of a two doublet with a large coupling constant due two *trans* olefinic protons. For the complete signal assignment of compound **130** is done as similar to the compound **128AB**.

2.3.3. Study of the mechanism of formation of the hydantoins

Once established unambiguously the structure of the hydantoin **126** and **130**, we tried to understand the mechanism of formation. Looking at the *N*-acylurea used as starting material, the possibility of an aza-Michael intramolecular reaction was considered (Scheme 47) where the nucleophilic NHR could attack the electrophilic carbon (C-7) of the α,β-unsatured system; nevertheless, in this case the product **128B** would be formed, with a six-member cyclic ring: in addition, there is no role for the enzyme and it is difficult to think that in the mild reaction conditions employed for this reaction could occur spontaneously. So this hypothesis was easily ruled out. On the other hand, it is well-known that laccases and polyphenol oxidases[91] are able to catalyze the oxidation of *ortho*-diphenolic compounds to the corresponding quinones: if this occurs, a reasonable mechanistic hypothesis is that the caffeic quinone results in an 'activated form' of the *N*-acylurea, and the electron-withdrawing effect of one quinone oxygen could justify the attach at the electron-poor position C-8, thus realizing a 5-member cycle as reported in structure **128A**. In order to support this hypothesis we tried to carry out similar reactions starting from ferulic acid, where the 'activating' oxygen is blocked, or *p*-coumaric acid, where only the *p*-

phenolic group is present: in these systems the *ortho*-quinone cannot be formed.

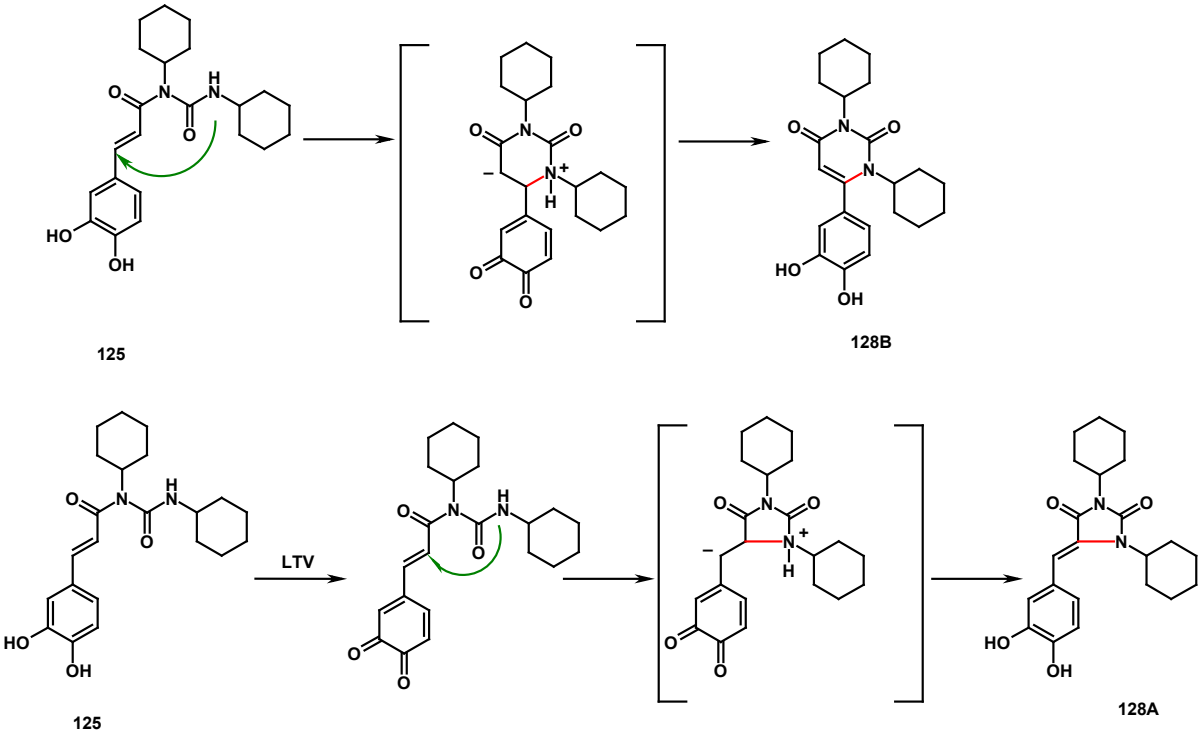

Scheme 47

2.3.4 Attempted Synthesis of Ferulic and Coumaric Hydantoin

2.3.4.1 Step1. Synthesis of Ferulic acid N,N'-dicyclohexylurea ***132***

We used ferulic acid **131** is starting material in the presence of DCC and *N*-ethyldiisopropylamine as base for the synthesis of ferulic *N*,*N*'-dicyclohexylurea **132** (Scheme 48); the product **132** was obtained by column chromatography purification (yield 30%). The structure of **132** has not been previously reported, so we run both ^{1}H and ^{13}C NMR spectra (reported in Figure 117 and 118, respectively)

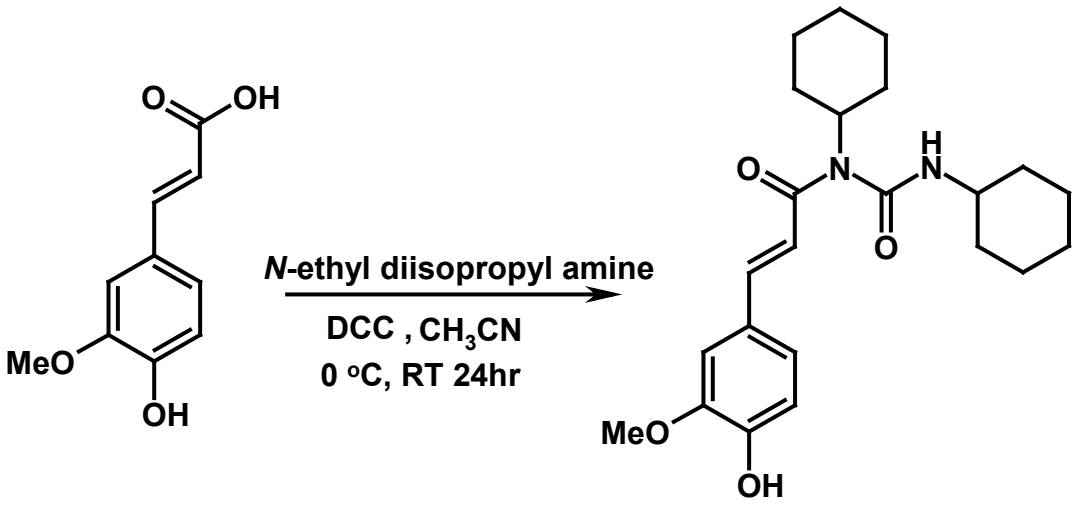

131 **132**

Scheme 48

The complete characterization of the compound **132** has been carried out by ^{1}H and ^{13}C NMR spectroscopy. ^{1}H NMR suggest that in the lower field region there are five signals, which have integrated to five hydrogens. Two doublet signals at δ 7.55 and 6.55 with large coupling constant 15.0 Hz gives two olefinic α,β-unsaturated hydrogens, and reaming three signals, one is double of doublet at δ 7.01 with coupling constant 8.0 and 2.0Hz, and other two doublets with coupling constant 2.0 and 8.0 Hz at δ 7.09 and 6.80 respectively to assign ferulic ring moiety hydrogens. In upper field of the spectra a set of multiplet were observed, which have been overlapped each other and assigned to hexane ring moiety integrated to 22 hydrogens. And a singlet at δ 3.87 integrated to three hydrogens assign to –O$\underline{C}H_3$ function.^{13}C NMR shows there are 19 signals of ferulic acid *N,N'*-dicyclohexylurea **132**, in which 10 signals in sp^2 region at δ 165.1 to δ 109.6 and 9 signal in upper field of the spectra which are assignable to two hexane rings, which corroborate us formation of ferulic acid *N*-acylurea **132**. Two carbons in lower field of the spectra at δ 165.1 and δ 154.6 are assignable for carbonyl carbons ($\underline{C}$=O).

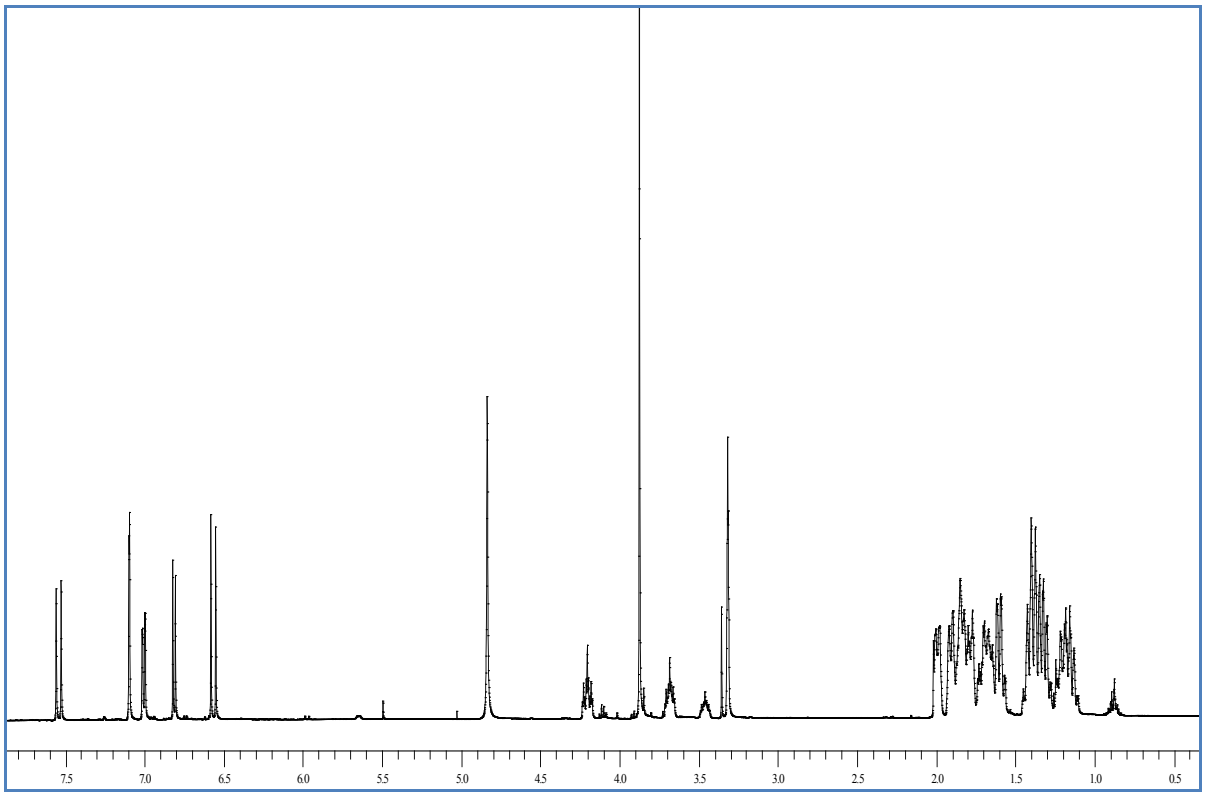

Figure 117: ^{1}H NMR spectrum of compound **132**

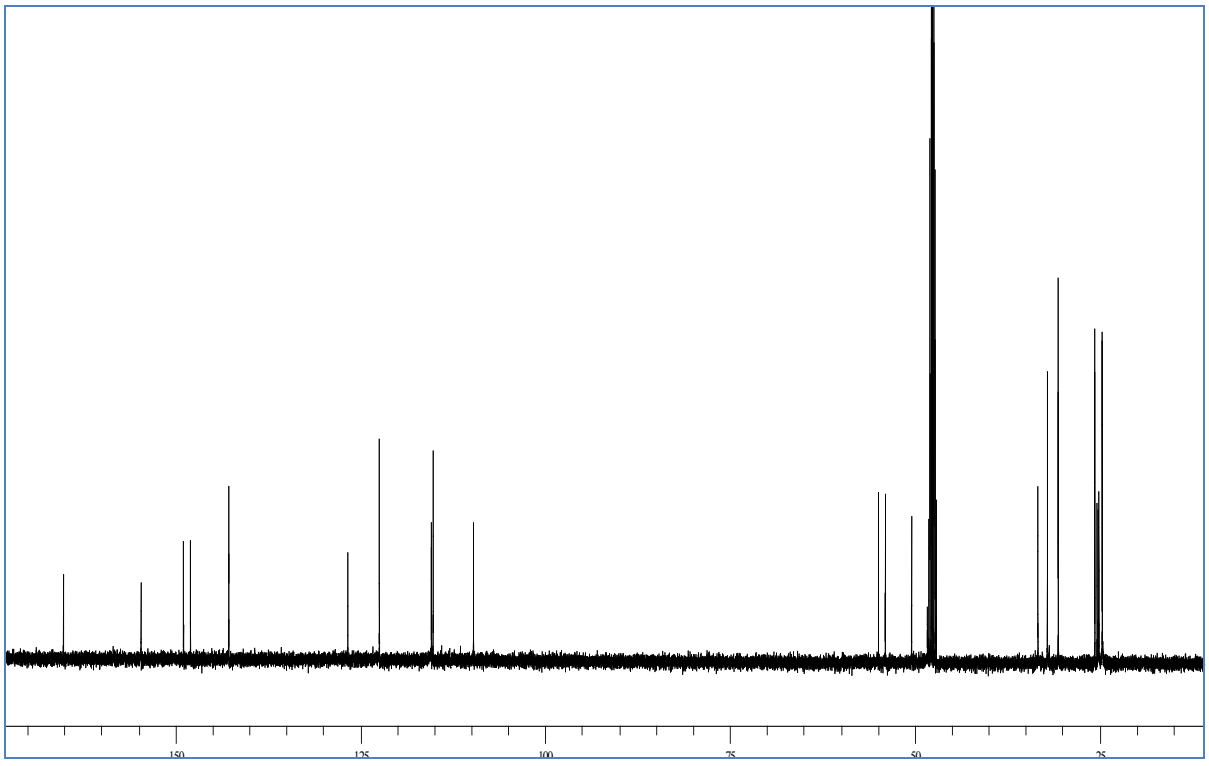

Figure 118: ^{13}C NMR spectrum of compound **132**

2.3.4.2 *Step2 Attempted Synthesis of Ferulic Hydantoin*

The ferulic *N,N'-dicyclohexylurea* **132** was maintained in the presence of LTV enzyme for 24 hrs, as reported in Scheme 49, and there is no conversion of

substrate **132** was observed. This shows catechol or quinone moiety is critically important to the formation of hydantoin.

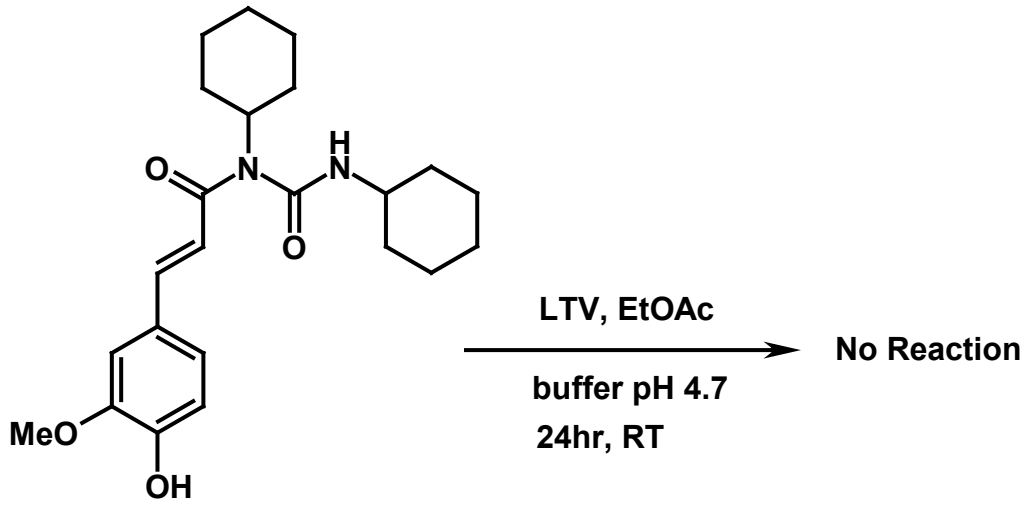

132

Scheme 49

*2.3.4.3 Step1. Synthesis of Coumaric acid N-acylurea **134***

We used coumaric acid **133** as starting material in the presence of DCC and *N*-ethyldiisopropylamine as base (Scheme 50) for the synthesis of coumaric *N*-dicyclohexylylurea **134**. The reaction was carried in the best conditions previously found for the synthesis of **125**, **130** and **131**; the product **134** was obtained by column chromatography purification (yield 30%).

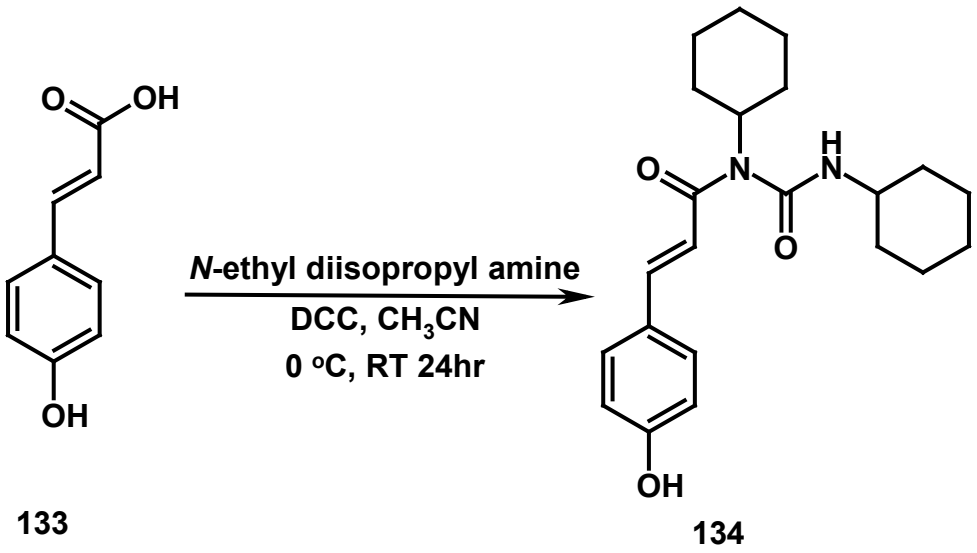

133 **134**

Scheme 50

The structure of **134** has not been previously reported, so we run both ^{1}H and ^{13}C NMR spectra; the ^{1}H and ^{13}C NMR spectra are reported in Figure 119 and 120

The complete characterization of the compound **134** has been carried out by ^{1}H NMR and ^{13}C NMR spectroscopy. In the lower region of ^{1}H NMR spectrum there are four signals, which are integrated to six hydrogens. Two doublet signals at δ 7.55 and 6.53 with large coupling constant 15.5 Hz gives two olefinic α,β-unsaturated hydrogens, and reaming two signals, two doublets with coupling constant 8.5 Hz at δ 7.09 and δ 6.80 to assign coumaric ring moiety AA'BB' system. In upper field of the spectra a set of multiplet were observed, which have been overlapped each other and assigned to hexane ring moiety integrated to 22 hydrogens. ^{13}C NMR shows there are 18 signals of coumaric *N,N'*-dicyclohexylurea **134**, in which 10 signals in sp^2 region at δ 165.2 to δ 115.4 and 8 signal in upper field of the spectra which are assignable to two hexane rings. Two carbons in lower field of the spectra at δ 165.2 and δ 154.6 are assignable for carbonyl carbons (C=O).

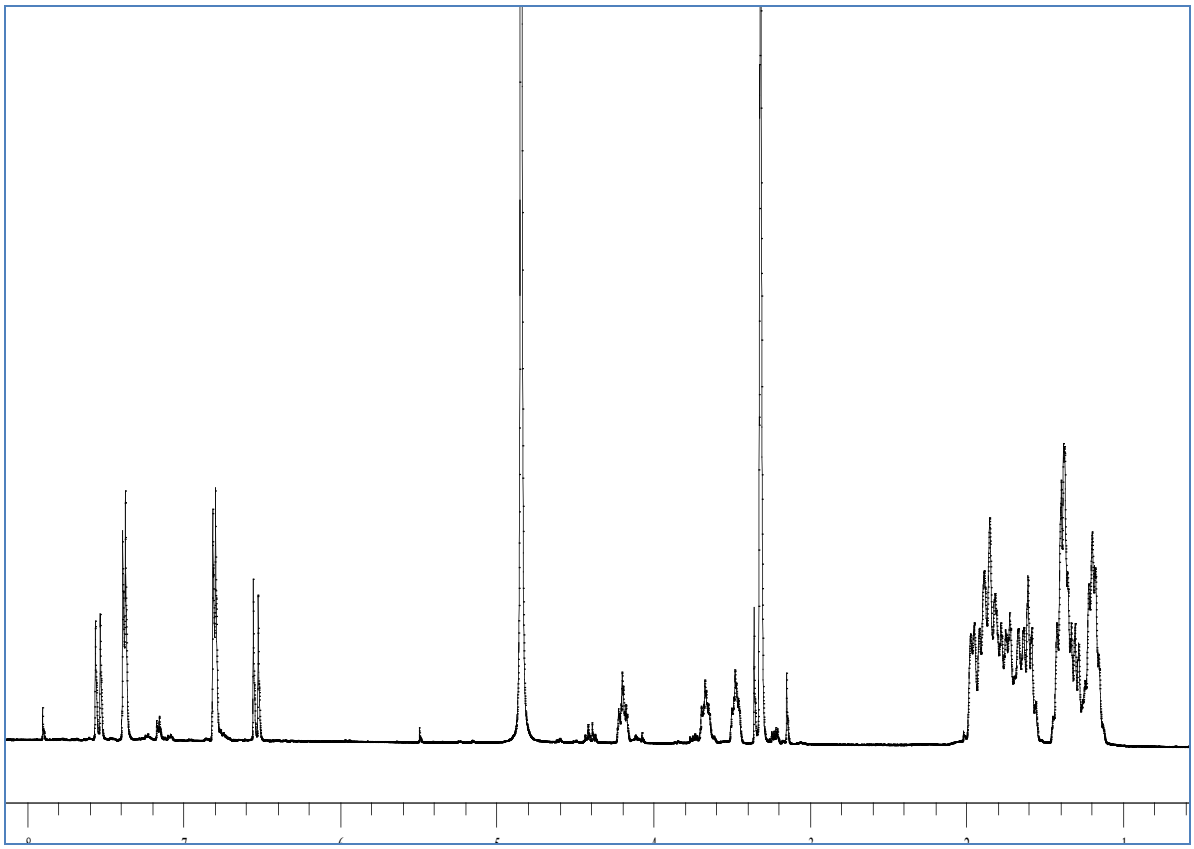

Figure 119: ^{1}H NMR spectrum of compound **134**

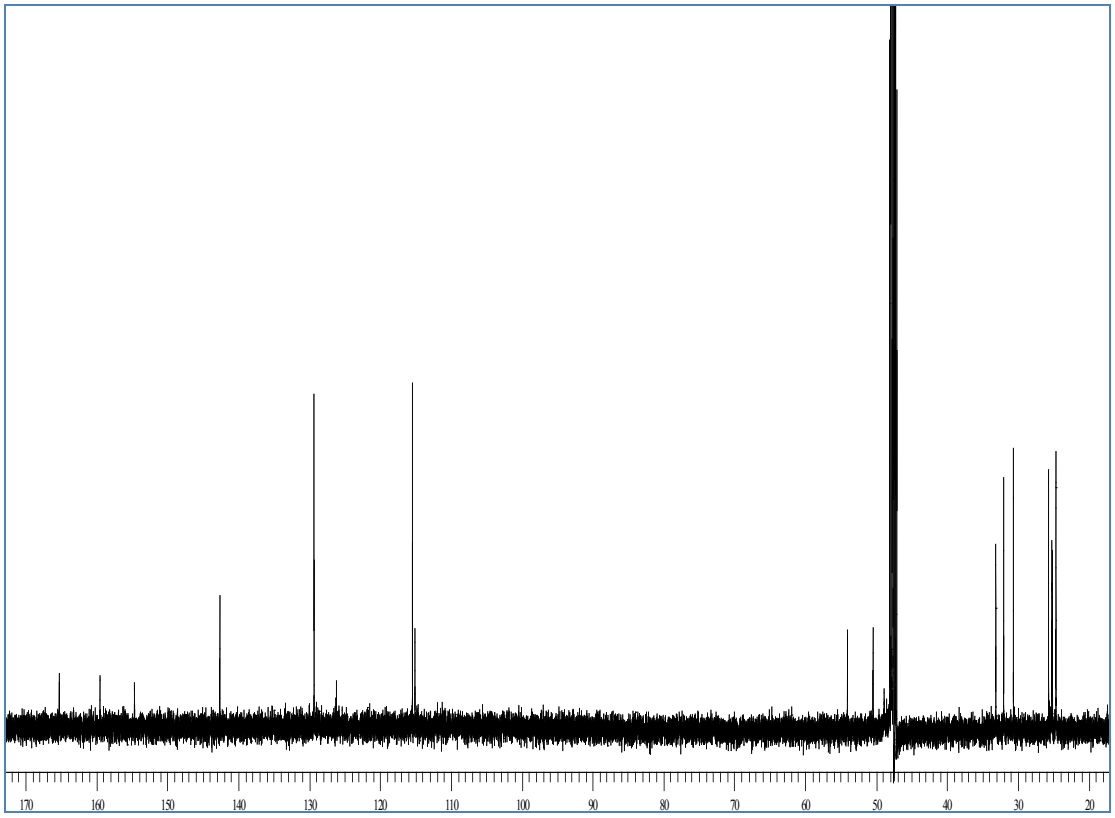

Figure 120: ^{13}C NMR spectrum of compound **134**

2.3.4.4 Step2. Attempted Synthesis of Coumaric Hydantoin

The coumaric *N,N'-dicyclohexylurea* **134** was maintained in the presence of LTV enzyme for 24 hrs, as reported in Scheme 51, and there is no conversion of substrate **134** was observed.

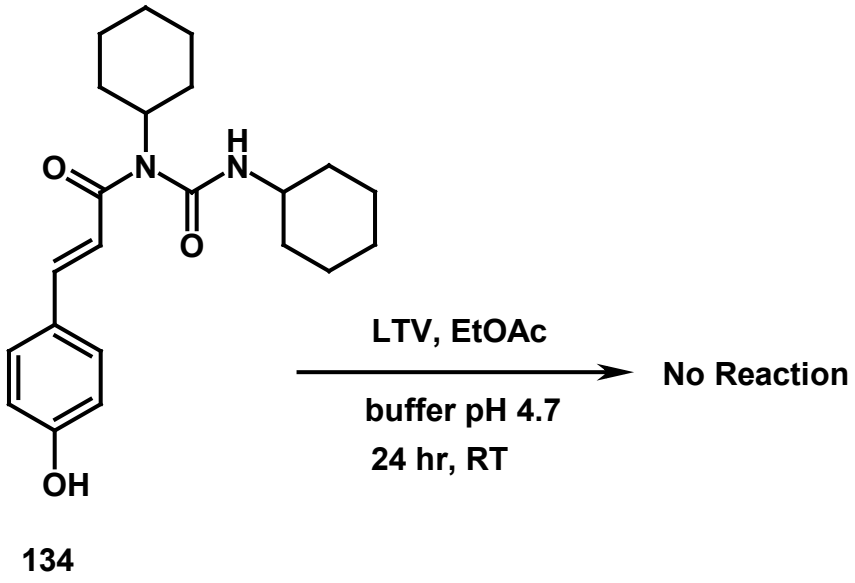

134

Scheme 51

On the basis of these data we can conclude that the *ortho*-diphenolic function is crucial for the formation of compound **128** and **130**. In order to support this mechanistic hypothesis, in collaboration with Prof. Rescifina – University of Catania - a theoretical in silico study at semiempirical AM1 level was carried out.

2.4 Theoretical Study of the mechanism of formation of the hydantoins 128A

The formation of cyclic compound **128** was further rationalized by means of a theoretical in silico study at semiempirical AM1 level starting from the not isolated intermediate *o*-quinone **135**, whose existence was experimentally demonstrated and in accord with literature date.

Mechanistically speaking, the most direct and easy method to obtain the hydantoin **128** is an intramolecular anti-aza-Michael reaction between the

amidic nitrogen atom and the C_α double bond, rationalized by the presence of a much stronger electron-withdrawing β-substituent, such as the *o*-quinone moiety, that induce an umpolung of the C=C double bond of the α,β-unsaturated carbonyl system.

This depicted scenario, taking into account that both C=C double bond and amidic moiety are soft acid and base, respectively, can be rationalized on the basis of HOMO and LUMO interactions of the compound **128**. From the HOMO and LUMO surfaces reported in Figure 121 it is possible to observe that in the HOMO the electrons are localized mainly on the amidic oxygen and nitrogen atoms with the nitrogen one that possess the more high orbital coefficient whereas in the LUMO the coefficients of importance for the nucleophilic attack are localized on C_α, C_{ipso} and C_6 atoms; however, the intramolecular cyclization on these last two carbon atoms would produce a seven- or eight-member ring and is entropically unfavourable.

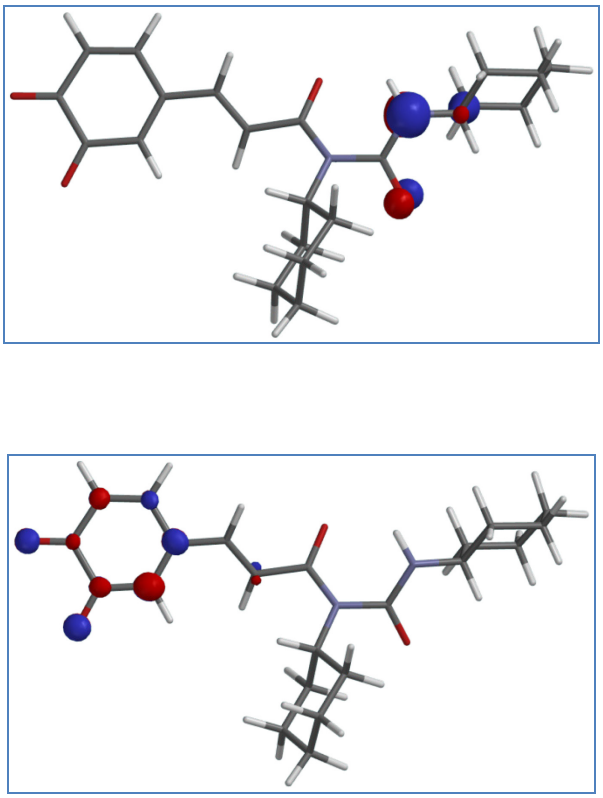

Figure 121: HOMO and LUMO plot for quinone **135**

To get more insights into the mechanism of this intramolecular anti-aza-Michael reaction we studied the entire process from reactant to product considering all the possible transition states. To do this, let us introduce some considerations.

On the basis of the knowledge acquired on the analogue addition of amines, the addition of a neutral amide to an activated carbon-carbon double bond can be described by Scheme 52a. A nucleophilic attack on the activated double bond in **135** leads to the charge-separated intermediate **136**, which can yield the neutral product **137** through several pathways. In many cases, the significant pathways that lead from **137** to **138** are either deprotonation of the amide moiety to form a negatively charged molecule or intramolecular proton transfer. The possible pathway through initial protonation of the negatively charged carbon to produce a positively charged intermediate followed by deprotonation of the amide is not significant. Evidence for the participation of the zwitterionic intermediate **136** in the addition reaction derives from the dependence of the rate and equilibrium constants on both the pK_a, of the nucleophilic amide and the capability of the activating group (see Scheme 52a) to delocalize the negative charge formed on C_α. From structure-reactivity relationships, it was shown that the intramolecular proton transfer is a dominant pathway in the addition of amines, and therefore amides, to activated double bonds, thus establishing the importance of the conversion of the zwitterions **136** to the product **137**. However, the precise mechanism of the intramolecular proton transfer is not known. Several possibilities have been considered, and a direct transfer from the amine to the carbanion has been discounted on the basis of a proton inventory study. On the other hand, a solvent (or reactant-assisted) proton transfer, such as described by **140** in Scheme 52b, is a

feasible mechanism for the intramolecular proton transfer. This suggestion is supported by early observations that in aprotic solvents, addition reactions of this type are second order in the concentration of the amine. A recent analysis of the addition of amines to an activated double bond in *trans*-2-furylnitroethylene confirmed the proposed participation of the second amine molecule in the proton transfer in the transition structure. The catalytic role of discrete water molecules in the addition of ammonia to formaldehyde was characterized in a detailed computational study in which the cyclic, activated transition complexes were shown to include one or two solvent molecules.

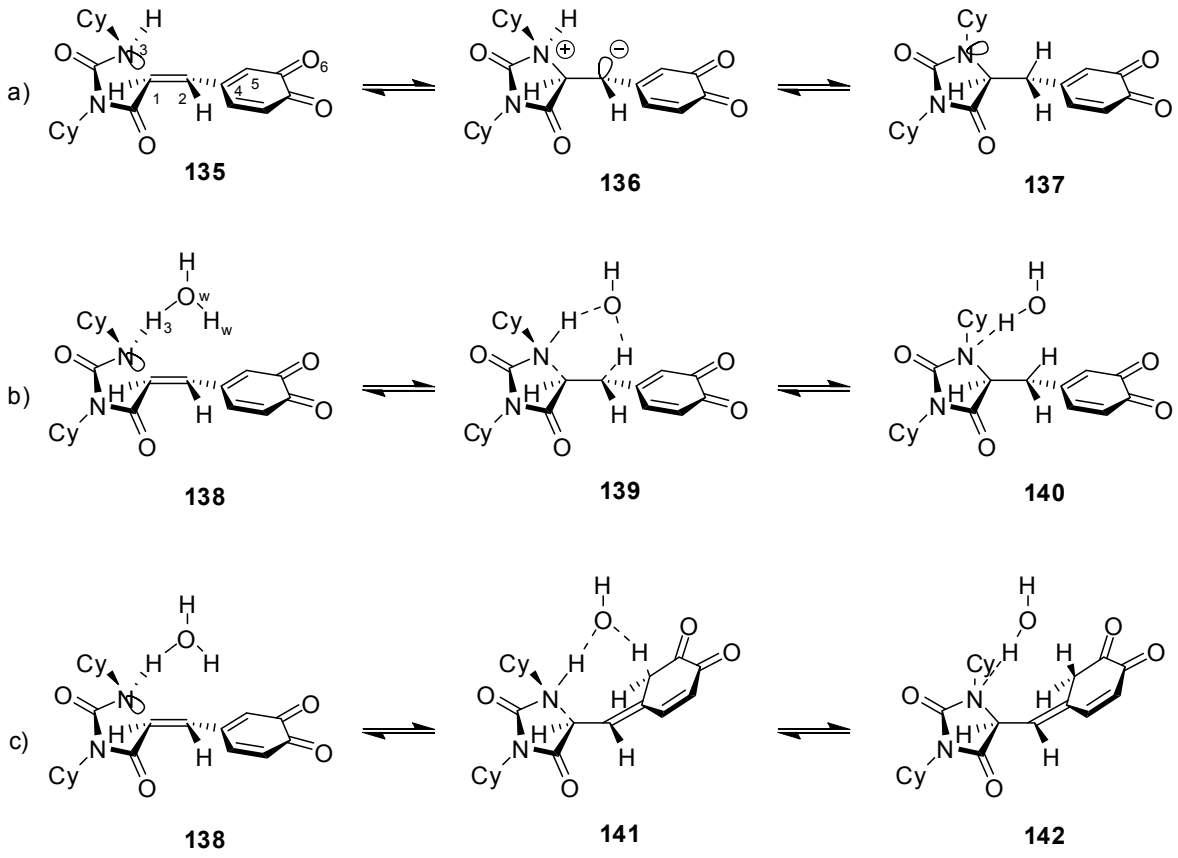

Scheme 52: Proposed mechanisms for the anti-aza-Michael intramolecular cyclization

Theoretically are possible three type of nucleophilic addition named 1,2- (Scheme 52b), 1,4- (Scheme 52c), and 1,6- (not showed), that depend from the proton transfer on C_2, C_5, or O_6, respectively. Since this transfer occurs between a hard acid (H^+) and a hard base (C^- or O^-) the interaction is governed

by charges and a rough evaluation can be made on optimizing the compound derived from the attack of the anionic amide (Figure 122). From this calculation results that the more high negative charge is on C_5 whereas C_2 and O_6 have the same value, then the 1,4-addition should be the expected one. However, we have optimize both 1,2- and 1,4- transition states excluding the 1,6- one because (i) it generate a negative charge of the same intensity of the 1,2-attack and then it is, supposedly, energetically comparable, and (ii) this transition state presume a more extended network of water molecules (almost three) and then it is more difficult to manage.

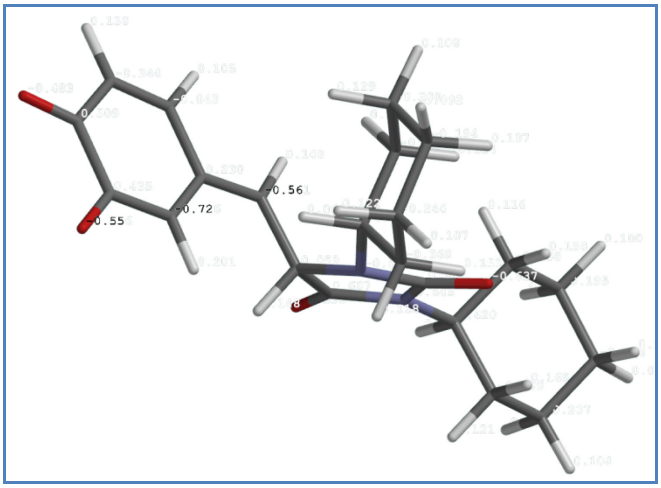

Figure 122: Anionic intermediate from **135**

2.4.1 Mechanism of the Nucleophilic 1,2- and 1,4-Addition

In a computational simulation of the formation of **139** in vacuum, we observed that the interaction is monotonically repulsive for distances between C_1 and N_3 (see Scheme 52 for numbering of atoms) ranging from 3.0 to 1.5 Å. An attempt to calculate the stabilization of the zwitterionic form by a polar solvent, such as water, also resulted in an unfavorable state relative to the separated molecules. Taken together, these findings and considerations lead to the hypothesis that in the process of amide addition to an activated double bond, the aqueous solution provides not only a polar medium for the reaction but also a discrete

water molecule that participates in the reaction. The reaction path is shown in Scheme 52b and represents the nucleophilic 1,2-addition of an amide assisted by a discrete water molecule. The role of the explicit water molecule in this mechanism is to act as a shuttle for the proton between N_3 and C_2 and is thus added to the effect of bulk solvent computed here from a model of continuum dielectric (see below).

The potential energy surface for the 1,2-nucleophilic addition of CONH---OH_2 to the activated double bond in **135** was scanned with the semiempirical AM1 method. The results showed that the nucleophilic attack of amide is characterized by (i) the C_1–N_3 distance to the attacked carbon, (ii) the N_3–H_3 distance of the hydrogen bond between amide and the water molecule, and (iii) the C_2–H_w, distance of the nascent bond to the second carbon of the double bond (see Scheme 52b for numbering of atoms).

Moreover, these results showed that two of the internal coordinates, N_3–H_3 and C_2–H_w, are coupled to their complementary internal coordinates, the H_3–O_w and the O_w–H_w distances, respectively.

The energetic relationships among the various positions in the reaction path are reflected in the potential energy surface constructed from the energies of the movement of the protons (H_3 and H_w) for fixed C_1–N_3 distances of 2.0, 1.8, 1.6, and 1.427 Å (the C_1–N_3 distance of 1.427 Å represents the optimized bond in the product of addition).

Similar considerations be worth for 1,4-addition according to Scheme 52c.

2.4.2 Transition-State Structures

The transition states were identified, as described in the Methods section, from AM1 calculations of the potential energy surface around the structures initially identified. The harmonic vibrational frequencies characterize these stationary

points as real TS in which the matrices of force constants have a single negative eigenvalue. For 1,2-attack the major contribution to the eigenvector with the negative eigenvalue comes from C_2–H_w, a minor contribution comes from the C_1–N_3 internal coordinate, and no significant contribution comes from the N_3–H_3 internal coordinate. The most relevant geometrical parameters of the optimized TS **139** and product **140** are depicted in Figure 123.

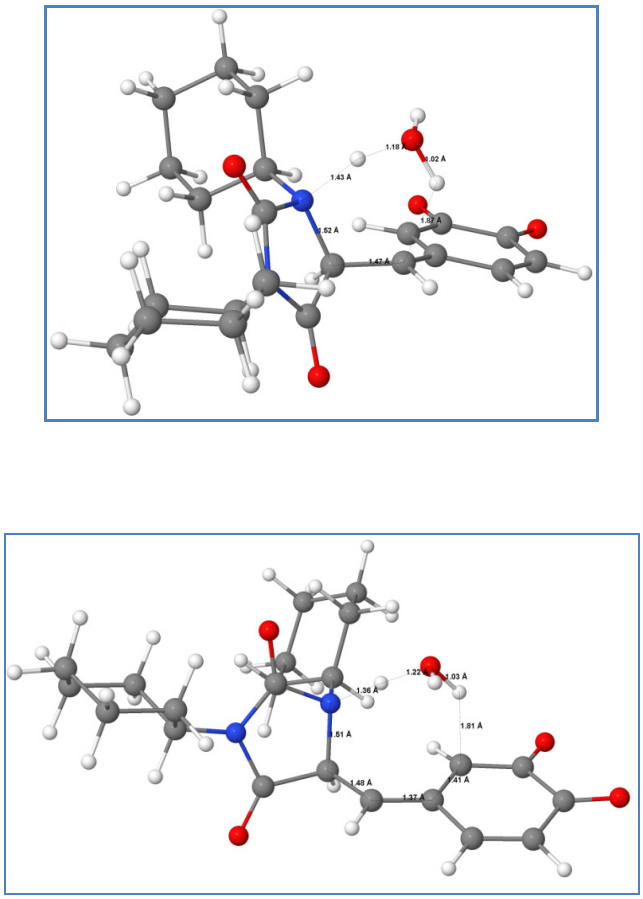

Figure 123: Bond distances in TSs **139** and **140**.

The initial approach to the CONH---OH_2 complex to C_1 is at an incident N_3–C_1–C_2 angle of 112.17° in a plane nearly perpendicular to the C_1–C_2–C_4 one. The orientation dihedral angle N_3–C_1–C_2–C_4 is 101.24°. Along this approach, the energy increases monotonically until the C_1–N_3 distance reaches an approximate value of 1.5 Å. Due to the approach of the CONH---OH_2 complex, C_1 and C_2 are pyramidalized, the charge density of the TS is polarized, and C_2

acquires negative charge following the attack of CONH on C_1. Clearly, the charge on C_2 changes from neutral in the reactant to –0.57 in the TS **139**. In parallel, the charge on N_3 changes from neutral to positive. The attraction of the water molecule by the negative charge on C_2 brings H_w to the proximity of C_2 by bending the previously linear N_3–H_3---O_w hydrogen bond. An important consequence of this structural change is a significant stretch of the O_w–H_w bond while the N_3–H_3 bond remains nearly unchanged. These findings suggest that the movement of H_w from the water to C_2 occurs at an earlier stage along the reaction coordinate than the movement of H_3 from amide to water.

The sequential movement of both protons (H_3 and H_w) leads to the product of the nucleophilic addition. Thus, we find that the minimum reaction path involves the attack of the proton of the water molecule on the negative charge generated on C_2 due to the nucleophilic attack of amide on the reactive double bond. From this point, the movement of H_3 from amide to water is energetically a downhill process.

For the 1,4-attack, the C_5–H_w and N_3–H_3 internal coordinates are the major components of the eigenvector of the Hessian matrix with the negative eigenvalue, and the C_1–N_3 makes no significant contribution because the bond is almost completely formed with a value of 1.513 Å.

The 1,4-nucleophilic addition can be described as follows. The approach to C_1 of amide hydrogen bonded to a discrete water molecule converts the atoms forming the reactive double bond into nearly tetrahedral carbons. The presence of amide causes a negative charge density to be shifted in the conjugated double bond, with a major concentration on C_5, as already demonstrated (Figure 122). This fact is reflected in the charges of the heavy atoms; the charge on C_5 is –0.65 while the charge on C_2 in **139** is only –0.57. The more

negative charge density on C_5 facilitates the attraction of H, to C_5, leading to a TS in which the distance C_5–H_w is significantly shorter than C_2–H_w in the 1,2-addition (1. 81 Å vs 1.87 Å, see Figure 123). At the same time, C_1–N_3 remains very similar to that in the 1,2-addition mechanism (1.51 Å vs 1.52 Å, see Figure 123).

Thus, the susceptibility of C_1 to nucleophilic attack is approximately the same in both the 1,2- and the 1,4-addition mechanisms, but the electrostatic stabilization of the O_w---H_w---C_5 hydrogen bond compared to O_w---H_w---C_2 is responsible for the different activation energies in these two processes (see below). Furthermore, analysis of the structural parameters of transition structures **139** and **141** reveals another important difference. In the 1,2-addition, the movement of H_w from the water to C_2 occurs at an earlier stage along the reaction coordinate than the movement of H_3 from amide to water; in the I,4-addition, both H_3 and H_w are almost midway in their movement to O_w and C_5, respectively (see N_3–O_w, H_3–H_3, O_w–C_5, and C_5–H_w distances of structure **141** in Figure 123). Therefore, the minimum reaction path of the proton movement from N_3 to C_5 takes advantage of a concerted mechanism in which H_3 moves toward O_w and H_w moves from O_w to C_5. Thus, the discrete water molecule acts as a catalyst in this proton rearrangement, contributing primarily to the lowering of the barrier to the proton shuttle.

After the TS is reached, a concerted mechanism of proton rearrangement yields the enol intermediate **143** that successively evolve to hydantoin **128** (Scheme 53).

2.4.3 Energetics of the 1,2- and 1,4-Nucleophilic Addition

The differences in formation enthalpies relative to reactant **138**, for **138**, the optimized TSs **139** and **140** ($\Delta H_{f\,act}$) and the products **141** and **142** ($\Delta H_{f\,react}$) are

given in Table 14. Both the reactions are exothermic with $\Delta H_{f\ react}$ of 6.57 and 8.00 kcal/mole. The barrier to the 1,2-nucleophilic addition is of 52.43 kcal/mol while the barrier to 1,4-nucleophilic addition is 49.68 kcal/mol. The energy of activation was calculated not from the linear structure of the reactant but from the *s-cis* conformation, that is adopted for cyclization. This conformational change is estimated to be of the order of 6.42 kcal/mol.

From this study emerge that the nucleophilic 1,4-attack is preferred to the 1,2-one by 2.75 kcal/mol and then the only practicable.

Table 14. Formation enthalpies and their differences relative to reactant **138**, for **138**, the optimized TSs **139** and **141** ($\Delta H_{f\ act}$) and the products **140** and **142** ($\Delta H_{f\ react}$), expressed in kcal/mol.

Compounds	ΔH_f	$\Delta\Delta H_f$
138	–172.64	0.00
139	–120.21	52.43
141	–122.96	49.68
140	–180.64	–8.00
142	–179.21	–6.57

2.4.4 Formation of hydantoin 128

Finally, after an enolic tautomerization, the intermediate **143**, that can exist in two principal conformation, namely *s-Z* and *s-E*, evolve, by a 1,6-prototropic shift, to the more stable hydantoin *Z*-**128** (Scheme 53).

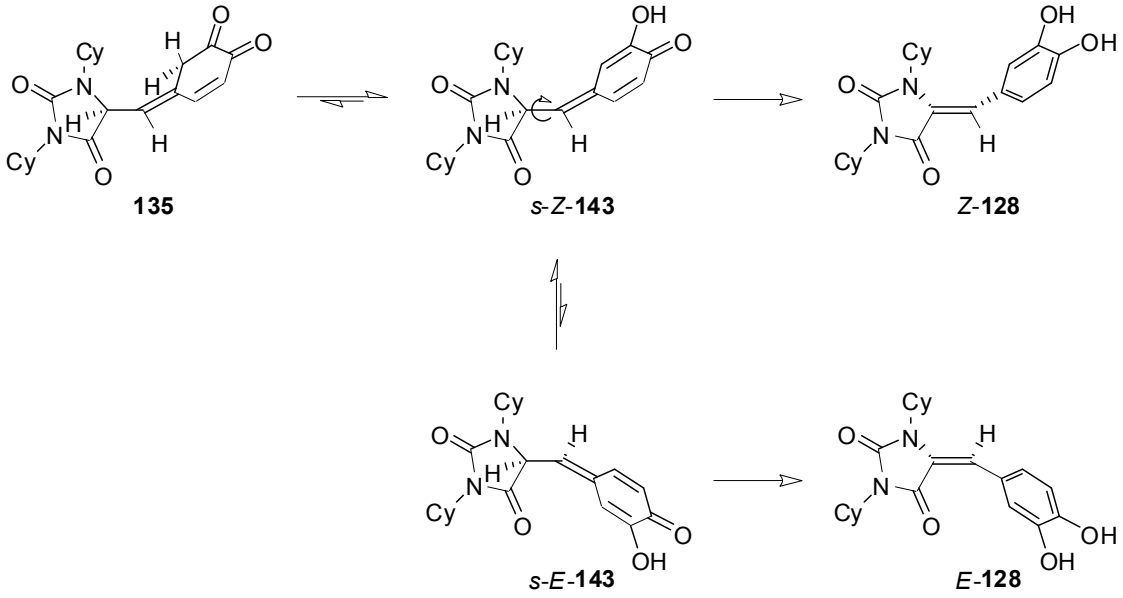

Scheme 53

The present study of the molecular mechanism of nucleophilic addition of amide to the activated double bond in **135** indicates that the addition proceeds through the formation of a transition state, in which the rate-determining step is an intramolecular proton transfer from the nucleophile to the ligand, assisted by a discrete water molecule which acts as a catalyst of this process (the catalysis by a H_2O molecule was shown to arise from the increase in hydrogen bonding to the zwitterion-like moiety in the activated complex). In the TS of nucleophilic 1,4-addition, the intramolecular proton transfer proceeds from the nucleophile to the C_5 carbon of aromatic ring via the discrete water molecule through a concerted mechanism in which both protons H_3 and H_w are midway in their movement. The structural preference observed for the I,4-mechanism is due to the electrostatic stabilization of the TS by the high negative charge on the terminal carbon of the aromatic ring conjugated to the double bond. By comparison, the charge on the carbon of the double bond is much smaller, resulting in less stabilization of the TS.

3. CONCLUSIONS

My three year doctoral work was devoted to work on three sections:

1. Biomimetic synthesis of stilbenolignans
2. Biomimetic synthesis of benzo[*k,l*]xanthene lignanamides
3. Synthesis of hydantoin-related compounds

In section one, we have synthesized (±)-**99**-**106** stilbenolignans and these were evaluated for antiproliferative activity, and apart from (**±**)-**104** and (**±**)-**105** all the other racemic mixtures resulted significantly active; therefore these mixtures were subjected to separation of the pure enantiomers through preparative chiral HPLC and Circular Dichroism (CD) spectra were run to establish their absolute configuration. The pure enantiomers were submitted to bioassays for antiproliferative activity towards SW-480 colon carcinoma cells. The following considerations can be made as a basis for possible future studies on these stilbenolignans:

a) all the active dimers results significantly more potent that the reference natural compounds resveratrol (**1**) and ε-viniferin (**29**). This suggests that in addition to a 4-phenoxy function, other structural requirements and probably a higher lipophilic character are necessary for higher activity;

b) the number and position of substituents on the second ring (that not bearing an oxygenated group in C-4) may significantly influence the activity;

c) the configuration of the stereogenic centers may have a role in the activity, at least for dimers where other factors (diffusion, membrane permeability, metabolic stability) result less important.

In section two, we have synthesized five new benzo[*k,l*]xanthene lignanamides **112**, **115**, **118**, **121**, and **124** biomimetically and characterized them using mono and bi dimensional NMR spectroscopy. Among these

benzo[*k,l*]xanthenes, **115** obtained in 70% yield and in radical coupling reaction this is a competitive yield. At moment these compounds are under investigation, in collaboration with Prof. Condorelli group's - University of Catania - to evaluate their antiproliferative activity towards different cancer cell lines and in collaboration with Prof. Bifulco group's - University of Salerno – to evaluate their DNA interacting properties.

In third section, we reported the synthesis and spectroscopic characterization of hydantoin-related compounds unexpectedly products obtained from *N*-acylureas. In particular the hydantoin **128** was obtained in 68% yield with an enzymatic reaction. To the best our knowledge this is the first report on hydantoin synthesis by chemo-enzymatic method. In collaboration of Prof. Rescifina - University of Catania- the formation of **128** was rationalized by means of a theoretical in silico study at semiempirical AM1 level.

4. EXPERIMENTAL SECTION

4.1 General Section

NMR spectra were run on Bruker 300 (^{1}H) and a Varian Unity Inova spectrometer operating at 499.86 (^{1}H) and 125.70 MHz (^{13}C) and equipped with gradient-enhanced, reverse-detection probe. Chemical shifts (δ) are indirectly referred to TMS using solvent signals. All NMR experiments, including two-dimensional spectra, were performed using software supplied by the manufacturers and acquired at constant temperature (298 K) and CD_3OD or $CDCl_3$ or $(CD_3)_2CO$ as solvent.

Electrospray ionization mass spectra (ESI-MS) were recorded on ThermoFinnigan LCQ-DECA ion trap mass spectrometer equipped with an ESI ion source operating in MS negative ion mode under the following conditions: capillary temperature 180 °C, sheat gas 20 a.u; spray voltage 4 KV.

CD spectra were run on Circular Dicroism Jasco J610.

High-performance liquid chromatography (HPLC) was carried out using an Agilent Series G1354A pump and a detector UV G1314A (Agilent). An auto-sampler Series 1100 G1313A (Agilent) was used for sample injection. The chiral HPLC of racemates was carried out by HPLC-UV using a column Chiralpak® IA (5 µm; 4.6 × 250 mm) with isocratic elution and flow rate is described below.

Flash chromatography was performed on silica gel 60 (Merck) and DIOL silica gel (Merck) using the different solvent systems or Biotage system. TLC was carried out using pre-coated silica gel F_{254} plates (Merck). Cerium sulphate and phosphomolybdic acid were used as spray reagents.

4.2 Materials and method

Benzotriazole-1-yl-oxy-tris-(dimethylamino)-phosphonium hexafluorophosphate (BOP), $Mn(OAc)_3$, Caffeic acid, Ferulic acid, Coumaric acid, Tyramine were purchased from Sigma, dicyclohexylcarbodiimide (DCC), diisopropylcarbodiimide (DIC), *N*,*N*-dimethylformamide (DMF), triethylamine (Et_3N), *N*-ethyldiisopropylamine, diethylamine, n-butylamine, dicyclohexylamine, dimethylaminopyridine (DMAP), Horseradish peroxidase and Laccase from *Trametes versicolor* (LTV), Laccase from *Pleurotus ostreatus* (LPO) were purchased from Sigma; *N*-hydroxybenzotriazole (HOBt) was purchased from Aldrich. Hydroxystilbenes (**90**, **91**, **92**, **95**, **96**, and **98**) were gained from France collaborator. All chemicals were of reagent grade and used without further purification.

4.3 Biomimetic synthesis of stilbenolignans

4.3.1 Synthesis of monomers

*4.3.1.1 Synthesis of monomer **83***

Step1: Preparation of hydroxy protected benzaldehyde **80**

The starting material 4-hydroxy benzaldehyde (**78**, 10 g, 81 mmol) was dissolved in dry pyridine in inert atmosphere (argon gas). To the solution chlorotrimethylsilane **79** (10.6 g, 98 mmol) was added slowly. Reaction is oxygen sensitive, so reaction was refluxed under argon gas for 10 hours. Reaction mixture was subjected to fractional distillation to separate pyridine and protected aldehyde **80**. At pressure 9 torrs with 25 °C pyridine was separated and at 118 °C protected aldehyde was distilled with 11.1g of 80% yield. **^{1}H NMR** ($CDCl_3$, 300 MHz, 298 K): δ 0.25 (s, 9 H), 6.86 (d, *J* = 8.5, 2 H), 7.72 (d, *J* = 8.5, 2 H), 9.82 (s, 1H, -CHO).

Step2: Preparation of tri phenyl phosphonium salt **82**

The starting material 1-Iodomethyl-4-vinylbenzene **81** (10 g, 43 mmol) was dissolved in dry toluene. To the solution triphenylphosphine (12.5g, 47 mmol) was added slowly. Reaction was refluxed for 4 hours and formation of insoluble triphenylphosphonium ylide **82** was observed. By filtration **82** was separated and thoroughly washed with heptane and dried over vacuum. **^{1}H NMR** ($CDCl_3$, 300 MHz, 298 K): δ 7.67(m, 15H, PPh_3), 7.15 (m, 4H, H-4,5,7,8), 6.56 (dd, 1H, *J* = 17.6, 10.9 Hz, H-2), 5.64 (d, 1H, *J* = 17.6 Hz, H-1), 5.2 (m, 2H, H-9). **^{31}P NMR** ($CDCl_3$, 121.47 MHz, 298 K): δ (ppm) 22.6 ppm (s,1P).

Step3: Preparation of compound **83**

The starting material triphenylphosphonium salt **82** (10.2 g, 20 mmol) was dissolved in dry THF. To the solution hydroxy protected benzaldehyde **80** (3.9 g, 20 mmol) was added in inert atmosphere (argon gas). After five min BuLi (in ether) was added slowly up to 30 min, in the course of addition of BuLi, the reaction mixture was cooled to – 80 ^{o}C by using liquid nitrogen and acetone in a container. The reaction was carried out 45 min in -80 ^{o}C and subsequently at room temperature for 24 hr. After 24 hr, 100 ml water was added to reaction mixture and stirred for 2 hour for deprotection of hydroxy function. Finally crude was extracted by using EtOAc and purified through column chromatography with 20% EtOAc, heptane solvent as elution, only *trans* isomer was isolated about 33% yield. **^{1}H NMR** ($CDCl_3$, 500 MHz, 300 K): δ (ppm) 7.46 (d, *J* = 8.0, H-3',5'), 7.39 (m, H-2',6',2,6), AB system 7.06 (d, 1H, *J* = 16.5 Hz), 6.96 (d, 1H, *J* = 16.5 Hz), 6.78 (dd, *J* = 6.5, *J*= 2.0, H-3,5), 6.72 (dd, *J* = 17.5 Hz, *J* = 10.75 Hz -C$\underline{H}_a$=C$H_b$$H_c$), 5.76 (d, *J*=17.5 Hz, -CH=C$H_b$$\underline{H}_c$), 5.24 (d, *J* = 10.75 Hz, -CH_a=C$\underline{H}_b$$H_c$), 5.77 (d, *J* = 17.5 Hz, H-10'), 5.91 (s,1H,OH). **^{13}C NMR** ($CDCl_3$, 125 MHz, 300 K): δ (ppm) 157.0, 137.5, 136.4, 136.3, 129.0, 128.0, 127.4 (2C), 126.0 (2C), 125.9 (2C), 124.9, 115.1 (2C), 112.0.

*4.3.1.2 Synthesis of monomer **86***

Step1: Preparation of compound **85**

The starting material 4-bromobenzyl bromide **84** (5 g, 20 mmol) was dissolved in dry toluene. To the solution triphenylphosphine (5.7 g, 22 mmol) was added slowly. Reaction was refluxed for 4 hours. After the formation of **85** reaction was stopped and by filtration product was recovered and dried under reduced pressure. **^{1}H NMR** ($CDCl_3$, 300 MHz, 298 K): δ (ppm) 7.78 (m,15 H, PPh_3), 7.17 (d, *J* = 8.5Hz , H-2,6), 7.06 (d, *J* = 8.5 Hz, H-3,5), 5.56 (d, $^{2}J_{PH}$ =15.6 Hz, -CH_2-P^{+}-Ph_3). **^{31}P NMR** ($CDCl_3$, 121.47 MHz, 298 K): δ (ppm) 23.2 (s,1P).

Step2: Preparation of compound **86**

The starting material triphenylphosphonium salt **85** (10.2 g, 20 mmol) was dissolved in dry THF. To the solution hydroxy protected benzaldehyde **80** (3.9 g, 20 mmol) was added slowly in inert atmosphere (argon gas). After five min BuLi (in ether) was added slowly up to 30 min, in the course of addition of BuLi reaction mixture was cooled to -80 ^{o}C by using liquid nitrogen and acetone solvent. The reaction was carried out 45 min in -80 ^{o}C and subsequently at room temperature for 24 hr. After 24 hr 100 ml water was added to reaction mixture and stirred for 2 hour for deprotection of hydroxy function. Finally crude was extracted by using EtOAc and purified through column chromatography with 10% EtOAc, heptane solvent as elution and only *trans* isomer was isolated about 41% yield. **^{1}H NMR** ($CDCl_3$, 300 MHz, 298 K); δ (ppm) 7.45 (d, *J* = 8.0, H-2' and H-,6'),7.41(d, *J* = 8.0, 2H, H-5' and H-3'), 7.35 (d, *J* = 9.0, H-2 and H-6), system (AB) 7.02 (d, 1H, *J* = 16.5 Hz), 6.91(d, 1H, *J* = 16.5Hz), 6,84 (d, 2H, H-3 and H-5), 4,88 (s, 1H, OH). **^{13}C NMR** ($CDCl_3$, 75 MHz, 298 K): δ (ppm) 155.5, 136.6, 131.7 (2C), 130.0, 128.6, 128.0 (2C), 127.9, 127.7 (2C), 125.4, 115.6 (2C).

*4.3.1.3 Synthesis of monomers **90-92**, **95-96** and **98***

These monomers were gained from French laboratory by collaboration with Prof. Dominique Fasseur-Vervandier, at the Institut de Chimie Moléculaire de l'Université de Bourgogne, Dijon (France).

4.3.2 Synthesis of Dimers

*4.3.2.1 Biomimetic synthesis of stilbenolignan (±)-**99***

Enzyme mediated method: Substrate **83** (30 mg, 0.06 mmol) was dissolved in 20 mL EtOAc, while the laccase from *Trametes versicolor* (10 U,15 mg) was dissolved in 15 mL of acetate buffer, pH 4.7. The biphasic system was stirring at room temperature for 24 hrs and monitored by TLC. When the TLC spots indicated that the products were prevalent with respect to the initial substrate, the reaction was quenched by phase separation followed by EtOAc extraction of the water solution, and the organic solvent was evaporated. The crude residue was purified by flash chromatography using (eluent: petroleum ether /dichloromethane, 6/4) to give 5 mg of (±)-**99** (20% yield). Obtained (±)-**99** was subjected to chiral column chromatography with the aim to get enantiopure compounds. The chiral HPLC of racemates was carried out by HPLC-UV using a column Chiralpak® IA (5 µm; 4.6 × 250 mm) and a isocratic elution with 60 % iso-propanol-hexane, flow rate *0*.6 mL. The pure enantiomer 7*R*,8*R* is isolated with retention time 12.0 min and 7*S*,8*S* is isolated with retention time 14.0 min.

Metal mediated method: Substrate **83** (300 mg, 1.3 mmol) was dissolved in 50 mL dichloromethane and subsequently $Mn(OAc)_3$ (720 mg, 2.6 mmol) was added to the solution. The reaction mixture was stirring at room temperature for 30 hours and monitored by TLC. Then, the solvent was distil off, and reaction mixture was quenched with solution of ascorbic acid in methanol; methanol was distilled off completely and to the mixture 100 ml water was added and reaction

mixture was recovered by ethyl acetate. The crude residue was purified by flash chromatography using (eluent: petroleum ether /dichloromethane, 6/4) to give (±)-**99** (10% yield). The mass spectrum shows ESI-MS peak at *m*/*z* 465.1 $[M + Na]^+$ confirming the formation of a dimer. **^{1}H** and **^{13}C NMR** data are reported in Table 1.

*4.3.2.2 Biomimetic synthesis of stilbenolignan (±)-**100***

Enzyme mediated method: Substrate **86** (50 mg, 0.2 mmol) was dissolved in 20 mL EtOAc, while the laccase from *Trametes versicolor* (10 U, 15 mg) was dissolved in 10 mL of acetate buffer, pH 4.7. The biphasic system was stirring at room temperature for 5 days and monitored by TLC. When the TLC spots indicated that the products were prevalent with respect to the initial substrate, the reaction was quenched by phase separation followed by EtOAc extraction of the water solution, and the organic solvent was evaporated. The crude residue was purified by flash chromatography using 6% ethyl acetate-petroleum ether as eluent to give 19 mg of (±)-**100** (38% yield) with 80% NMR purity. Further purification was made by preparative TLC in 0.5 % MeOH-$CHCl_3$ as eluent. Finally obtained dimer (±)-**100** gives 97% purity with yield 20%. Obtained (±)-**100** was subjected to chiral column chromatography with the aim to get enantiopure compound. The chiral HPLC of racemate was carried out by HPLC-UV using a column Chiralpak® IA (5 µm; 4.6 × 250 mm) and an isocratic elution with 50 % iso-propanol-hexane, flow rate *0*.8 mL. The pure enantiomer 7*R*,8*R* is isolated with retention time 10.4 min and 7*S*,8*S* is isolated with retention time 12.5 min.

Metal mediated method: Substrate **86** (100 mg, 0.4 mmol) was dissolved in 50 mL dichloromethane and subsequently $Mn(OAc)_3$ (350 mg, 1.2 mmol) was added to the solution. The reaction mixture was stirring at room temperature for

24 hour and monitored by TLC. Then, the solvent was distilled off, and reaction mixture was quenched with saturated solution of ascorbic acid in methanol. After one hour methanol was distilled off completely and to the mixture 100 ml water was added and crude was extracted by ethyl acetate. The residue was subjected to column chromatography by using silica gel and 6% ethyl acetate, petroleum ether as eluent to give (±)-**100** in 80% purity. Again this product was purified by using preparative TLC in 0.5% MeOH-$CHCl_3$ as eluent. Finally obtained dimer (±)-**100** gives 96% purity with yield 22%. The mass spectrum shows ESI-MS peak at *m*/*z* 546.9 $[M-H]^-$ confirming the formation of a dimer. **^{1}H** and **^{13}C NMR** data are reported in Table 2.

*4.3.2.3 Biomimetic synthesis of stilbenolignan (±)-**101***

The substrate **90** (140 mg, 0.7 mmol) was dissolved in 35 mL CH_2Cl_2, while the laccase from *Trametes versicolor* (10 U, 30mg) was dissolved in 15 mL of acetate buffer, pH 4.7. The biphasic system was stirring at room temperature for 10 hrs and monitored by TLC. When the TLC spots indicated that the products were prevalent with respect to the initial substrate, the reaction was quenched by phase separation followed by EtOAc extraction of the water solution, and the organic solvent was evaporated. The crude residue was purified by flash chromatography using eluent: petroleum ether: dichloromethane (6:4) to give 28% yield of (±)-**101**. The mass spectrum shows ESI-MS peak at *m*/*z* 413.1 $[M + Na]^+$ confirming the formation of a dimer. **^{1}H** and **^{13}C NMR** data are reported in Table 3 and are in agreement with reported data in literature. Obtained (±)-**101** was subjected to chiral column chromatography with the aim to get enantiopure compounds. The chiral HPLC of racemates was carried out by HPLC-UV using a column Chiralpak® IA (5 µm; 4.6× 250 mm) and an isocratic elution with 80 % iso-propanol-hexane,

flow rate 0.4 mL. The pure enantiomer 7*R*,8*R* is isolated with retention time 14.3 min and 7*S*,8*S* is isolated with retention time 18.1 min.

4.3.2.4 *Biomimetic synthesis of stilbenolignan (±)-**102***

Enzyme mediated method: The substrate **91** (100 mg, 0.4 mmol) was dissolved in 40 mL EtOAc, while the laccase from *Trametes versicolor* (10 U, 15 mg) was dissolved in 10 mL of acetate buffer, pH 4.7. The biphasic system was stirring at room temperature for 20 hrs and monitored by TLC. When the TLC spots indicated that the products were prevalent with respect to the initial substrate, the reaction was quenched by phase separation followed by EtOAc extraction of the water solution, and the organic solvent was evaporated. The crude residue was purified by flash chromatography using petroleum ether/ethyl acetate (8/2) to give 65 mg (65% yield) of (±)-**102**. The mass spectrum shows ESI-MS peak at *m*/*z* 449.3 $[M-H]^-$ confirming the formation of a dimer. **^{1}H** and **^{13}C NMR** data are reported in Table 4 and are in agreement with reported data in literature.[29] Obtained (±)-**102** was subjected to chiral column chromatography with the aim to get enantiopure compound. The chiral HPLC of racemate was carried out by HPLC-UV using a column Chiralpak® IA (5 µm; 4.6 × 250 mm) and an isocratic elution with 30% iso-propanol-hexane, flow rate *0*.5 mL. The pure enantiomer 7*R*,8*R* is isolated with retention time 21.0 min and 7*S*,8*S* is isolated with retention time 25.1 min.

Metal mediated method: Compound **91** (100 mg, 0.4 mmol) was dissolved in 10 mL dichloromethane and subsequently $Mn(OAc)_3$ (116 mg, 0.4 mmol) was added to the solution. The reaction mixture was stirring at room temperature for 9 hours and monitored by TLC. Then, the solvent was distilled off, and reaction mixture was quenched with solution of ascorbic acid in methanol. To the mixture 100 ml water was added and reaction mixture was recovered by ethyl

acetate. The residue was subjected to column chromatography by using Diol silica gel and 20% ethyl acetate, petroleum ether as eluent to give (±)-**102** (yield 50%).

*4.3.2.5 Biomimetic synthesis of stilbenolignan (±)-**103***

Substrate **92** (85 mg, 0.3 mmol) was dissolved in 30 mL chloroform and subsequently $Mn(OAc)_3$ (200mg, 0.7 mmol) was added to the solution. The reaction mixture was stirring at room temperature for 8 hours and monitored by TLC. Then, the solvent was distilled off, and reaction mixture was quenched with solution of ascorbic acid in methanol. To the mixture 100 ml water was added and reaction mixture was recovered by ethyl acetate. The residue was subjected to column chromatography by using DIOL silica gel and 20% ethyl acetate-petroleum ether as eluent to give (±)-**103** (yield 25%). **^{1}H NMR** data is reported in Table 5 and is agreement with reported data in literature(S. Velu *et al*). Obtained (±)-**103** was subjected to chiral column chromatography with the aim to get enantiopure compound. The chiral HPLC of racemate was carried out by HPLC-UV using a column Chiralpak® IA (5 µm; 4.6× 250 mm) and an isocratic elution with 60% iso-propanol-hexane, flow rate *0*.6 mL. The pure enantiomer 7*R*,8*R* is isolated with retention time 13.4 min and 7*S*,8*S* is isolated with retention time 16.0 min.

*4.3.2.6 Biomimetic synthesis of stilbenolignan (±)-**104***

The substrate **95** (30 mg, 0.1mmol) was dissolved in 15 mL EtOAc, while the laccase from *Trametes versicolor* (10 U, 10 mg) was dissolved in 10 mL of acetate buffer pH 4.7. The biphasic system was stirring at room temperature for 24 hrs and monitored by TLC. When the TLC spots indicated that the products were prevalent with respect to the initial substrate, the reaction was quenched by phase separation followed by EtOAc extraction of the water solution, and the

organic solvent was evaporated. The crude residue was purified by flash chromatography using 20% ethyl acetate-petroleum ether as eluent to give 20 mg of (±)-**104** (67% yield) with 96% NMR purity. **^{1}H** and **^{13}C NMR** data are reported in Table 6 and are in agreement with reported literature data.[29]

*4.3.2.7 Biomimetic synthesis of stilbenolignan (±)-**105***

The substrate **96** (100 mg, 0.3 mmol) was dissolved in 25 mL EtOAc, while the laccase from *Trametes versicolor* (10 U, 15 mg) was dissolved in 15 mL of acetate buffer pH 4.7. The biphasic system was stirring at room temperature for 8 hrs and monitored by TLC. When the TLC spots indicated that the products were prevalent with respect to the initial substrate, the reaction was quenched by phase separation followed by EtOAc extraction of the water solution, and the organic solvent was evaporated. The crude residue was purified by flash chromatography using 40% ethyl acetate-petroleum ether as eluent to give 30 mg of (±)-**105** (30% yield) with 96% NMR purity. The mass spectrum shows ESI-MS peak at *m*/*z* 629.2 $[M-H]^-$ confirming the formation of a dimer. **^{1}H** and **^{13}C NMR** data are reported in Table 7.

*4.3.2.8 Biomimetic synthesis of stilbenolignan (±)-**106***

The substrate **98** (30 mg, 0.1mmol) was dissolved in 15 mL EtOAc, while the laccase from *Trametes versicolor* (10 U, 10 mg) was dissolved in 10 mL of acetate buffer pH 4.7. The biphasic system was stirring at room temperature for 24 hrs and monitored by TLC. When the TLC spots indicated that the products were prevalent with respect to the initial substrate, the reaction was quenched by phase separation followed by EtOAc extraction of the water solution, and the organic solvent was evaporated. The crude residue was purified by flash chromatography using 20% ethyl acetate-petroleum ether as eluent to give 7 mg of (±)-**106** (20% yield) with 96% NMR purity. The mass spectrum shows

ESI-MS peak at *m m/z* 533.1 $[M+ Na]^+$ confirming the formation of a dimer. **^{1}H NMR** ($CDCl_3$, 500 MHz, 300 K): δ 3.68 (s), 3.76 (s), 4.62 (m), 4.74 (d, *J* = 13.5), 4.97 (d, *J* = 13.5), 6.62 (d, *J* = 17.0 , 1H, −CH=CH_a−), 7.34 (d, *J* = 17.0, 1H, −CH_b=CH−), 6.55(d, *J* = 8.5), 6.67 (d, *J* = 9.0), 6.84(d, *J* = 8.0), 6.92(d, *J* = 10.0), 6.97(bs), 7.12(m), 7.32(s), 7.29(bs), 7.38(d, *J* = 8.5).

4.4 Biomimetic synthesis of benzo[*k,l*]xanthene lignans

4.4.1 Synthesis of benzo[*k,l*]xanthene **112**

*4.4.1.1. Step1. Preparation of amide **111***

Caffeic acid (**7**, 100 mg, 0.5 mmol) was dissolved in 8 mL of DMF and 0.07 mL (0.5 mmol) of triethylamine. The solution is cooled in an ice-water bath and 0.173 mL (0.5 mmol) of tyramine **110** was added followed by a solution of 236 mg (0.5mmol) of BOP reagent in 5 mL of CH_2Cl_2. The mixture is stirred at 0 ^oC for 30 min and then at room temperature for 24 h. CH_2Cl_2 was removed under reduced pressure and the solution is diluted with 40 ml of water. The products are extracted with ethyl acetate. The extract is washed successively with 1*N* HCl, water, 1*M* $NaHCO_3$, and water, dried over Na_2SO_4, filtered and evaporated. The residue is purified on silica gel column with eluent 9:1 dichloromethane-methanol and obtained yield was 70%. **^{1}H NMR** (CD_3OD, 500 MHz, 300 K): δ 2.75 (t, *J* = 7.75, 2H, CH_2−Ar), 3.46 (t, *J* = 7.25, 2H, −NH−CH_2−), 6.34 (d, *J* = 15.5, 1H, −CH=CH_a−), 7.39 (d, *J* = 15.5, 1H, −CH_b=CH−), caffeic acid ring: 6.71 (d, *J* = 2.0, 1H, H-2), 6.76 (d, *J* = 8.5, 1H, H-5), 6.9 (dd, *J* = 2.0, *J* = 8.5, 1H, H-6), tyramine ring: 6.99 (d, *J* = 2, 2H, H-2‘, H-6‘), 7.05 (d, *J* = 8.5, 2H, H-3‘, H-5‘). **^{13}C NMR** (CD_3OD, 125 MHz, 300 K): δ 34.4, 41.13, 113.6, 114.8, 115.0, 117.0, 120.6, 126.9, 129.3, 129.9, 140.7, 145.2, 147.3, 155.5, 167.8.

*4.4.1.2 Step2. Preparation of compound **112***

To a stirred suspension of $Mn(OAc)_3$ (55 mg, 0.2 mmol) in 20 mL EtOH solution, caffeic amid **111** (30 mg, 0.1 mmol) was added. The reaction mixture was then stirred at room temperature for 1 hr and treated with a saturated solution of ascorbic acid in methanol. After filtration, the solvent was completely removed under reduced pressure and greenish residue obtained was treated with purified by column chromatography over silica gel using a gradient of 4% EtOH-CH_2Cl_2 gives dimer **112** with 75% purity. Which again purified by using column chromatography with elution 1:1 EtOAc-petroleum ether, gives 97% NMR purity of 6 mg with 20% yield. The mass spectrum shows ESI-MS peak at *m*/*z* 591.3 $[M-H]^-$ confirming the formation of a dimer. **^{1}H** and **^{13}C NMR** data are reported in Table 9.

4.4.2 Synthesis of benzo[*k,l*]xanthene **115**

*4.4.2.1. Step1. Preparation of amide **114***

Caffeic acid (**7**, 300 mg, 1.6 mmol) was dissolved in 8 mL of DMF and 0.23 mL (1.6 mmol) of triethylamine. The solution is cooled in an ice-water bath and 0.173 mL (1.6 mmol) of diethyl amine **113** was added followed by a solution of 733 mg (1.6 mmol) of BOP reagent in 10 mL of CH_2Cl_2. The mixture is stirred at 0 ^oC for 30 min and then at room temperature for 24 h. CH_2Cl_2 was removed under reduced pressure and the solution is diluted with 40 ml of water. The products are extracted with ethyl acetate. The extract is washed successively with 1*N* HCl, water, 1*M* $NaHCO_3$, and water, dried over Na_2SO_4, filtered and evaporated. The residue is purified on silica gel column with eluent 1:1 ethyl acetate, petroleum ether and obtained yield was 50%. **^{1}H NMR** (CD_3OD, 500 MHz, 300 K): δ 1.17 (t, 7.0, 3H), 1.25 (t, 7.0, 3H), 3.46 (m, 2H), 3.52 (m, 2H), 4.88 (s, OH)), 6.76 (d, *J* = 15.3, 1H,−CH=CH $_a$−), 7.47 (d, *J* = 15.3, 1H,

−CH_b=CH−), caffeic acid ring: 6.78 (d, *J* = 8.5, 1H, H-5), 7.05 (d, *J* = 2.0, 1H, H-2), 6.96 (dd, *J* = 8.5, *J* = 2.0, 1H, H-6). **^{13}C NMR** (CD_3OD, 125 MHz, 300 K): δ 13.4, 15.1, 42.3, 43.6, 115.0, 115.2, 116.5, 122.2, 128.5, 144.4, 146.7, 148.8, 168.5.

*4.4.2.2 Step2. Preparation of compound **115***

To a stirred suspension of $Mn(OAc)_3$ (136 mg, 0.5 mmol) in 20 mL EtOH solution, caffeic amid **114** (60 mg, 0.2 mmol) was added. The reaction mixture was then stirred at room temperature for 1 hr and treated with a saturated solution of ascorbic acid in methanol. After filtration, the solvent was completely removed under reduced pressure and greenish residue obtained was treated with purified by column chromatography over silica gel using a gradient of 2% MeOH-CH_2Cl_2 gives dimer **115** with 80% purity. Which again purified by using column chromatography with elution 1:1 EtOAc-petroleum ether, gives 97% NMR purity with 70% yield. **^{1}H NMR** and **^{13}C NMR** data are reported in Table 10.

4.4.3 Synthesis of benzo[*k,l*]xanthene **118**

*4.4.3.1 Step 1. Preparation of amide **117***

Caffeic acid (300 mg, 1.6 mmol) was dissolved in 8 mL of DMF and 0.23 mL (1.6 mmol) of triethylamine. The solution is cooled in an ice-water bath and 0.19 mL (1.6 mmol) of *n*-butyl amine **116** was added followed by a solution of 733 mg (1.6 mmol) of BOP reagent in 10 mL of CH_2Cl_2. The mixture is stirred at 0 ^oC for 30 min and then at room temperature for 24 h. CH_2Cl_2 was removed under reduced pressure and the solution is diluted with 40 ml of water. The products are extracted with ethyl acetate. The extract is washed successively with 1*N* HCl, water, 1*M* $NaHCO_3$ and water, dried over Na_2SO_4, filtered and evaporated. The residue is purified on silica gel column with eluent 60% ethyl

acetate, petroleum ether and obtained yield was 58%.**^{1}H NMR** (CD_3OD, 500 MHz, 300 K): δ 0.94 (t, *J* = 7.5, 3H),1.38 (m, 2H), 1.53 (m, 2H), 3.28 (t, *J* = 7.0, 2H), 4.89 (s, OH and NH), 6.38 (d, *J* = 15.3, 1H, −CH=CH_a−), 7.40 (d, *J* = 15.3, 1H, −CH_b=CH−), caffeic acid ring: 6.76 (d, *J* = 8.5, 1H, H-5), 7.01 (d, *J* = 2.0, 1H, H-2), 6.96 (dd, *J* = 8.0, *J* = 1.5, 1H, H-6). **^{13}C NMR** (CD_3OD, 125 MHz, 300 K): δ14.0, 21.1, 32.5, 40.2, 115.0, 116.4, 118.4, 122.0, 128.3, 142.0, 146.6, 148.6, 169.2.

*4.4.3.2 Step2. Preparation of compound **118***

To a stirred suspension of $Mn(OAc)_3$ (112 mg, 0.4 mmol) in 10 mL EtOH solution, caffeic amid **117** (50 mg, 0.2 mmol) was added. The reaction mixture was then stirred at room temperature for 1 h and treated with a saturated solution of ascorbic acid in methanol. After filtration, the solvent was completely removed under reduced pressure and greenish residue obtained was purified by column chromatography over silica gel using a gradient of 3% MeOH-CH_2Cl_2 gives dimer 63 with 15% yield. **^{1}H** and **^{13}C NMR** data are reported in Table 11.

4.4.4 Synthesis of benzo[*k,l*]xanthene **121**

*4.4.4.1 Step1. Preparation of amide **120***

Caffeic acid (150 mg, 0.8 mmol) was dissolved in 8 mL of DMF and 0.12 mL (0.8 mmol) of triethylamine. The solution is cooled in an ice-water bath and 0.18 mL (0.8 mmol) of dicyclohexylamine **119** was added followed by a solution of 368 mg (0.8 mmol) of BOP reagent in 10 mL of CH_2Cl_2. The mixture is stirred at 0 ^{o}C for 30 min and then at room temperature for 24 h. CH_2Cl_2 was removed under reduced pressure and the solution is diluted with 40 ml of water. The products are extracted with ethyl acetate. The extract is washed successively with 1*N* HCl, water, 1*M* $NaHCO_3$ and water, dried over Na_2SO_4, filtered and

evaporated. The residue is purified on silica gel column with eluent 3% EtOH-CH_2Cl_2 and obtained yield was 20%. **^{1}H NMR** (CD_3OD, 500 MHz, 300 K): Cyclohexane ring, δ 1.32 (m, 4H),1.89 (m,8H), 2.06 (m, 8H), 3.19 (m, 2H); AB system 6.73 (d, *J* = 15.5, 1H, −CH=CH $_a$−), 7.31 (d, *J* = 15.5, 1H, −CH_b=CH−); caffeic acid moiety: 6.78 (d, *J* = 8.0, 1H, H-5), 7.02 (d, *J* = 2.0,1H, H-2), 6.92 (dd, *J* = 8.0, *J* = 2.0, 1H, H-6). **^{13}C NMR** (CD_3OD, 125 MHz, 300 K): δ 25.4 (4C), 26.1 (2C), 30.5 (4C), 54.5 (2C), 114.8, 116.5, 118.2, 121.7, 128.7, 142.7,146.7, 148.6, 169.3.

*4.4.4.2 Step2. preparation of compound **121***

To a stirred suspension of $Mn(OAc)_3$ (23 mg, 0.08 mmol) in 5 mL EtOH solution, caffeic amid **120** (15 mg, 0.04 mmol) was added. The reaction mixture was then stirred at room temperature for 1 hr and treated with a saturated solution of ascorbic acid in methanol. After filtration, the solvent was completely removed under reduced pressure and greenish residue obtained was purified by column chromatography over silica gel using a gradient of 2.5% MeOH-CH_2Cl_2 gives dimer **121** with 95% NMR purity. **^{1}H NMR** (CD_3COCD_3, 500 MHz, 300 K): Cyclohexane ring, δ 1.12-3.62 (m, 44H, four cyclohexane ring moiety), 7.63 (s, H-6'), 7.27 (s, H-4), 6.69 (s, H-3'), 7.34 (d, *J* = 9.0, H-5), 7.21 (d, *J* = 9.0, H-6).

4.4.5 Synthesis of benzo[*k,l*]xanthene **124**

*4.4.5.1 Step1. Preparation of amide **123***

Caffeic acid (222 mg 1.2 mmol) was dissolved in 8 mL of DMF and 0.25 mL (1.2 mmol) of triethylamine. The solution is cooled in an ice-water bath and 0.14 mL 1.2 mmol of benzylamine **122** was added followed by a solution of 550 mg (1.2 mmol) of BOP reagent in 10 mL of $CHCl_3$. The mixture is stirred at 0 ^oC for 30 min and then at room temperature for 24 h. $CHCl_3$ was removed under

reduced pressure and the solution is diluted with 40 mL of water. The products are extracted with ethyl acetate. The extract is washed successively with 1*N* HCl, water, 1*M* $NaHCO_3$ and water, dried over Na_2SO_4, filtered and evaporated. The residue is purified on silica gel column with eluent 3% EtOH-CH_2Cl_2 and obtained yield was 10%. **^{1}H NMR** (CD_3OD, 500 MHz, 300 K)**:** δ 4.46 (s), 6.44 (d, *J* = 15.5, 1H, −CH=CH_a−), 7.46 (d, *J* = 15.5, 1H, −CH_b=CH−), Caffeic ring, 6.78 (d, *J* = 8.5, 1H, H-5), 6.92 (d, *J* = 8.0,1H, H-6), 7.03 (s, H-2). Benzyl ring, 7.22-7.30 (m, 5H). **^{13}C NMR** (CD_3OD, 125 MHz, 300 K) δ 43.3, 114.4, 115.9, 118.8, 121.2, 127.3, 127.8, 128.0 (2C), 128.8 (2C), 139.9, 140.9, 145.8, 147.6, 166.2.

*4.4.5.2 Step2. Preparation of compound **124***

To a stirred suspension of $Mn(OAc)_3$ (220 mg, 0.8 mmol) in 20 mL $CHCl_3$ solution, caffeic amid **123** (65 mg, 0.2 mmol) was added. The reaction mixture was then stirred at room temperature for 5 hr and treated with a saturated solution of ascorbic acid in methanol. After filtration, the solvent was completely removed under reduced pressure and greenish residue obtained was purified by column chromatography over silica diol gel using a gradient of 4% EtOH-CH_2Cl_2 gives dimer **124**.

4.5 Synthesis of caffeic hydantoins

4.5.1. Enzymatic synthesis of caffeic hydantoin **128**

*4.5.1.1 Step 1. Synthesis of caffeic N,N'-dicyclohexylurea **125***

The starting material caffeic acid **7** (300 mg, 1.6 mmol) was soluble in 200 mL of CH_3CN solvent. To the solution *N*-ethyldiisopropylamine (0.28 ml, 1.6 mmol) was added. The reaction mixture was cooled to 0 ^oC in ice bath, and DCC (340 mg, 1.6 mmol) was added to it. For 30 min reaction was stirred at 0 ^oC, subsequently stirred at room temperature for 24 hr. The complete solvent was

distilled off and crude was extracted using EtOAc solvent. Crude was purified by column chromatography with the elution 1.5% MeOH-CH_2Cl_2, gives compound **125**, yielding 42%. The mass spectrum shows a peak at *m/z* 385.3 $[M-H]^-$ supporting the expected structure of *N,N'*-dicyclohexylurea product **125** incorporating two *N*-cyclohexyl moieties. **^{1}H NMR** (CD_3OD, 500 MHz, 300 K)**:** DCC ring, δ 1.31 (m, 4H),1.58(m, 8H), 1.78 (m, 8H),3.66 (m, 1H), 4.19 (m,1H), 6.46 (d, *J* = 15.5, 1H, −CH=CH_a−), 7.46 (d, *J* = 15.5, 1H, −CH_b=CH−), caffeic acid ring: 6.77 (d, *J* = 8.0, 1H, H-5), 6.97 (d, *J* = 2.0, 1H, H-2), 6.87 (dd, *J* = 8.0, *J* = 2.0, 1H, H-6). **^{13}C NMR** (CD_3OD, 125 MHz, 300 K)**:** δ 24.6 (2C), 25.1, 25.2, 25.6 (2C), 32.0 (2C), 30.6(2C), 54.0, 50.4,113.4, 114.9, 115.1, 121.1, 126.7, 143.0, 145.4, 147.8, 154.6, 165.2.

*4.5.1.2 Step 2. Enzymatic conversion of **125** to caffeic hydantoin **128***

The substrate **125** (25 mg, 0.2 mmol) was dissolved in 25 mL EtOAc, while the laccase from *Trametes versicolor* (LTV) or Laccase from *Pleurotus ostreatus* (LPO) (10 U, 15 mg) was dissolved in 15 mL of acetate buffer, pH 4.7. The biphasic system was stirring at room temperature for 24 hr and monitored by TLC. When the TLC spots indicated that the products were prevalent with respect to the initial substrate, the reaction was quenched by phase separation followed by EtOAc extraction of the water solution, and the organic solvent was evaporated. The crude residue was purified by flash chromatography using 0.3% MeOH-CH_2Cl_2 as eluent to give 17 mg of **128** (68% yield). The mass spectrum shows a peak at *m/z* 385.3 $[M-H]^-$ supporting the structure of **128** with the loss of two hydrogens from substrate **125**. **^{1}H** and **^{13}C NMR** data are reported in Table 12.

4.5.2. Enzymatic synthesis of caffeic hydantoin **130**

*4.5.2.1 Step1. Synthesis of caffeic N,N'-diisopropylurea **129***

The starting material caffeic acid **7** (100 mg, 0.5 mmol) was soluble in 100 mL of CH_3CN solvent. To the solution *N*-ethyldiisopropylamine (0.04 ml, 0.2 mmol) was added. The reaction mixture was cooled to 0 ^oC in ice bath, and DIC (0.09 mL, 0.5 mmol) was added to it. For 30 min reaction was stirred at 0 ^oC, subsequently stirred at room temperature for 24 hr. The complete solvent was distilled off and crude was extracted using EtOAc solvent. Crude was purified by column chromatography with the elution 1% MeOH-CH_2Cl_2, gives compound **129**, yielding 30%. **^{1}H NMR** (CD_3OD, 500 MHz, 300 K): isopropyl moiety: δ 1.25 (d, *J* = 6.5, 6 H),1.31 (d, *J* = 6.5, 6H), 4.03 (octet,1H), 4.55 (heptet, 1H), AB system: 6.62 (d, *J* = 15.25, 1H, $-CH=CH_a-$), 7.46 (d, *J* = 15.25, 1H, $-CH_b=CH-$), aromatic ring: 6.86 (d, *J* = 8.0, 1H, H-5), 7.11 (d, *J* = 2.0, 1H, H-2), 6.97 (dd, *J* = 8.0, *J* = 2.0, 1H, H-6). **^{13}C NMR** (CD_3OD, 125 MHz, 300 K): δ 20.7 (2C), 22.2 (2C), 43.5, 46.8, 114.6, 116.1, 117.4, 121.8, 128.0, 142.8, 146.0, 148.0, 154.7, 165.5.

*4.5.2.2.Step 2. Enzymatic conversion of **129** to caffeic hydantoin **130***

The substrate **129** (65 mg, 0.2 mmol) was dissolved in 30 mL EtOAc, while the laccase from *Pleurotus ostreatus* (LPO) (10 U, 12 mg) was dissolved in 20 mL of acetate buffer, pH 4.7. The biphasic system was stirring at room temperature for 24 hr and monitored by TLC. When the TLC spots indicated that the products were prevalent with respect to the initial substrate, the reaction was quenched by phase separation followed by EtOAc extraction of the water solution, and the organic solvent was evaporated. The crude residue was purified by flash chromatography using 0.1% MeOH-$CHCl_3$ as eluent to give 33 mg of **130** (52% yield). **^{1}H** and **^{13}C NMR** data are reported in Table 13.

4.5.3 Attempted Synthesis of Ferulic and Coumaric Hydantoin

4.5.3.1 Step1. Synthesis of Ferulic acid N,N'-dicyclohexylurea ***132***

The starting material ferulic acid **131** (50 mg, 0.2 mmol) was soluble in 100 mL of CH_3CN solvent. To the solution *N*-ethyldiisopropylamine (0.047 ml, 0.2 mmol) was added. The reaction mixture was cooled to 0 ^oC in an ice bath, and DCC (53 mg, 0.2 mmol) was added to it. For 30 min reaction was stirred at 0 ^oC, subsequently stirred at room temperature for 24 hr. The complete solvent was distilled off and crude was extracted using EtOAc solvent. Crude was purified by column chromatography with the elution 25% EtOAc-petroleum ether gives compound **132**, yielding 30%. **^{1}H NMR** (CD_3OD, 500 MHz, 300 K): DCC ring, δ 1.23 (m, 4H), 1.63 (m, 8H), 1.97 (m, 8H),3.68 (m, 1H), 4.20 (m,1H), 3.87 (s, -OCH_3), 6.55 (d, *J* = 15.0, 1H, −CH=CH_a−), 7.55 (d, *J* = 15.0, 1H, −CH_b=CH−), aromatic ring: 6.80 (d, *J* = 8.0, 1H, H-5), 7.09 (d, *J* = 2.0,1H, H-2), 7.01 (dd, *J* = 8.0, *J* = 2.0, 1H, H-6). **^{13}C NMR** (CD_3OD, 125 MHz, 300 K): δ 24.6 (2C), 25.1, 25.2, 25.6 (2C), 30.6 (2C), 32.0 (2C), 50.4, 53.9, 54.9 (OCH_3), 109.6, 115.1, 115.3, 122.4, 126.6, 142.7, 147.9, 148.9, 154.6, 165.1.

4.5.3.2 Step2 Attempted Synthesis of Ferulic Hydantoin

The substrate **132** (5mg, 0.01 mmol) was dissolved in 3 mL of EtOAc, while the laccase from *Pleurotus ostreatus* (LPO, 10 U, 5 mg) was dissolved in 2 mL of acetate buffer, pH 4.7. The biphasic system was stirring at room temperature for 24 hr and monitored by TLC. There is no progress in reaction.

*4.5.3.3 Step1. Synthesis of Coumaric acid N-acylurea **134***

The starting material coumaric acid **133** (450 mg, 2.7 mmol) was soluble in 100 mL of CH_3CN solvent. To the solution *N*-ethyldiisopropylamine (0.47 ml, 2.4 mmol) was added. The reaction mixture was cooled to 0 ^oC in ice bath, and DCC (565 mg, 2.7 mmol) was added to it. For 30 min reaction was stirred at 0 ^oC, subsequently stirred at room temperature for 24 hr. The complete solvent was distilled off and crude was extracted using EtOAc solvent. Crude was

purified by recrystallization with EtOAc solvent gives compound **134**, yielding 50%. **^{1}H NMR** (CD_3OD, 500 MHz, 300 K): DCC ring: δ 1.25 (m, 4H),1.58 (m, 8H), 1.78 (m, 8H), 3.67 (m, 1H), 4.19 (m,1H), AB system: 6.53 (d, *J* = 15.5, 1H, −CH=CH_a−), 7.55 (d, *J* = 15.5, 1H, −CH_b=CH−), aromatic ring: 6.80 (d, *J* = 8.5, 2H, H-3, H-5), 7.37 (d, *J* = 8.5,2H, H-2, H-6). **^{13}C NMR** (CD_3OD, 125 MHz, 300 K)**:** δ 24.6 (2C), 25.1, 25.2, 25.6 (2C), 33.1 (2C), 31.9 (2C), 50.4, 54.0, 115.0, 115.4 (2C), 126.1, 129.3 (2C), 142.6, 154.6, 159.5, 165.2.

4.5.3.4 *Step2. Attempted Synthesis of Coumaric Hydantoin*

The substrate **134** (5mg, 0.01 mmol) was dissolved in 3 mL of EtOAc, while the laccase from *Pleurotus ostreatus* (LPO, 10 U, 5 mg) was dissolved in 2 mL of acetate buffer, pH 4.7. The biphasic system was stirring at room temperature for 24 hr and monitored by TLC. There is no progress in reaction.

4.6 Theoretical Approach

Semiempirical quantum mechanical calculations were performed with the MOPAC 2009 (11.038W) program using the AM1 Hamiltonian.

The simulation of the nucleophilic addition of either amide or amide hydrogen bonded to a discrete water molecule (CONH---OH_2) to double bond in **135** includes structure optimizations of reactant and transition structures (TS) at the same level of calculations. Characterization of critical points in the potential energy surface was carried out through diagonalization of the Hessian matrix.

The parameters chosen to characterize the nucleophilic addition are $\Delta H_{f\ act}$, which is the barrier for the nucleophilic addition and is defined as the difference in energy between the TSs and the reactant, $\Delta H_{f\ inter}$, which is the difference in energy between any intermediate created in the reaction path and the reactant, and $\Delta H_{f\ react}$, which is the difference in energy between the products and the reactant. The system CONH---OH_2 was constructed to leave the lone pair of

the nitrogen free for the nucleophilic attack. Thus, the amide is the hydrogen donor, and the oxygen of water is the hydrogen acceptor (NH---O hydrogen bond instead of N---HO).

5. REFERENCES

[1] Nichenametla, S. N.; Taruscio, T. G.; Barney, D. L.; Exon, J. H. *Crit. Rev. Food Sci. Nutr.*, **2006**, *46*,16-183.

[2] Aggarwal, B. B.; Shishodia, S. *Resveratrol in health and disease* in Oxidative Stress and Disease. Taylor & Francis, London, United Kingdom, **2006**; Vol 20, pp 1-712.

[3] (a) Thompson, L. U.; Rickard, S. E.; Orcheson, L. J.; Seidl, M. M. *Carcinogenesis* **1996**, *17*, 1373-1376. (b) Kitts, D. D.; Yuan, Y. V.; Wijewickreme, A. N.; Thompson, L. U. *Mol. Cell Biochem.* **1999**, *202*, 91-100. (c) Saarinen, N. M.; Warri, A.; Makela, S. I.; Eckerman, C.; Reunanen, M.; Ahotupa, M.; Salmi, S. M.; Franke, A. A.; Kangas, L.; Santti, R. *Nutr. Cancer* **2000**, *36*, 207-216. (d) Katsuda, S.-I.; Yoshida, M.; Saarinen, N.; Smeds, A.; Nakae, D.; Santti, S.; Maekawa, A. *Exp.Biol. Med.* **2004**, *229*, 417-424.

[4] Pieters, L.; Van Dyck, S.; Gao, M.; Bai, R.; Hamel, E.; Vlietinck, A.; Lemiere. G. *J. Med. Chem.* **1999**, 42, 5475-5481.

[5] Moss, G. P. *Pure Appl. Chem.* **2000**, *72*, 1493-1523.

[6] http://www.chem.qmul.ac.uk/iupac/lignan/

[7] Dewick, P. M. *Medicinal Natural Products*. *A Biosynthetic Approach*; 2nd Edition; John Wiley & Sons: Chichester, UK, 2001; p. 133

[8] Davin, L. B.; Lewis, N. G. *Phytochem. Rev.* **2004**, *2*, 257-288.

[9] a) Apers, S.; Vlietinck, A.; Pieters, L. *Phytochem. Rev.* **2004**, *2*, 201–207; b) Van Miert, S.; Van Dyck, S.; Schmidt, T. J.; Brun, R.; Vlietinck, A.; Lemiere, G.; Pieters, L. *Bioorg. Med. Chem.* **2005**, *13*, 661-669; c) Prasad, A. K.; Kumar, V.; Arya, P.; Kumar, S.; Dabur, R.; Singh, N.; Chhillar, A. K.; Sharma, G. L.; Ghosh, B.; Wengel, J.; Olsen, C. E.; Parmar, V. S. *Pure Appl. Chem.* **2005**, *77*, 25-40.

[10] Ralph, J.; Quideau, S.; Grabber, J. H.; Hatfield, R. D. *J. Chem. Soc., Perkin Trans.1* **1994**, *23*, 3485-3498.

[11] Mayer, A. M.; Staples, R. *Phytochemistry* **2002**, *60*, 551-565.

[12] Xu, F. *J. Biol. Chem.* **1997**, *272*, 924-928.

[13] (a) Claus, H. *Micron* 2004, *35*, 93-96. (b) Solomon, E. I., Sundaram UM, Machonkin TE. *Chem. Rev.* 1996, *96*, 2563-2605.

[14] Piontek, K.; Antorini, M.; Choinowski, T. *J. Biol. Chem*. **2002**, *277*, 37663-37669.

[15] Berka, R. M.; Schneider, P.; Golightly, E. J.; Brown, S. H.; Madden, M.; Brown, K.; Halkier, T.; Mondorf, K.; Xu, F. *Appl. Environ. Microbiol.* **1997**, 63, 3151-3157.

[16] Tzeng, S.-C.; Liu Y.-C. *J. Mol. Catal. B: Enzym.* **2004**, *32*, 7-13.

[17] a) Sy, L. K.; Saunders, R. M. K.; Brown, G. D. *Phytochemistry* **1997**, *44*, 1099-1108; b) Kouno, I.; Morisaki, T.; Hara, Y.; Yang, C.-S. *Chem. Pharm*. *Bull.* **1991**, *39*, 2606-2608; c) Sarker, S. D. *Fitoterapia* **1997**, *68*, 3-8.

[18] Lajide, L.; Escoubas, P.; Mizutani, J. *Phytochemistry* **1995**, *40*, 1105-1112.

[19] Ohyama, M.; Tanaka, T.; Ito, T.; Iinuma, M.; Bastow, K. F.; Lee, K.-H. *Bioorg. Med. Chem. Lett.* **1999**, *9*, 3057-3060.

[20] Barjot, C.; Tournaire, M.; Castagnino, C.; Vigor, C.; Vercauteren, J.; Rossi, J.-F. *Life Sci.* **2007**, 81, 1565-1574.

[21] Colin, D.; Gimazane, A.; Lizard, G.; Izard, J.-C.; Solary, E.; Latruffe, N.; Delmas, D. *Int. J. Cancer* **2009**,*124*, 2780-2788.

[22] Langcake, P.; Pryce, R. J. *Experientia* **1977**, 33151-33152.

[23] Cichewicz, R. H.; Kouzi, S. A. *Studies in Natural Products Chemistry Bioactive Natural Products*, Part G, **2002**, *26,* 507-579.

[24] a) Langcake, P.; Pryce, R. J. *J. Chem. Soc. Chem. Commun*. **1977**, 208-210; b) Hirano, Y.; Kondo, R.; Sakai, K. *J. Wood Sci*. **2002**, *48*, 64-68.

[25] Breuil, A. C.; Adrian, M.; Pirio, N.; Meunier, P.; Bessis, R.; Jeandet, P. *Tetrahedron Lett*. **1998**, *39*, 537-540; b) Cichewicz, R. H.; Kouzi, S. A.; Hamann, M. T. *J. Nat. Prod*. **2000**, *63*, 29-33.

[26] Wang, M.; Jin, Y.; Ho, C.-T. *J. Agric. Food Chem.* **1999**, *47*, 3974-3977.

[27] (a) Huang, K.-S.; Lin, M.; Yu, L.-N.; Kong, M. Tetrahedron **2000**, *56*, 1321-1329. (b) Huang, K.-S.; Lin, M.; Wang, Y. H. *Chin. Chem. Lett.* **1999**, *10*, 817-820.

[28] Nicotra, S.; Cramarossa, M. R.; Mucci, A.; Pagnoni, U. M.; Riva, S.; Forti, L. *Tetrahedron* **2004**, *60*, 595-600.

[29] Ponzoni, C.; Beneventi, E.; Cramarossa, M. R.; Raimondi, S.; Trevisi, G.; Pagnoni, U.M.; Riva, S.; Forti, L. *Adv. Synth. Catal.* **2007**, *349*, 1497-1506.

[30] a) Snyder, S. A.; Zografos, A. L.; Lin, Y. *Angew. Chem.* **2007**, *119*, 8334-8339; b) Snyder, S. A.; Zografos, A. L.; Lin, Y. *Angew. Chem. Int. Ed.* **2007**, *46*, 8186-8191.

[31] Sako, M.; Hosokawa, H.; Ito, T.; Inuma, M. *J. Org.Chem.* **2004**, *69*, 2598-2600.

[32] Takaya, Y.; Terashima, K.; Ito, J.; He, Y.-H.; Tateoka, M.; Yamaguchi, N.; Niwa, M. *Tetrahedron* **2005**, *61*, 10285-10290.

[33] Shang, Y.-J.; Qian, Y.-P.; Liu, X.-D.; Dai, F.; Shang, X.-L.; Jia, W.-Q.; Liu, Q.; Fang, J.-G.; Zhou, B. *J. Org. Chem.* **2009**, *74*, 5025-5031.

[34] a) Zhou, L. X.; Lin, M.; *Chin. Chem. Lett*. **2000**, *11*, 515-516; b) Yao, C. S.; Zhou, L. X.; Lin, M. *Chem. Pharm. Bull*. **2004**, *52*, 238-243.

[35] Li, W.; Li, H.; Li, Y.; Hou, Z. *Angew. Chem*. **2006**, *118*, 7771–7773. b) Li, W.; Li, H.; Li, Y.; Hou, Z. *Angew. Chem. Int. Ed*. **2006**, 45, 7609-7611.

[36] Velu, S. S.; Buniyamin, I.; Ching, L. K.; Feroz F.; Noorbatcha, I; Gee, L. C.; *Awang,* K.; Wahab, I. A.; Weber, J.-F. F. *Chemistry* - A *European Journal,* **2008**, *14*, 11376-11384.

[37] Lee, D.; Cuendet, M.; Vigo, J. S.; Graham, J. G.; Cabieses, F.; Fong, H. H. S.; Pezzuto, J. M.; Kinghorn, A. D. *Org. Lett.* **2001**, *3*, 2169-2171.

[38] Banwell, M. G.; Bezos, A.; Chand, S.; Dannhardt, G.; Kiefer, W.; Nowe, U.; Parish, C. R; Savage, G. P.; Ulbrich, H. *Org. Biomol. Chem.* **2003**, *1*, 2427-2429.

[39] Ferro, V.; Devine, P. *Chem. Aust.* **2001**, *68*, 18-21.

[40] Tanaka, T.; Nishimura, A.; Kouno, I.; Nonaka, G.; Yang, C.R. *Chem.Pharm. Bull.*, **1997**, *45*, 1596-1600.

[41] Souza da Silva, S. A.; Souto, A. L.; de Fatima Agra, M.; Leitao da-Cunha, E. V.; Barbosa-Filho, J. M.; Sobral da Silva, M.; Braz-Filho, R., *Arkivoc*, **2004**, *6*, 54-58.

[42] Shi, S.; Zhang, Y.; Huang, K.; Liu, S.; Zhao, Y. *Food Chem.*, **2008**, *108*, 402-406.

[43] a) Maeda, S.; Masuda, H.; Tokoroyama, T. *Chem. Pharm. Bull.*,**1994**, *42*, 2506–2513; b) Maeda, S.; Masuda, H.; Tokoroyama, T. *Chem. Pharm. Bull.*, **1995**, *43*, 935–940.

[44] Li, X.; Shi, S.; Xu, Y.; Tao, Q.; Stockhit, J.; Zhao, Y. CN Pat.,101024640, **2007**.

[45] Kikuchi, T.; Kadota, S.; Yanada, K.; Tanaka, K.; Watanabe, K.; Yoshizaki, M.; Yokoi, T.; Shingu, T. *Chem. Pharm. Bull.* **1983**, *31*, 1112-1114.

[46] Seikel, M. K.; Hostettler, F. D.; Johnson, D. B. *Tetrahedron* **1968**, *24*, 1475-1488.

[47] Hostettler, F. D.; Seikel, M. K. *Tetrahedron* **1969**, *25*, 2325-2337.

[48] Agata, I.; Hatano, T.; Nishibe, S.; Okuda, T. *Chem. Pharm. Bull.* **1988**, *36*, 3223-3225.

[49] Daquino, C.; Rescifina, A.; Spatafora, C.; Tringali C. *E. Jour. Org. Chem.*, **2009**, 6289-6300.

[50] Da Cunha, F. M.; Duma, D.; Assreuy, J.; Buzzi, F. C.; Niero, R.; Campos, M. M.; Calixto, J. B. *Free Radical Res.* **2004**, *38*, 1241-1253; b) Lee, Y.-T.; Don, M.-J.; Hung, P.-S.; Shen, Y.-C.; Lo, Y.-S.; Chang, K.-W.; Chen, C.-F.; Ho, L.-K. *Cancer Lett.* **2005**, *223*, 19–25; c) Debing, X.; Dong, W.; Yujun, H.; Jiayin, X.; Zhaoyang, Z.; Zengpeng, L.; Jiang, X. *Anti-Cancer Drugs* **2006**, *17*, 753–762; d) Jin, H. H.; Joo, P.

H.; Hwa-Jin, C.; Hye-Young, M.; Eun-Jung, P.; Ji-Young, H.; Kook, L. S. *J. Nutr. Biochem*. **2006**, *17*, 356-362.

[51] Maeda, S.; Masuda, H.; Tokoroyama, T. *Chem. Pharm. Bull.* **1994**, 42, 2500-2505.

[52] Di Micco, S.; Mazué, F.; Daquino, C.; Spatafora, C.; Delmas, D.; Latruffe, N.; Tringali, C.; Riccio, R.; Bifulco, G. *Org. Biomol. Chem.*, **2011**, *9*, 701-710.

[53] Bayer, A. Ann. **1861**, *117*, 178-180.

[54] a) Jimenez, C.; Crews, P. *Tetrahedron Lett*. **1994**, *35*, 1375-1378. b) Fathi-Afshar, R.; Allen, T. M. *Can J. Chem*. **1988**, *66*, 45-50. c) Chevolot, L.; Padua, S.; Ravi, B. N.; Blyth, P. C.; Scheuer, P. J. *Heterocycles* **1977**, *7*, 891-894.

[55] Sutherland, J. J.; Weaver, D. F. *J. Chem. Inf. Comput. Sci*. **2003**, 43, 1028-1036.

[56] Djura, P.; Stierle, D. B.; Sullivan, B.; Faulkner, D. J.; Arnold, E. V.; Clardy, J. *J. Org. Chem*. **1980**, *45*, 1435-1441.

[57] Khanfar, M. A.; Abu Asal, B.; Mudit, M.; Kaddoumi, A.; El Sayed, K. A. *Bioorg. Med. Chem.* **2009**, *17*, 6032-6039.

[58] Shah, G. V.; Muralidharan A.; Thomas, S.; Gokulgandhi, M.; Mudit, M.; Khanfar, M.; El Sayed, K. A. *Mol. Cancer Ther*. **2009**, *8*, 509-520.

[59] Carmi, C.; Cavazzoni, A.; Zuliani, V.; Lodola, A.; Bordi, F.; Plazzi, P. V.; Alfieri, R. R.; Petronini, P. G.; Mor, M. *Bioorg. Med. Chem. Lett.* **2006**, *16*, 4021-4025.

[60] Zuliani, V.; Carmi, C.; Rivara, M.; Fantini, M.; Lodola, A.; Vacondio, F.; Bordi, F.; Plazzi, P. V.; Cavazzoni, A.; Galetti, M.; Alfieri, R. R.; Petronini, P. G.; Mor. M. *E. Jour. Med. Chem.* **2009**, *44*, 3471-3479.

[61] McNamara, J. O. In Goodman & Gilman's *The Pharmacological Basis of Therapeutics, Tenth Edition*; Hardman, J. G., Limbird, L. E., Eds.; McGraw-Hill: New York, **2001**, Chapter 21, pp 528-531.

[62] Thenmozhiyal, J. C.; Wong, P. T. H.; Chui, W. K.; *J. Med. Chem.* **2004**, *47*, 1527-1535.

[63] a) Bazil, C. W.; Pedley, T. A. *Annu. Rev. Med.* **1998**, *49*, 135-162; b) Luer, M. S. *Neurol. Res.* **1998**, *20*, 178-182.

[64] a) Matsukura, M.; Daiku, Y.; Ueda, K.; Tanaka, S.; Igarashi, T.; Minami, N. *Chem. Pharm. Bull.* **1992**, *40*, 1823-1827; b) Knabe, J.; Baldauf, J.; Ahlhelm, A. *Pharmazie* **1997**, *52*, 912-919.

[65] Somsák, L.; Kovács, L.; Tóth, M.; Ösz, E.; Szilágyi, L.; Györgydeák, Z.; Dinya, Z.; Docsa, T.; Tóth, B.; Gergely, P. *J. Med. Chem.* **2001**, *44*, 2843-2848.

[66] a) Moloney, G. P.; Robertson, A. D.; Martin, G. R.; MacLennan, S.; Mathews, N.; Dodsworth, S.; Sang, P. Y.; Knight, C.; Glen, R. *J. Med. Chem.* **1997**, *40*, 2347-2362; b) Moloney, G. P.; Martin, G. R.; Mathews, N.; Milne, A.; Hobbs, H.; Dodsworth, S.; Sang, P. Y.; Knight, C.; Williams, M.; Maxwell, M.; Glen, R. C., *J. Med.Chem.* **1999**, *42*, 2504-2526.

[67] Jansen, M.; Potschka, H.; Brandt, C.; Löscher, W.; Dannhardt, G.; *J. Med. Chem.* **2003**, *46*, 64-73.

[68] Last-Barney, K.; Davidson, W.; Cardozo, M.; Frye, L. L.; Grygon, C. A.; Hopkins, J. L.; Jeanfavre, D. D.; Pav, S.; Qian, C.; Stevenson, J. M.; Tong, L.; Zindell, R.; Kelly, T. A. *J. Am. Chem. Soc.* **2001**, *123*, 5643-5650.

[69] Koenig, W.; Zoller, G.; Just, M.; Jablonka, B. *Ger. Offen.* **1993**, 17 pp. CODEN: GWXXBX DE 4126277 A1 19930211 CAN 119:181238 AN 1993:581238

[70] Sutherland, J. C.; Hess, G. P. *Nat. Prod. Rep.* **2000**, *17*, 621-631.

[71] a) Syldatk, C.; Müller, R.; Siemann, M.; Krohn, K.; Wagner, F. *Biocatalytic Production of Amino Acids and Derivatives*, Hanser, München, **1992**, p. 75; b) Drauz, K.; Waldmann, H. *Enzyme Catalysis in Organic Synthesis*, VCH, Weinheim, **1995**, p. 409.

[72] Altenbuchner, J.; Siemann-Herzberg, M.; Syldatk, C. *Curr. Opin. Biotechnol*. **2001**, *12*, 559-563.

[73] Ware, E. *Chem. Rev* **1950**, *46*, 403-470.

[74] Paul, S.; Gupta, M.; Gupta, R.; Loupy, A. *Synthesis*, **2002**, 75-78.

[75] Zhao, B.; Du, H.; Shi, Y. *J. Am. Chem. Soc.* **2008**, *130*, 7220-7221.

[76] a) Greene, F. D.; Stowell, J. C.; Bergmark, W. R. *J. Org. Chem.* **1969**, *34*, 2254-2263; b) For leading references on the reaction of diaziridines with ketenes, see: c) Shevtsov, A. V.; Petukhova, V. Yu.; Strelenko, Yu. A.; Lyssenko, K. A.;Makhova, N. N.; Tartakovsky, V. A. *Russ. Chem. Bull., Int. Ed.* **2005**, *54*,1021-1031; d) Shevtsov, A. V.; Ananikov, V. P.; Makhova, N. N. *Russ. J. Org. Chem.* **2007**, *43*, 1101-1105.

[77] Zhang, D.; Xing, X.; Cuny, G. D. *J. Org. Chem.* **2006**, *71*, 1750-1753.

[78] For a review concerning the synthesis and the structural and chemical properties of carbodiimides, see: Williams, A.; Ibrahim, I. T. *Chem. Rev.* **1981**, *81*, 589-636.

[79] Sheehan, J. C.; Hess, G. P. *J. Am. Chem. Soc.* **1955**, *77*, 1067-1068.

[80] (a) Klausner, Y. S.; Bodansky, M. *Synthesis* **1972**, *1*, 453-463 and references cited therein. (b) Rebek, J.; Fitler, D. *J. Am. Chem.Soc.* **1973**, *95*, 4052-4053.

[81] a) Volonterio, A.; Zanda, M. *Tetrahedron Lett.* **2003**, *44*, 8549-8551; b) Volonterio, A.; Ramirez de Arellano, C.; Zanda, M. *J. Org. Chem.* **2005**, *70*, 2161-2170.

[82] Olimpieri, F.; Bellucci, M. C.; Volonterio, A.; Zanda, M. *Eur. J. Org. Chem.* **2009**, 6179-6188.

[83] Olimpieri, F.; Volonterio, A.; Zanda, M. *Synlett* **2008**, 3016-3020.

[84] Sarkanen, K. V.; Wallis, A. F. A. *J. Chem. Soc., Perkin Trans. 1*, **1973**, 1869-1878.

[85] Lemiere, G.; Gao, M.; De Groot, A.; Dommisse, R.; Lepoivre, J.; Pieters, L.; Buss, V. *J. Chem. Soc., Perkin Trans. 1*, **1995**, 1775-1779.

[86] a) Park, J. B.; Schoene, N. *Cancer Letters* **2003**, *202*, 161-171; b) Park, J. B.; Schoene, N. *BBRC* **2002**, *292*,1104-1110; c) Albericio, F.; Carpino, L. A. *Methods Enzymol*. **1997**, *289*, 104-126.

[87] Son, S.; Lewis, B. A. *J. Agric. Food Chem.* **2002**, *50,* 468-472.

[88] Fu, J.; Cheng, K.; Zhang, Z.-M.; Fang, R.-Q ; Zhu, H.-L. *Eur. J. Med. Chem.* **2010**, *45*, 2638-2643.

[89] Marder, O.; Albericio, F. CHIMICA OGGI, *Chemistry Today,* June **2003**.

[90] a) S. Riva, *Trends in Biotechnology*, **2006**, *24*, 219-226; b) Witayakran, S.; Ragauskas, A. J.; *Advanced Synthesis & Catalysis.* **2009**, *351*,1187-1209.

[91] Edward I. Solomon, Peng Chen, Markus Metz, Sang-Kyu Lee, Amy E. Palmer. *Angew. Chem. Inter. Ed.* ***2001***, *40*, 4570-4590.